IL
NUOVO CIMENTO
ORGANO DELLA SOCIETÀ ITALIANA DI FISICA
SOTTO GLI AUSPICI DEL CONSIGLIO NAZIONALE DELLE RICERCHE

Vol. XIII, N. 1 | *Serie decima* | 1° Luglio 1959

Form Factor Influence on Processes of Bremsstrahlung and Pair Production on Protons.

P. S. Isaev and I. S. Zlatev

Joint Institute for Nuclear Research - Laboratory of Theoretical Physics
Dubna

(ricevuto il 30 Dicembre 1958)

Summary. — The differential cross-sections of the processes of electron bremsstrahlung and pair production by γ-quanta on protons in presence of the form factor were calculated. This calculation was made in the lowest order of perturbation theory. The formula of the differential bremsstrahlung cross-section was integrated over all angles, except the angle between the direction of the incident electron and that of the emitted photon. A comparison of the differential and integral bremsstrahlung cross-sections with the corresponding Bethe-Heitler formulae was made.

Introduction.

The processes of electron bremsstrahlung and pair production by γ-quanta on protons were calculated by Bethe and Heitler (1) in the lowest order of perturbation theory in the approximation of point and infinitely heavy proton.

The development of the accelerative techniques made it possible to carry out experiments at rather high energies of incident particles (electrons, γ-quanta). In the considered processes at these energies both the nucleon recoil and its structure may be found essential. In fact, the experiments, which have been made by Hofstadter and others (2) on electron scattering

(1) H. Bethe and W. Heitler: *Proc. Roy. Soc.*, A **146**, 83 (1934); see also W. Heitler: *Quantum Theory of Radiation* (Oxford, 1954).

(2) R. Hofstadter: *Rev. Mod. Phys.*, **28**, 214 (1956).

at 500 MeV on hydrogen show that to explain the experimental data some sort of structure must be attributed to the nucleon. In connection with this it is of interest to clear up the form factor and recoil influence on such processes as electron scattering bremsstrahlung and pair production on nucleons (3), which are similar to the processes of electron scattering.

We calculated the differential cross-sections of the considered processes in the lowest order of perturbation theory (see diagrams *a*, *b*, *c*, *d*). On these diagrams the double line is the proton line, the single line that of the electron and

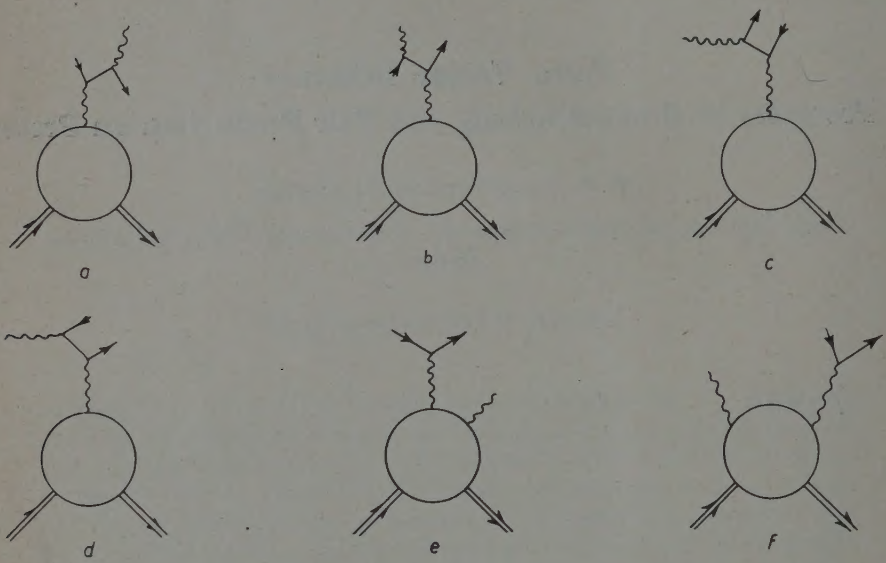

Fig. 1.

the waved line that of the photon. An additional contribution to the cross-sections will take place as a result both of the meson cloud of the nucleon (diagrams *e* and *f*) and the interference terms $(a, b)+e$; $(c, d)+f$. But its calculation is more complicated, than that of diagrams *a*), *b*), *c*), *d*), to which we limit ourselves in this paper. Recently in paper (4) the influence of the structure on the processes of bremsstrahlung and pair production was considered.

The consideration was made for angles θ satisfying the conditions:

$$(1) \qquad \theta^2 \ll \frac{M}{p}, \qquad p \gg M,$$

(3) I. Zlatev and P. S. Isaev: *Journ. Exp. Theor. Phys.*, **35**, 309 (1958).
(4) I. T. Dyatlov: *Journ. Exp. Theor. Phys.*, **35**, 155 (1958).

where θ is the angle between γ-quantum and electron (or positron), M is the nucleon mass and p the momentum of the electron (or that of the positron). We can see that the approximation (1) limits the consideration of this question and is convenient at energies of light particles $\gtrsim 10$ GeV and angles $\leqslant 5°$. In the case of $p \sim M$ one may extend the region of the angles up to $\theta \leqslant 15°$. However, in this case the form factor connected with an anomalous magnetic moment of the nucleon is omitted.

No limitation is imposed on the differential cross-sections given in this paper.

1. – Differential bremsstrahlung cross section.

The matrix element corresponding to the sum of the diagrams a) and b) has the following form:

$$M_{(a+b)} = \frac{ie^3}{(2\pi)^{\frac{7}{2}}} \cdot \frac{M \cdot m \cdot \delta(q_0 + p_0 - q - p - k)}{\sqrt{2\,|\boldsymbol{k}|\,\varepsilon_0 \varepsilon E_0 E}} \cdot \frac{1}{(p_0 - p)^2} \cdot$$
$$\cdot [\overline{w}^s(\boldsymbol{p}) \Gamma^\mu w^{s_0}(\boldsymbol{p}_0)] \left[\bar{u}^\sigma(\boldsymbol{q}) \left\{ \hat{l} \frac{1}{\hat{q}_0 + \hat{p}_0 - \hat{p} - m} \gamma_\mu + \gamma_\mu \frac{1}{\hat{q}_0 - \hat{k} - m} \hat{l} \right\} u^{\sigma_0}(\boldsymbol{q}_0) \right], \tag{2}$$

where M is the nucleon mass, m the electron mass, $p_0(E_0, \boldsymbol{p}_0)$, $p(E, \boldsymbol{p})$ the 4-momenta of the initial and final nucleon state; $q_0(\varepsilon_0, \boldsymbol{q}_0)$, $q(\varepsilon, \boldsymbol{q})$ the 4-momenta of the initial and final electron states; $k(k_0, \boldsymbol{k})$ the 4-momenta of the photon, $w^s(\boldsymbol{p})$ the spinor describing the nucleon with momentum $\boldsymbol{p}$ and spin direction s, $u^\sigma(q)$ the corresponding spinor of the electron, l the 4-vector of the photon polarization, $\hat{l} = \gamma^\alpha l_\alpha$, γ^μ the Dirac matrix, satisfying the condition $\gamma^\mu\gamma^\nu + \gamma^\nu\gamma^\mu = 2g^{\mu\nu}I$, I = unit matrix,

$$g^{\mu\nu} = \begin{pmatrix} 1 & 0 & 0 & 0 \\ 0 & -1 & 0 & 0 \\ 0 & 0 & -1 & 0 \\ 0 & 0 & 0 & -1 \end{pmatrix}.$$

$$\Gamma^\mu = \gamma^\mu F_1(|p_0 - p|^2) + \frac{\mu}{2M} \sigma^{\mu\nu}(p_0 - p)_\nu F_2(|p_0 - p|^2),$$

$F_i(|p_0 - p|^2)$ ($i = 1, 2$) is the form factor depending on the nucleon recoil, $F_i(0) = 1$.

1575

μ is the anomalous magnetic moment of the proton in nuclear magnetons,

$$\sigma^{\mu\nu} = \tfrac{1}{2}(\gamma^\mu\gamma^\nu - \gamma^\nu\gamma^\mu)$$

$$pq = g^{\mu\nu}p_\mu q_\nu \, .$$

We used the system of units $\hbar = c = 1$, $(e^2/4\pi) = (1/137)$.

In the system in which the nucleon is at rest in the initial state the formula of the differential bremsstrahlung cross-section has the form:

$$\begin{aligned}
(3)\qquad \mathrm{d}\sigma = {}& \frac{e^6}{8(2\pi)^5}\cdot\frac{\mathrm{d}k_0}{k_0 ME}\cdot\frac{1}{|\mathrm{d}f(\varepsilon)/\mathrm{d}\varepsilon|}\cdot\frac{|\boldsymbol{q}|}{|\boldsymbol{q}_0|}\cdot\frac{\mathrm{d}\Omega_{q_0}\mathrm{d}\Omega_k}{[(\varepsilon_0-\varepsilon-k_0)^2-Q^2]^2}\cdot \\
&\cdot\Bigg\{\Bigg[\left(\frac{\boldsymbol{q}^2\sin^2\theta}{(\varepsilon-|\boldsymbol{q}|\cos\theta)^2}+\frac{\boldsymbol{q}_0^2\sin^2\theta_0}{(\varepsilon_0-|\boldsymbol{q}_0|\cos\theta_0)^2}-\frac{2|\boldsymbol{q}_0||\boldsymbol{q}|\sin\theta\sin\theta_0\cos\varphi}{(\varepsilon-|\boldsymbol{q}|\cos\theta)(\varepsilon_0-|\boldsymbol{q}_0|\cos\theta_0)}\right)\cdot \\
&\cdot(2m^2-Q^2+(\varepsilon_0-\varepsilon-k_0)^2)-2k_0^2\frac{\varepsilon-|\boldsymbol{q}|\cos\theta}{\varepsilon_0-|\boldsymbol{q}_0|\cos\theta_0}-2k_0^2\frac{\varepsilon_0-|\boldsymbol{q}_0|\cos\theta_0}{\varepsilon-|\boldsymbol{q}|\cos\theta}\Bigg]\cdot \\
&\cdot[F_1(|p_0-p|^2)+\mu F_2(|p_0-p|^2)]^2(M^2-ME)+ \\
&+M^2\Bigg[\frac{\boldsymbol{q}^2\sin^2\theta}{(\varepsilon-|\boldsymbol{q}|\cos\theta)^2}((\varepsilon_0+\varepsilon+k_0)^2-Q^2)+\frac{\boldsymbol{q}_0^2\sin^2\theta_0}{(\varepsilon_0-|\boldsymbol{q}_0|\cos\theta_0)^2}\cdot \\
&\cdot((\varepsilon_0+\varepsilon-k_0)^2-Q^2)-\frac{2|\boldsymbol{q}||\boldsymbol{q}_0|\sin\theta\sin\theta_0\cos\varphi}{(\varepsilon-|\boldsymbol{q}|\cos\theta)(\varepsilon_0-|\boldsymbol{q}_0|\cos\theta_0)}\cdot \\
&\cdot((\varepsilon_0+\varepsilon+k_0)(\varepsilon_0+\varepsilon-k_0)-Q^2+2k_0^2)+2k_0^2\frac{\boldsymbol{q}^2\sin^2\theta+\boldsymbol{q}_0^2\sin^2\theta_0}{(\varepsilon-|\boldsymbol{q}|\cos\theta)(\varepsilon_0-|\boldsymbol{q}_0|\cos\theta_0)}\Bigg]\cdot \\
&\cdot\left[F_1^2(|p_0-p|^2)+2\left(\frac{\mu}{M}\right)^2F_2^2(|p_0-p|^2)(ME-M^2)\right]\Bigg\},
\end{aligned}$$

where

$$\begin{aligned}
Q^2 = {}& \boldsymbol{q}^2+\boldsymbol{q}_0^2+k_0^2-2|\boldsymbol{q}||\boldsymbol{q}_0|(\cos\theta\cos\theta_0+\sin\theta\sin\theta_0\cos\varphi)+ \\
&+2k_0|\boldsymbol{q}|\cos\theta-2k_0|\boldsymbol{q}_0|\cos\theta_0
\end{aligned}$$

$$f(\varepsilon) = E(\varepsilon)+\varepsilon+k_0-\varepsilon_0-M\,,$$

(ε and $E(\varepsilon)$ are found from the conservation law $p_0+q_0 = p+q+k$), θ_0 is the angle between the vector $\boldsymbol{k}$ and $\boldsymbol{q}_0$, θ the angle between the vectors $\boldsymbol{k}$ and $\boldsymbol{q}$, φ the angle between the vectors $[\boldsymbol{k}\times\boldsymbol{q}_0]$ and $[\boldsymbol{k}\times\boldsymbol{q}]$; $\mathrm{d}\Omega_{q_0}\mathrm{d}\Omega_k = \sin\theta\,\mathrm{d}\theta\sin\theta_0\,\mathrm{d}\theta_0\,\mathrm{d}\varphi\,\mathrm{d}\varphi_0$. To obtain from (3) the Bethe-Heitler formula it is

necessary to make the following transition

1) $M \to \infty$.

2) to consider the nucleon as a point nucleon: $r_0 = 0$, $F_i = 1$.

3) to assume that $\mu = 0$.

When this transition is made, the conservation law takes the form $\varepsilon_0 = k_0 + \varepsilon$.

The formula of the differential cross-section of pair production on nucleons may be obtained from (3) by means of the substitution:

$$\varepsilon \to -\varepsilon_+ , \qquad \varepsilon_0 \to \varepsilon_- , \qquad |\boldsymbol{q}_0| \to |\boldsymbol{q}_-|, \qquad |\boldsymbol{q}| \to |\boldsymbol{q}_+|$$

$$\theta \to \pi - \theta_+ , \qquad \theta_0 \to \theta_- , \qquad \varphi_+ \to \pi + \varphi$$

and

$$\frac{\mathrm{d}k_0}{|\mathrm{d}f(\varepsilon)/\mathrm{d}\varepsilon|} \cdot \frac{|\boldsymbol{q}|}{|\boldsymbol{q}_0|} \cdot \mathrm{d}\Omega_{q_0} \mathrm{d}\Omega_k \to -\frac{\mathrm{d}\varepsilon_+}{k_0^2} \frac{|\boldsymbol{q}_+||\boldsymbol{q}_-|}{|\mathrm{d}\psi(\varepsilon_-)/\mathrm{d}\varepsilon_-|} \mathrm{d}\Omega_{q_+} \mathrm{d}\Omega_{q_-} ,$$

where the sign $(+)$ is connected with the positron and the $(-)$ sign with the electron,

$$\psi(\varepsilon_-) = E(\varepsilon_-) + \varepsilon_- + \varepsilon_+ - M - k_0$$

$$\mathrm{d}\Omega_{q_+} \mathrm{d}\Omega_{q_-} = \sin\theta_+ \mathrm{d}\theta_+ \sin\theta_- \mathrm{d}\theta_- \mathrm{d}\varphi_+ \mathrm{d}\varphi_- .$$

The formula of the differential bremsstrahlung cross-section (3) depends in a complicated manner on the nucleon recoil. To obtain a clear view of the influence of recoil, form factor and anomalous magnetic moment of the proton μ on the bremsstrahlung cross-section, a comparison was made of formula (3) and that of Bethe-Heitler. We made the numerical calculations for the particular case, when the incident electron energy is equal to 0.54 and the energy of the γ-quantum is equal to 0.25 (in units $\hbar = c = M = 1$). The form of the form factors $F_1(|p^0 - p|^2)$ and $F_2(|p_0 - p|^2)$ was taken from Hofstadter's experiments on electron scattering on protons at incident electron energy ~ 500 MeV (exponential model, $F_1 = F_2$, $r_0 = 0.8 \cdot 10^{-13}$ cm). The choice of the γ-quantum energy was made from kinematic reasons (see Appendix). In Table I we give a part of the numerical data which characterize the influence of the recoil form factor and anomalous magnetic moment on the bremsstrahlung cross-section.

For other values of the angles θ_0, θ and φ we have approximately the same deviations from the Bethe-Heitler formula.

It is of interest to note that the presence of recoil only leads to a redistribution of the differential cross-section (3) with respect to that of Bethe-

1577

TABLE I.

θ_0	Differential Bethe-Heitler cross-section $\frac{d\sigma_{\text{B.-H.}} \cdot 10^{36}}{dk_0\, d\Omega_{q_0}\, d\Omega_k} \cdot$ $\cdot \text{cm}^2/(\text{sr})^2$ erg	Differential cross-section taking into account recoil and form factor $\frac{d\sigma \cdot 10^{36}}{dk_0 d\Omega_{q_0} d\Omega_k} \cdot$ $\cdot \text{cm}^2/(\text{sr})^2$ erg	$\frac{d\sigma}{d\sigma_{\text{B.-H.}}}$	Differential cross-section without taking into account the form factor $\cdot 10^{36} \frac{\text{cm}^2}{(\text{sr})^2 \text{ erg}}$	Differential cross-section without taking into account form factor and anomalous magnetic moment $\cdot 10^{36} \frac{\text{cm}^2}{(\text{sr})^2 \text{ erg}}$
1	2	3	4	5	6
		$\varphi = 0$ $\theta = 30°$			
6°	6 003 000	5 789 000	0.963 8	6 048 000	5 863 000
30°	136 260	126 480	0.929 7	137 370	129 590
60°	3 605	2 252	0.624 4	439 8	2 795
90°	544.4	218.0	0.400 5	827.5	314.0
120°	134.37	48.95	0.364 3	287.2	65.89
150°	36.71	21.35	0.581 4	155.95	23.77
		$\varphi = 0$ $\theta = 90°$			
6°	31 085	25 848	0.831 5	42 610	25 460
30°	3 214	2 787	0.867 3	3 471	2 588
60°	347.2	581.9	1.676 1	699.4	405.7
90°	179.40	125.89	0.701 7	261.0	129.67
120°	53.01	19.344	0.364 9	83.31	23.23
150°	20.39	5.721	0.280 6	38.05	6.184
		$\varphi = 0$ $\theta = 150°$			
6°	1 210.2	3 402	2.81	7 944	918.7
30°	121.15	182.13	1.534	391.3	99.79
60°	64.60	67.64	1.047 1	139.59	43.68
90°	25.85	34.43	1.331 7	79.67	20.84
120°	7.154	16.852	2.356	55.93	11.232
150°	3.705	7.538	2.034	40.65	6.306
		$\varphi = 90°$ $\theta = 30°$			
6°	2 177 000	2 018 000	0.926 7	2 267 000	2 090 000
30°	24 040	17 913	0.745 2	26 580	20 290
60°	1 625.2	901.3	0.554 6	2 391	1 200.6
90°	291.1	131.94	0.453 3	581.2	187.31
120°	71.70	38.49	0.536 8	236.9	50.03
150°	18.340	19.484	1.062 4	143.59	21.40
		$\varphi = 90°$ $\theta = 90°$			
6°	23 977	19 936	0.831 5	35 082	19 784
30°	825.8	642.6	0.778 1	1 289.8	666.2
60°	146.94	94.66	0.644 2	255.6	107.79
90°	45.09	22.86	0.507 1	89.74	27.72
120°	19.200	7.930	0.412 8	43.79	9.379
150°	11.136	3.795	0.346 7	26.45	4.393

TABLE I (*continued*).

θ_0	Differential Bethe-Heitler cross-section $\frac{d\sigma_{B.-M.}\cdot 10^{36}}{dk_0\, d\Omega_{q_0}\, d\Omega_k}\cdot$ $\cdot$cm²/(sr)² erg	Differential cross-section taking into account recoil and form factor $\frac{d\sigma\cdot 10^{36}}{dk_0\, d\Omega_{q_0}\, d\Omega_k}\cdot$ $\cdot$cm²/(sr)² erg	$\frac{d\sigma}{d\sigma_{B.-M.}}$	Differential cross-section without taking into account the form factor $\cdot 10^{36}\,\frac{\text{cm}^2}{(\text{sr})^2\,\text{erg}}$	Differential cross-section without taking into account form factor and anomalous magnetic moment $\cdot 10^{36}\,\frac{\text{cm}^2}{(\text{sr})^2\,\text{erg}}$
1	2	3	4	5	6
			$\varphi = 90°\quad \theta = 150°$		
6°	963.5	3 204	3.326	7 688	1 484.7
30°	63.00	137.59	2.184	341.2	75.12
60°	34.56	36.24	1.048 7	99.57	26.94
90°	22.22	16.012	0.720 5	53.11	13.420
120°	13.189	8.379	0.635 3	36.62	7.243
150°	8.168	5.295	0.648 3	31.25	4.633
			$\varphi = 150°\quad \theta = 30°$		
6°	1 388 500	1 243 200	0.895 4	1 482 000	1 310 700
30°	12 076	8 693	0.719 9	15 764	10 336
60°	929.2	531.7	0.572 2	1 682.1	716.8
90°	157.43	95.05	0.603 8	458.5	131.11
120°	30.42	32.32	1.062 5	205.2	40.78
150°	4.312	18.113	4.201	134.37	19.679
			$\varphi = 150°\quad \theta = 90°$		
6°	26 235	16 356	0.623 4	31 440	16 278
30°	350.7	314.5	0.897 0	812.1	322.2
60°	36.98	39.98	1.081 2	145.25	43.57
90°	8.509	11.267	1.324 1	54.67	12.867
120°	4.377	5.074	1.159 2	30.96	5.662
150°	5.258	3.382	0.643 2	24.19	3.471
			$\varphi = 150°\quad \theta = 150°$		
6°	760,5	3 042	4.00	7 465	1 407.7
30°	23.49	104.66	4.456	287.3	57.75
60°	11.723	23.83	2.033	77.29	17.531
90°	9.957	9.918	0.996 1	39.36	8.576
120°	8.913	5.606	0.628 9	27.94	5.029
150°	7.887	4.180	0.530 1	25.99	3.718

Heitler $d\sigma_{\text{B.-H.}}$. For example, at $\varphi=0$, $\theta=30°$, $\theta_0=6°, ..., 150°$ the cross-section (3) was found everywhere less than $d\sigma_{\text{B.-H.}}$ while at $\varphi=150°$, $\theta=90°$, $\theta_0=60°, 90°, 120°$ it is everywhere greater than $d\sigma_{\text{B.-H.}}$. The anomalous magnetic moment of the proton increases everywhere the cross-section while the form factor decreases this cross-section. Thus, there is no simple regularity of change of the differential cross-section (3) in comparison to the differential Bethe-Heitler cross-section.

2. – Integral bremsstrahlung cross-section.

For a comparison with the experimental results it is useful to integrate formula (3) over the angles φ and θ and to obtain the integral bremsstrahlung cross-section as a function of ε_0, k_0 and θ_0. We choose the exponential form factor model which well conforms to the experimental data on electron scattering on nucleons ([2]). The integration was made for the case when $F_1=F_2$. Before the integration of (3) the substitution $|\boldsymbol{q}_0|\to\varepsilon_0$, $|\boldsymbol{q}|\to\varepsilon-(m^2/2(\varepsilon_0-k_0))$ was made. The integration was carried out exactly: over φ in the limits $(0, 2\pi)$, and over θ in the limits $(0, \pi)$. The kinematic case $I(a, c)$ was chosen by this (see Appendix).

The formula which was obtained is too complicated and is given explicitly in paper ([5]).

In the extreme case $M\to\infty$, $r_0=0$, $\mu=0$ the integral formula transforms to the Bethe-Heitler formula ([6]) anagoulosly integrated within the accuracy of the terms proportional to m^2 which were omitted in ([6]). The detailed extreme transition was made in paper ([5]).

For a comparison of the integral cross section with that which was obtained by means of integration of the Bethe-Heitler formula we give the Table II.

TABLE II.

θ_0	$F(\varepsilon_0, k_0, \theta_0)$	$F_{\text{B.-H.}}(\varepsilon_0, k_0, \theta_0)$	$F/F_{\text{B.-H.}}$
10°	$0.12428\cdot10^{-28}$	$0.8922\cdot10^{-29}$	1.3930
20°	$0.8322\cdot10^{-30}$	$0.5514\cdot10^{-30}$	1.5092
30°	$0.13381\cdot10^{-30}$	$0.10727\cdot10^{-30}$	1.2474
60°	$0.3813\cdot10^{-32}$	$0.6295\cdot10^{-32}$	0.6057
90°	$0.4427\cdot10^{-33}$	$0.10958\cdot10^{-32}$	0.4040
120°	$0.13031\cdot10^{-33}$	$0.2732\cdot10^{-33}$	0.4770
150°	$0.7162\cdot10^{-34}$	$0.7535\cdot10^{-34}$	0.9505

([5]) P. S. ISAEV and I. ZLATEV: Preprint of J.I.N.R. 264 (1958).
([6]) P. V. C. HOUGH: *Phys. Rev.*, **74**, 80 (1948).

Note. – The integral cross-section is given by following formula:

$$d\sigma(\varepsilon_0, k_0, \theta_0) = \sin\theta_0 d\theta_0 d\varphi_0 dk_0 F(\varepsilon_0, k_0, \theta_0),$$

$F_{\text{B.-H.}}(\varepsilon_0, k_0, \theta_0)$ is the analogous quantity for the integrated Bethe-Heitler formula. The numerical calculation was made for the case when $\varepsilon_0 = 0.54$, $k_0 = 0.25$.

The comparison of F and $F_{\text{B.-H.}}$ carried out for $\theta_0 < 10°$ showed that with the decrease of θ_0 the quantity F is approaching $F_{\text{B.-H.}}$, so that when $\theta_0 = 5°$ the difference between them does not exceed 3%.

3. – Conclusion.

In the Bernstein and Panofsky experiment (7) on the measurement of the total cross-section of electron bremsstrahlung at $(500 \div 550)$ MeV on hydrogen it was shown that in the region of angles not exceeding $(7 \div 10)°$ the Bethe-Heitler formula is correct within a great degree of accuracy. Nevertheless the comparison which was made by us (see Table II) shows that at $\theta_0 = 10°$ the difference is equal to 40%. This apparent discrepancy is explained as follows: the angles $\theta_0 \ll 10°$ (the maximum of radiation is at $\theta_0 \sim m/\varepsilon_0$) give a principal contribution to the cross-sections where the influence of the form factor, the anomalous magnetic moment and the recoil are insignificant, therefore this difference at $\theta_0 = 10°$ makes no essential change in the total cross-section.

It follows from this that the experimental study of the form factor influence in the considered processes has to be made measuring the integral curve as a function of the angle even in the range of $(5 \div 30)°$.

If the experiment does not confirm our integral formula even in the given range it will mean that a marked contribution from the meson cloud of the nucleon exists and consequently it is necessary to take into account the diagrams (e, f) already at 500 MeV.

Thus the interest lies in the experimental measurement of the integral cross section at $(500 \div 600)$ MeV.

* * *

The authors express their gratitude to A. A. LOGUNOV and V. S. BARAŠENKOV for useful discussions.

---

(7) D. BERNSTEIN and W. K. H. PANOFSKY: *Phys. Rev.*, **102**, 522 (1956).

Appendix

Kinematics of the bremsstrahlung process.

At the given energies ε_0 and k_0 and the angles θ_0, θ and φ, the energy of the scattered electron ε is determined from the law of conservation of energy:

$$M + \varepsilon_0 - \varepsilon - k_0 - E = 0 \,,$$

and from the law of conservation of three-dimensional momentum

$$\boldsymbol{q}_0 - \boldsymbol{p} - \boldsymbol{q} - \boldsymbol{k} = 0 \,,$$

that is from the equation

$$B - \varepsilon - \sqrt{B^2 - 2C + \varepsilon^2 + 2A\sqrt{\varepsilon^2 - m^2}} = 0 \,, \tag{A.1}$$

where we have put:

$$\begin{aligned} A &= k_0 \cos\theta - |\boldsymbol{q}_0|(\cos\theta\cos\theta_0 + \sin\theta\sin\theta_0\cos\varphi)\,, \\ B &= M + \varepsilon_0 - k_0\,, \\ C &= M\varepsilon_0 - Mk_0 - \varepsilon_0 k_0 + m^2 + |\boldsymbol{q}_0| k_0 \cos\theta_0\,. \end{aligned}$$

It was found that the equation (A.1) has solutions only for particular values of the quantities ε_0, k_0, θ_0, θ, φ. The following cases are possible:

1) The equation (A.1) has exactly one solution in the interval $m \leqslant \varepsilon \leqslant \varepsilon_0 - k_0$. This will be happen when

(a) $\quad A \geqslant 0\,, \qquad C - Bm \geqslant 0\,;$

or

(b) $\quad A < 0\,, \qquad C - Bm \leqslant 0\,, \qquad |A| \geqslant \dfrac{B(\varepsilon_0 - k_0) - C}{\sqrt{(\varepsilon_0 - k_0)^2 - m^2}}\,.$

This equality may be satisfied only for one of the following conditions:

(c) $\quad A < 0\,, \qquad |A| < B\,, \qquad C - Bm > 0\,, \qquad |A| \leqslant \dfrac{B(\varepsilon_0 - k_0) - C}{\sqrt{(\varepsilon_0 - k_0)^2 - m^2}}\,.$

2) The equation (A.1) has one double root. This will take place under the following conditions:

$$A < 0\,, \qquad |A| < B\,, \qquad C - m\sqrt{B^2 - A^2} = 0\,, \qquad Bm \leqslant \sqrt{B^2 - A^2}(\varepsilon_0 - k_0)\,.$$

3) The equation (A.1) has two different roots, when

$$A<0\,, \qquad |A|<B\,, \qquad C-Bm\leqslant 0\,, \qquad Bm<\sqrt{B^2-A^2}(\varepsilon_0-k_0)\,,$$

$$C-m\sqrt{B^2-A^2}>0\,, \qquad |A|\leqslant\frac{B(\varepsilon_0-k_0)-C}{\sqrt{(\varepsilon_0-k_0)^2-m^2}}\,.$$

4) In all other cases the equation (A.1) has no roots.

RIASSUNTO (*)

È stata calcolata la sezione trasversale d'urto del processo di produzione degli elettroni di bremsstrahlung e della produzione di coppie da parte dei quanti γ sui fotoni in presenza del fattore di forma. Tale calcolo è stato fatto nel primo ordine d'approssimazione della teoria delle perturbazioni. La formula della sezione d'urto differenziale di bremsstrahlung è stata integrata rispetto a tutti gli angoli escluso quello compreso fra la direzione dell'elettrone incidente e quello del fotone emesso. È stato eseguito il raffronto fra le sezioni d'urto differenziale ed integrale della bremsstrahlung con la corrispondente formula di Bethe-Heitler.

(*) *Traduzione a cura della Redazione.*

IL NUOVO CIMENTO Vol. XIII, N. 1 1° Luglio 1959

The Crab and Cygnus A as Gamma Ray Sources.

M. P. Savedoff

Department of Physics and Astronomy, University of Rochester - Rochester, N.Y.

(ricevuto il 30 Dicembre 1958)

Summary. — The Crab is estimated to give a maximum nuclear γ-ray flux of $10^{-2}\ \text{cm}^{-2}\ \text{s}^{-1}$ from the decay of ^{251}Cf formed with ^{253}Cf during the supernova outburst. Although extrapolation of the radio and visual fluxes suggests the possibility of a flux as high as $10\ \gamma\ \text{cm}^{-2}\ \text{s}^{-1}$ between 1 and 2 MeV, model calculations suggest that $7\cdot10^{-5}\ \gamma\ \text{cm}^{-2}\ \text{s}^{-1}$ above about 10 MeV is more probable. Bremsstrahlung and Compton scattering yield considerably lower fluxes. Cygnus A, regarded as the result of a collision of matter and antimatter, should yield lower fluxes than the $\gamma\ \text{cm}^{-2}\ \text{s}^{-1}$ estimated by Morrison. The radio flux suggests a π^0 decay γ-flux of $4\cdot10^{-5}\ \gamma\ \text{cm}^{-2}\ \text{s}^{-1}$. For $E > 10$ MeV, any γ-ray flux exceeding $5\cdot10^{-5}\ \gamma\ \text{cm}^{-2}\ \text{s}^{-1}$ should be detectable from a balloon flown emulsion stack.

1. – Introduction.

Morrison (1) has pointed out the possibility of γ-ray observation of astronomical objects. This note makes more detailed estimates of what energy ranges and sensitivities would provide meaningful tests for current hypotheses of these objects. Radio and continuum observations of the Crab (M1) point to a high energy component (synchrotron radiation) which makes this one of the brightest objects in the sky at 100 MHz. The tremendous energy flux from Cygnus A implies the possibility that we are actually seeing the collision between two systems involving matter and antimatter. As this system is again one of the brightest systems in the sky in radio region, we may again expect high γ-ray fluxes.

For the Crab we will assume a distance of $3\cdot10^{21}$ cm, a radius of $10^{18.1}$ cm,

(1) P. Morrison: *Nuovo Cimento*, **7**, 858 (1958).

a volume of 10^{55} cm³, and an age of 900 years or $3\cdot10^{10}$ s. γ-ray may be expected from nuclei following α or β decay, from synchrotron radiation, and from collisional processes of high energy electrons and protons both with particles and photons.

2. – Radioactive decays.

Nuclear γ-ray fluxes from the Crab were estimated by MORRISON [1] to be of the order of 10^{-2} cm^{-2} s^{-1}. The model of the Crab proposed by BURBIDGE *et al.* [2] where the spontaneous fission of ^{254}Cf is assumed to be the energy source seems pertinent. Assuming the maximum total energy flux from a supernova ($6\cdot10^{8} L_\odot$) comes solely from this decay one estimates that the Crab contained $5\cdot10^{52}$ nuclei of ^{254}Cf initially. This amounts to $10^{-2} M_\odot$ in contrast with a comparable calculation by BURBIDGE *et al.* which yields $5\cdot10^{-4} M_\odot$. Here $L_\odot$ and $M_\odot$ represent respectively the energy flux and mass of the sun. The higher abundance is used in the computations which follow and should be considered an upper limit. Table I contains a selection of

TABLE I. – *Nuclear γ rays from the crab.*

Nucleus	Longest half-life (years)	Flux (cm^{-2} s^{-1})	Photon Energy (MeV)
$^{251}_{98}$Cf	700	$1.1\cdot10^{-2}$	0.180
$^{250}_{96}$Cm	$7.5\cdot10^{3}$	$1.4\cdot10^{-3}$	Sp. Fiss: 75%
$^{249}_{98}$Cf	470	$6.3\cdot10^{-3}$	.395
$^{243}_{95}$Am	7600	$1.6\cdot10^{-3}$	.075
$^{241}_{95}$Am	470	$1.0\cdot10^{-2}$	.060
$^{233}_{92}$U	$1.6\cdot10^{5}$	$4.2\cdot10^{-5}$	.04
$^{231}_{91}$Pa	$3.4\cdot10^{4}$	$3.0\cdot10^{-4}$	.110, .329
$^{226}_{88}$Ra	1620	$1.5\cdot10^{-3}$	.188 (5%)

radioactive nuclei chosen as most likely to dominate the γ-ray spectrum of a 900 year old supernova. Morrison's statement about the dominance of $^{226}_{88}$Ra seems unfounded as only 5% of the α decays are to the excited state of the daughter. The principal γ-ray energy has been found using the compilation of SEABORG *et al.* [3] and available nuclear data cards. Branching

(2) G. R. BURBIDGE, E. M. BURBIDGE, W. FOWLER and F. HOYLE: *Rev. Mod. Phys.*, **29**, 547 (1957).

(3) D. STROMINGER, J. M. HOLLANDER and G. T. SEABORG: *Rev. Mod. Phys.*, **30**, 585 (1958).

and internal conversion will reduce the rate from that given in column 3 which is the number of disintegrations times the fractional solid angle subtended by 1 cm^2 at the earth's distance.

CAMERON (private communication) claims that certain light nuclei ignored in this calculation are formed abundantly by (n, γ) processes with decay γ-rays above 1 MeV. His estimates are not available in detailed form. It should also be noted that an appreciable number of spontaneous fissions by ${}^{250}_{96}Cm$ occur which give rise to a large number of possible γ-ray lines.

3. – Spectrum extrapolation.

To produce γ-rays ($h\nu > 1$ MeV) by magnetic bremsstrahlung in a field of 10^{-2} gauss, electrons must have an energy exceeding 10^{+13} eV. If we extrapolate the estimated luminosity of $1.4 \cdot 10^{24}$ erg s^{-1} Hz^{-1} at 100 MHz and of $3.4 \cdot 10^{21}$ erg s^{-1} Hz^{-1} at 4 250 A ([4]), we obtain $1.7 \cdot 10^{19}$ erg s^{-1} Hz^{-1} at 1 MeV. In the band $(1 \div 2)$ MeV the total flux is approximately $3.4 \cdot 10^{39}$ erg s^{-1} or $3.4 \cdot 10^{-5}$ erg $^{-1}$ cm^{-2} at the earth. This is equivalent to a flux of $10\ \gamma\ cm^{-2}\ s^{-1}$. Power law extrapolation over these ranges from 10^8 Hz and 10^{14} Hz to 10^{20} Hz seem dubious since the observed exponent in the power spectrum is -0.4 and implies infinite integrated power without a high energy cut-off. For example, the radiation lifetime of a $10^{13.5}$ eV electron in a 10^{-2} gauss field is about 10^{-3} that for the electrons producing visual light and is about 10 hours, excessively short compared to any time scale in the system.

It should also be noted that most of the observed visible radiation arises from electrons with $\nu \sim \nu_c$. These do not contribute appreciably to the MeV range, the asymptotic spectrum being $(\nu/\nu_c)^{\frac{1}{2}} \exp[-\nu/\nu_c]$ powerwise.

4. – Burbidge's primary proton model.

If we take the recent model of the Crab proposed by BURBIDGE ([5]) in which a high energy proton component provides the relativistic electrons by p-p scattering through meson production, we obtain Table II. We record respectively the magnetic field, proton energy, total number of protons, electron energy, total number of electrons and the electron radiation lifetime.

We further expect that about 1 $M_\odot$ of material possibly of mean atomic mass 20 and charge 10 is contained in the volume of the amorphous emitter.

([5]) R. MINKOSKI: *Astrophys. Journ.*, **96**, 199 (1942).
([3]) G. R. BURBIDGE: *Astrophys. Journ.*, **127**, 48 (1958).

Thus the heavy particle density is about $6\ \text{cm}^{-3}$. BURBIDGE *et al.* [2] estimate $10^3\ \text{cm}^{-3}$. We adopt $10^2\ \text{cm}^{-3}$ for the nuclear density and $10^3\ \text{cm}^{-3}$ for the electron density.

5. – Meson decay and gamma production.

With the data of Table II, assuming that the electrons are produced via π-meson production by proton bombardment of the heavy nuclei, we obtain by combining the number of electrons and their lifetimes a production rate of $7\cdot10^{39}$ electrons per second. From the known statistics on π^+, π^0, and π^- production one estimates one γ will be produced per $\pi^\pm$ from decay of the

TABLE II. – *High energy components of the crab.*

B (G)	E_{proton} (eV)	N_{proton}	E_{electron} (eV)	N_{electron}	Electron half-life (s)
10^{-2}	$1.8\cdot10^{13}$	$2\cdot10^{49}$	$6\cdot10^{10}$	$2\cdot10^{48}$	$1.5\cdot10^{8}$
$3\cdot10^{-2}$	$7\ \ \cdot10^{12}$	$5\cdot10^{49}$	$3\cdot10^{40}$	$2\cdot10^{47}$	$3\ \ \cdot10^{7}$

π^0 and another γ by the later electron annihilation radiation. Thus the flux at the earth of γ-rays of either type is about $7\cdot10^{-5}\ \text{cm}^{-2}\ \text{s}^{-1}$. It is interesting to note that the mass surface density of the Crab is about $10^{-3}\ \text{g cm}^{-2}$ hence little conversion should occur in the source.

6. – Bremsstrahlung.

Although we have indicated that only an infinitesimal part of the synchrotron radiation of relativistic electrons at $3\cdot10^{10}$ eV in a field of 10^{-2} gauss will fall in the MeV region, bremsstrahlung will in general produce appreciable fluxes in this energy range. This flux can be estimated from HEITLER [6]. Since $E \gg mc^2$,

$$\sigma_\nu = 20\,\bar{\varphi}\,\mathrm{d}K/K = 10^{-24}\,\mathrm{d}\nu/\nu\ \ \text{cm}^{-2}\,.$$

The γ-ray number flux expected is therefore

$$N_e n_H \sigma_\nu c = 3\cdot10^{36}\quad \text{photons s}^{-1}$$

(6) W. HEITLER: *The Quantum Theory of Radiation*, 2-nd ed. (Oxford, 1944), p. 170, Fig. 14.

1587

or $3 \cdot 10^{-8}\, \mathrm{d}\nu/\nu$ photons $\mathrm{cm}^{-2}\,\mathrm{s}^{-1}$ at the distance of the earth. The integrated flux above 10 MeV should be $2 \cdot 10^{-7}\,\mathrm{cm}^{-2}\,\mathrm{s}^{-1}$ and a factor 1.5 larger above 100 keV. There is of course considerable uncertainty in the factors entering this estimate. The radio radiation from the Crab indicates that N_e is 10^3 larger for electrons at $10^{7.5}$ eV. These would contribute $6 \cdot 10^{-5}$ photons $\mathrm{cm}^{-2}\,\mathrm{s}^{-1}$ between .1 and 1 MeV.

7. – Compton scattering.

The only other obvious process leading to observable γ-rays is the collision of relativistic electrons with photons. The electron energy loss by this process has been previously calculated. The question is whether it leads to observable photon fluxes.

An electron with energy $mc^2(1-\beta^2)^{-\frac{1}{2}}$ in the observer's system sees a photon of frequency ν in the observer's system Doppler shifted to ν', where

$$\nu\left(\frac{1-\beta}{1+\beta}\right)^{\frac{1}{2}} < \nu' < \nu\left(\frac{1+\beta}{1-\beta}\right)^{\frac{1}{2}},$$

depending upon the relative direction of motion. If $\nu' < mc^2$, we have classical Compton scattering and the scattered photons are nearly isotropic in the electron rest system. Transforming back to the observer's system the energy range of the scattered photons is

$$\nu\left(\frac{1-\beta}{1+\beta}\right) < \nu'' < \nu\left(\frac{1+\beta}{1-\beta}\right) = \nu_m\,.$$

The maximum energy amplification by electrons of energy $3 \cdot 10^{10}$ eV is $1.5 \cdot 10^{10}$. Since the electron velocity distribution is isotropic in the observers system the radiation is again nearly isotropic. The intensity distribution in each transformation is

$$I_{\nu'} = I_\nu(1-\beta^2)^{\frac{1}{2}}/2\beta\nu\,.$$

The convolution of the two transformations yields the approximate distribution in the observer's system. Computation of the predicted γ-ray flux requires integration over the photon frequency distribution. We introduce a relation between the electron energy and the maximum amplification factor valid for relativistic particles $(1+\beta=2)$ and since the distributions described above are very flat (logarithmic) we assume that a fraction $(1-\nu/\nu_m)$ of the scattered photons are scattered to frequencies above ν where ν_m is the maximum frequency attainable in the collision. We further assume that the number

of electrons per energy interval is proportional to E^{-2} (which corresponds to the decay spectrum by synchrotron radiation for injection at a definite large E), and that the photon energy density is proportional to the inverse half power of the frequency up to a cut-off frequency of 10^{15} Hz. The minimum frequency amplified to the MeV range is taken as $1.4\cdot10^{8}$ Hz. The flux appears to be $2\cdot10^{-12}$ photons cm^{-2} s^{-1} above 10^{6} eV and proportional to $\nu^{-\frac{1}{2}}$.

8. – Cygnus A.

It has been suggested by HOYLE and BURBIDGE that the energy radiated by the colliding galaxies may result from the annihilation of matter. It is apparent that the average of 5 mesons produced by $\mathrm{p}+\tilde{\mathrm{p}}$ annihilation satisfy the relation $n_{\pi^+}=n_{\pi^0}=n_{\pi^-}$. The average energy per meson is thus about 400 MeV or about $2.7\,m_\pi c^2$. In the decay $\pi\to\mu+\nu$, the average total energy of the muon is then nearly $\sim 2.7\,m_\mu c^2$. The neutrino carries off the remainder of the energy. In the further decay $\mu\to\beta+2\nu$, the rest mass of the electron is negligible compared to the available energy. On the average therefore the electron energy is $\sim 0.9\,m_\pi c^2$ or ~ 100 MeV. This argument was suggested by C. GOEBEL. It should be noted that at 100 MeV the parameter $\nu_c=1.6\cdot10^{11}$ Hz^{-1} hence radio radiation at $(10\div10^3)$ MHz implies magnetic fields from 10^{-4} to 10^{-2} gauss unless Fermi amplification occurs. Since the π^0 decays into two γ, we may estimate the γ-ray production as one per each 100 MeV input into the charged particle component. Since the radio radiation of Cygnus A is measurable and leads to a flux of $1.18\cdot10^{-22}$ W m^{-2} Hz^{-1} s^{-1} at 10^{8} Hz with a power law dependence $\nu^{-\gamma}$ where $\gamma=-.66$ for $\nu<3.5\cdot10^{8}$ Hz and $\gamma=-1.02$ for $\nu>3.5\cdot10^{8}$ Hz (WHITFIELD [7]), the total flux integrated over frequency at the earth between 10^{7} Hz and 10^{11} Hz is $7\cdot10^{-11}$ erg cm^{-2} s^{-1}. Expressing this in units of 100 MeV/cm^{-2} s^{-1} we obtain a γ-ray flux estimate of $4\cdot10^{-7}$ cm^{-2} s^{-1}. Higher fluxes would be expected if an appreciable fraction of the available energy went into other than the radio emission while lower fluxes would result if an appreciable part of the electron energy arose from interaction with the colliding magnetic field systems of the two galaxies. If the energy source is not annihilation, pions will still be produced by proton interactions in flight as considered earlier in the Crab. The flux would be much lower than predicted above in this case as the pions produced in this case would be highly relativistic and the energy per charged particle higher.

A higher estimate has been given by MORRISON. Apparently this is based upon the flat-on collision of two galaxies at a velocity of 1000 km s^{-1}. For

(7) G. R. WHITFIELD: *Month. Not. Roy. Astron. Soc.*, **117**, 680 (1957).

an effective radius of 10^4 ps ($3\cdot10^{22}$ cm) for each galaxy and a hydrogen density comparable to that in our galaxy, 1 cm^{-3}, and finally a distance of 10^8 ps ($3\cdot10^{26}$ cm) we expect about 0.3 γ $cm^{-2}\,s^{-1}$. This is probably an overestimate since inhomogeneities, tilt, and hydromagnetic interactions and diffusion would lower the annihilation rate calculated above.

At present, some of the fluxes calculated above seem to be within the range of nuclear emulsion technology. M. F. KAPLON has estimated an oriented emulsion stack flown for eight hours could safely detect any flux of γ-rays with $E > 10$ MeV which exceeds $5\cdot10^{-5}\,\gamma\,cm^{-2}\,s^{-1}$. It is assumed that the directional properties of pair production can be used to reduce background difficulties.

RIASSUNTO

La nebulosa del Granchio (?) probabilmente emette un flusso massimo di radiazione γ di $10^{-2}\,cm^{-2}\,s^{-1}$ dovuto al decadimento del ^{251}Cf chè si formò col ^{253}Cf nella esplosione della supernova. Sebbene una estrapolazione dei flussi nel campo delle radiazioni visibili e delle radioonde suggerisca la possibilità di flussi dell'ordine fino a $7\cdot10^{-5}\,cm^{-2}\,s^{-1}$, i calcoli basati su un modello determinato mostrano che è più probabile un flusso maggiore di 10 MeV. Si ha un effetto assai minore per bremsstrahlung e scattering Compton. Il Cigno A, considerato come prodotto da un urto fra materia e antimateria, dovrebbe dare un flusso di γ al disotto 1 $cm^{-2}\,s^{-1}$, secondo le valutazioni di Morrison. Si mostra che il flusso di radioonde suggerisce un flusso di γ di $4\cdot10^{-5}\,cm^{-2}\,s^{-1}$ corrispondente al decadimento di π^0. Per $E > 10$ MeV, ogni flusso di raggi γ superiore a $5\cdot10^{-5}\,\gamma\,cm^{-2}\,s^{-1}$ dovrebbe essere osservabile sperimentalmente in emulsioni nucleari esposte nella stratosfera.

IL NUOVO CIMENTO Vol. XIII, N. 1 1° Luglio 1959

Investigation on Quantum Electrodynamics at Short Distances by Means of Bremsstrahlung and Pair Production.

G. Poiani and I. Reina

Istituto di Fisica dell'Università - Trieste
Istituto Nazionale di Fisica Nucleare - Sottosezione di Trieste

(ricevuto il 6 Febbraio 1959)

Summary. — By means of a study of bremsstrahlung and pair production the possibility is examined of extending the limits of the validity of electrodynamics to values beyond those at present known. For this purpose the cross-sections for these two processes are calculated by introducing a covariant function which takes account of the form factors relative to the electrodynamic vertices. These calculations are then applied to some cases of experimental tests which would be more sensitive to the limits of electrodynamics.

1. – Introduction.

The important problem on the limits of validity of quantum electrodynamics (ED) at short distances has grown new interest in recent times. Experiments on the elastic diffusion of electrons by protons with the scope of determining the charge distribution for nuclei and nucleons have in fact left a certain indetermination in the results since the influence of eventual modifications of the laws of ED at short distances is unknown.

It is clear that the straightforward way of determining these limits should be the experimental study of electron-electron (or photon-electron) scattering. In view of the small electron mass and of the fact that the critical element in these phenomena is the momentum transfer in the center-of-mass system, it can easily be seen that in order to improve present knowledge of the validity of ED at short distances it would be necessary either to use energies much greater than those at present available (in the laboratory system) or carry out the experiments with a precision which is difficult to realize in practice.

To get round this difficulty one can think that use be made of the atomic nucleus or of proton to « anchor » the center of mass and so allow large momentum transfers even with relatively modest laboratory energies: this may be realized with large angle experiments involving the production of bremsstrahlung or electron pairs (1).

Recently this possibility has been taken into consideration also by DRELL (2) who carried out a critical study of the limits of validity of ED considering the experimental data available and assuming that eventual deviations from the local theory can be described by modifying only the virtual electron and photon propagators: he then examined the possibility of lowering these limits with experiments on pair production at large angles in hydrogen

In the present paper, general expressions for the bremsstrahlung cross-section are given which are obtained from a lagrangian with non-local covariant form factors; it is shown that the case considered by DRELL is a special case; some numerical values are given which illustrate the experimental possibilities when form factors of the type considered by DRELL are used.

2. – Calculation of the bremsstrahlung cross-section.

A simple method for introducing covariant form-factors is to start from the lagrangian interaction density:

$$\mathcal{L}_{\text{int}}(x) = e\int \overline{\psi}(x)\gamma_\mu\psi(x_2)A_\mu(x_1)f(x, x_1, x_2)\,\mathrm{d}^4x_1\,\mathrm{d}^4x_2\,, \tag{1}$$

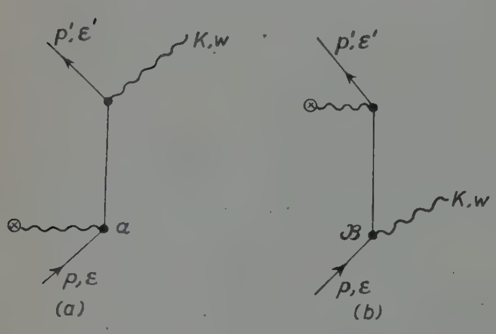

Fig. 1.

where $f(x, x_1, x_2)$ is a scalar function, normalized to unity. In the following the lagrangian will have a purely phenomenological meaning, leaving out questions of causality, of convergence and of the unitarity of the S-matrix. Further, one may state that the results obtained are identical to those which can be obtained starting from a lagrangian which is different from (1) and which sacrifices only the unitarity of the purely electrodynamic S matrix, respecting however the principle of causality (3).

---

(1) P. BUDINI, G. POIANI and I. REINA: *International Conference on Mesons* (Padua-Venice, 1957), pp. IX-17.

(2) S. D. DRELL: *Ann. of Phys.*, **4**, 75 (1958).

(3) These ideas will be fully developed in a subsequent paper.

The matrix element for the bremsstrahlung process, represented by the diagrams given in Fig. 1 can be easily calculated using for example the method of YANG and FELDMANN ([4]), and becomes:

$$\text{(2)}\qquad \mathcal{M}^{\text{Br.}} = \frac{\alpha^{\frac{3}{2}} Z m}{2\pi^2\sqrt{\varepsilon'\varepsilon\omega}} \frac{|F(q)|}{|\boldsymbol{q}|^2}\, \bar{u}(\boldsymbol{p}')\left\{A(p'+k,\,p)A'(p',\,p'+k)\boldsymbol{e}\,\frac{i\boldsymbol{p}'+i\boldsymbol{k}-m}{(p'+k)^2+m^2}+\right.$$

$$\left. +B(p-k,\,p)B'(p',\,p-k)\boldsymbol{n}\,\frac{i\boldsymbol{p}-i\boldsymbol{k}-m}{(p-k)^2+m^2}\boldsymbol{e}\right\}u(\boldsymbol{p})\,,$$

where $F(q)$ is the Fourier transform of the nuclear form factor; A, A', B, B', are the Fourier transforms of the form factors relative to the vertices indicated in the figure, and the other symbols follow the usual conventions ([5]).

If one admits that deviations of ED from local theory can be represented by a modification of the virtual electron and photons propagators then A, A', B, B' reduce to only three functions of the intermediate momenta, as done by DRELL: $\varphi(q)\,\mathcal{G}_1(p'+k)$ and $\varphi(q)\,\mathcal{G}_2(p-k)$.

The matrix element then becomes:

$$\text{(3)}\qquad \mathcal{M}^{\text{Br.}} = \frac{\alpha^{\frac{3}{2}} Z m}{2\pi^2\sqrt{\varepsilon'\varepsilon\omega}} \frac{|\varphi(q)|\,|F(q)|}{|\boldsymbol{q}|^2}\, \bar{u}(\boldsymbol{p}')\left\{G_1(p'+k)\boldsymbol{e}\,\frac{i\boldsymbol{p}'+i\boldsymbol{k}-m}{(p'+k)^2+m^2}\boldsymbol{n}+\right.$$

$$\left. +\,G_2(p-k)\boldsymbol{n}\,\frac{i\boldsymbol{p}-i\boldsymbol{k}-m}{(p-k)^2+m^2}\,\boldsymbol{e}\right\}u(\boldsymbol{p})\,,$$

where $\varphi(q)$ represents the modification of the virtual photon propagator.

At this point it should be noted that an exact calculation of the cross-section should take into account certain corrective effects amongst which that due to the recoil of the nucleus and that due to the radiative processes. The calculation of these latter effects, carried out by BJORKEN *et al.* ([6]), has shown that their contribution to the cross-section is relatively small. Similar calculations have been performed also by ISAYEW and ZLATEV ([7]).

The introduction into the calculation of the effect of the recoil of the nucleus leads to a factor which cannot be factorized. In any case, since the corrections due to these effects are relatively small it can be maintained that the substance of the final result is not modified, especially in view of the fact that these results concern the ratios between cross-sections.

([4]) C. N. YANG and D. FELDMANN: *Phys. Rev.*, **79**, 972 (1950).

([5]) See J. M. JAUCH and F. ROHRLICH: *The Theory of Photons and Electrons* (Cambridge, 1955).

([6]) J. D. BJORKEN, S. D. DRELL and S. C. FRAUTSCHI: *Phys. Rev.*, to be published.

([7]) I. ISAYEW and S. ZLATEV: *Nuovo Cimento*, to be published.

By means of the usual procedures one can calculate, starting from (2) or (3), the bremsstrahlung cross-section

$$(4)\quad \mathrm{d}\sigma^{\mathrm{Br.}}=\frac{\alpha Z^2 r_0^2}{(2\pi)^2}\frac{m^2}{|\boldsymbol{q}|^4}\frac{|\boldsymbol{p}'|}{|\boldsymbol{p}|}\frac{\mathrm{d}\omega}{\omega}\,\mathrm{d}\Omega'\,\mathrm{d}\Omega_k|F(q)|^2\left\{A^2A'^2\frac{\beta'^2\sin^2\theta'}{(1-\beta'\cos\theta')^2}(4\varepsilon^2-q^2)+\right.$$

$$+B^2B'^2\frac{\beta^2\sin^2\theta}{(1-\beta\cos\theta)^2}(4\varepsilon'^2-q^2)-2AA'BB'\frac{\beta\beta'\sin\theta\sin\theta'\cos\varphi}{(1-\beta\cos\theta)(1-\beta'\cos\theta')}(4\varepsilon\varepsilon'-q^2)-$$

$$-\frac{2\omega^2}{\varepsilon\varepsilon'(1-\beta\cos\theta)(1-\beta'\cos\theta')}[[AA'\varepsilon(1-\beta\cos\theta)-BB'\varepsilon'(1-\beta'\cos\theta')]^2-$$

$$-q^2AA'BB']+2\omega\left[\frac{1}{\varepsilon(1-\beta\cos\theta)}(\beta\beta'\varepsilon\varepsilon'\sin\theta\sin\theta'\cos\varphi-\beta^2\varepsilon^2\sin^2\theta-2\varepsilon'\omega)BB'+\right.$$

$$\left.\left.+\frac{1}{\varepsilon'(1-\beta'\cos\theta')}(\beta\beta'\varepsilon\varepsilon'\sin\theta\sin\theta'\cos\varphi-\beta'^2\varepsilon'^2\sin^2\theta'+2\varepsilon\omega)AA'\right](AA'-BB')\right\}.$$

From expressions (4), with the usual conversion, one may obtain the cross-section for pair production

$$(5)\quad \mathrm{d}\sigma^{\mathrm{P.P.}}=-\frac{\alpha Z^2 r_2}{(2\pi)^2}\frac{m^2}{|\boldsymbol{q}|^4}|\boldsymbol{p}_-||\boldsymbol{p}_+|\frac{\mathrm{d}\varepsilon_+}{\omega^3}\mathrm{d}\Omega_+\mathrm{d}\Omega_-|F(q)|^2\cdot$$

$$\cdot\left\{A^2A'^2\frac{\beta_-^2\sin^2\theta_-}{(1-\beta_-\cos\theta_-)^2}(4\varepsilon_+^2-q^2)+B^2B'^2\frac{\beta_+^2\sin^2\theta_+}{(1-\beta_+\cos\theta_+)^2}(4\varepsilon_-^2-q^2)+\right.$$

$$+2AA'BB'\frac{\beta_+\beta_-\sin\theta_+\sin\theta_-\cos\varphi_+}{(1-\beta_-\cos\theta_-)(1-\beta_+\cos\theta_+)}(4\varepsilon_+\varepsilon_-+q^2)+$$

$$+\frac{2\omega^2}{\varepsilon_+\varepsilon_-(1-\beta_-\cos\theta_-)(1-\beta_+\cos\theta_+)}[[AA'\varepsilon_+(1-\beta_+\cos\theta_+)+BB'\varepsilon_-(1-\beta_-\cos\theta_-)]^2-$$

$$-q^2AA'BB']+2\omega\left[\frac{1}{\varepsilon_+(1-\beta_+\cos\theta_+)}(-\beta_+\beta_-\varepsilon_+\varepsilon_-\sin\theta_+\sin\theta_-\cos\varphi_+-\right.$$

$$-\beta_+^2\varepsilon_+^2\sin^2\theta_++2\varepsilon_-\omega)BB'-\frac{1}{\varepsilon_-(1-\beta_-\cos\theta_-)}(-\beta_+\beta_-\varepsilon_+\varepsilon_-\sin\theta_+\sin\theta_-\cos\varphi_+-$$

$$\left.\left.-\beta_-^2\varepsilon_-^2\sin^2\theta_-+2\varepsilon_-\omega)AA'\right](AA'-BB')\right\}.$$

In the hypothesis that only propagators are modified, one has to substitute the form factors given by (3).

Substituting $F=1$, $A=A'=B=B'=1$ into expressions (4) and (5), one obtains the cross-sections of Bethe and Heitler.

3. – Evaluation of the electrodynamical effects.

It is now necessary, in order to discuss the effects of the modifications of ED at small distances, to give a form to the functions $\mathcal{G}_1$ and $\mathcal{G}_2$, which appear in (3), The choice of these is very arbitrary, provided that they are both relativistically invariant, and consequently there is considerable freedom in the interpretation of the results. We will therefore follow the example of other authors [2,8], and choose for the form factors expressions of the type:

$$\frac{\Lambda^2}{|q^2|+\Lambda^2}, \tag{6}$$

where q is the intermediate momentum and Λ acquires the significance of a cut-off parameter for the electron propagator. This cut-off introduces a limitation for the 4-momentum, and its reciprocal gives an indication of the minimum distance of action. It is necessary in (6) to take the modulus of q^2 (which is equivalent to taking an expression of the form $\Lambda^4/(q^4+\Lambda^4)$) since otherwise the form factor for process ($1a$) results greater than unity.

One is now in a position to calculate the ratio:

$$R=\frac{(\mathrm{d}\sigma)^{\mathrm{E.D.}}_{\mathrm{N.L.}}}{(\mathrm{d}\sigma)_{\mathrm{N.L.}}}, \tag{7}$$

between on the one hand the cross-section containing the electrodynamic modifications and the nuclear form factor, and on the other that containing only the nuclear form factor. R then depends only on the electrodynamic form factors and equals one in the local theory; in the following sections certain specific coplanar cases will be considered and values of R will be derived.

The first case considered is that of the production of pairs of electrons in which both particles are produced with the same energy and are symmetrically emitted with respect to the incident photon. This case leads to the equality of the two functions $\mathcal{G}_1$ and $\mathcal{G}_2$ and the ratio R is then simply $\mathcal{G}^2$. In Fig. 2 the value of R is given for incident photon energies of 700 MeV and 1000 MeV and for various values of the parameter Λ^{-1}. These values of Λ^{-1} have been chosen so as to examine the effect for distances less than the present limits for the validity of ED. The figure indicates a situation which is very favourable for an experimental investigation, especially at higher energies and at large angles; however the corresponding cross-sections precipitate rapidly.

---

(8) W. K. H. Panofsky: *Ann. Int. Conf. CERN* (1958).

An analogous situation is encountered in the bremsstrahlung process when, for equal energies of the diffused electron and photon, the choice of the angles which these two particles make with the incident electron (χ, θ) is such that

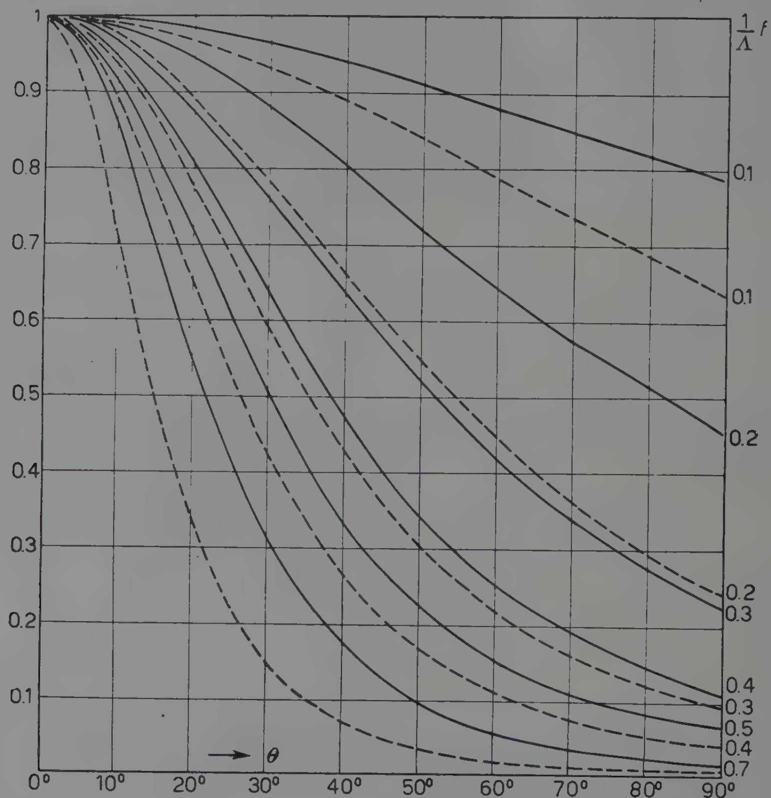

Fig. 2.

the form factors $\mathcal{G}_1$ and $\mathcal{G}_2$ are equal. This happens when the following relation holds between the angles:

$$\cos(\theta + \chi) = 2\cos\theta - 1\,. \tag{8}$$

Another particularly interesting case for bremsstrahlung is when the two diffused particles both lie on the same side of the incident particle (see Fig. 3*a*).

Fixing the value of the angle χ for the diffused electron and varying the angle θ for the photon up to a maximum value $\theta = \chi$ the Bethe-Heitler cross-section shows two unequal maxima, one for $\theta \approx 0$ (*i.e.* $\theta = m/\varepsilon$) and the other for $\theta \approx \chi$.

In Fig. 4 the ratio R is given as a function of θ for two values of the parameter Λ^{-1}. Each curve is roughly symmetrical about the value of θ equal

to $\chi/2$, which also corresponds to the minimum value of R for a given χ and therefore particularly suitable for obtaining interesting information were it not for the fact that as in the case previously considered, this also corresponds to a trough in the cross-section.

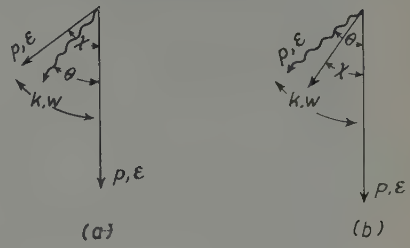

Fig. 3.

The complementary case is indicated in Fig. 3*b* in which this time the angle θ is fixed and it is the angle χ which is varied up to a maximum θ. If now the two new angles Δ and δ are introduced so that $\Delta=(\chi+\theta)/2$, $\delta=(\theta-\chi)/2$, it may be shown that for equal energies of the diffused particles the modulus of the momentum transferred to the nucleus can be held constant for large variations of δ, to which correspond only small

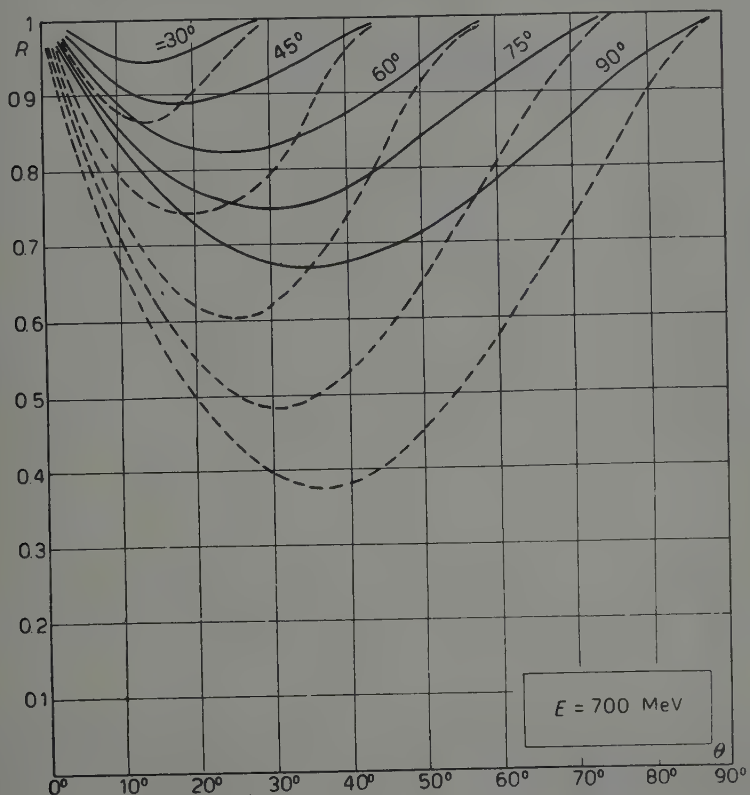

Fig. 4.

variations in Δ. By keeping the momentum transfer constant in this way, the effect of the poorly known nuclear form factor (on which R might de-

pend, even if only weakly, in a theory which takes into account the recoil of the nucleus) can be notably attenuated.

The behaviour of the phenomenon in the vicinity of $\theta = \chi$ both for case 3*a* and case 3*b*, presents another aspect which could be interesting from the experimental point of view. In fact the relative maximum which one has for $\theta = \chi$ is much less in absolute value than the maximum for $\theta \simeq 0$ (one has $d\sigma^{Br.}(\theta = \chi) \simeq \frac{1}{16} d\sigma^{Br.}(\theta \simeq 0)$ for equal χ and for $\varepsilon' = \omega = \varepsilon/2$). This signifies that a fairly precise measurement could be carried out near this maximum since, owing to the large angle between the line of observation and the machine beam, the background should be low while the number of interesting events remains high. For this point R is equal to unity (see Fig. 4). If now the angle between the two diffused particles is increased (keeping the momentum transfer constant) a study can be made of the behaviour of the ratio R, normalizing the experimental cross-section to the value obtained for $\theta \approx \chi$, for which $R = 1$. Thus one can proceed by relative measurements, compensating in this way for the eventual errors committed in the theoretical evaluation of the cross-section. As can be seen from Fig. 4 the expected effects with form factors other than those which represent the present limits of validity of ED ($\Lambda^{-1} \simeq 0.7$ fermi) are notable and consequently it can be maintained that the introduction of further approximation into the calculations will not change the order of magnitude of these effects. This leads to the hope that experiments using present techniques might permit a revision of the limits of validity of ED at small distances.

* * *

In conclusion the authors wish to express their appreciation to Prof. P. Budini for many helpful discussions and criticism throughout this work.

RIASSUNTO

Viene esaminata la possibilità di portare la conoscenza dei limiti di validità dell'elettrodinamica al di sotto dei valori attualmente noti mediante lo studio della bremsstrahlung e della creazione di coppie. Allo scopo si calcolano le sezioni d'urto per questi due processi facendo intervenire una funzione covariante che tenga conto dei fattori di forma relativi ai vertici elettrodinamici. Come applicazione si studiano diversi casi di possibili disposizioni sperimentali che consentirebbero di mettere in evidenza la validità dell'elettrodinamica a livelli più bassi di quelli attualmente noti.

IL NUOVO CIMENTO Vol. XIII, N. 1 1° Luglio 1959

Antiproton Interaction Cross Sections.

A. G. Ekspong and B. E. Ronne
Institute of Physics - Uppsala

(ricevuto il 9 Febbraio 1959)

Summary. — A study has been made of 374 antiproton tracks in nuclear emulsions in the energy region $(0 \div 250)$ MeV. A path length of 37.3 m has been followed. Ten new elastic $\overline{\text{p}}$-p scattering events together with eleven events published earlier yield an elastic scattering cross section of (77 ± 17) mb. The total and the differential elastic cross sections are consistent with the theory by Chew and Ball. The mean free path for annihilation in the energy region 30 to 250 MeV is (26.8 ± 1.6) cm, and the interaction mean free path is (18.3 ± 1.3) cm. An effective antiproton-nucleon cross section of (150^{+27}_{-22}) mb has been deduced from an optical model calculation. Six new inelastic scattering events are reported. Putting these together with the 8 or 9 events published by Goldhaber *et al.* one gets an inelastic scattering cross section of (42 ± 11) mb per emulsion nucleus (hydrogen excluded). The low value of the cross section is discussed in the light of the optical model. The elastic scattering on complex nuclei seems to agree with a combination of Rutherford and diffraction scattering from a completely absorbing nucleus.

1. – Introduction.

In continuing the study of antiproton interactions in nuclear emulsions [1-3], we had one stack exposed at the Bevatron at Berkeley in January 1958 to

(1) O. Chamberlain, W. W. Chupp, A. G. Ekspong, G. Goldhaber, S. Goldhaber, E. J. Lofgren, E. Segrè, C. Wiegand, E. Amaldi, G. Baroni, C. Castagnoli, C. Franzinetti and A. Manfredini: *Phys. Rev.*, **102**, 921 (1956).

(2) W. H. Barkas, R. W. Birge, W. W. Chupp, A. G. Ekspong, G. Goldhaber, S. Goldhaber, H. H. Heckman, D. H. Perkins, J. Sandweiss, E. Segrè, F. M. Smith, D. H. Stork, L. Van Rossum, E. Amaldi, G. Baroni, C. Castagnoli, C. Franzinetti and A. Manfredini: *Phys. Rev.*, **105**, 1037 (1957).

(3) A. G. Ekspong, S. Johansson and B. E. Ronne: *Nuovo Cimento*, **8**, 84 (1958).

the separated antiproton beam [4,5]. The stack consisted of 175 pellicles of Ilford G-5 emulsions, each $5\frac{3}{4}$ in. $\times$ 9 in. $\times$ 600 μm. The beam momentum was 740 MeV/c, and the stack was exposed for $2\cdot 10^{14}$ protons on the target. This should give an antiproton flux of about 10 per cm² in the central part of the beam together with a flux of background particles of minimum ionization of $1\cdot 10^{5}$ particles per cm².

This paper is concerned with measurements of cross-sections in the energy interval $(30\div 250)$ MeV for various types of antiproton events, namely annihilation in flight, elastic antiproton-proton scattering, and inelastic scattering on complex nuclei. In dealing with the interactions in flight, we give the experimental result also in the form of an interaction radius. For an understanding of the reactions on complex nuclei, an optical model calculation has been carried out. Small angle scattering on complex nuclei is reported. The experimental results are compared with other published data and with theoretical predictions.

2. – Scanning and identification of antiprotons.

The antiproton tracks were selected on the basis of grain density and angle of entrance relative to minimum ionizing tracks. The scanning started about 3 mm from the side of the stack in which the beam entered. All tracks with a grain density relative to minimum grain density of 2.0 ± 0.4 and with entrance angles within $\pm 10°$ of the beam direction were followed. We have scanned an area of 110 cm² perpendicular to the beam.

The tracks followed consisted mainly of antiprotons. However, there was also a small background of protons mostly. Other particles in the background, for instance π- and K-mesons, could easily be ruled out through mass determinations by a combination of range and ionization measurements.

Thus the problem is to determine the possible admixture of protons. In Table I we have grouped all tracks picked up by the scanners where the particle has protonic mass. They are arranged into five phenomenological groups according to the appearance at the end of the track. The first group consists of 167 particles which come to rest and give rise to stars. These particles of protonic mass can be antiprotons only. Their mean range and range straggling is (14.4 ± 0.7) cm. The second group contains 15 particles which come to rest without giving rise to a visible interaction at the end. These particles

(4) L. Agnew, T. Elioff, W. B. Fowler, L. Gilly, R. Lander, L. Oswald, W. Powell, E. Segrè, H. Steiner, H. White, C. Wiegand and T. Ypsilantis: *Phys. Rev.*, **110**, 994 (1958).

(5) O. Chamberlain, G. Goldhaber, L. Jauneau, T. Kalogeropoulos, E. Segrè and R. Silberberg: UCRL-8424.

TABLE I. – *Number of tracks with proton mass followed and their identification.*

Phenomenological groups	Possible interpretations of particle nature and physical process	Total number of tracks	Number of tracks interpreted as		Path length of $\overline{\text{p}}$ (m)
			$\overline{\text{p}}$	p	
I. - Particles which come to rest and give a star.	Antiproton annihilations at rest.	167	167	0	23.15
II. - Particles which come to rest without giving a star.	1) Antiproton annihilations into 0-prong stars. 2) Protons.	15	8	7	1.16
III. - Particles giving a star in flight with $\geqslant 1$ prong.	1) Antiproton annihilations in flight. 2) Antiproton charge exchange scatterings. 3) Proton inelastic scatterings or charge exchange scatterings.	179	176	3	11.00
IV. - Particles disappearing in flight.	1) Antiproton annihilations in flight into 0-prong stars. 2) Antiproton charge exchange scatterings. 3) Proton charge exchange scatterings.	7	7	0	0.33
V. - Particles which leave the stack.	1) Antiprotons. 2) Protons.	16	16	0	1.63
Number of antiprotons and path length			374 ± 3		37.27

may be either antiprotons or protons. If antiprotons they would represent annihilation into only neutral particles ($\overline{\text{p}}_\rho$-events). In order to determine the proton admixture, we have plotted in Fig. 1 the number of tracks versus range between the limits 8 and 28 cm. The connection between range and relative ionization (g/g_0) of a particle of protonic mass is shown in the second abscissa scale in Fig. 1. There is a pronounced peak right at the position where established antiprotons stop. If we assume that the scanning efficiency is a smooth function of relative ionization between the limits used, *i.e.* 1.6 to 2.4 times minimum ionization, and further assume that positive protons have no preferred energy in the interval considered, we must conclude

1601

that most of the particles in the pronounced peak in Fig. 1 are antiprotons. From the background outside the peak, we have estimated the number of protons to about 7, leaving about 8 antiprotons to be described as $\bar{p}_\rho$-events. Our proportion of $\bar{p}_\rho$ is about 5% of all antiprotons coming to rest. The possible existence of $\bar{p}_\rho$ events can be inferred from the observation by FRYE (6) of an antiproton which annihilated at rest into only neutral particles. The electron pair emitted was interpreted as a Dalitz pair from a decaying neutral pion. If the annihilation leads to five neutral pions, each event of the Frye type corresponds to 16 $\bar{p}_\rho$ events.

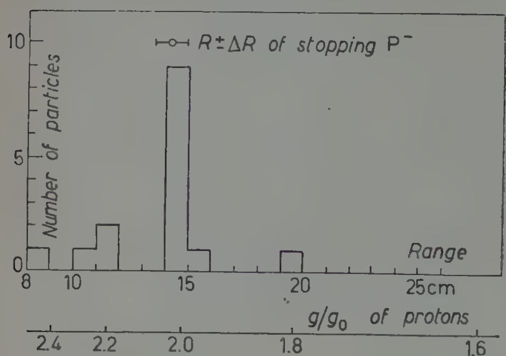

Fig. 1. – Range distribution of particles coming to rest without giving rise to secondary prongs. The lower scale shows the relative ionization of protons corresponding to the range on the upper scale.

In the third group all particles are collected which give rise to a star in flight. The number of such particles is 179. When the visible energy in the star is above the kinetic energy of the incoming particle, the event is certainly due to an antiproton. As this is not always the case, we might expect some small admixture of protons. From our result above that 7 protons come to rest, we conclude that we should expect about 3 stars in flight to be proton events. This is based on the observed range of the protons and the assumption of a geometric cross-section for inelastic interactions with emulsion nuclei. This leaves 176 antiprotons in this group. In the last two groups in Table I there could in principle be proton admixtures. However, we estimate that the groups contain antiprotons only, because the proton contamination is small and the number of events in the groups is low.

In conclusion, we estimate the proton background to be about 3% in the sample picked up during scanning. We have finally a total of (374 ± 3) antiprotons, of which about 90% are unambiguously identified. Included in this sample are ten antiprotons published earlier (3).

3. – Antiproton-proton elastic scattering.

Experimental results on elastic antiproton-proton scattering are of great interest as recently some models have been proposed from which the cross-

(6) G. M. FRYE jr.: *Phys. Rev. Lett.*, 1, 14 (1958).

sections may be derived. BALL and CHEW (7) have given a model for the antinucleon-nucleon interaction where they use a modification of the Signell-Marshak-Gartenhaus nucleon-nucleon potential, which describes the nucleon-nucleon interaction correctly up to 150 MeV. FULCO (8) has calculated from the theory of Ball and Chew the differential cross-section for $\bar{p}$-p elastic scattering at an energy of 140 MeV. This curve is plotted in Fig. 2. By integrating the theoretical cross-section over the forward and backward hemispheres separately, he finds that the ratio is 14 to 1.

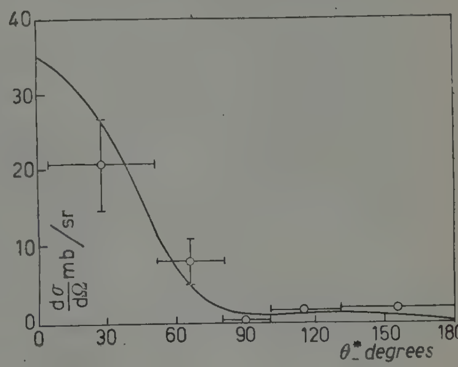

Fig. 2. – Differential cross sections for elastic $\bar{p}$-p scattering. The solid curve is calculated by FULCO (8) on the basis of the theory of Ball and Chew (7).

COOMBES *et al.* (9) have measured the differential cross-section for $\bar{p}$-p scattering in a scintillation counter experiment. They get good agreement with Fulco's curve for the forward scattering. However, backward scattered antiprotons have a short range and annihilate inside the target. Such events are therefore indistinguishable from normal annihilations. To observe large angle scatterings, one has to make observations inside the target. This is for instance possible in emulsion and bubble chamber experiments (4). The determination of the large angle scattering gives information on the details of the antiproton-nucleon interaction. The forward scattering is mainly due to diffraction.

The elastic scattering of antiprotons from free protons can in general be easily identified in nuclear emulsions. In severely distorted regions of the emulsions, there may be difficulties in the analysis, but these may be overcome. One can recognize scattering events in the angular region of about $5^\circ \div 175^\circ$ in the center of mass system at an energy of about 150 MeV. In the remaining cases the recognition is rendered difficult or impossible by the fact that one of the scattered particles is emitted with a very short range, $< 3\ \mu\text{m}$. As the unobservable solid angle is only 0.4%, this limitation is of minor importance.

In our analysis of the antiproton-proton events, we use the following notations:

---

(7) J. S. BALL and G. F. CHEW: *Phys. Rev.*, **109**, 1385 (1958).

(8) J. R. FULCO: *Phys. Rev.*, **110**, 784 (1958).

(9) C. A. COOMBES, B. CORK, W. GALBRAITH, G. R. LAMBERTSON and W. A. WENZEL: UCRL-8279.

T, p = energy and momentum of incoming antiproton,
T_-, p_- = energy and momentum of outgoing antiproton,
T_+, p_+ = energy and momentum of positive proton,
θ_- = space angle between outgoing and incoming directions of antiproton (θ_-^* in center of mass system),
θ_+ = corresponding space angle for outgoing positive proton,
$\theta_\pm$ = space angle between the two outgoing tracks (opening angle).

For an event to be classified as an elastic $\bar{p}$-p scattering, we require energy and momentum to be conserved according to the following analysis:

a) The three tracks must be coplanar. The deviation from coplanarity is here measured as the angle between the normals to the planes ($\bar{p}_{in}$, $\bar{p}_{out}$) and ($\bar{p}_{in}$, p^+).

b) The opening angle $\theta_\pm$ must not differ significantly from $90° - \delta$, where δ is the relativistic correction to the opening angle.

c) Agreement is required between the values of the incoming antiproton energy computed or measured in two or more ways, according to the relations:

(1) $$T = T_+ + T_-\,,$$

(2) $$\frac{T}{p} = \frac{T_+}{p_+ \cos\theta_+}\,,$$

(3) $$\frac{T}{p} = \frac{T_-}{p_- \cos\theta_-}\,,$$

(4) T measured from observed range or ionization on incoming track.

Relation (1) is used when both p^+ and $\bar{p}$ come to rest, relation (2) when p^+ comes to rest, and (3) when $\bar{p}$ comes to rest.

Results on our eleven $\bar{p}$-p scattering events are collected in Table II.

One of the events, 6-83, fulfilled at first all criteria with the exception of conditions *b*) and *c*-3). The event occurs at high energy and is thus situated rather close to the leading edge of the plate in a region where distortion is severe. The distortion influenced most strongly the outgoing antiproton track which had the large dip angle of 63°. The first order distortion correction changed the projection of θ_- on the plane of emulsion by as much as 20°. After application of distortion corrections, we found that the event 6-83 fulfilled all the criteria. This $\bar{p}$-p scattering event is important because it is one of the rare backward scatterings in the center of mass system with a scattering angle of 139.5°.

TABLE II. – *Elastic antiproton-proton scattering events.*

Anti-proton number	Deviation from coplanarity (°)	Opening angle (°) $\theta_\pm$	Opening angle (°) $90-\delta$	Antiproton kinetic energy T MeV from $T_+ + T_-$	T_+, θ_+	T_-, θ_-	g^* or $R_{obs.}$	Average energy T MeV (lab. syst.)	Scatt. angle c. m. system θ^*_-
6 - 156	—	87 ±3	89.2	200 ±2	—	200 ± 3	206 ± 7	200	11.6°
6 - 14	0.8 ± 0.9	89.3 ± 1.5	88.3	—	215 ± 33	—	223 ± 8	222	31.2°
6 - 95	1.6 ± 1.5	87.0 ± 2.0	87.8	—	162 ± 28	—	223 ± 8	218	41.8°
6 - 6 (*)	0.2 ± 0.4	89.3 ± 0.3	88.2	—	206 ± 9	—	182 ± 6	189	44.4°
6 - 49	4.0 ± 2.8	87.5 ± 1.2	89.1	80.2 ± 0.5	79 ± 6	77 ± 1	80 ± 6	80	44.5°
6 - 322	0.7 ± 1.0	88.9 ± 0.6	88.6	129 ± 1.0	128 ± 6	133 ± 2	118 ± 9	130	47.4°
6 - 144	3 ± 3	89 ± 2	88.6	105 ± 1.0	103 ± 11	113 ± 3	104 ± 12	106	58.3°
6 - 358	0.2 ± 0.8	87.5 ± 0.6	88.0	168 ± 3	159 ± 13	171 ± 5	160 ± 11	168	59.5°
6 - 26	2.2 ± 1.8	88.0 ± 1.5	89.6	32.3 ± 0.5	27 ± 2	33.3 ± 0.6	34 ± 2	32.6	65.1°
6 - 248	1.4 ± 1.0	87.1 ± 0.5	88.0	144 ± 1	138 ± 5	145 ± 4	136 ± 8	144	75.1°
6 - 83	3.5 ± 3.5	88.2 ± 2.5	87.6	250 ± 2	244 ± 6	262 ± 80	242 ± 7	249	139.5°

(*) 6 - 6 has been published earlier, ref. (8).

The proton track in event 6-156 is very short and is emitted near 90° to the incoming track. The coplanarity criterion is insensitive to events where one of the angles θ_+ and θ_- is small and the other almost 90°. Therefore we find it meaningless to give the deviation from coplanarity of this event.

After adding the 9 events reported by G. GOLDHABER *et al.* (10), the number of elastic $\bar{\text{p}}$-p scatterings observed in emulsions is 20 and the path length in hydrogen is 431 g/cm² (of which 199 g/cm² come from our data). Consequently the total cross-section for elastic antiproton-proton scattering is

$$\sigma_{\text{el.}} = (77 \pm 17)\ \text{mb}\,.$$

The angular distribution of the events from Uppsala and Berkeley (10) is shown in Table III and in Fig. 2. The events have been grouped into five

TABLE III. – *Number of elastic* $\bar{\text{p}}$-p *events and differential cross section as a function of c.m. angle* (*Uppsala and Berkeley*).

θ^*_-	5° ÷ 50°	50° ÷ 80°	80° ÷ 100°	100° ÷ 130°	130° ÷ 175°
Number of $\bar{\text{p}}$-p	12	6	0	1	1
$(\text{d}\sigma/\text{d}\Omega)$ mb/sr	20.7	7.9	0	1.3	1.8

(10) G. GOLDHABER, T. KALOGEROPOULOS and R. SILBERBERG: *Phys. Rev.*, **110**, 1474 (1958).

approximately equal solid angles. The agreement with Fulco's theoretical curve is good. The number of scatterings in the forward hemisphere is 18 and in the backward hemisphere 2. This should be compared with the theoretical expectation of 14 : 1. It should be mentioned that the theoretical curve is for 140 MeV, whereas the emulsion data are from an energy interval ranging from about 30 MeV to 250 MeV with a mean energy near 160 MeV. Our results are in agreement with those of COOMBES *et al.* [9], who get $\sigma_{\text{el.}} = (72^{+9}_{-11})$ mb at 133 MeV. The agreement is not so good with the propane bubble chamber result of AGNEW *et al.* [4] who get the rather low value of $\sigma_{\text{el.}} = (41^{+10}_{-7})$ mb at an energy of 120 MeV between 15° and 165° in the center of mass system, (if one adds about 4 mb one would get the total elastic cross section).

4. – Mean free path in G-5 emulsions.

The energy of each antiproton interacting in flight has been determined by ionization measurements or has been calculated from the observed track length and the mean total range of antiprotons coming to rest. The ranges of stopping antiprotons depend only slightly on the position (y) of the entrance point into the stack. The relation is $R = 15.08 - 0.087\,y$ cm with the center of the plates at $y = 7.3$ cm. The range spread was found to be 0.67 cm. Above an energy of about 140 MeV, the method of ranges is superior and has been used here. Below 140 MeV, the energy has been estimated from a measurement of the ionization (gapcoefficient method). The resulting error in the kinetic energy of the interacting antiproton is about 5%. In Table IV

TABLE IV. – *Annihilation mean free path and cross section in* G-5 *emulsions.*

Energy interval (MeV)	Observed track length (cm)	Number of annihilations	λ (cm)	σ_a/σ_0
250 ÷ 225	633.5	30	21 ± 4	1.7 ± 0.3
225 ÷ 200	681.2	39	18 ± 3	2.1 ± 0.3
200 ÷ 165	839.4	34	25 ± 4	1.5 ± 0.3
165 ÷ 115	811.9	38	21 ± 3	1.7 ± 0.3
115 ÷ 30	692.9	35	20 ± 3	1.9 ± 0.3
250 ÷ 30	3658.9	176	20.8 ± 1.6	1.76 ± 0.13

we give results for the mean free path for annihilation in G-5 emulsions. The data have been grouped into five classes with about 35 annihilations in each.

The mean free path for annihilation in the energy region 30 to 250 MeV in G-5 emulsion is

$$\lambda_a = (20.8 \pm 1.6)\ \text{cm}.$$

The results are also shown in terms of the annihilation cross-section as a function of energy in Fig. 3, where the reference cross-section is $\sigma_0 = \pi(1.2\cdot 10^{-13} A^{\frac{1}{3}})^2_{\text{av.}}$ cm². At an average antiproton energy of $T = 170$ MeV, we get:

$$\sigma_a/\sigma_0 = 1.76 \pm 0.13\ .$$

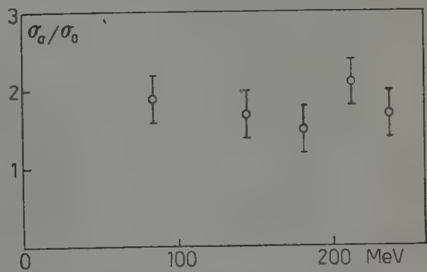

Fig. 3. – The annihilation cross section σ_a relative to $\sigma_0 = \pi(1.2\cdot 10^{-13} A^{\frac{1}{3}})^2_{\text{av}}$ cm² in G-5 emulsions as a function of antiproton energy.

We have determined an interaction mean free path for which also interactions other than annihilation have been included, namely antiproton-proton elastic scattering, charge exchange scattering, and inelastic scattering on complex nuclei. We get a total number of (200 ± 2) interactions in the energy interval 30 to 250 MeV. This gives an interaction mean free path of

$$\lambda_{\text{int}} = (18.3 \pm 1.3)\ \text{cm}.$$

An optical model calculation, to be described below, suggests that the total interaction cross-sections can be written in the form

$$\sigma = \pi(R + C)^2\ ,$$

where $R = 1.25 A^{\frac{1}{3}}$ fermis, A is the mass number, and C is a constant. Using this formula and the result $\lambda_{\text{int}} = (18.3 \pm 1.3)$ cm, we obtain $C = (1.5 \pm 0.1)$ fermis.

5. – Optical model calculation of total effective $\overline{\text{p}}$-nucleon cross section.

We have performed an optical model calculation and obtained the effective antiproton-nucleon cross-section from our observed mean free path for interaction in emulsion.

The nuclei have been represented by a nucleon density formula

$$\varrho(r) = \frac{\varrho_0}{\exp[(r - R)/a] + 1}, \tag{1}$$

where r is the distance from the center of the nucleus. The half-density radius R has been taken as $R=1.07A^{\frac{1}{3}}$ fermis and the surface thickness parameter $a=0.55$ fermis. These values are in accordance with the values for medium heavy nuclei in HOFSTADTER's paper [11]. The density parameter ϱ_0 ($\approx$ central density) is obtained from the formula

$$\varrho_0 = \frac{A}{\frac{4}{3}\pi R^3(1+(\pi^2 a^2/R^2))}\,. \tag{2}$$

This expression can be found from a complex integration of the type

$$\int \frac{(1/3a)Z^3+\frac{4}{3}\pi^2 aZ}{\exp[(Z-R)/a]+1}\,\mathrm{d}Z$$

around the pole at $Z=R+i\pi a$.

The absorption coefficient has been put equal to the number of nucleons in a cylinder with cross-section equal σ and axis along the classical path of an antiproton. This means that the density according to equ. (1) has been averaged to $\bar{\varrho}$ over an area equal to the assumed elementary cross-section. Then we integrate along the classical path, s, for a given impact parameter b, to obtain the absorption coefficient. The total reaction cross-section in a specified nucleus (i) is then computed from the formula

$$\sigma_i = 2\pi\int_0^\infty\left[1-\exp\left[-\sigma\int_{-\infty}^{+\infty}\bar{\varrho}\,\mathrm{d}s\right]\right]b\,\mathrm{d}b\,. \tag{3}$$

In this expression we have only one parameter at our disposal, namely the effective $\bar{\mathrm{p}}$-N cross-section σ, since the nuclear size and shape parameters R and a were fixed by the model. When we finally sum over the nuclei in emulsion (N_i), we obtain a theoretical interaction mean free path $\lambda=(\sum N_i\sigma_i)^{-1}$ as a function of the elementary effective cross section σ, see Fig. 4.

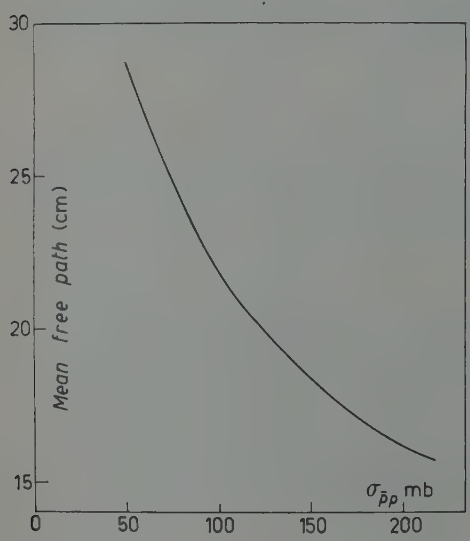

Fig. 4. – The theoretical interaction mean free path based on the optical model as a function of the effective cross section $\sigma_{\bar{\mathrm{p}}\mathrm{p}}$ per nucleon in nuclear matter.

[11] R. HOFSTADTER: *Rev. Mod. Phys.*, **28**, 214 (1956).

All integrations in equ. (3) were carried out graphically. The integral in the exponent was calculated in a way which can be described by referring to Fig. 5, where circles of constant density ϱ are shown. The cross-section area was divided into ten equal parts such that the nucleon density in each part is approximately constant. The correct way to divide the area depends on the impact parameter b and the cross-section assumed. We therefore constructed five different templates for each cross-section assumed to be used in five corresponding regions of impact parameter. One example is shown in Fig. 5. At each measuring point (we had about 100) on the b-s-diagram of Fig. 5, the average density $\bar{\varrho}$ was obtained from the readings at the ten midpoints. The effect of this averaging procedure is such that the effective nucleon density is raised at large impact parameters thereby increasing the total cross-section. At small impact parameters the effective nucleon density is reduced. This, however, does not change the total cross section contribution because the reduction occurs only in a region of impact parameters where there is still nearly 100% absorption. The contribution to the total cross-section from different impact parameters can be seen in Fig. 6 for the case $A = 108$ (silver) and $\sigma_{\bar{p}p} = 150$ mb. If averaging had not been performed, the dashed curve holds, resulting in a total cross section 16% smaller. Our model is different from the one used by GOLDHABER ([12]) and somewhat different from the one employed by AGNEW *et al.* ([13]).

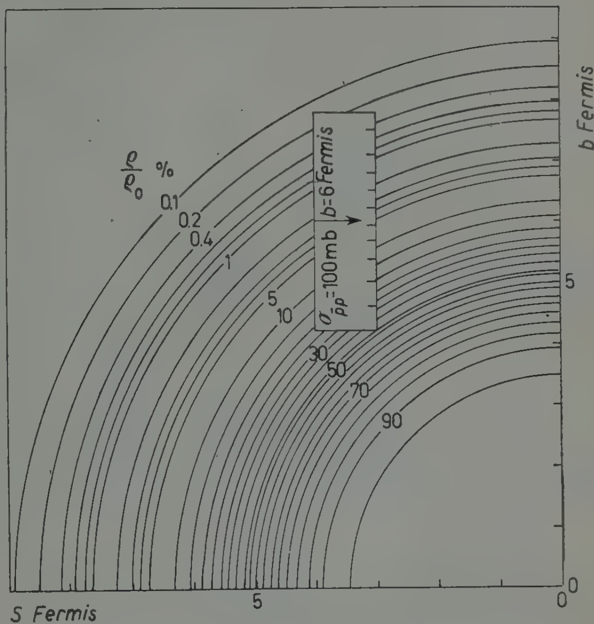

Fig. 5. – With the center of the nucleus at the origin, the figure shows circles of constant nucleon density for silver. The antiproton moves on a path parallel to the s-axis with an impact parameter b. Inserted is a representation of the cross section with its ten reading points.

([12]) G. GOLDHABER: *Proc. of 7th Rochester Conference on High Energy Nuclear Physics* (1957).

([13]) L. E. AGNEW, O. CHAMBERLAIN, D. V. KELLER, R. MERMOD, E. H. ROGERS, H. M. STEINER and C. WIEGAND: *Phys. Rev.*, **108**, 1545 (1957).

The results of our computations are shown in Table V and Fig. 7. Three representative nuclei in emulsions were selected, namely oxygen, bromine, and silver. The calculations were carried out for four assumed elementary cross-sections, $\sigma = 50$, 80, 100 and 150 mb. It is easy to find values for the cross-section on other nuclei and also for other elementary cross-sections by a formula of the

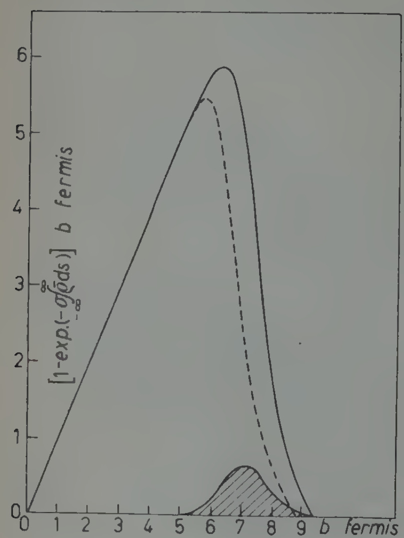

Fig. 6. – The solid curve shows the contributions to the total cross section for different impact parameters b, for the case $A=108$ (silver) and $\sigma_{\bar{p}p}=150$ mb. The dashed curve shows the contributions in the case when no density averaging over the cross section area has been made. The cross-hatched area shows the contributions to the inelastic scattering cross section. The three cross sections are in this case 1745, 1465, and 60 mb, respectively.

TABLE V. – *Total cross sections for three nuclei resulting from optical model calculations. σ_{eff} is the effective $\bar{\text{p}}$-nucleon cross section per nucleon in nuclear matter.*

σ_{eff} (mb)	σ_{total} (mb)		
	Oxygen	Bromine	Silver
50	400	1060	1255
80	500	1225	1430
100	555	1320	1530
150	670	1520	1745

type $\sigma_i = (\alpha R + \beta\sigma)^2$ where α and β are constants in limited regions of R and σ.

Our observed interaction mean free path (hydrogen included) is $\lambda = (18.3 \pm 1.3)$ cm. This yields a fit with the optical model calculations if the antiproton-nucleon effective cross-section is $\sigma = (150^{+27}_{-22})$ mb.

For the interpretation we note that the resulting cross-section is the effective cross-section in nuclear matter which can be written

$$\sigma_{\text{eff.}} = \sigma_{\text{a}} + f_1\sigma_{\text{el}} + \frac{Z}{A} f_2 \sigma_{\text{ch ex.}}\,, \tag{4}$$

where σ_a, $\sigma_{el.}$, and $\sigma_{ch.ex.}$ denote the annihilation, elastic scattering, and charge exchange cross-section, respectively. The last two cross-sections should be reduced by a factor ($f \leqslant 1$) due to the effect of the Pauli exclusion principle ([14]).

Compairing our results with those obtained on free protons by COOMBES *et al.* ([9]) interpolated at a corresponding energy (170 MeV), we find the following:

a) the elastic scatterings on protons compare favourably,
$\sigma = (77 \pm 17)$ mb (emulsion data),
$\sigma = (70^{+9}_{-11})$ mb (counter-experiment);

b) the total cross-sections are approximately equal;
$\sigma_{eff.} = (150^{+27}_{-22})$ mb (emulsion),
$\sigma_{total} = (153 \pm 8)$ mb (counter exp.).

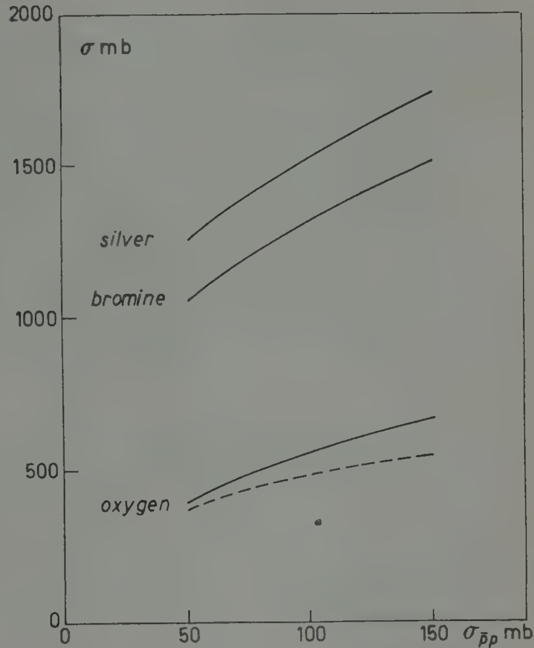

Fig. 7. – Interaction cross sections for three different nuclei as a function of the effective antiproton-nucleon cross section, $\sigma_{\bar{p}p}$, computed with the optical model. The dashed curve is calculated with no density averaging (for oxygen).

This means that everything fits well into the picture provided the factors f_1 and f_2 are close to unity.

This result, however, is very surprising as one has reasons to think that the reduction of the elastic scattering cross-section should be strong in this case where the scattering involves preferentially small momentum transfers. With regard to the experimental errors in the cross-sections, it is too early to say that a discrepancy exists. We estimate that one standard deviation change the right way would give results compatible with a reduction factor $f_1 = 0.6$. A theoretical calculation gave $f_1 = 0.62$ and $f_2 = 0.90$ at our mean energy (to be published in *Ark. f. Fysik*).

([14]) M. L. GOLDBERGER: *Phys. Rev.*, **74**, 1269 (1948).

1611

6. – Charge exchange.

From Table I group IV we find that 7 tracks which disappear in flight are interpreted as due to antiprotons. These may either have annihilated into stars with zero visible prongs or have given rise to charge exchange and emission of an antineutron. It has not been possible to distinguish between these two classes. Thus we can only get an upper limit of the number (7) of charge exchange events included in this group. On the other hand we may also have some charge exchange events among the stars in flight with small energy release (group III). The two effects work in opposite directions but whether they cancel each other or not we cannot say. At present we have not determined the charge exchange cross-section on complex nuclei.

7. – Inelastic scattering on complex nuclei.

We have observed 6 events which we interpret as inelastic scatterings of antiprotons on complex nuclei (Table VI). A scattering is called inelastic if we see at least one additional prong at the point of scattering ($\overline{\mathrm{p}}$-p scatterings excluded) or a sudden change of grain density in the antiproton track. It is

TABLE VI. – *Inelastic scattering events.*

Anti-proton number	Scatt. angle (lab. syst.)	Antiproton kinetic energy (MeV) initial	final	Energy loss $\Delta T/T$	Deviation from coplanarity	Additional prongs Num-ber	Energy or range	Angle θ (lab. syst.)
6 - 287	24°	220 ± 7	133	0.40	—	0	—	—
6 - 55	26°	172 ± 9	108	0.37	40°	1	27.5 MeV	103°
6 - 347	53°	110 ± 6	75	0.32	—	3	13 MeV, 12 μm, 3 μm	—
6 - 195	18°	122 ± 11	86	0.30	30°	1	11.4 MeV	88°
6 - 340	15°	176 ± 10	136	0.23	—	0	—	—
6 - 156	46°	$\simeq 162$	154	$\simeq 0.05$	12°	1	7 μm	73°

difficult to establish the existence of inelastic scattering events where the energy loss is small and no additional prong is seen. For that reason some of these events may have been included among the elastic scatterings. This problem will be more fully discussed in connection with the treatment of elastic scattering on complex nuclei.

1612

Two of the events in Table VI have no additional prong, three have one prong, and one has three prongs. The additional prongs in events 6-55 and 6-195 are presumably protons. As the range of the additional prong in 6-156 is only 7 μm, we can not establish its nature.

After adding the 8 or 9 events reported by G. GOLDHABER *et al.* [10], we find that the cross-section for inelastic scattering per emulsion nucleus (excluding hydrogen) is (42 ± 11) mb.

This cross-section is very low compared with the total interaction cross-section (hydrogen excluded) which is found to be 1020 mb per nucleus. It is possible, however, to see from the optical model calculations that the inelastic scattering cross-section must be very suppressed. The upper curve in Fig. 6 gives the contribution to the total interaction cross-section from different impact parameters b. The fraction of the total cross-section which comes from elastic scatterings allowed by the Pauli exclusion principle is $f_1\sigma_{\text{el}}/\sigma_{\text{eff.}}$, where the notation is the same as in equ. (4). The mean free path of antiprotons in nuclear matter is very short. We can then expect to get contributions to inelastic scatterings mainly from such fringe collisions where the antiproton after the scattering continues towards lower nuclear density. The probability that the scattered antiproton will escape from the nucleus is $\exp[-\sigma\int_s^\infty \bar{\varrho}\,\mathrm{d}s]$, where the integration is along the new path. To get an approximate value on the inelastic cross-section (σ_{inel}), we substitute for the correct average escape probability the expression $\frac{1}{2}\exp[-\sigma\int_0^\infty \bar{\varrho}\,\mathrm{d}s]$ where the integration is along the original path,

$$\sigma_{\text{inel}} = \frac{1}{2}\frac{f_1\sigma_{\text{el.}}}{\sigma_{\text{eff.}}}\int_0^\infty 2\pi \exp\left\{-\sigma\int_0^\infty \bar{\varrho}\,\mathrm{d}s\right\}\left[1-\exp\left\{-\sigma\int_{-\infty}^{\infty}\bar{\varrho}\,\mathrm{d}s\right\}\right] b\,\mathrm{d}b\;.$$

The cross hatched area in Fig. 6 shows the contributions to the inelastic scattering cross-section in silver for different impact parameters b, for an assumed value of $f_1\sigma_{\text{el}}/\sigma_{\text{eff.}} = 0.3$. Here we used the theoretical value $f_1 = 0.6$. The area corresponds to 60 mb to be compared with a total cross-section of 1745 mb.

We have also calculated the inelastic scattering cross-section in oxygen and bromine for $\sigma_{\text{eff.}} = 150$ mb. Finally, after averaging over the nuclei in the emulsion, we get a cross-section for inelastic scattering of $\sigma_{\text{inel}} \approx 45$ mb per nucleus.

When comparing this with the experimental value of 42 mb, one must remember that the experimental result does not include scatterings with very small energy transfers and further that the theoretical value is a rather crude estimate.

8. – Elastic scattering on complex nuclei.

When studying elastic scattering, we have selected tracks which are identified as antiprotons by their annihilation stars. All scattering events in the energy interval 20 to 250 MeV with a projected angle of scattering greater than 2° were recorded. The scattering was taken as elastic if no visible prong or change of grain density was seen.

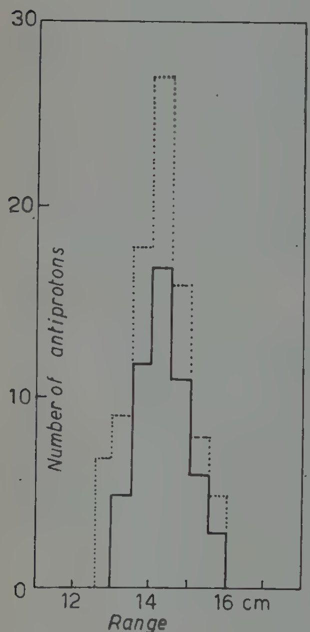

Fig. 8. – The solid curve shows the range distribution of stopping antiprotons which are scattered less than a projected angle of 2°. The dashed curve shows the range distribution of stopping antiprotons which are scattered in our sense.

Some inelastic scattering events may have been included. In order to find out whether this effect is important we have examined the range distribution of stopping antiprotons which are scattered less than a projected angle of 2° and of stopping antiprotons which are scattered in our sense. The resulting distributions are seen in Fig. 8. The first, not scattered group, consists of 54 antiprotons with a mean range of (14.26 ± 0.66) cm. The second, scattered group, consists of 90 antiprotons with a mean range of (14.17 ± 0.77) cm. The given errors are the standard deviations. The errors of the mean values are about 0.1 cm. The mean values are consequently not significantly separated. The difference between the standard deviations is also not significant according to a test by means of Fisher's z-distribution. Thus we can not find any significant admixture of inelasticly scattered particles.

The scanning efficiency has been checked by rescanning and by comparing the number of scatterings for different angles per meter path length.

The rescanning has been carried out in such a way that two scanners (A and B) have followed the same tracks. It is then possible to calculate the efficiency of both scanners and the total number of scatterings of the rescanned tracks. We use the following notations:

ε_A and ε_B = the efficiency of scanners A and B, respectively; $\varepsilon = \varepsilon_A + \varepsilon_B - \varepsilon_A \varepsilon_B$ = the total efficiency of A and B,

N_A and N_B = the number of scatterings found by A and B respectively,

N = the total number of scatterings found by A and B,

N_0 = the true total number of scatterings.

We get at once the following equations:

$$\varepsilon_A N_0 = N_A$$
$$\varepsilon_B N_0 = N_B$$
$$\varepsilon N_0 = N$$

from which ε_A, ε_B and N_0 can be calculated. The efficiences are in general functions of the scattering angle.

One of the scanners (A) was found to have an efficiency of 100% for scattering events with a projected angle greater than 2°. A comparison of the number of scatterings per meter path length for different angles found by A and by the other scanners (C) shows (Table VII) that the scanners C have an efficiency of 100% for projected angles greater than 3° but show a loss between 2° and 3°.

TABLE VII. – *Scanning efficiency for small angle scattering.*
Number of scatterings per meter path length in the entire energy interval 20 to 250 MeV as a function of projected scattering angle. Scanner A (about 100% efficiency for projected angles greater than 2°) has 101 scatterings in 12.4 m and scanners C 118 scatterings in 18.8 m.

Projected angle (°)	2° ÷ 3°	3° ÷ 4°	4° ÷ 5°	⩾ 5°	⩾ 2°
Scanner A	4.2 ± 0.6	1.5 ± 0.4	0.6 ± 0.3	1.8 ± 0.4	8.1 ± 0.8
Scanners C	1.2 ± 0.2	1.8 ± 0.3	1.0 ± 0.2	2.3 ± 0.4	6.3 ± 0.6

In Fig. 9 and 10 we give the experimental distributions of space angles for the energy interval 50 to 200 MeV;

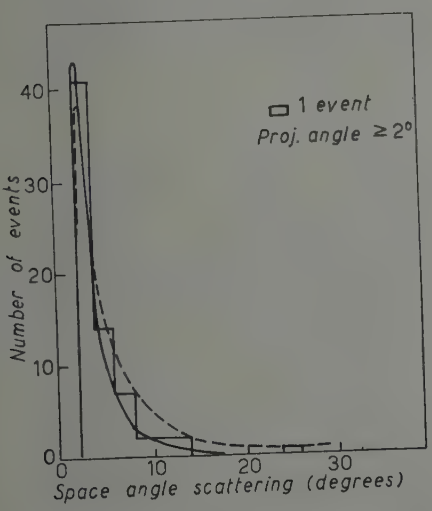

Fig. 9. – Number of scattering events with projected angle greater than 2° as a function of the space angle of scattering. The histogram shows the observed number (69) of elastic scattering events on 7.53 m of antiproton tracks for the energy interval 50 to 200 MeV (Scanner A). The solid curve shows the distribution expected from point-nucleus Rutherford scattering and the dashed curve from the charged-black-sphere model ([15]). Both curves are corrected according to the 2° cut-off criterion in projected angle.

1615

in Fig. 9 the data from scanner A for projected angles greater than 2° and in Fig. 10, the data from all scanners for projected angles greater than 3°. We have also given the distributions expected from pure Rutherford scattering (solid curve) and from the charged-black-sphere model (dashed curve) [15].

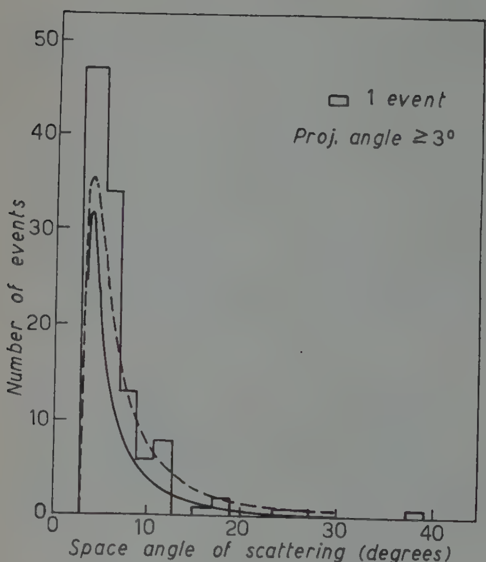

Fig. 10. – Number of scattering events with projected angle greater than 3° as a function of the space angle of scattering. The histogram shows the observed number (114) of events in 19.07 m for the energy interval 50 to 200 MeV (scanner A: 37 events in 7.53 m; scanners C: 77 events in 11.54 m). As in Fig. 9 the solid and dashed curves give the distributions expected from point-nucleus Rutherford scattering and from the charged-black-sphere model.

When calculating the number of scatterings expected from the point nucleus Rutherford scattering, we have taken into consideration the composition of the emulsion and the path length followed for different energies. A correction according to the 2° or 3° cut-off of projected angles has also been applied to the computed curves.

The angular distribution expected from a charged-black-sphere model has been calculated by G. GOLDHABER and J. SANDWEISS [15]. Their angular distribution was averaged over the energy interval 50 to 200 MeV as well as for the elements in nuclear emulsion. The given curves are also corrected to take account of the cut-off criterion in projected angles.

It is evident from Fig. 9 and 10 that the observed number of scatterings is significantly more than what is expected from Rutherford scattering only. The combination of Rutherford and diffraction scattering from a completely absorbing nucleus seems to agree better.

9. – Conclusions.

The large antiproton-proton scattering cross-section of $\sigma_{el} = (77 \pm 17)$ mb and the forward to backward ratio are in good agreement with theoretical predictions based on the Chew and Ball theory. The short interaction mean

---

[15] G. GOLDHABER and J. SANDWEISS: *Phys. Rev.*, **110**, 1476 (1958).

1616

free path in emulsion, $\lambda = (18.3 \pm 1.3)$ cm, gives an effective antiproton-nucleon cross-section of $\sigma_{\text{e f}} = (150^{+27}_{-22})$ mb when interpreted in terms of an optical model. If the reduction of the scattering cross-sections are carried out, the resulting annihilation cross-section comes out higher ((98^{+30}_{-25}) mb per nucleon) than that measured directly on protons by COOMBES *et al.* (9), namely (80 ± 13) mb. This discrepancy may indicate that the $\overline{\text{p}}$-n cross-sections are somewhat larger than the $\overline{\text{p}}$-p cross-sections. In view of the errors on the measured cross-sections we can only say that the $\overline{\text{p}}$-n cross-sections are at least as large as the corresponding $\overline{\text{p}}$-p cross-sections. The smallness of the inelastic scattering cross-section on complex nuclei seems to be possible to understand as due to quasi-elastic scattering and to the high reabsorption probability in the same nucleus which leaves only fringe collisions effective. Finally, the elastic scattering on complex nuclei seems to be accounted for by the combined results of Rutherford and diffraction scattering.

* * *

We express our deep gratitude to Dr. E. J. LOFGREN, head of the Bevatron, and to Prof. G. GOLDHABER and Prof. E. SEGRÈ for all of their help in planning and carrying out of the successful exposure. Our thanks are extended to Mr. J. F. GARFIELD, Brookhaven, who developed the stack.

The facilities put at our disposal by Prof. KAI SIEGBAHN are greatfully acknowledged as is his continued interest in this work.

For all their help in scanning we thank Mrs. I. NILSSON, Mrs. S. EKLUND, Miss I. DURÈN, Miss B. LUNDKVIST, and Miss V. BRAUN.

The research was supported in part by a contract with the Air Research and Development Command, U.S.A.F., through its European Office. Support was also obtained from the Swedish Atomkommitté.

RIASSUNTO (*)

Si è fatto uno studio su 374 tracce di antiprotoni in emulsioni nucleari nell'intervallo di energia $(0 \div 250)$ MeV. È stata seguita una lunghezza di traccia di 37.3 m. Dieci nuovi scattering $\overline{\text{p}}$-p elastici assieme ad undici eventi pubblicati precedentemente danno per lo scattering elastico una sezione d'urto di (77 ± 17) mb. Le sezioni d'urto totale e differenziale si accordano con la teoria di Chew e Ball. Il cammino libero medio per l'annichilazione nell'intervallo di energia $(30 \div 250)$ MeV è (20.8 ± 1.6) cm e il cammino libero medio d'interazione è (18.3 ± 1.3) cm. Da un calcolo in base a un modello ottico si è dedotta una sezione d'urto antiprotone-nucleone effettiva di (150^{+27}_{-22}) mb. Si riportano 6 nuovi scattering anelastici. Mettendo questi assieme agli 8 o 9 eventi pubblicati da G. GOLDHABER *et al.* si ottiene una sezione d'urto di scattering anelastico di (42 ± 11) mb per nucleo dell'emulsione (escluso l'idrogeno). Si discute il basso valore della sezione d'urto al lume del modello ottico. Lo scattering elastico su nuclei complessi sembra accordarsi con una combinazione di scattering di Rutherford e di diffrazione su un nucleo completamente assorbente.

(*) *Traduzione a cura della Redazione.*

Irreducibility Constraints and Field Equations for the Elementary Particles.

II. Fermions.

G. C. Bollini (*)

Imperial College of Science and Technology - London

(ricevuto il 12 Febbraio 1959)

Summary. — The conditions needed to describe an elementary particle by an irreducible quantity in the Lorentz group, are here taken as constraint equations to be imposed on the field entity. The independent components are extracted in a covariant way. The field equations are deduced from a Lagrangian in which only the free components are permitted to be varied. The communication relations, compatible with the constraints, are also given. In Part I the field entity was a tensor. In the present paper we are going to consider spin-tensors and simple Dirac spinors for which second order equations are proposed. In a general summary we give a brief and unifying treatment for elementary particles of any spin. In a future paper we intend to consider the interaction with the electromagnetic field.

1. – Introduction.

The field of an elementary particle with half-integer spin may be represented by means of a spin-tensor [1] $\Psi_{\mu_1 \dots \mu_s}$. To assure irreducibility under the Lorentz group and the uniqueness of spin it is necessary to impose the following conditions [2]: $\Psi_{\mu_1 \dots \mu_s}$ must be: *a*) completely symmetric; *b*) « perpendicular » to γ_μ; *c*) divergenceless. Conditions *b*) and *c*) are usually deduced, whenever possible, from a suitable (and complicated) Lagrangian [1,3,4], being then dependent on the equations of motion.

(*) On leave of absence from « Comisión Nacional de la Energía Atómica » Argentina.

(1) W. Rarita and J. Schwinger: *Phys. Rev.*, **60**, 61 (1941).

(2) H. Umezawa: *Quantum Field Theory* (1956), p. 64-66.

(3) H. Umezawa: *Quantum Field Fheory* (1956), p. 120.

(4) M. Fierz and W. Pauli: *Proc. Roy. Soc.*, A **173**, 211 (1939).

1618

Our viewpoint is different. We are going to take a), b) and c) as constraint conditions to be imposed on the spin-tensor independently of the equation of motion. It will be shown that they allow one to express the spin-tensor in terms of simple Dirac spinors. We have now two possibilities. Either a first or a second order wave equation may be taken for the Dirac spinors (5). The connection between spin and statistics is indeed independent of the field equations (6). With our point of view the second possibility seems more logical, because a Dirac spinor in itself has two components too many to represent a particle with only two intrinsic degrees of freedom. Of course, Dirac's equation allows the elimination of the redundant components, but we mean to start with a covariant field entity having as many degrees of freedom as the represented particle has. So, we are going to change c) in favour of a natural and more stringent condition (implying c)). Once this is accomplished a unified treatment for bosons and fermions will be possible. This is shown in the brief general summary ending the paper.

2. – Polarization matrices.

In I (7) we found an orthonormal system of $2s+1$ tensor operators $p^{(\sigma)}_{\mu_1\dots\mu_s}$ ($\sigma=0, 1, \dots, 2s$), which are symmetric, traceless and perpendicular to $p_\mu = -i\partial_\mu$. Let us define now the following matrix operators:

$$N^{(r)}\boldsymbol{p}^{(r)}_{\mu_1\dots\mu_s} = (p^{(2r-1)}_{\mu_1\dots\mu_{s+1}}\,p^{(1)}_\nu + p^{(2r)}_{\mu_1\dots\mu_{s+1}}p^{(2)}_\nu)\gamma_{\mu_{s+1}}\gamma_\nu\,, \qquad r=1, 2, \dots, s+1. \tag{2.1}$$

These matrices evidently are symmetric, traceless and perpendicular to ∂_μ. We also have

$$\gamma_{\mu_1}\boldsymbol{p}^{(r)}_{\mu_1\dots\mu_s} = 0\,, \tag{2.2}$$

$$\gamma\cdot\partial\boldsymbol{p}^{(r)}_{\mu_1\dots\mu_s} = \boldsymbol{p}^{(r)}_{\mu_1\dots\mu_s}\gamma\cdot\partial \tag{2.3}$$

and the normalization constants $N^{(r)}$ are so adjusted that

$$\overline{\boldsymbol{p}}^{(r)}_{\mu_1\dots\mu_s}\boldsymbol{p}^{(t)}_{\mu_1\dots\mu_s} = \delta^{rt}\,. \tag{2.4}$$

Where $\overline{\boldsymbol{p}}^{(r)}$ is the transposed of $\boldsymbol{p}^{(r)}$.

With the orthonormal system given by (2.1) we can form the projection

(5) R. P. Feynman and M. Gell-Mann: *Phys. Rev.*, **109**, 193 (1958).
(6) N. Burgoyne: *Nuovo Cimento*, **8**, 607 (1958).
(7) C. G. Bollini: *Nuovo Cimento*, **11**, 342 (1959).

operator

$$P_{\mu_1\ldots\mu_s;\,\nu_1\ldots\nu_s} = \sum_{r=1}^{s+1} p^{(r)}_{\mu_1\ldots\mu_s}\overline{p}^{(r)}_{\nu_1\ldots\nu_s}\,. \tag{2.5}$$

Of course, having all the properties of a projection operator for the conditions a), b) and c), and because of (cf. (2.3))

$$\gamma\cdot\partial P_{\mu_1\ldots\mu_s;\,\nu_1\ldots\nu_s} = P_{\mu_1\ldots\mu_s;\,\nu_1\ldots\nu_s}\gamma\cdot\partial \tag{2.6}$$

the projection matrix $P_{\mu_1\ldots\mu_s;\,\nu_1\ldots\nu_s}$ coincides with that investigated by C. FRONSDAL [8].

3. – Spinor components of the field.

Any spin-tensor field satisfying conditions a), b) and c), belongs to the space for which (2.5) is the projector.

I.e.

$$\Psi_{\mu_1\ldots\mu_s} = P_{\mu_1\ldots\mu_s;\,\nu_1\ldots\nu_s}\Psi_{\nu_1\ldots\nu_s}\,. \tag{3.1}$$

With (2.5) this is changed into

$$\Psi_{\mu_1\ldots\mu_s} = \sum_r p^{(r)}_{\mu_1\ldots\mu_s}\overline{p}^{(r)}_{\nu_1\ldots\nu_s}\Psi_{\nu_1\ldots\nu_s}\,,$$

$$\Psi_{\mu_1\ldots\mu_s} = \sum_r p^{(r)}_{\mu_1\ldots\mu_s}\Psi^{(r)}\,, \tag{3.2}$$

where

$$\Psi^{(r)} = \overline{p}^{(r)}_{\nu_1\ldots\nu_s}\Psi_{\nu_1\ldots\nu_s}\,. \tag{3.3}$$

(3.2) expresses the field in terms of $S+1$ simple Dirac spinors given by (3.3).

4. – Constraint equation for Dirac spinors.

We have found the spinor components of the spin-tensor field, but we have already said that a Dirac spinor in itself has too many degrees of freedom. Our viewpoint compels us to eliminate the redundant components by means of a constraint. As a matter of fact something of the kind was accomplished by R. P. FEYNMANN and M. GELL-MANN [4] using a « parity non-conserving »

---

[8] R. E. BEHRENDS and C. FRONSDAL: *Phys. Rev.*, **106**, 345, (1957).

projection operator. However, it is equally possible and perhaps preferable to use a completely covariant projection operator.

The wanted constraint equation can easily be found. Let us first take the vector field as a guide. A_μ has one component in excess to represent a spin one elementary particle. Under purely spacial rotations the four-vector A_μ is reducible $A_\mu \to A_i, A_4$. The « scalar » component A_4 is redundant and in the rest system of the particle is eliminated by means of the Lorentz condition

$$p_\mu A_\mu = 0 \Rightarrow A'_4 = 0 .$$

The prime referring to the rest system.

Let us now take a Dirac spinor $\Psi(p)$. It is also reducible under pure rotations. In the rest system *e.g.*

$$\Psi'(p) \to \Psi'_1(p), \Psi'_2(p) ,$$

Ψ'_1 and Ψ'_2 are Pauli spinors. One of them is redundant. We eliminate Ψ'_1 when the energy is positive and Ψ'_2 when it is negative (9). This is equivalently expressed by means of the following « Dirac condition »:

(4.1) $$\left(\beta \frac{E'}{|E'|} + 1\right)\Psi' = 0 ; \qquad \operatorname{diag}(\beta) = (1, 1, -1, -1) ,$$

i.e.

$$(i\beta p'_4 + |p'_4|)\Psi' = 0 ,$$

$$(i\gamma_\mu p'_\mu + p')\Psi' = 0 ,$$

where

$$p' = |p'_4| = +\sqrt{-p'_\mu p'_\mu} = +\sqrt{-p_\mu p_\mu} = p .$$

Or generally, in any system:

(4.2) $$(i\gamma\cdot p + p)\Psi(p) = 0 ,$$

which is the covariant expression of the constraint (4.1). Note that p is not the mass of the particle, it merely is the modulus of p_μ. The dynamical « value » of p remains to be fixed by the equation of motion.

---

(9) See however the final note.

Condition (4.2) together with condition b (Section **1**), imply the Lorentz condition:

$$(i\gamma\cdot p + p)\Psi_{\mu_1\dots\mu_s} = 0 = \gamma_{\mu_1}(i\gamma\cdot p + p)\Psi_{\mu_1\dots\mu_s} = i\gamma_{\mu_1}\gamma\cdot p\Psi_{\mu_1\dots\mu_s} + p\gamma_{\mu_1}\Psi_{\mu_1\dots\mu_s} =$$
$$= i\gamma_{\mu_1}\gamma\cdot p\Psi_{\mu_1\dots\mu_s} = i(2p_{\mu_1} - \gamma\cdot p\gamma_{\mu_1})\Psi_{\mu_1\dots\mu_s} = 2ip_{\mu_1}\Psi_{\mu_1\dots\mu_s}$$

i.e.

$$p_{\mu_1}\Psi_{\mu_1\dots\mu_s} = 0 \, .$$

5. – Projection operators and polarization spin-tensors.

The projection operator for the Dirac condition (4.2) is easily found. It is

$$\boldsymbol{P} = \frac{1}{2}\left(1 - \frac{i\gamma\cdot p}{p}\right), \tag{5.1}$$

with the properties

$$\boldsymbol{P}^2 = \boldsymbol{P} \, ,$$
$$(i\gamma\cdot p + p)\boldsymbol{P} = 0 \, ,$$
$$\mathrm{Tr}\,\{\boldsymbol{P}\} = 2 \, .$$

The condition (4.2) is also expressed by the following constraint equation

$$\Psi = \boldsymbol{P}\Psi \, . \tag{5.2}$$

Introducing now two special spinors $u^{(1)}$ and $u^{(2)}$ such that

$$\overline{u}^{(i)}u^{(j)} = \delta^{ij} \, ,$$
$$\sum_i u^{(i)}\overline{u}^{(i)} = \boldsymbol{P} \, .$$

We have

$$\Psi = \boldsymbol{P}\Psi = \sum_i u^{(i)}\overline{u}^{(i)}\Psi = \sum_i u^{(i)}Q^{(i)} \tag{5.3}$$

with

$$Q^{(i)} = \overline{u}^{(i)}\Psi \, . \tag{5.4}$$

Then, if Dirac condition (4.2) is imposed as a constraint equation, the decomposition (3.2) must be supplemented with

$$\Psi^{(r)} = \sum_i u^{(i)}Q^{(r,i)} \, , \tag{5.5}$$

1622

where

$$Q^{(r,i)} = \overline{u}^{(i)}\Psi^{(r)} .$$

(3.2) is now changed into

(5.6) $$\Psi_{\mu_1\dots\mu_s} = \sum_{r,i} p^{(r)}_{\mu_1\dots\mu_s} u^{(i)} Q^{(r,i)} .$$

New polarization spin-tensor operators are defined by

(5.7) $$\begin{cases} \boldsymbol{P}^{(r)}_{\mu_1\dots\mu_s} u^{(1)} = q^{(2r-1)}_{\mu_1\dots\mu_s} \\ \boldsymbol{P}^{(r)}_{\mu_1\dots\mu_s} u^{(2)} = q^{(2r)}_{\mu_1\dots\mu_s} \end{cases} \qquad r=1, \dots, s+1.$$

With them, (5.6) takes the form

(5.8) $$\Psi_{\mu_1\dots\mu_s} = \sum_{\varrho=1}^{2s+2} q^{(\varrho)}_{\mu_1\dots\mu_s} Q^{(\varrho)} ,$$

(5.9) $$Q^{(\varrho)} = \overline{q}^{(\varrho)}_{\mu_1\dots\mu_s} \Psi_{\mu_1\dots\mu_s} .$$

(5.8) is a decomposition of the field entity in $2s+2$ scalar quantities $Q^{(\varrho)}$ [10] which may be taken as the free co-ordinates of the field satisfying conditions a), b) and (4.2)

The complete projection operator, *i.e.* the projection operator for the conditions a), b) and (4.2) is

(5.10) $$\sum_{\varrho} q^{(\varrho)}_{\mu_1\dots\mu_s} \overline{q}^{(\varrho)}_{\nu_1\dots\nu_s} = \boldsymbol{P}\boldsymbol{P}_{\mu_1\dots\mu_s;\,\nu_1\dots\nu_s} ,$$

where $\boldsymbol{P}$ is given by (5.1) and $\boldsymbol{P}_{\mu_1\dots\mu_s;\,\nu_1\dots\nu_s}$ by (2.5).

It is easily seen that [10]

(5.11) $$\mathrm{Tr}\,\{\boldsymbol{P}\boldsymbol{P}_{\mu_1\dots\mu_s;\,\mu_1\dots\mu_s}\} = (s+1)\,\mathrm{Tr}\,\{\boldsymbol{P}\} = 2(s+\tfrac{1}{2})+1 .$$

6. – Lagrangians and free field equations.

An essentially unique Lagrangian for the free field is

(6.1) $$L = -\frac{1}{2m}\left(m^2 \overline{\Psi}_{\mu_1\dots\mu_s} \Psi_{\mu_1\dots\mu_s} + \partial_\nu \overline{\Psi}_{\mu_1\dots\mu_s} \partial_\nu \Psi_{\mu_1\dots\mu_s}\right) .$$

The constant factor is chosen so as to conform with the usual normalization.

---

[10] Remember that the spin of the represented particle is $s+\frac{1}{2}$.

In order for the equation of motion to be deduced only the independent components must be varied in the action integral

$$\mathcal{A} = \int d^4x\, L\,,$$

$$\mathcal{A} = -\frac{1}{2m}\int d^4x(m^2\overline{\Psi}_{\mu_1\dots\mu_s}\Psi_{\mu_1\dots\mu_s} + \dots)\,.$$

We now use (5.8) and its adjoint

$$\mathcal{A} = -\frac{1}{2m}\int d^4x\,(m^2\sum_{\varrho,\sigma}\overline{q}^{(\varrho)}_{\mu_1\dots\mu_s}Q^{(\varrho)*}\, q^{(\sigma)}_{\mu_1\dots\mu_s}Q^{(\sigma)} + \dots)\,.$$

The polarization spin-tensor operators may be treated as hermitian operators, so that

$$\mathcal{A} = -\frac{1}{2m}\int d^4x(m^2\sum_{\varrho,\sigma}Q^{(\varrho)*}\overline{q}^{(\varrho)}_{\mu_1\dots\mu_s}\, q^{(\sigma)}_{\mu_1\dots\mu_s}Q^{(\sigma)} + \dots)\,,$$

$$\mathcal{A} = -\frac{1}{2m}\int d^4x\,(m^2\sum_{\sigma,\varrho}Q^{(\varrho)*}\delta_{\varrho\sigma}Q^{(\sigma)} + \dots)\,,$$

$$\mathcal{A} = \sum_{\varrho}\int d^4x L^{(\varrho)}\,. \tag{6.2}$$

$$L^{(\varrho)} = -\frac{1}{2m}\,(m^2Q^{(\varrho)*}Q^{(\varrho)} + \partial_\nu Q^{(\varrho)*}\partial_\nu Q^{(\varrho)})\,. \tag{6.3}$$

The variation of the free components $Q^{(\varrho)*}$ gives

$$(\partial_\mu\partial_\mu - m^2)Q^{(\varrho)} = 0\,, \tag{6.4}$$

which may also be written (cf. (5.8))

$$(\partial_\mu\partial_\mu - m^2)\Psi_{\mu_1\dots\mu_s} = 0 \tag{6.5}$$

or

$$(-p_\mu p_\mu - m^2)\Psi_{\mu_1\dots\mu_s} = (p^2 - m^2)\Psi_{\mu_1\dots\mu_s} = 0\,.$$

Coming back to the constraint condition (4.2), we see that

$$(i\gamma\cdot p + p)\Psi = (i\gamma\cdot p + m)\Psi = 0$$

which is Dirac's equation.

7. – Quantization.

Applying the « canonical » procedure to the independent components of the spin-tensor we find [11]

$$\frac{1}{2m}\{Q^{(\varrho)}(x),\, Q^{(\sigma)}(x')\} = -\,i\delta^{\varrho\sigma}\Delta(x-x')\,. \tag{7.1}$$

where $\Delta(x-x')$ is the invariant function of Pauli and Jordan. Taking (5.8) into account we obtain

$$\begin{aligned}\frac{1}{2m}\{\Psi_{\mu_1\dots\mu_s}(x),\, \overline{\Psi}_{\nu_1\dots\nu_s}(x')\} &= -\,i\sum_{\varrho,\sigma}\delta^{\varrho\sigma}q^{(\varrho)}_{\mu_1\dots\mu_s}\overline{q}^{(\sigma)\prime}_{\nu_1\dots\nu_s}\Delta(x-x') = \\ &= -\,i\sum_{\varrho}q^{(\varrho)}_{\mu_1\dots\mu_s}\overline{q}^{(\varrho)}_{\nu_1\dots\nu_s}\Delta(x-x') = -\,i\boldsymbol{P}_{\mu_1\dots\mu_s;\,\nu_1\dots\nu_s}\boldsymbol{P}\Delta(x-x')\,.\end{aligned} \tag{7.2}$$

But

$$2m\boldsymbol{P}\Delta(x-x') = m\left(1-\frac{i\gamma\cdot p}{p}\right)\Delta(x-x')\,,$$

and $\Delta(x-x')$ satisfies the Klein-Gordon equation

$$p^2\Delta(x-x') = m^2\Delta(x-x')\,,$$

$$\frac{1}{p}\,\Delta(x-x') = \frac{1}{m}\,\Delta(x-x')\,.$$

Then

$$\begin{aligned}2m\boldsymbol{P}\Delta(x-x') &= m\left(1-\frac{i\gamma\cdot p}{m}\right)\Delta(x-x') \\ &= -\,(i\gamma\cdot p - m)\,\Delta(x-x') \\ &= -\,S(x-x')\,.\end{aligned} \tag{7.3}$$

So that

$$\{\Psi_{\mu_1\dots\mu_s}(x),\, \overline{\Psi}_{\nu_1\dots\nu_s}(x')\} = i\boldsymbol{P}_{\mu_1\dots\mu_s;\,\nu_1\dots\nu_s}S(x-x')\,. \tag{7.4}$$

For the spinor field (7.4) is just the usual anticommutation relation. But this is not the case with the vacuum expectation value of the chronological product. In fact, from

$$\frac{1}{2m}\langle 0\,|\,T\{Q^{(\varrho)}(x),\, Q^{(\sigma)*}(x')\}\,|\,0\rangle = -\,i\delta^{\varrho\sigma}\,\Delta_F(x-x')\,,$$

---

[11] See (6.1) and (6.3) for the factor $1/2m$.

1625

we deduce

$$(7.5)\quad \langle 0|T\{\Psi(x),\overline{\Psi}(x')\}|0\rangle = -2im\boldsymbol{P}\Delta_F(x-x') = i\left(\frac{m}{p}\,i\gamma\cdot p - m\right)\Delta_F(x-x')\,.$$

The right hand member of (7.5) does not coincide with the usual definition if $iS_F(x-x')$. The difference is due to the presence of m/p which must be retained because Δ_F does not satisfy the homogeneous Klein-Gordon equation.

8. – General summary. Particles of any spin.

a) Any elementary particle with spin s is represented by means of a Lorentz covariant entity Ψ_a, a representing either a set of s tensor indexes if s is integer, or a set of $s-\frac{1}{2}$ tensor indices plus one spinor index if s is half-integer.

b) For each field Ψ_a there exists a Lorentz covariant projection operator $P_{a;b}$ which is a $2s$-th degree polynomial function of the normalized impulse operator p_μ/p and is such that the constraint condition

$$\Psi_a = P_{a;b}\,\Psi_b$$

reduces the number of the independent components of Ψ_a to $2s+1$. Furthermore, the constraint equation implies irreducibility of the field entity not only under the Lorentz group but also under the rotation group in the rest system of the represented particle.

c) With the choice of a suitable base, the projection operator may be expressed in the form

$$P_{a;b} = \sum_{\sigma=1}^{2s+1} p_a^{(\sigma)}\,\overline{p}_b^{(\sigma)}$$

with

$$\overline{p}_a^{(\varrho)}\,p_a^{(\sigma)} = \delta^{\varrho\sigma}\,.$$

The $2s+1$ operators $p^{(\sigma)}$ may be called « polarization operators » for the field Ψ_a. As a consequence of this possibility we have

$$P_{a;a} = 2s+1\,.$$

d) The constraint equation allows one to write

$$\Psi_a = P_{a;b}\Psi_b = \sum_\sigma p_a^{(\sigma)}\,\overline{p}_b^{(\sigma)}\,\Psi_b = \sum_\sigma p_a^{(\sigma)}\,Q^{(\sigma)}\,,$$

1626

where the $2s+1$ scalar quantities

$$Q^{(\sigma)} = \overline{p}_b^{(\sigma)} \Psi_b$$

may be taken as the independent components of Ψ_a.

e) An invariant Lagrangian is constructed by means of a quadratic (bilinear) function of Ψ_a (and $\overline{\Psi}_a$) and its derivatives. In order for the equation of motion to be deduced, only the independent components must be varied in the action integral. All free elementary particles obey the Klein-Gordon equation. In the presence of interaction the equation of motion takes the form (see I)

$$(\partial_\mu \partial_\mu - m^2)\Psi_a = P_{a;b} J_{bc} \Psi_c \,,$$

which is compatible with the constraint equation. J_{bc} depends on the kind of interaction.

f) The commutation or anticommutation relations are

$$[\Psi_a, \overline{\Psi}_b]_\pm = -i \Delta_{a,b}(x - x') \,,$$

where

$$\Delta_{ab}(x - x') = P_{a;c} \Delta_{c,b}(x - x') \,.$$

For the free fields we have

$$\Delta_{a,b}(x - x') = P_{a;b} \Delta(x - x') \,,$$

$\Delta(x - x')$ being the usual Pauli-Jordan function. These relations are compatible with the constraints.

g) The vacuum expectation value of the chronological product is

$$\langle 0 | T[\Psi_a, \overline{\Psi}_b]_\pm | 0 \rangle = -i P_{a;b} \Delta^{(F)}(x - x') \,,$$

where $\Delta^{(F)}(x - x')$ is the Feynman function. As a consequence, the asymptotic behaviour (for $p \to \infty$) of the propagators is dominated by that of $\Delta^{(F)}(x - x')$.

Note. – The projection operator for half-integer spin has the expression (5.10) $P_{a;b} \equiv \boldsymbol{P}\boldsymbol{P}_{\mu_1 \dots \mu_s;\, \nu_1 \dots \nu_s}$. The projector operator $\boldsymbol{P}_{\mu_1 \dots \mu_s;\, \nu_1 \dots \nu_s}$ and that for integer spin may be found in the paper by R. E. BEHRENDS and C. FRONSDAL [8]. For $\boldsymbol{P}$ there are several possibilities. If we adopt first order equations of motion for all fermion fields then $\boldsymbol{P}$ must be taken to be one. For second order wave equations and Feynman-Gell-Mann's procedure is $\boldsymbol{P} = \frac{1}{2}(1 \pm \gamma_5)$. With Dirac's

1627

convention $\boldsymbol{P}$ is given by (5.1). If the same kind of spinor for both signs of the energy is adopted, then $\boldsymbol{P}=\frac{1}{2}(1\pm \operatorname{sg}(E)(i\gamma\cdot p)/p)$.

Summarizing: $\boldsymbol{P}$ is

$$
\begin{array}{ll}
1 & \text{for first order wave quation.}\\[1ex]
\frac{1}{2}(1\pm\gamma_5) & \text{Feynman-Gell-Mann.}\\[1ex]
\dfrac{1}{2}\left(1\pm i\dfrac{\gamma\cdot p}{p}\right) & \left.\begin{matrix}\text{Negative}\\ \text{Positive}\end{matrix}\right\}\ \text{energy}\ \left\{\begin{matrix}\text{second}\\ \text{first}\end{matrix}\right\}\ \text{kind spinor},\\[2ex]
\dfrac{1}{2}\left(1\pm i\operatorname{sg}(E)\dfrac{\gamma\cdot p}{p}\right) & \text{Both signs of energy}\ \left\{\begin{matrix}\text{second}\\ \text{first}\end{matrix}\right\}\ \text{kind spinor}.
\end{array}
$$

Not all the assertions made in the General Summary are valid if $P=1$ or $P=\frac{1}{2}(1+\gamma_5)$.

RIASSUNTO (*)

Le condizioni necessarie a descrivere una particella elementare per mezzo di una grandezza irriducibile nel gruppo di Lorentz sono considerate qui come equazioni di costrizione da imporre al campo. Le componenti indipendenti si ricavano in modo covariante. Le equazioni del campo si deducono da un lagrangiano in cui solo le componenti libere possono variare. Si danno anche relazioni di comunicazione, compatibilmente colle costrizioni. Nella parte I il campo era considerato tensoriale. Nel presente lavoro considereremo tensori spinoriali e semplici spinori di Dirac pei quali proporremo equazioni di second'ordine. In una ricapitolazione generale diamo un breve trattamento unitario per particelle di spin qualsiasi. In un prossimo lavoro prenderemo in esame l'interazione col campo elettromagnetico.

(*) *Traduzione a cura della Redazione.*

IL NUOVO CIMENTO Vol. XIII, N. 1 1° Luglio 1959

On the Unphysical Region in Dispersion Relations (*).

R. F. Streater

Mathematics Department, Imperial College of Science and Technology - London

(ricevuto il 19 Febbraio (1959)

Summary. — Conditions on the masses of four particles are written down such that present methods can prove inelastic dispersion relations for processes of the type $A+B \to C+D$. One necessary condition is that both elastic relations $A+B \to A'+B'$ and $C+D \to C'+D'$ can be proved for forward scattering at least. The masses of $p\,n\,\pi^-\pi^0$ satisfy the conditions, and also photomeson production, and the model K-meson system $K=3\Pi/2$, $\Lambda \simeq N$ (where these are the masses of the particles). Using dispersion relations and the unitarity condition for the unphysical region of this model system, integral equations for the unphysical region in $KN \to \Lambda\pi$ relations are obtained; these equations have solutions in terms of physical S matrix elements. It is also possible to set up a model $KN \to KN$ system such that the usual dispersion relations can be proved by present methods, and also all the inelastic relations which the method of this paper needs in order to interpret the unphysical region. However, a model can be constructed such that dispersion relations can be proved, but such that their unphysical region cannot be interpreted by present methods.

1. – Introduction.

A difficulty which occurs in the theory of dispersion relations is the interpretation of the unphysical region in terms of physical data. When a relation is rigorously proved, the meaning of the unphysical region is defined in the course of the proof; it will not necessarily be in terms of physical S-matrix elements: for instance, it could be given by the analytic continuation of a

(*) Supported by the Department of Scientific and Industrial Research.

matrix-element of a product of field operator between specified states. This mathematical definition must be related to experimentally determinable quantities, such as scattering amplitudes. H. LEHMANN has shown [1] that for π-n elastic scattering the unphysical region occurring in the non-forward dispersion relation is uniquely determined by the nearly-forward amplitudes at the same energy: it is in fact determined by analytic continuation in the momentum transfer. LEHMANN has shown [1] that this continuation is valid just in the region where the dispersion relations are proved, which is a satisfactory result. He proves that

$$\operatorname{Im} T(W,\theta) = \int_{-1}^{+1} d(\cos\alpha) \int_{2x_0^2-1}^{\infty} dy \, \frac{\Phi(W,\cos\alpha,y)}{y-\cos(\theta-\alpha)},$$

where W is the energy, and θ the scattering angle; regularity in $\cos\theta$ follows, as θ enters only in the kernel $1/(y-\cos(\theta-\alpha))$. Note that $\operatorname{Im} T$ is not at all regular in W, since Φ is an arbitrary distribution. This is illustrated in Fig. 1. Here p_1, k_1, are the initial momenta of the nucleon and meson, and p_2, k_2 the final momenta. Spin and isotopic spin are inessential complications, and can be ignored provided all the selection rules are obeyed. We use the time-like metric $(+1\ -1\ -1\ -1)$; the scattering is determined by the two invariants $W^2=(p_1+k_1)^2$ and $\Delta^2=-\frac{1}{4}(p_1-p_2)^2$, the « energy » and «momentum transfer ». In Fig. 1, $DAEF$ is the physical region; dispersion relations are valid if $\Delta < \Delta_{max}$. $DABC$ is the region occurring in the dispersion relations, of which ABE is unphysical. A point X of ABE is reached by continuing the physical region YZ in Δ, W being fixed.

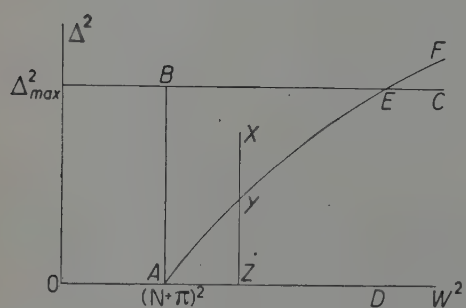

Fig. 1. – Nucleon-pion elastic scattering. Showing the physical region $DAEF$; region of validity of dispersion relations $DABC$; region of validity of the continuation procedure ABE; the point X is reached by continuation along the line YZ.

Although K-meson dispersion relations have not yet been proved, it is worth considering the same problem here. For the sake of argument we deal with a model K-meson of mass $3\Pi/2$ (Π is the mass of the π-meson); then dispersion relations for KN-KN can be proved, for example, by the method

---

[1] H. LEHMANN: *Nuovo Cimento*, **10**, 597 (1958).

described by Lehmann [1]. Here the relations are

$$T(W, \varDelta) = \text{bound state terms} + \frac{1}{2\pi}\int\limits_{W'=\varLambda+\Pi}^{\infty} \frac{A_1(\omega', \varDelta)}{\omega' - \omega}\, \mathrm{d}\omega' + \frac{1}{2\pi}\int\limits_{W'=K+N}^{\infty} \frac{A_2(\omega', \varDelta)}{\omega' + \omega}\, \mathrm{d}\omega',$$

where

$$\omega = \frac{(k_1 + k_2)(p_1 + p_2)}{2\sqrt{(p_1 + p_2)^2}} = \omega(W, \varDelta)\,.$$

The first integral runs from $\varLambda + \Pi$ to ∞. The physical region is $K+N$ to ∞, and so there is an unphysical region even for forward scattering ($\varDelta = 0$). In Fig. 2 we can continue from $\varDelta = 0$ up to $\varDelta = \varDelta_{\max}$ with W^2 fixed. In our model $\varDelta^2_{\max} > 0$. Now there is a region $ABCD$ in Fig. 2 which cannot be reached by analytic continuation from any physical region, since A is not regular in W. If we could obtain an interpretation in the neighbourhood of AD (or any other region in the complex $\varDelta$-plane where $W < K+N$ and $A(\varDelta, W)$ is regular in $\varDelta$), a continuation into the whole of $ABCD$ would be possible, by a slight extension of Lehmann's result.

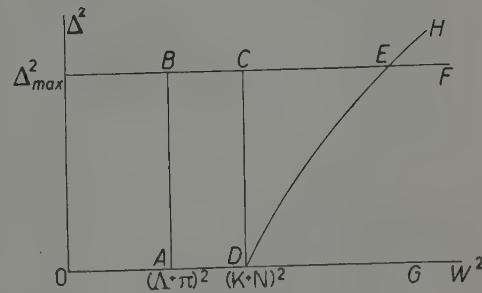

Fig. 2. – K-meson-nucleon elastic scattering. *GDEH* physical region; *FBAG* region occurring in dispersion relations; *DCE* region of validity of continuation; *ABCD* region requiring interpretation.

A programme for the interpretation will be given and the mathematical justification given in subsequent sections.

We consider in detail the similar problem for the inelastic dispersion relations for (KN, $\Lambda\pi$). These are conjectured to hold for the actual masses of KN$\Lambda\pi$; they will be proved for our model. Let $T(W\varDelta)$ denote the transition matrix for the process $\mathrm{K}+\mathrm{N} \to \Lambda + \pi$. The masses will be denoted by KN, $\varLambda\Pi$. T is related to the S-matrix by

$$S = 2\pi\, \delta(p_1 + k_1 - p_2 - k_2) T\,.$$

For inelastic processes, the « straight through » term $\delta(k_1 - k_2)\,\delta(p_1 - p_2)$ vanishes. The transition matrix equals [1]

$$(1.1)\quad T_1(W, \varDelta) = -\int \langle p_1 | \theta(x) \left[j_K\left(\frac{x}{2}\right), j_\pi\left(-\frac{x}{2}\right)\right] | p_2 \rangle \exp\left[i(k_1 + k_2)\frac{x}{2}\right] \mathrm{d}^4x\,,$$

1631

where $j_K(x)$ and $j_\pi(x)$ are the K, π currents respectively. Define T_2 and the « absorptive parts » $\frac{1}{2}A_1$ and $\frac{1}{2}A_2$ by

$$(1.2)\quad T_2(W,\Delta) = -\int \langle p_1|\theta(x)\left[j_\pi\left(\frac{x}{2}\right), j_K\left(-\frac{x}{2}\right)\right]|p_2\rangle \exp\left[i(k_1+k_2)\frac{x}{2}\right] d^4x\,,$$

$$(1.3)\quad A_1(W,\Delta) = \int \langle p_1|j_K\left(\frac{x}{2}\right) j_\pi\left(-\frac{x}{2}\right)|p_2\rangle \exp\left[i(k_1+k_2)\frac{x}{2}\right] d^4x\,,$$

$$(1.4)\quad A_2(W,\Delta) = \int \langle p_1|j_\pi\left(\frac{x}{2}\right) j_K\left(-\frac{x}{2}\right)|p_2\rangle \exp\left[i(k_1+k_2)\frac{x}{2}\right] d^4x\,.$$

By introducing a complete set of states in A_1 or A_2 it is easily shown that they vanish unless $W>0$ using the fact that every state has positive energy. For a theory invariant under TP, we can use (²)

$$\operatorname{Im} T_1 = \frac{1}{2}\int \langle p_1|\left[j_\pi\left(\frac{x}{2}\right), j_K\left(-\frac{x}{2}\right)\right]|p_2\rangle \exp\left[i(k_1+k_2)\frac{x}{2}\right] d^4x =$$

$$= \frac{1}{2}[A_1(\omega,\Delta) - A_2(-\omega,\Delta)] = \frac{1}{2}A_1(\omega,\Delta)\,, \quad \text{if } \omega>0\,.$$

So A_1 and A_2 are related to the imaginary part of T_1 and T_2.

The T's and A's are at first physically meaningful only on the mass-shells $p_1^2=N^2$, $p_2^2=\Lambda^2$, $k_1^2=K^2$, $k_2^2=\Pi^2$ and the energy shell $p_1+k_1=p_2+k_2$ and in the physical region of Δ, W; in terms of field theory, (1.1), (1.2), (1.3) and (1.4) define them for all real k_1+k_2 as Fourier transforms. We shall always maintain $p_1+k_1=p_2+k_2$. We have the dispersion relations ($\operatorname{Im} W\neq 0$)

$$(1.5)\quad T_1(W,\Delta) = \frac{g_1}{\omega-\omega_0} + \frac{g_2}{\omega+\omega_0'} + \frac{1}{2\pi}\int_{W'=\Lambda+\Pi}^{\infty} \frac{A_1(\omega',\Delta)}{\omega'-\omega}\,d\omega' + \frac{1}{2\pi}\int_{W'=\Pi+N}^{\infty} \frac{A_2(\omega',\Delta)}{\omega'+\omega}\,d\omega'\,,$$

$$(1.6)\quad T_2(W,\Delta) = \frac{g_3}{\omega-\omega_0'} + \frac{g_4}{\omega+\omega_0} + \frac{1}{2\pi}\int_{W'=N+\Pi}^{\infty} \frac{A_2(\omega',\Delta)}{\omega'-\omega}\,d\omega' + \frac{1}{2\pi}\int_{W'=\Lambda+\Pi}^{\infty} \frac{A_1(\omega',\Delta)}{\omega'+\omega}\,d\omega'\,.$$

In (1.5) and (1.6) g_1, g_2, g_3, g_4 are related to renormalized coupling constants, and ω_0, ω_0' are the « bound state » energies coming from the one-nucleon intermediate state. We have ignored the question of convergence of dispersion relations, which introduces no new features. After introducing a complete

---

(²) R. OEHME: *Phys. Rev.*, **100**, 1503 (1955), Appendix.

set of states $|\gamma\rangle$ and using translational invariance, the absorptive parts are seen to equal:

$$A_1(W, \Delta) = (2\pi)^4 \sum_\gamma \langle p_1 | j_K(0) | \gamma\rangle\langle\gamma | j_\pi(0) | p_2\rangle\, \delta^4(p_1 + k_1 - \gamma)\,, \tag{1.7}$$

$$A_2(W, \Delta) = (2\pi)^4 \sum_\gamma \langle p_1 | j_\pi(0) | \gamma\rangle\langle\gamma | j_K(0) | p_2\rangle\, \delta^4(p_1 + k_1 - \gamma)\,. \tag{1.8}$$

For $W \geqslant K+N$, Λ we «know» A_1 and A_2, since they are the absorptive parts for physical energies. Below $K+N$, *i.e.* in $ABCD$ of Fig. 2, we are going to use (1.7) and (1.8) for A_1 and A_2. Suppose $W < K+N$. In our model, $\Lambda + 2\Pi > K+N$, and $N+2\Pi > K+\Lambda$ so the only intermediate states if $W < K+N$ are the two-particle states $|N, \pi\rangle$ and $|\Lambda, \pi\rangle$. So (1.7) and (1.8) become

$$A_1(W, \Delta) = (2\pi)^4 \int_{-1}^{+1} \mathrm{d}(\cos\theta') \int \mathrm{d}\varphi'\, \frac{K_2}{2W}\, \langle p_1 | j_K(0) | \Lambda', \pi'\rangle\langle\Lambda', \pi' | j_\pi(0) | p_2\rangle\,, \tag{1.9}$$

$$A_2(W, \Delta) = (2\pi)^4 \int_{-1}^{+1} \mathrm{d}(\cos\theta') \int \mathrm{d}\varphi'\, \frac{K_2}{2W}\, \langle p_1 | j_\pi(0) | N'\pi'\rangle\langle N'\pi' | j_K(0) | p_2\rangle\,. \tag{1.10}$$

In (1.9) and (1.10), θ' and φ' are angles specifying the momenta Λ', π' (or N', π') of the intermediate states; $K_2(W)$ is the magnitude of the momentum, given by (2.1) below.

Of the quantities appearing in the R.H.S. of (1.9), $+(2\pi)^{\frac{3}{2}} i\langle\Lambda', \pi' | j_\pi(0) | p_2\rangle = T_{\Lambda\pi}$ say, the amplitude for (Λ, π) elastic scattering, where W is $> \Lambda + \Pi$, *i.e.* above threshold. It is therefore known from the S-matrix, provided that the vectors p_2 and k_2 are physical vectors, *i.e.* $p_2^2 = \Lambda^2$, $k_2^2 = \Pi^2$ and p_2, k_2 real. This can always be chosen to be the case, but for $W < K+N$ it will be impossible to choose k_1, p_1 also physical, if we wish to keep $k_1 + p_1 = k_2 + p_2$. For instance, if we insist on $p_1^2 = N^2$, $k_2^2 = K^2$ the components of k_1 and p_1 would be complex. Then the Δ of (1.9), (1.10) will in general be complex. Similarly in (1.10), $+i(2\pi)^{\frac{3}{2}}\langle p_1 | j_\pi(0) | N', \pi'\rangle = T_{N\pi}$ is known from N-π scattering. The other functions occurring in (1.9), (1.10) are $i(2\pi)^{\frac{3}{2}}\langle p_1 | j_K(0) | \Lambda', \pi'\rangle$ and $i(2\pi)^{\frac{3}{2}}\langle N', \pi' | j_K(0) | p_2\rangle$. These are respectively equal to $T_1(W, \Delta_1')$ and $T_2(W, \Delta_2')$ where Δ_i' is the momentum transfer to the intermediate baryon in each case. Δ_i' depends on W and θ' according to

$$\Delta_1'^2(W, \theta') = -\tfrac{1}{4}(p_1 - p_\Lambda')^2\,,$$

$$\Delta_2'^2(W, \theta') = -\tfrac{1}{4}(p_2 - p_N')^2\,.$$

By our choice of p_2, k_2 to be physical in (1.9), Δ_1' will be complex. Also if in (1.10) we choose p_1, k_1 physical, then Δ_2' will be complex. So (1.9) and (1.10)

look like

(1.9*) $A_1(W, \Delta) =$

$$= -2\pi\int \frac{K_2}{2W}\,\mathrm{d}(\cos\theta')\,\mathrm{d}\varphi' T_1(W, \Delta_1'(W, \theta'))\, T_{\Lambda\pi}(W, \Delta_1''(\Delta, W, \theta', \varphi')) ,$$

(1.10*) $$A_2(W, \Delta) = -2\pi\int \frac{K_2}{2W}\,\mathrm{d}(\cos\theta')\mathrm{d}\varphi' T_2(W, \Delta_2'(W, \theta'))\, T_{N\pi}(W, \Delta_2''(\Delta, W, \theta', \varphi')) .$$

Here Δ_1'' and Δ_2'' are equal to $-\frac{1}{4}(p_2 - \Lambda')^2$ and $-\frac{1}{4}(p_1 - N')^2$ and are physical. Δ_1' Δ_2' are complex, and so the equations need justification. We will do this by showing that these values of Δ' lie in the domain of regularity of T_1, T_2. We can use (1.5) and (1.6) to eliminate T_1 and T_2, provided (as will be shown) that the dispersion relations are valid for these complex values of Δ'. We then obtain two coupled equations for A_1 and A_2 in the unphysical region of W.

Write the dispersion relations (1.5), (1.6) as

(1.11) $$T_1(W, \Delta) = \varphi_1(W, \Delta) + \int_{(\Pi+\Delta)^2}^{(K+N)^2} \mathfrak{K}_1(W, W') A_1(W', \Delta)\,\mathrm{d}W'^2 + \int_{(N+\Pi)^2}^{(\Lambda+K)^2} \mathfrak{K}_2(W', W, \Delta) A_2(W', \Delta)\,\mathrm{d}W'^2 ,$$

(1.12) $$T_2(W, \Delta) = \varphi_2(W, \Delta) + \int_{(N+\Pi)^2}^{(K+\Lambda)^2} \mathfrak{K}_1(W, W') A_2(W', \Delta)\,\mathrm{d}W'^2 + \int_{(\Lambda+\Pi)^2}^{(K+N)^2} \mathfrak{K}_2(W', W, \Delta) A_1(W', \Delta)\,\mathrm{d}W'^2 ,$$

where

(1.13) $$\left\{\begin{aligned} &\mathfrak{K}_1(W, W') = \frac{1}{2\pi(W'^2 - W^2)}, \quad \mathfrak{K}_2 = \frac{1}{2\pi(W'^2 + W^2 - 4\Delta^2 - N^2 - \Lambda^2 - K^2 - \Pi^2)} \\ &\varphi_1(W, \Delta) = \frac{g_1}{\omega - \omega_0} + \frac{g_2}{\omega + \omega_0'} + \\ &\qquad + \int_{(K+N)^2}^{\infty} A_1(W', \Delta)\mathfrak{K}_1(W, W')\,\mathrm{d}W'^2 + \int_{(K+\Lambda)^2}^{\infty} A_2(W', \Delta)\mathfrak{K}_2(W, W', \Delta)\,\mathrm{d}W'^2 \\ &\varphi_2(W, \Delta) = \frac{g_3}{\omega - \omega_0'} + \frac{g_4}{\omega + \omega_0} + \\ &\qquad + \int_{(K+\Lambda)^2}^{\infty} \mathfrak{K}_1(W, W') A_2(W', \Delta)\,\mathrm{d}W'^2 + \int_{(K+N)^2}^{\infty} \mathfrak{K}_2(W, W', \Delta) A_1(W', \Delta)\,\mathrm{d}W'^2 \end{aligned}\right.$$

1634

All the quantities in (1.13) are «known», since as will be shown, all the quantities involved can be obtained from physical ones by continuation, even for $\Delta^2 = \Delta_1'^2$ or $\Delta_2'^2$ needed in (1.9)* and (1.10)*. Substituting (1.11) and (1.12) in (1.9)*, (1.10)*, we get

$$(1.14)\qquad A_1 = f_1(\Delta, W) + \iint G_{11}(\Delta, W, \Delta', W')A_1(\Delta', W)\,\mathrm{d}(\cos\theta')\,\mathrm{d}W'^2 + \\ + \iint G_{12}(\Delta, W, \Delta', W')A_2(\Delta_1', W')\,\mathrm{d}(\cos\theta')\,\mathrm{d}W'^2,$$

$$(1.15)\qquad A_2(W, \Delta) = f_2(\Delta, W) + \iint G_{21}(\Delta, W, \Delta_2', W')A_1(\Delta_2', W')\,\mathrm{d}(\cos\theta')\,\mathrm{d}W'^2 + \\ + \iint G_{22}(\Delta, W, \Delta_2', W')A_2(\Delta_2', W')\,\mathrm{d}(\cos\theta')\,\mathrm{d}W'^2.$$

These equations are of the Fredholm type, and will have solutions under very general conditions on the functions involved. In (1.14) and (1.15)

$$(1.16)\qquad \left\{\begin{aligned}
&f_1(\Delta, W) = -\frac{\pi K_{2\Lambda}}{W}\int \varphi_1(W, \Delta_1'(W, \theta'))\, T_{\Lambda\pi}(W, \Delta(\Delta_1'', W, \theta', \varphi'))\,\mathrm{d}(\cos\theta')\,\mathrm{d}\varphi', \\
&f_2(\Delta, W) = -\frac{\pi K_{2N}}{W}\int \varphi_2(W, \Delta_2'(W, \theta'))\, T_{N\pi}(W, \Delta_2''(\Delta, W, \theta', \varphi'))\,\mathrm{d}(\cos\theta')\,\mathrm{d}\varphi', \\
&G_{11}(\Delta, W, \Delta_1'(W,\theta'), W') = -\pi\frac{K_{2\Lambda}}{W}\,\mathfrak{K}_1(W, W')\int T_{\Lambda\pi}(W, \Delta_1''(W, \Delta, \theta', \varphi'))\,\mathrm{d}\varphi', \\
&G_{12}(\Delta, W, \Delta_1'(W,\theta'), W') = \\
&\qquad = -\pi\frac{K_{2\Lambda}}{W}\,\mathfrak{K}_2(W, W', \Delta_1'(W, \theta'))\int T_{\Lambda\pi}(W, \Delta_1''(W, \Delta, \theta', \varphi'))\,\mathrm{d}\varphi', \\
&G_{21}(\Delta, W, \Delta_2'(W, \theta'), W') = -\pi\frac{K_{2N}}{W}\,\mathfrak{K}_1(W, W)\int T_{N\pi}(W, \Delta_2''(\Delta, W, \theta', \varphi'))\,\mathrm{d}\varphi', \\
&G_{22}(\Delta, W, \Delta_2'(W,\theta'), W') = -\pi\frac{K_{2N}}{W}\,\mathfrak{K}_2(W, W', \Delta_2')\int T_{N\pi}(W, \Delta_2''(\Delta, W, \theta', \varphi'))\,\mathrm{d}\varphi'.
\end{aligned}\right.$$

All quantities in (1.16) are «known». The integral in (1.14), $\int \mathrm{d}(\cos\theta')$ is in fact a contour integral $\mathrm{d}\Delta'^2$ whose exact path will be given in Section **4**, where it is also seen that Δ is a value on the path.

The main part of the paper is devoted to proving that (1.9) and (1.10) hold, (with $T_{\Lambda\pi}$ and $T_{N\pi}$ physical for each intermediate state $|\gamma\rangle$); and also that the dispersion relations (1.11), (1.12) are in fact valid for all Δ' which are needed in the sum over intermediate states. It turns out that a sufficient

condition for this is that the relations be valid near the physical threshold $W=K+N$ (or $K+\Lambda$ in the case of T_2).

For elastic KN, KN in our model, there is an unphysical region $\Lambda+\Pi\leqslant \leqslant W<K+N$. For W in this range

$$A(W,\Delta)\,(2\pi)^4 \sum_{\gamma} \langle p\,|\,j_K(0)\,|\,\Lambda,\pi\,\gamma\rangle\langle\gamma,\Lambda\,\pi\,|\,j_K(0)\,|\,p_2\rangle\,\delta^4(p_1+p_1-\gamma)$$

and we know the whole of the R.H.S. by the above method. It is possible however, to set up a model KN system such that KN relations can be proved but not the $K\Lambda$; the latter have a larger unphysical region. Then the $K\Lambda$ associated production relations cannot be proved by present methods; since these relations are needed to link the equations for the unphysical region, the unphysical region of such a model cannot be interpreted in terms of scattering data.

For the realistic KN system, we can interpret the unphysical regions supposing all the relevent relations to hold. Then using unitarity as here, we get a finite system of coupled equations which have solutions in terms of S-matrix elements. The dispersion relations needed to link them are those for all the processes with contributions below threshold: (KN, $\Lambda\pi$), (KN, $\Lambda 2\pi$), (πN, ΛK), (2πN, ΛK), etc.; and ($\Lambda\pi$, $\Lambda 2\pi$).

We hope to treat (πN/2πN) relations rigorously in another paper.

2. – Kinematics.

In this Section we fix the notation to be used, and write down the physical region. We wish to determine the physical region of the process $p_1+k_1\to p_2+k_2$ where $p_1^2=N^2$, $k_1^2=K^2$, $p_2^2=\Lambda^2$, $k_2^2=\Pi^2$. This is the Λ production, $p+K^-\to\Lambda+\pi^0$. We assume $K+N>\Lambda+\Pi$. All that follows also applies to $\pi^-+P\to N+\pi^0$ where the small mass differences $N>P$, $\pi^->\pi^0$ are taken into account; this last example is perhaps not interesting, because in proving the dispersion relations we ignore other electromagnetic effects which are possibly as large. If $N=\Lambda$, $K=0$ we reduce to photomeson production [3]. Here no unphysical region appears, in the approximation in which they are proved.

Define as the two invariants

$$W^2=(p_1+k_1)^2=(p_2+k_2)^2\,,\qquad \Delta^2=-\tfrac{1}{4}(p_1-p_2)^2=-\tfrac{1}{4}(k_1-k_2)^2\,.$$

---

(3) J. G. Taylor: *Proof of certain dispersion relations in quantised field theories*, preprint.

2·1. *Centre of mass frame* $p_1+k_1=(W, 0, 0, 0)$.

$$p_1=(p_{10}, 0, 0, K_1), \qquad k_1=(k_{10}, 0, 0 -K_1),$$

where

$$p_{10}=\frac{W^2+N^2-K^2}{2W};$$

$$k_{10}=\frac{W^2+K^2-N^2}{2W}; \qquad K_1^2=p_{10}^2-N^2=\frac{(W^2+N^2-K^2)^2}{4W^2}-N^2;$$

and

$$p_2=(p_{20}, 0, K_2\sin\theta, K_2\cos\theta), \qquad k_2=(k_{20}, 0, -K_2\sin\theta, -K_2\cos\theta),$$

where

$$p_{20}=\frac{W^2+\Lambda^2-\Pi^2}{2W}; \qquad k_{20}=\frac{W^2-\Lambda^2+\Pi^2}{2W}; \qquad K_2^2=p_{20}^2-\Lambda^2,$$

$\cos\theta$ is related to Δ by

$$K_1K_2\cos\theta=p_{10}p_{20}-\frac{N^2}{2}-\frac{\Lambda^2}{2}-2\Delta^2. \tag{2.1}$$

The physical region is given by

$$K_1^2\geqslant 0; \quad K_2^2\geqslant 0; \quad p_{10}, p_{20}, k_{10}, k_{20}>0; \quad -1\leqslant\cos\theta\leqslant 1.$$

These imply $W\geqslant \text{Max}\,(N+K, \Lambda+\Pi)=N+K$

$$-K_1K_2\leqslant p_{10}p_{20}-2\Delta^2-\tfrac{1}{2}N^2-\tfrac{1}{2}\Lambda^2\leqslant K_1K_2. \tag{2.2}$$

For $N=\Lambda$, $\Pi=K$ (2.2) reduces to $K_1=K_2$; $0\leqslant\Delta^2\leqslant K_1^2$.

2·2. *Breit system* $\boldsymbol{p}_1+\boldsymbol{p}_2=0$.

Define

$$\overline{W}^2=(p_1+p_2)^2=2N^2+2\Lambda^2+4\Delta^2,$$

and

$$\overline{K}^2=\frac{(\overline{W}^2+N^2-\Lambda^2)}{4\overline{W}^2}-N^2=\Delta^2, \qquad \text{if } N=\Lambda.$$

Then

$$p_1 = \left(\frac{W^2+N^2-\Lambda^2}{2W}, 0, 0, K\right), \quad p_2 = \left(\frac{W^2+\Lambda^2-N^2}{2W}, 0, 0, -K\right).$$

Define

$$\omega = \frac{(k_1+k_2)(p_1+p_2)}{2\sqrt{(p_1+p_2)^2}} = \frac{2W^2-K^2-\Pi^2-N^2-\Lambda^2-4\Delta^2}{2W}.$$

Then $q=\frac{1}{2}(k_1+k_2)$ has the value

$$q_0=\omega\,, \qquad q_1=0\,,$$

$$q_2=\left[\omega^2-\frac{2K^2+2\Pi^2+4\Delta^2}{4}-\left\{\frac{2\omega}{4KW}(N^2-\Lambda^2)+\frac{K^2-\Pi^2}{4K}\right\}^2\right]^{\frac{1}{2}},$$

$$q_3=\frac{1}{4K}\left(\frac{2\omega}{W}(N^2-\Lambda^2)+K^2-\Pi^2\right).$$

3. – Dispersion relations.

It is convenient to work with ω and Δ at first. We are interested in the regularity of the transition matrix for $p_1+k_1\to p_2+k_2$ in the upper W-plane To exhibit regularity in W, write T as in (1.1), $q=(k_1+k_2)/2$ and choose the Breit frame, in which p_1 and p_2 depend on Δ but not on ω.

Equation (1.1) coincides with the transition amplitude T_1 when k_1, p_1, k_2, p_2 are possible 4-momenta of a scattering process. But (1.1) also defines T for all real q and for those complex q for which the Laplace transform converges. In this case the resulting function is regular in q and T is obtained as the limit of this function, as $\operatorname{Im} q\to 0$. Due to the support properties of the retarded commutator, which causality requires to be zero outside the forward cone, $T_1(W,\Delta)$ is regular in ω if $\operatorname{Im} q$ is time-like, *i.e.* if $\operatorname{Im} q_0>[(\operatorname{Im} q)^2]^{\frac{1}{2}}$. This makes, the integral converge. Therefore $T_1(W,\Delta)$ can be continued as a regular function of ω in the region R (the forward tube)

$$A\operatorname{Im}\omega > \operatorname{Im}(A\omega^2+B\omega+c)^{\frac{1}{2}}\,, \qquad (R)$$

where

$$A^2=1-\frac{1}{4K^2W^2}(N^2-\Lambda^2)^2>0\,, \qquad B=\frac{2(K^2-\Pi^2)(N^2-\Lambda^2)}{16K^2W}\,,$$

$$C=\frac{K^2}{2}-\frac{\Pi^2}{2}-\Delta^2-\left(\frac{K^2-\Pi^2}{4K}\right)^2.$$

If we consider T as a function of the masses of the K- and π-meson, say ζ and β, then (1.1) defines a function of $(\omega, \Delta, \zeta, \beta)$ regular in (ω, ζ, β) in (R). As usual [1,3,4] we see that (R) is the upper ω-plane if ζ and β are sufficiently small: if $\zeta=\zeta_1+i\zeta_2$, $\beta=\beta_1+i\beta_2$ and $\zeta_2=\beta_2$ the region (R) is

$$\omega_2\left(2A\omega_1+B-\sqrt{2A(2A\omega_1^2+2B\omega_1-\zeta_1-\beta_1-2\Delta^2)}\right)\leqslant\frac{\zeta_2+\beta_2}{2}\leqslant$$

$$\leqslant\omega_2\left(2A\omega_1+B+\sqrt{2A(2A\omega_1^2+2B\omega_1-\zeta_1-\beta_1-2\Delta^2)}\right),$$

$$A\omega_1^2+B\omega_1-\zeta_1/2-\beta_1/2-\Delta^2>0\,.$$

The second condition says: ω_1 is a possible physical energy for masses ζ_1 and β_1. If $\zeta_1=\beta_1<-\Delta^2$, (R) is the region $\omega_2>0$, the upper half plane.

Similarly the advanced amplitude.

$$(3.1)\qquad T_a=\int\langle p_1|\theta(-x)\left[j_K\left(\frac{x}{2}\right),\,j_\pi\left(-\frac{x}{2}\right)\right]|p_2\rangle\exp[iqx]\,\mathrm{d}^4x\,,$$

is regular in the lower-half-plane if $\zeta_1=\beta_1<-\Delta^2$. On the real axis,

$$T_a-T=A_1-A_2=\int\langle p_1|\left[j_K\left(\frac{x}{2}\right),\,j_\pi\left(-\frac{x}{2}\right)\right]|p_2\rangle\exp[iqx]\,\mathrm{d}^4x\,,$$

vanishes for a region $W\neq\Lambda$, $W<\Lambda+\Pi$. So T_1 and T_a continue one-another in the cut plane, and we can take a Cauchy contour round C.

We then get the dispersion relation

$$T(W^2,\Delta^2,\zeta,\beta)=\frac{1}{2\pi i}\int\limits_{-\infty}^{\infty}\frac{[\int\langle p_1|[j_K(x/2),\,j_\pi(-x/2)]|p_2\rangle\exp[iq'x]\,\mathrm{d}^4x]}{\omega'-\omega}\,\mathrm{d}\omega',$$

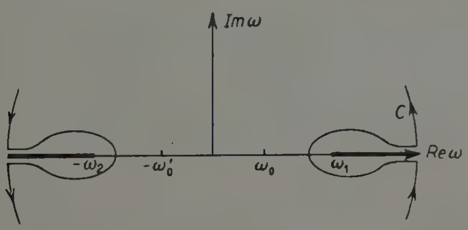

Fig. 3. – Regularity of T in ω'. The poles $-\omega_0'$ and ω_0 are at $W=+N$ and $+\Lambda$ and the cuts are from $W=+(N+K)$, to $-\infty$, and from $W=\Lambda+\Pi$ to $+\infty$.

---

(4) H. J. Bremmermann, R. Oehme and J. G. Taylor: *Phys. Rev.*, **109**, 2178 (1958).

and this can be written

$$(3.2)\quad T(W^2, \Delta^2, \zeta, \beta) = \frac{g_1(\zeta, \beta)}{\omega - \omega_0} + \frac{g_2(\zeta, \beta)}{\omega + \omega_0'} + \frac{1}{2\pi}\int_{\omega_1}^{\infty} \frac{A_1(\Delta, \omega', \zeta, \beta)}{\omega' - \omega}\, \mathrm{d}\omega' + \frac{1}{2\pi}\int_{\omega_2}^{\infty} \frac{A_2(\Delta, \omega', \zeta, \beta)}{\omega' + \omega}\, \mathrm{d}\omega' .$$

Here $g_1(K^2, \Pi^2)$, $g_2(K^2, \Pi^2)$ are related to renormalized coupling constants; $-\omega_0'$, ω_0 are the poles $W = N, \Lambda$ and ω_1, $-\omega_2$ are the beginnings of the cuts. A_1 and A_2 are given by (1.3) and (1.4). The limit $\mathrm{Im}\, W \to 0$ from above gives the retarded function T_1 and the limit from below gives the advanced function T_a. As in (1).(4) (5), we wish to continue both sides of (3.2) to give a physical dispersion relation. Suppose we have shown that $A_{1,2}(\zeta, \beta)$, $g_{1,2}(\zeta, \beta)$ are regular functions of ζ, β in the neighbourhood S of the real axis, from $\zeta = \beta < -\Delta^2$ up to $\zeta = K^2$, $\beta = \Pi^2$. This would continue the left side of (3.2) also, and would define a regular function of W in the upper-half plane. We must then show that this continuation of $T(W, \Delta^2, \zeta, \beta)$ does in fact lead to the physical value defined by (1.1) if $\mathrm{Im}\, \omega \to 0$. This would be true if there is a path in the intersection of the forward tube (R) (where T can be defined as the integral (1.1)), and the domain S, the path such that it leads to $\omega_2 \to 0$, $\zeta_2 \to 0$, $\beta_2 \to 0$, $\zeta_1 = K^2$, $\beta_1 = \Pi^2$ and ω_1 physical. For continuation is unique, and the function in the forward tube has the Fourier transform (1.1) as its limit. There is clearly such a path in R if we keep $\zeta_2 = \beta_2$ and both small enough, provided

$$A\omega_1^2 + B\omega_1 - K^2/2 - \Pi^2/2 - \Delta^2 > 0$$

which is the condition for a physical ω_1. This identifies the T found by continuation of (3.2) as the original Fourier transform (1).

It remains to find out what conditions on the masses are sufficient to ensure that $A_1(\zeta, \beta)$ and $A_2(\zeta, \beta)$ are regular in S. This is done as in Ref. (1,3); for example:

$$(3.3)\quad A_1(\Delta, W, \zeta, \beta) = \sum_\gamma \int \langle 0 | \theta(x_1) \left[f_{\mathrm{P}}\left(\frac{x_1}{2}\right), j_{\mathrm{K}}\left(\frac{-x_1}{2}\right)\right] | \gamma\rangle \exp\left[\frac{i(k_1 - p_1)}{2}\, x_1\right] \mathrm{d}^4 x_1 \cdot \int \langle \gamma | \theta(x_2) \left[j_\pi\left(\frac{x_2}{2}\right), f_\Lambda\left(\frac{-x_2}{2}\right)\right] | 0\rangle \exp\left[\frac{-i(k_2 - p_2)}{2}\, x_2\right] \mathrm{d}^4 x_2 ,$$

1610

where $f_P(x)$, $f_\Lambda(x)$ are the nucleon and Λ currents. Just as in [1,3], we arrive at

$$(3.4)\quad A_1(W, \Lambda^2, \zeta, \beta) = \\ = \int \mathrm{d}u_i\, \mathrm{d}u_{0i}\, \mathrm{d}\varkappa_i^2 \int_0^\pi \mathrm{d}\alpha\, \varphi(u_{i0}, u_i; \varkappa_i^2, \alpha, W) \left(\frac{y_1}{\sqrt{y_1^2 - K_1^2}} + \frac{y_2}{\sqrt{y_2^2 - K_2^2}}\right) \cdot \\ \cdot \frac{1}{y_1 y_2 + \sqrt{y_1^2 - K_1^2}\sqrt{y_2^2 - K_2^2} - K_1 K_2 \cos(\theta - \alpha)}; \qquad i = 1, 2.$$

Here

$$K_1^2 = \left(\frac{W^2 + N^2 - \zeta}{2W}\right)^2 - N^2; \qquad K_2^2 = \left(\frac{W^2 + \Lambda^2 - \beta}{2W}\right)^2 - \Lambda^2,$$

$$y_1 = \frac{u_1^2 + \varkappa^2 + K_1^2(\zeta) - ((N^2 - \zeta)/2W - u_{01})^2}{2u_1};$$

$$y_2 = \frac{u_2^2 + K_2^2(\beta) + \varkappa_2^2 - ((\Lambda^2 - \beta)/2W - u_{20})^2}{2u_2},$$

and u_i, u_{0i}, $\varkappa_i^2$ vary over the region (9) of Ref. [1]

$$0 \leqslant u \leqslant w/2; \qquad -W/2 - u \leqslant u_0 \leqslant W/2 - u,$$

$$\varkappa_1^2 \geqslant \max\left\{0;\, m_1 - \sqrt{(W/2 + u_{10})^2 - u_1^2};\quad m_2 - \sqrt{(W/2 - u_{10})^2 - u_1^2}\right\}, \qquad \begin{aligned} m_1 &= K + 2\Pi, \\ m_2 &= N + \Pi, \end{aligned}$$

$$\varkappa_1^2 \geqslant \max\left\{0;\, m_3 - \sqrt{(W/2 + u_{20})^2 - u_2^2};\, m_4 - \sqrt{(W/2 - u_{20})^2 - u_2^2}\right\}, \qquad \begin{aligned} m_3 &= 3\Pi, \\ m_4 &= \Lambda + \Pi. \end{aligned}$$

For A_2 the masses are $m_1 = 3\Pi$; $m_2 = N + \Pi$; $m_3 = K + 2\Pi$; $m_4 = \Lambda + \Pi$.

Singularities in ζ, β occur if the denominators in (3.4) vanish over the region of integration. In practice, $y_i^2 > K_i^2$ is always satisfied; y_i diverges when $u_i = 0$. To prevent singularities in the kernel of (3.4) we wish y to be bounded below, and so must go to $+\infty$ when $U = 0$ and not $-\infty$. The condition for this is

$$(3.5)\qquad K_{1,2}^2 + \frac{(m_{1,3}^2 - \zeta, \beta)(m_{2,4}^2 - N^2, \Lambda^2)}{W^2 - (m_{1,3} - m_{2,4})^2} > 0\,.$$

This is the condition for NK-NK and $\Lambda\pi$-$\Lambda\pi$ elastic scattering relations to hold for forward at least. Thus both these must be provable for the in-

elastic ones to follow. If (3.5) is not satisfied, y_1 or y_2 can take any value, and so can:

$$Y = y_1 y_2 + \sqrt{y_1^2 - K_1^2}\sqrt{y_2^2 - K_2^2}\,,$$

Then singularities in ζ, β in the kernel

$$\frac{1}{Y - K_1 K_2 \cos(\theta - \alpha)}$$

of (3.4) occur, and the proof fails at this point.

Singularities occur when

$$K_1 K_2 \cos\theta = Y \cos\alpha + i\sqrt{Y^2 - K_1^2 K_2^2}\sin\alpha\,,$$

that is, if Δ is real, when

$$\left(\frac{W^2 + N^2 - \zeta}{2W}\right)\left(\frac{W^2 + \Lambda^2 - \beta}{2W}\right) - 2\Delta^2 - \frac{N^2}{2} - \frac{\Lambda^2}{2} = \pm Y\,.$$

The minimum value of Y is when y_1 and y_2 have their minima, $\zeta = K^2$ and $\beta = \Pi^2$. This is also when the L.H.S. has its greatest modulus. The minimum value of y as u_0, u, $\varkappa^2$ vary over the allowed region, can be calculated in an elementary manner. It turns out then that the continuation in ζ, β of (3.2) is possible if (1)

$$(3.6)\qquad 2\Delta^2 < \left(\frac{W^2 + N^2 - K^2}{2W}\right)\left(\frac{W^2 + \Lambda^2 - \Pi^2}{2W}\right) - \frac{N^2}{2} - \frac{\Lambda^2}{2} + \bar{y}_1\bar{y}_2 + X_1 X_2\,,$$

where

$$X_i^2 = \min\,(y_i^2 - K_i^2)\ (^1)\,;\qquad \bar{y}_i^2 = X_i^2 + K_i^2\,,$$

$$X_1^2 = \frac{(m_1^2 - K^2)(m_2^2 - N^2)}{W^2 - (m_1 - m_2)^2}\,;\qquad X_2^2 = \frac{(m_3^2 - \Pi^2)(m_4^2 - \Lambda^2)}{W^2 - (m_3 - m_4)^2}\,.$$

The one nucleon intermediate state has not been treated in detail, but it gives no trouble (4).

Eq. (3.6) must hold for all values of W in the range of the dispersion integral. This is true of N, P, π^0, π^-; $\gamma P \to \pi P$ (3) and our model $KN\Lambda\pi$.

The condition for a physical scattering is $W \geqslant K+N$. When $W=K+N$

$$N\left(\frac{(N+K)^2+\Lambda^2-\Pi^2}{2(N+K)}\right)=2\Delta^2_{\text{thresh}}+\frac{N^2}{2}+\frac{\Lambda^2}{2},$$

and in order to prove a physical dispersion we must have (3.6) holding for this value of Δ; that is to say, we must have

$$(3.7)\quad N\left(\frac{(N+K)^2+\Lambda^2-\Pi^2}{2(N+K)}\right)<\left(\frac{W^2+N^2-K^2}{2W}\right)\left(\frac{W^2+\Lambda^2-\Pi^2}{2W}\right)+\bar{y}_1\bar{y}_2+X_1X_2\,.$$

A similar, but not identical, condition is sufficient for $(\pi\text{N}, \Lambda\text{K})$ relations to be proved.

We will now suppose the masses are such that (3.7) holds for $\text{NK}\to\Lambda\pi$ and $\pi\text{N}\to\Lambda\text{K}$. Then we have dispersion relations proved for this model, and there is an unphysical region to interpret.

4. – The unphysical region.

In our model with $N+2\Pi>K+\Lambda$ the unphysical region is $\Lambda+\Pi\leqslant W<$ $<N+K$ for A_1, and $N+\Pi\leqslant W<\Lambda+K$ for A_2. The values of Δ to be put in the unphysical region in (3.2) are given by the continuation of $A_{1,2}(W, \Delta, \zeta, \beta)$ defined for $\zeta+\beta<-\Delta^2$ by eqns. (1.3) and (1.4).

Consider A_1 in detail: A_2 is treated similarly. For $W<K+N$, A is given by (3.3) with $|\gamma\rangle=|\Lambda',\pi'\rangle$. For $\sqrt{\zeta}+N<W$ let us consider

$$(4.1)\qquad -\int\langle 0|\theta(x)\left[f_N\left(\frac{x}{2}\right), j_K\left(\frac{-x}{2}\right)\right]|\Lambda',\pi',\gamma\rangle\exp\left[i(k_1-p_1)\frac{x}{2}\right]\mathrm{d}^4x\,,$$

which is the first factor in (3.3). We can choose k_1, p_1 real. Then (4.1) can be expressed, by the usual methods [6], as

$$(4.2)\qquad -\int\langle p_1|\theta\left[j_K\left(\frac{x}{2}\right), j_\pi\left(\frac{-x}{2}\right)\right]|\Lambda'\rangle\exp\left[i(k_1+\pi')\frac{x}{2}\right]\mathrm{d}^4x\,,$$

$$\Lambda'=(\Lambda_0', K_2(\sin\varphi'\sin\theta', \cos\varphi'\sin\theta', \cos\theta'))\,;\qquad \Lambda_0'=\frac{W^2+\Lambda^2-\Pi^2}{2W}\,.$$

([5]) N. N. Bogoljubov, B. V. Medvedov and M. K. Polivanov: translated lecture notes.

([6]) H. Lehmann, K. Symanzik and W. Zimmermann: *Nuovo Cimento*, 10, 319 (1957).

1613

We suppose the continuation up to $\beta = \Pi^2$ to be made. This is always possible for some ζ. Then (4.2) is, by definition (centre of mass frame):

$$T_1(W^2, \Lambda'^2(\zeta, \theta'), \zeta, \beta = \Pi^2)\,,$$

where the momentum transfer depends on the intermediate state Λ' as

$$(4.3)\quad \Delta_1'^2(\zeta, \theta') = -\frac{1}{4}\left(N^2 + \Lambda^2 + 2K_1(\zeta)K_2\cos\theta' - \left(\frac{W^2+N^2-\zeta}{2W}\right)\left(\frac{W^2+\Lambda^2-\Pi^2}{2W}\right)\right),$$

and $\sum_\gamma$ of (3.3) means

$$\int \frac{K_2(\zeta)}{2W}\sin\theta' \mathrm{d}\theta' \mathrm{d}\varphi' :$$

The second factor in the expression (3.3) for A is

$$(4.4)\qquad -\int \langle \Lambda'\pi' | \theta \left[j_\pi\left(\frac{x}{2}\right), f_\Lambda\left(\frac{-x}{2}\right)\right] | 0 \rangle \exp\left[\frac{-ik_2 - p_2}{2}\, x\right] \mathrm{d}^4x =$$
$$= T_{\Lambda\pi}\,(W, \Delta''(\theta, \theta', \varphi', \zeta))\,.$$

By Lorentz invariance, $T_{\Lambda\pi}$ depends only on W and

$$\Delta''(\theta, \theta', \varphi', \zeta) = \frac{-1}{4}\,(p_2 - \Lambda')^2 =$$
$$= \frac{-1}{4}\left(2\Lambda^2 - 2\left(\frac{W^2+\Lambda^2-\Pi^2}{2W}\right)^2 - K_2^2(\sin\theta\sin\theta'\cos\varphi' + \cos\theta\cos\theta')\right).$$

If k_2 and p_2 are physical 4-vectors, $T_{\Lambda\pi}$ is the scattering amplitude $(1/2)\pi\langle\Lambda\pi|\Lambda\pi\rangle$ for physical values of the parameters, and is thus known from experiment. Actually we need only bother with $\Lambda + \Pi \leqslant W < K + N$. The condition for k_2 and p_2 to be real is found easily. From Section 2·1

$$p_2 = (p_{20}, 0, K_1\sin\theta, K_2\cos\theta)\,, \qquad k_2 = (k_{20}, 0, -K_2\sin\theta, -K_2\cos\theta)\,.$$

The angle θ is given by

$$(4.3)^*\qquad K_1K_2\cos\theta = p_{10}p_{20} - \tfrac{1}{2}N^2 - \tfrac{1}{2}\Lambda^2 - 2\Delta^2\,.$$

So p_2 and k_2 are real provided K_1 is real $(\sqrt{\zeta} < W - N)$ and $-1 \leqslant \cos\theta \leqslant 1$,

and in this case we have the equation (1.9)* at ζ:

$$(4.5)\quad A_1(W, \Delta(\theta, \zeta), \zeta) = -2\pi\cdot$$
$$\cdot\int \frac{K_2}{2W}\,\mathrm{d}(\cos\theta')\,\mathrm{d}\varphi'\, T_1(W, \Delta_1'(\theta', \zeta), \zeta)\, T_{\Delta\pi}(W, \Delta''(\theta(\zeta), \theta', \varphi')) ,$$

$\Delta(\theta, \zeta)$ is given by (4.3).

In order to get (1.14) we wish to use the dispersion relation (3.2) for each $T_1(W, \Delta(\theta', \zeta), \zeta)$ in the range of θ' integration. The dispersion relation

$$T_1(W, \Delta'(\theta', \zeta), \zeta) = \frac{1}{2\pi}\int \frac{A_1(W', \Delta'(\theta', \zeta), \zeta)\,\mathrm{d}\omega'}{\omega' - \omega} + \frac{1}{2\pi}\frac{A_2(W', \Delta'(\theta', \zeta), \zeta)}{\omega' + \omega}\,\mathrm{d}\omega' +$$
$$+\ \text{bound states},$$

will be valid provided we can continue (3.2) to this value of ζ and Δ. (In particular we are interested in continuing up to $\zeta = K^2$.) Eq. (4.5) then becomes

$$(4.5^*)\quad A_1(W, \Delta(\theta, \zeta), \zeta) = -2\pi\int \frac{K_2}{2W}\, T_{\Delta\pi}(W, \Delta''(\theta, \theta', \varphi'))\cdot$$
$$\cdot\left[\text{B.S.} + \frac{1}{2\pi}\int \frac{A_1(W', \Delta_1'(\theta', \zeta), \zeta)}{\omega' - \omega}\,\mathrm{d}\omega' + \frac{1}{2\pi}\int \frac{A_2(W', \Delta_1'(\theta', \zeta), \zeta)}{\omega' + \omega}\,\mathrm{d}\omega'\right]\mathrm{d}(\cos\theta')\,\mathrm{d}\varphi',$$

and it can be continued in ζ *keeping* θ *fixed*, provided $A_i(W, \Delta(\theta, \zeta), \zeta)$ is regular in ζ up to K^2 for all $-1 \leqslant \cos\theta \leqslant 1$. This is continuation in (ζ, Δ) along the path (4.3).

We can continue $A_1(W')$ of (4.5)* provided

$$(4.6)\quad \left(\frac{W'^2 + N^2 - \zeta}{2W'}\right)\left(\frac{W'^2 + \Lambda^2 - \Pi^2}{2W'}\right) - 2\Delta_1'^2(W, \zeta, \theta') -$$
$$-\frac{\Lambda^2}{2} - \frac{N^2}{2} \neq Y_1' \cos\alpha + i\sqrt{Y_1'^2 - K_1'^2 K_2'^2}\,\sin\alpha ,$$

and for A_2

$$(4.7)\quad \left(\frac{W'^2 + N^2 - \Pi^2}{2W'}\right)\left(\frac{W'^2 + \Lambda^2 - \zeta}{2W'}\right) -$$
$$-2\Delta_1'^2(W, \theta', \zeta) - \frac{\Lambda^2}{2} - \frac{N^2}{2} \neq Y_2' \cos\alpha + i\sqrt{Y_1'^2 - K_1'^2 K_2'^2}\,\sin\alpha .$$

1645

For an intermediate state $|\gamma\rangle$ (4.6) reads, using (4.3)

$$(4.8)\qquad K_1K_2\cos\theta' + \left(\frac{W'^2+N^2-\zeta}{2W'}\right)\left(\frac{W'^2+\Lambda^2-\Pi^2}{2W'}\right) - \\ -\left(\frac{W^2+N^2-\zeta}{2W}\right)\left(\frac{W^2+\Lambda^2-\Pi^2}{2W}\right) \neq Y'\cos\alpha + i\sqrt{Y'^2-K_1'^2K_2'^2}\sin\alpha\,.$$

It is shown in the Appendix that the worst case is when $W'=\Lambda+\Pi$ and $\zeta=K^2$. Then $K_2'=0$, $K_1^2=0$ and for singularities

$$\sin\alpha=\frac{|K_1|K_2}{Y'}\,;\qquad \sin^2\alpha=\frac{-K_1^2K_2^2}{Y'^2}\,.$$

Then (4.8) becomes $(W'=\Lambda+\Pi)$

$$(4.9)\qquad \left(\frac{W^2+N^2-K^2}{2W}\right)\left(\frac{W^2+\Lambda^2-\Pi^2}{2W}\right)<\left(\frac{W'^2+N^2-K^2}{2W'}\right)\Lambda+\sqrt{Y'^2+K_1^2K_2^2}\,.$$

We would like to use (4.5) for each value of W in $\Lambda+\Pi\leqslant W<K+N$. At the top of the range $W=K+N$ and $K_1=0$. Then (4.9) reduces to (3.7), the condition (assumed to hold) for $\mathrm{NK}\to\Lambda\pi$ relations to be proved. For W at the bottom of the range, $W=\Lambda+N$, $K_2=0$ and (4.9) is satisfied *a fortiori*. It is shown in the Appendix that (4.9) is satisfied for all W in between as well. So for each (W,θ) we can continue (4.5) up to $\zeta=K^2$ to obtain the equation (1.14). In this equation $d\theta'$ is an integral in the Δ'^2 plane, the path being defined by $\zeta=K^2$ and $-1\leqslant\cos\theta'\leqslant 1$ in (4.3). Δ is any complex value on the path. The path in (1.15) is slightly different.

* * *

Acknowledgment is due to Dr. J. C. TAYLOR for many critical discussions. We would also like to thank Prof. A. SALAM for suggesting the investigation.

APPENDIX

We must show that

$$K_1K_2\cos\theta+\left(\frac{W'^2+N^2-\zeta}{2W'}\right)\left(\frac{W'^2+\Lambda^2-\Pi^2}{2W'}\right)-\left(\frac{W^2+N^2-\zeta}{2W}\right)\left(\frac{W^2+\Lambda^2-\Pi^2}{2W}\right)\neq \\ \neq Y'\cos\alpha+\sqrt{Y'^2-K_1'^1K_2'^2}\sin\alpha\,,$$

for any $0\leqslant\alpha\leqslant\pi$, $0\leqslant\theta\leqslant\pi$, $W'>\Lambda+\Pi$, $\zeta\leqslant K^2$ and $\Lambda+\Pi\leqslant W\leqslant K+N$

and u_0, u_1, $\varkappa^2$ in the region of integration.

1616

K is pure imaginary. The worst case is when $\cos\theta = \pm 1$ for then $\sin\alpha$ is largest, and $Y'\cos\alpha$ smallest. Then

$$\sin\alpha = \frac{|K_1|K_2}{\sqrt{Y'^2 - K_1'^2 K_2'^2}},$$

and for a singularity

$$\left(\frac{W'^2 + N^2 H \zeta}{2W'}\right)\left(\frac{W'^2 + \Lambda^2 - \Pi^2}{2W'}\right) - \left(\frac{W^2 + N^2 - \zeta}{2W}\right)\left(\frac{W^2 + \Lambda^2 - \Pi^2}{2W}\right) = \pm Y'\cos\alpha\,.$$

The minus sign on the R.H.S. is the worst case. $\cos\alpha$ is smallest when $Y'^2 - K_1'^1 K_2'^2$ is smallest, which is when $W' = \Lambda + \Pi$. This is also when Y' and

$$\left(\frac{W'^2 + N^2 - \zeta}{2W'}\right)\left(\frac{W'^2 + \Lambda^2 - \Pi^2}{2W'}\right),$$

are smallest. So the worst case is $W' = \Lambda + \Pi$, $K_2^2 = 0$. Then we get, for no singularities

$$\text{(A.1)}\qquad \left(\frac{W^2 + N^2 - \zeta}{2W}\right)\left(\frac{W^2 + \Lambda^2 - \Pi^2}{2W}\right) < \\ < \left(\frac{W'^2 + N^2 - \zeta}{2W'}\right)\left(\frac{W'^2 + \Lambda^2 - \Pi^2}{2W'}\right) + \sqrt{Y'^2 + K_1^2 K_2^2}\,.$$

Coeff. of $-\zeta$ on R.H.S. is

$$\frac{1}{2W'}\left(\frac{W'^2 + \Lambda^2 - \Pi^2}{2W'}\right) = \frac{1}{4} + \frac{1}{4}\frac{(\Lambda^2 - \Pi^2)}{(\Lambda + \Pi)^2} > \frac{1}{4} + \frac{\Lambda^2 - \Pi^2}{4W^2},$$

the last being the coeff. of $-\zeta$ on the L.H.S. Hence these terms have the worst case when ζ is largest. This is also true of Y' and $K_1^2 K_2^2$. Hence, as stated in the text, $\zeta = K^2$ is the worst case.

If $\zeta = K^2$ (A.1) becomes, on writing $a = \Lambda\left(((\Lambda + \Pi)^2 + N^2 - K^2)/2(\Lambda + \Pi)\right)$

$$\text{(A.1*)}\qquad \sqrt{K_1^2 + N^2}\sqrt{K_2^2 + \Lambda^2} < a + \\ + \sqrt{Y'^2 + K_1^2 K_2^2}\,,$$

or

$$\text{(A.2)}\qquad K_1^2\Lambda^2 + K_2^2 N^2 + N^2\Lambda^2 + \\ + a^2 - 2a\sqrt{K_1^2 + N^2}\sqrt{K_2^2 + \Lambda^2} < Y'^2\,.$$

The L.H.S. of (A.2) is of the form $Q(W^2)/W^2 + B$ where Q is quadratic in

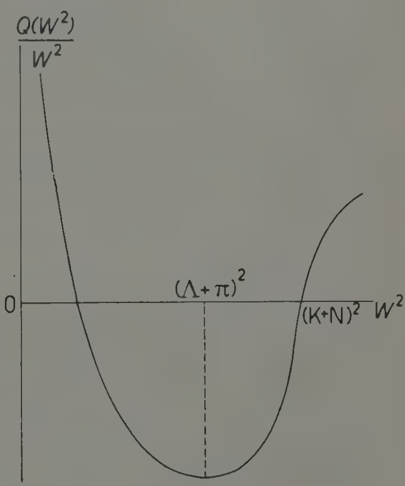

Fig. 4.

W^2. Hence the graph of the L.H.S. of (A.2) is as shown (Fig. 4). In the text it was shown that the value at $W^2 = (K+N)^2$ was $< Y'^2$ but bigger than the value at $W = \Lambda + \Pi$.

Hence the value at $W = K + N$ from the graph, is larger than any value in $\Lambda + \Pi \leqslant W \leqslant K + N$ and $W = K + N$ is the worst case.

RIASSUNTO (*)

Si scrivono le condizioni imposte alle masse di quattro particelle in modo tale che coi metodi oggi in uso si possono dimostrare le relazioni di dispersione per processi del tipo $A+B \to C+D$. Una condizione necessaria è che si possano dimostrare le due relazioni elastiche $A+B \to A'+B'$ e $C+D \to C'+D'$ almeno per lo scattering in avanti. Le masse del p, n, π^-, π^0 soddisfano alle suddette condizioni ed anche alla produzione dei fotomesoni, ed al modello del sistema dei mesoni K, $K = 3\Pi/2$, $\Pi \simeq N$ (dove queste sono le masse delle particelle). Servendosi delle relazioni di dispersione e della condizione di unitarietà per la regione non fisica di questo sistema preso come modello, si ottengono delle equazioni integrali per la regione non fisica, in $KN \to \Lambda\pi$; si hanno soluzioni di tali equazioni in termini di elementi di matrice S fisici. Si può anche costruire un modello di sistema $KN \to KN$ che consente di dimostrare con metodi usuali le consuete relazioni di dispersione ed anche tutte le relazioni anelastiche che nel metodo seguito dal presente lavoro occorrono per descrivere la regione non fisica. Tuttavia, si può costruire un modello che consente di provare le relazioni di dispersione, ma tale che la loro regione non fisica non può essere descritta coi metodi attuali.

(*) *Traduzione a cura della Redazione.*

IL NUOVO CIMENTO Vol. XIII, N. 1 1° Luglio 1959

Antiproton Annihilation in Nuclear Emulsion (*).

A. H. Armstrong and G. M. Frye, Jr. (**)

Los Alamos Scientific Laboratory, University of California
Los Alamos, N. Mex.

(ricevuto il 23 Febbraio 1959)

Summary. — Sixteen antiproton stars observed in an emulsion stack exposed at the Berkeley Bevatron to a beam of negative particles of momentum 700 MeV/c have been analyzed in detail. It is found that in the «elementary» antiproton-nucleon annihilation an average of (4.7 ± 0.6) mesons are produced, each with an average total energy of (348 ± 28) MeV. No strange particles were observed as annihilation products.

1. – Introduction.

Up to the present time the most detailed information on the annihilation of antiprotons has come from the study of annihilation stars in nuclear emulsions [1-4]. Although the annihilation usually takes place in one of the emulsion nuclei other than hydrogen so that nucleons and nuclear fragments are

---

(*) Work performed under the auspices of the U.S. Atomic Energy Commission.

(**) Now with U.S. Atomic Energy Commission, Division of Research, Washington, D.C.

(1) W. H. Barkas, R. W. Birge, W. W. Chupp, A. G. Ekspong, G. Goldhaber, S. Goldhaber, H. H. Heckman, D. H. Perkins, J. Sandweiss, E. Segrè, F. M. Smith, D. H. Stork, L. van Rossum, E. Amaldi, G. Baroni, C. Castagnoli, C. Franzinetti and A. Manfredini: *Phys. Rev.*, **105**, 1037 (1957). (Antiproton Collaboration Experiment).

(2) E. Amaldi, C. Castagnoli, M. Ferro-Luzzi, C. Franzinetti and A. Manfredini: *Nuovo Cimento*, **5**, 1797 (1957).

(3) A. G. Ekspong, S. Johansson and B. E. Ronne: *Nuovo Cimento*, **8**, 84 (1958).

(4) A. G. Ekspong: *Proceedings of the Seventh Rochester Conference*, Chap. X-18 (1957).

observed in addition to mesons, the following conclusions have been reached about the antiproton-nucleon process:

1) The products of the « elementary annihilation act » are charged and neutral pions;
2) The average number of mesons per annihilation is 5 ± 0.5;
3) The average pion total energy is 340 MeV;
4) K-mesons are produced in less than 5% of the annihilation events.

The pion multiplicity of 5 is larger than predicted by the Fermi statistical theory and an interaction volume 20 times the usual volume is required to give this multiplicity. Also the Fermi model predicts $K\overline{K}$ production in $\sim 10\%$ of the annihilation events. There have been several recent theoretical attempts to modify the Fermi theory so as to explain the large pion multiplicity without using such a large interaction volume [5-10].

In this paper we present the results of detailed measurements on 16 antiproton annihilation events which further substantiate the above conclusions. Two of these events gave experimental evidence for the production of a neutral pion and have been reported in detail earlier [11,12]. They are included here for completeness.

2. – Experimental method and plate analysis.

A stack of 180 Ilford G-5 emulsions, 600 μm thick, was exposed in May 1956 at the Bevatron. Negative particles of momentum 700 MeV/c produced in the forward direction by 6.2 GeV protons incident on a Cu target were focussed on the stack. Further details of the experimental arrangement are given in reference one. At this momentum mesons have minimum ionization while particles of protonic mass have an ionization of twice minimum. An « along the track » scan was made 5 mm from the entrance edge of the stack for tracks which had an ionization $(1.5 \div 2.3) I_0$ and an angle within 5° of the beam direction as defined by the large number of minimum ionization tracks. None of the antiproton tracks had an angle which differed by more than 2° from the beam angle.

(5) N. Yajima and K. Kobayakawa: *Prog. Theor. Phys.*, **19**, 192 (1958).
(6) Z. Koba and G. Takeda: *Prog. Theor. Phys.*, **19**, 269 (1958).
(7) M. Kretzschmar: *Zeits. f. Phys.*, **150**, 247 (1958).
(8) P. P. Srivastava and G. Sudarshan: *Phys. Rev.*, **110**, 765 (1958).
(9) E. Eberle: *Nuovo Cimento*, **8**, 610 (1958).
(10) T. Gotō: *Nuovo Cimento*, **8**, 625 (1958).
(11) G. M. Frye Jr. and A. H. Armstrong: *Phys. Rev.*, **110**, 170 (1958).
(12) G. M. Frye Jr.: *Phys. Rev. Letters*, **1**, 14 (1958).

Of the sixteen antiproton events found, nine were at rest and seven in flight. Each prong of the resultant annihilation was identified as completely as possible. For the prongs which ended in the stack a gap length *vs.* range measurement was made if enough track length was available; otherwise the particle was assumed to be a proton. For tracks which left the stack the g^* *vs.* $p\beta$ method was used. The scattering was measured by the sagitta method for tracks with a dip angle $< 20°$. For steeper tracks the surface angle method was employed [1]. Ionization was determined by blob counting ($g^* < 2.5$) or gap length ($g^* > 2.5$).

The density of samples of the stack was determined [13] just after the exposure and found to differ by less than 0.5% from the standard density of 3.815 g/cm³. Thus the range-energy relationship of BARKAS *et al.* [14] was used directly to obtain the energy of stopping tracks. The thickness of each pellicle was also measured before development.

A question of special importance is the determination of the detection efficiency for finding prongs of minimum ionization from the annihilation stars. Each of our events was carefully studied by at least three different observers. In an attempt to see how often a minimum ionization track could be found originating at a point, 129 μ-e endings in the same stack were examined and the electron was found in 128 of them. This test suffers from two defects: 1) the electrons are of « plateau » ionization, whereas pions may be of minimun ionization which for this stack was 0.90 of the plateau value; 2) there is a « psychological » difference in examining μ endings and annihilation stars, because in the former case one knows there is one and only one decay electron, while for the latter the number of charged pions from an annihilation event can vary from zero to six [15]. However, since the μ-e electrons were seen quite easily (in the one exception the μ ending was near the bottom of the emulsion), we conclude that all the minimum ionization prongs were detected. One reason for this success in finding minimum tracks may be that we were fortunate in having very fresh emulsion. Only two weeks elapsed between manufacture and development and the single grain and slow electron background was correspondingly low.

3. – Results.

A summary of the results of the measurements on the annihilation stars is given in Table I. To facilitate comparison the notation is the same as used

---

(13) A. J. OLIVER: *Rev. Sci. Instr.*, **25**, 326 (1954); UCRL-5077 (1958).

(14) W. H. BARKAS, P. H. BARRETT, P. CÜER, H. HECKMAN, F. M. SMITH and H. K. TICHO: *Nuovo Cimento*, **8**, 185 (1958).

(15) Six prongs of near minimum ionization is the greatest number we have seen in a later $\overline{p}$ stack.

1651

TABLE I. – *Details of the individual antiproton stars.*

Event number	Anti-proton energy $T_{\bar{p}}$	Number of charged pions $N_{\pi^\pm}$	Charged pion kinetic energies $T_{\pi^\pm}$	Sum of pion total energies $\Sigma E_{\pi^\pm}$	Number of heavy prongs N_H	Total heavy prong energy ΣE_H	Total visible energy $E_{vis} = \Sigma E_\pi + \Sigma E_H$	E_{vis}/W ($W = 2M_pc^2 + T_{\bar{p}}$)	Number of neutral pions N_{π^0}	Lower limit of π^0 total energy $E_{\pi^0} >$
1-101-4	0	5	315 ± 110 245 ± 75 215 ± 60 150 ± 45 70 ± 20	1693	2	27	1720	0.92		
1-69-6	0	4	310 ± 110 175 ± 50 110 ± 20 $95\ (\pi^+)$	1248	2	23	1271	0.68		
1-95-2	0	3	250 ± 75 > 175 160 ± 50	> 1004	2	162	> 1166	> 0.62		
1-74-4	0	3	350 ± 60 65 ± 20 $48\ (\pi^+)$	882	4	381	1263	0.68		
1-91-1	9	2	> 250 40 ± 10	> 569	5	405	> 974	> 0.52		
1-136-4	0	2	160 ± 20 $70\ (\pi^-)$	509	4	212	721	0.39		
1-60-9	0	2	140 ± 40 $59\ (\pi^-)$	478	4	73	551	0.29		

1652

1-99-3	0	1	340 ± 70	480	8	208	688	0.37		
1-131-3 [a]	0	0	0	0	0	0	0	0	1	231
1-82-2	190	5	360 ± 110 340 ± 100 70 ± 20 36 (π^-) 26 (π^-)	1530	9	496	2026	0.98		
1-85-3 [b]	110	3	495 ± 138 488 ± 131 74 (π^+)	1476	4	280	1756	0.89	1	190
1-46-3	206	3	~ 500 215 ± 85 13.6 (π^-)	1147	0	0	1147	0.55		
1-86-1	185	3	425 ± 130 130 ± 40 70 ± 20	1044	3	74	1118	0.54		
1-118-1	179	2	> 190 100 ± 30	> 569	12	569	> 1138	> 0.56		
1-80-2	184	1	230 ± 40	370	7	228	598	0.29		
1-106-4 [c]	203	0	0	0	3	79	79	0.04		
		$\Sigma N_{\pi^\pm}=39$ $\overline{N}_{\pi^\pm}=$ $=2.44\pm0.39$	$\overline{T}_{\pi^\pm}=$ $=194\pm24$ MeV							

([a]) Reference ([18]).
([b]) Reference ([11]).
([c]) This event could be a proton collision star since $E_{vis} < T_{\bar{p}}$.

in the Antiproton Collaboration Experiment (ACE) (1). The total energy E includes the rest energy in the case of the pions and a binding energy of 8 MeV per nucleon for the heavy particles. The visible energy per star is $E_{\text{vis}} = \Sigma E_\pi + \Sigma E_{\text{H}}$. The energy available to the annihilation star is $W = 2M_{\bar{p}}c^2 + T_{\bar{p}}$, where $T_{\bar{p}}$ is the kinetic energy of the antiproton. The kinetic energies of the pions, T_π, are given individually. In four cases it was possible only to make an estimate or to set an upper limit to the meson energy. These values will be treated as actual values rather than limits in computing the average meson energy. The average number of charged pions per event is

$$\bar{N}_{\pi^\pm} = 2.44 \pm 0.39 \,,$$

and the average pion total energy is

$$\bar{E}_{\pi^\pm} = (334 \pm 24) \text{ MeV} \,.$$

Eight mesons stopped in the stack, 3 π^+'s and 5 π^-'s.

In the two events where evidence was found for neutral pion emission, only a lower limit on the π^0-energy may be set, since one γ-ray from the π^0-decay remains undetected. This energy is not included in the « visible » energy.

Although a careful search was made, no K-mesons or hyperons were observed.

4. – Conclusions.

The average energy of the charged pions, $\bar{E}'_{\pi^\pm}$, and the average number of charged and neutral pions, $\bar{N}_\pi$, emitted in the « elementary » antiproton-nucleon annihilation can be calculated from the observed number of heavy prongs and their energies combined with other experimental information on the interaction of π-mesons in nuclear emulsion. Energy will be transmitted to the nucleus if a pion is absorbed or inelastically scattered. To find the total energy received by the nucleus, an estimate must be made of the amount carried away by neutrons. The procedure followed (1) is to divide the protons into two groups: 1) $T_p > 35$ MeV; and 2) $T_p < 35$ MeV. The protons in the first group are assumed to arise from a knock-on process and a similar energy spectrum is taken for knock-on neutrons, multiplied by a factor of 1.2, the n/p ratio in emulsion. The average knock-on energy per star for our sixteen events is $U_{k0} = 191$ MeV. Protons in the second group exhibit an evaporation type spectrum and it is assumed that four times as many neutrons are emitted as protons with an average kinetic energy of 3 MeV. The average evaporation

energy per star is $U_{\text{evap}} = 195$ MeV. Thus the average total energy U transferred to the nucleus is

$$U = U_{k0} + U_{\text{evap}} = 386 \text{ MeV} .$$

It has been shown [1,3] that if charge independence is assumed the following relations hold:

$$U = \nu \overline{E}'_{\pi^\pm} + b\nu E_0 ,$$

$$\overline{N}_{\pi^\pm} \overline{E}_{\pi^\pm} = (\overline{N}_{\pi^\pm} - \tfrac{2}{3} b\nu)\overline{E}'_{\pi^\pm} + \tfrac{2}{3} b\nu E_0 ,$$

where ν is the number of mesons which interact with the nucleus, b is the fraction of the interacting mesons which is inelastically scattered, and E_0 is the total energy of a meson which has been inelastically scattered. E_0 and b may be estimated from meson interaction experiments [1] as $b = 0.25$ and $E_0 = 180$ MeV (the calculation is insensitive to E_0). Then

$$\nu = 1.3 ,$$

$$\overline{E}'_{\pi^\pm} = (348 \pm 28) \text{ MeV} .$$

And, if one again assumes charge independence, the average number of pions produced in the « elementary » antiproton-nucleon annihilation is

$$\overline{N}_{\pi} = \tfrac{3}{2} \overline{N}_{\pi^\pm} + \nu(1 - b) = 4.7 \pm 0.6 .$$

These values of $\overline{E}_{\pi^\pm}$ and $\overline{N}_{\pi}$ are compared in Table II with previous results. They are in agreement within the stated statistical accuracy.

TABLE II. – *A comparison of the results from various experiments of* $\overline{N}_{\pi}$, *the average number of pions emitted in the antiproton-nucleon annihilation; and* $\overline{E}'_{\pi^\pm}$, *the average energy of the charged mesons emitted in the antiproton-nucleon annihilation. All energies are in* MeV.

	Ref. (1)	Ref. (3)	Ref. (4)	This work
$\overline{N}_{\pi}$	5.3 ± 0.6	5.1 ± 1.0	4.7 ± 0.4	4.7 ± 0.6
$\overline{E}'_{\pi^\pm}$	(346 ± 20) MeV	283 MeV	343 MeV	(348 ± 28) MeV

* * *

The authors would like to thank Dr. E. J. LOFGREN and his team for use of the Bevatron facilities, Dr. HARRY HECKMAN for assistance in making the

exposure, and Mr. A. J. OLIVER and Dr. R. S. WHITE for the development of the stack. Dr. LOUIS ROSEN encouraged the experiment throughout. The plate analysis would not have been possible without the untiring efforts of Mmes. PAT AGEE, DAGNY DERR, MARTHA DOWNS, MARY HOUSLEY, OPAL MILLIGAN, VIRGINIA STOVALL, MARJORIE WORK, MARY WORMAN, and Mr. PETER VANDERVOORT.

RIASSUNTO (*)

Si sono dettagliatamente analizzate sedici stelle di antiprotoni osservate in un pacco di emulsioni esposte nel Bevatrone di Berkeley a un fascio di particelle negati vedi 700 MeV/c. Si trova che nell'annichilamento antiprotone-nucleone elementare si produce una media di (4.7 ± 0.6) mesoni, ciascuno di energia totale media di (348 ± 28) MeV. Non furono osservate particelle strane fra i prodotti di annichilamento.

(*) *Traduzione a cura della Redazione.*

IL NUOVO CIMENTO Vol. XIII, N. 1 1° Luglio 1959

Effect of $\overline{\mathrm{K}}^0$-K^- Mass Difference on K^--N Interactions at Low Energies.

J. D. Jackson and H. W. Wyld, Jr.
University of Illinois - Urbana, Illinois

(ricevuto il 2 Marzo 1959)

Summary. — The R matrix formalism of Wigner and Eisenbud is used to modify the zero range S wave analysis of the scattering and absorption of K^--mesons on protons proposed by Jackson, Ravenhall and Wyld so as to take into account the kinematical effects of the $\overline{\mathrm{K}}^0$-K^- mass difference. It is found that even with a mass difference, the elastic, charge exchange, and absorption cross sections can be expressed in terms of two complex scattering lengths. The elastic and absorption cross sections exhibit cusps at the threshold for charge exchange scattering. The shape of the cusps can be used to distinguish between otherwise indistinguishable sets of scattering lengths. If the $\overline{\mathrm{K}}^0$ and K^- have opposite parities there is no cusp in the elastic scattering cross section, so that in principle it is possible to determine the relative parity of K^0 and K^- from the energy dependence of the K^- scattering cross section.

1. – Introduction.

Analysis of recent bubble chamber experiments at Berkeley (1) on the charge exchange scattering of K^- mesons on protons,

$$\mathrm{K}^- + \mathrm{p} \to \overline{\mathrm{K}}^0 + \mathrm{n}\,,$$

has shown the $\overline{\mathrm{K}}^0$ meson to be heavier than the K^- meson,

$$m_{\overline{\mathrm{K}}^0} - m_{\mathrm{K}^-} = (3.9 \pm 0.6)\ \mathrm{MeV}\,,$$

(1) A. H. Rosenfeld, F. T. Solmitz and R. D. Tripp: *Phys. Rev. Lett.*, **2**, 110 (1959). F. S. Crawford, M. Cresti, M. L. Good, M. L. Stevenson and H. K. Ticho: *Phys. Rev. Lett.*, **2**, 112 (1959).

so that the charge exchange scattering is actually an endothermic reaction with a threshold of 8.0 MeV incident energy.

This breakdown in charge independence presumably has its origin in electromagnetic effects similar to those responsible for the n-p and $\pi^{\pm}-\pi^0$ mass difference although it is difficult to understand even the sign of the mass difference in this way let alone calculate its magnitude. Another possibility has been envisaged by PAIS (2), who has investigated the consequences of assuming that the K^- and $\overline{K}^0$ have opposite parities. In such a theory the K^-, $\overline{K}^0$ mesons do not form an isotopic spin doublet and there is no reason that they should have the same mass.

Leaving aside this deeper theoretical problem of the origin of the mass difference, we assume that the K^-, $\overline{K}^0$ form an approximate isotopic spin doublet. The existence of a mass difference will have certain essentially kinematic effects, not only on the charge exchange scattering, but also on the elastic scattering,

$$K^- + p \to K^- + p \, .$$

and reactions

$$K^- + p \to \begin{cases} \Lambda^0 + \pi^0 \\ \Sigma^0 + \pi^0 , \qquad \Sigma^{\pm} + \pi^{\pm} \end{cases}$$

at very low energies.

It is our aim to investigate these effects along the lines of the zero range S wave analysis proposed by JACKSON, RAVENHALL and WYLD (3) and employed by ASCOLI, HILL and YOON (4) and DALITZ (5) in an analysis of the K^- scattering and absorption on protons. These authors have shown that the low energy scattering and absorption of K^- on protons can be characterized by two complex scattering lengths

$$A_T = a_T + ib_T \tag{1}$$

related to the corresponding complex S wave phase shifts by

$$\operatorname{tg} \delta_T = kA_T \, , \tag{2}$$

where $T = 0$ or 1 is the isotopic spin. In particular DALITZ (5) has shown

---

(2) A. PAIS: *Phys. Rev.*, **112**, 624 (1958).

(3) J. D. JACKSON, D. G. RAVENHALL and H. W. WYLD jr.: *Nuovo Cimento*, **9**, 834 (1958), referred to as JRW in the text.

(4) G. ASCOLI, R. D. HILL and T. S. YOON: *Nuovo Cimento*, **9**, 813 (1958).

(5) R. H. DALITZ: *Proc. of the Ann. Intern. Conference on High Energy Physics at CERN* (Geneva, 1958), p. 187.

that these zero range formulas are capable of giving a reasonably good fit to the energy dependence of the elastic scattering and absorption of K^- on protons and has found two equally acceptable sets of scattering lengths:

$$(3)\qquad \begin{cases} & a_0 + ib_0 & a_1 + ib_1 \\ \text{Dalitz solution A} & 0.28 + i\,0.54 & 1.19 + i\,0.22 \\ \text{Dalitz solution B} & 1.28 + i\,0.71 & 0.43 + i\,0.18 \end{cases}$$

Here the unit is 10^{-13} cm.

In discussing the effects of the $\overline{K}^0$-K^- mass difference it is convenient to distinguish between two kinds of charge independence violating effects—intrinsic dynamical effects and kinematic effects. The intrinsic dynamical effects, which arise from violation of charge independence in the underlying short range interaction, we expect to be small, of the order of $\Delta m/m \simeq 1\%$. The kinematic effects, while negligible at high energies, will be pronounced at low energies in the neighborhood of the threshold for charge exchange scattering. We shall ignore the small intrinsic dynamical effects and consider only the kinematic effects.

It is convenient to carry through this analysis in terms of the R matrix or derivative matrix of Wigner and Eisenbud. On the one hand it turns out, as we show in Section 2, that the zero range analysis is equivalent to assuming that the elements of the R matrix are energy independent; and it is possible to express the complex scattering lengths in terms of the elements of the R matrix. On the other hand the R matrix formalism provides a natural separation of the intrinsic dynamical effects and the kinematic effects. In fact the R matrix formalism was devised just to achieve this separation. Thus we shall assume, in accordance with the discussion above, that the R matrix itself is charge independent. In relating the R matrix to the scattering and absorption cross-sections it is then easy to put in the kinematic effects related to the $\overline{K}^0$-K^- mass difference. The result is that it is possible to express the scattering and absorption cross-sections in terms of the scattering lengths A_T by formulas similar to those in JRW [3] with certain kinematic corrections.

2. – *R* matrix formalism.

A simple discussion of the R matrix formalism for S wave reactions is given in Chapter X of BLATT and WEISSKOPF [6]. We reproduce the essential results here. The cross-section leading from an entrance channel α to an exit

[6] J. M. BLATT and V. F. WEISSKOPF: *Theoretical Nuclear Physics* (New York, 1952).

channel β is given in terms of the S matrix by

$$\sigma_{\alpha\beta} = \frac{\pi}{k_\alpha^2} |\delta_{\alpha\beta} - S_{\alpha\beta}|^2 , \tag{4}$$

where k_α is the wave number in the entrance channel. The S matrix is in turn given in terms of the R matrix by the matrix equation

$$S = \omega \frac{1 + iBRB}{1 - iBRB} \omega . \tag{5}$$

Here B and ω are diagonal matrices:

$$B_{\alpha\beta} = \delta_{\alpha\beta} \sqrt{k_\alpha} , \tag{6}$$

$$\omega_{\alpha\beta} = \delta_{\alpha\beta} \exp[-ik_\alpha \mathcal{R}_\alpha] . \tag{7}$$

The dependence of B on the channel momenta contains the kinematic effects associated with different particle masses in the entrance and exit channels. ω is determined by the channel radii $\mathcal{R}_\alpha$. We shall set $\omega = 1$ in what follows, as is consistent with a zero range analysis. The R matrix itself can be shown to be real and symmetric.

The explicit forms of B and ω given by (6) and (7) are valid for S wave scattering in the absence of Coulomb interactions. Coulomb effects in the entrance channel enter in two places—a Rutherford scattering amplitude must be added to the strong interaction amplitude (this produces interference effects in the angular distribution), and the relation (2) between phase shift and scattering length is altered. The interference effects at forward angles will be useful in determining the sign of the scattering lengths, but will not appreciably affect the S wave scattering at backward angles for energies above 2 or 3 MeV. To a good approximation the altered relation between phase shift and scattering length is equivalent to replacing kA by C^2kA, where C^2 is the Coulomb penetration factor ($C^2 = 2\pi\eta/(1 - \exp[-2\pi\eta])$, with $\eta = e^2/\hbar v$). At threshold for the charge exchange reaction $C^2 \simeq 1.13$. For simplicity we will neglect Coulomb effects in this preliminary work.

Let us first neglect the $\overline{\text{K}}^0$-K^- mass difference and consider a single isotopic spin state, for example $T = 0$. Then the system under consideration has two channels—a scattering channel involving a mixture of K^-p and $\overline{\text{K}}^0\text{n}$ and a reaction channel involving a combination of $\Sigma^0\pi^0$, $\Sigma^\pm\pi^\mp$. The R matrix will then have the form

$$R = \begin{pmatrix} R_1 & R_2 \\ R_2 & R_3 \end{pmatrix} , \tag{8}$$

where R_1, R_2, and R_3 are real numbers. The matrix B will be of the form

$$B = \begin{pmatrix} \sqrt{k} & 0 \\ 0 & \sqrt{q} \end{pmatrix} , \tag{9}$$

where k is the wave number in the KN system and q the wave number in the reaction channel. A simple calculation shows that

$$(1-S)_{11} = -2ik\,\frac{R_1 + iq(R_2^2 - R_1R_3)}{1 - iqR_3 - ik[R_1 + iq(R_2^2 - R_1R_3)]}\,. \tag{10}$$

We can compare this with the prediction of the zero range analysis

$$(1-S)_{11} = 1 - \exp[2i\delta] = -2ik\,\frac{A}{1-ikA} = -2ik\,\frac{a+ib}{1-ik(a+ib)}\,. \tag{11}$$

Thus the two approaches give the same result provided we have

$$a + ib = \frac{1}{1-iqR_3}[R_1 + iq(R_2^2 - R_1R_3)] = R_1 + \frac{iqR_2^2}{1-iqR_3}\,. \tag{12}$$

Since the hyperon producing reactions are exothermic, q is nearly constant at low energies and we see that if the elements of the R matrix are energy independent the scattering length $A = a + ib$ will be energy independent as assumed in the zero range analysis [7].

If we assume isotopic spin is rigorously conserved but take account of both isotopic spin states the R matrix will have the form [8]

$$R = \begin{pmatrix} R_1 & R_2 & 0 & 0 \\ R_2 & R_3 & 0 & 0 \\ 0 & 0 & R_4 & R_5 \\ 0 & 0 & R_5 & R_6 \end{pmatrix}, \tag{13}$$

---

(7) R. H. DALITZ has pointed out to us in a private communication that if the intrinsic parity of the $\Lambda\pi$ or $\Sigma\pi$ system is opposite to that of the $\mathrm{K}^-\mathrm{p}$ system so that the reaction products come off in a P wave, the momentum dependence of Eq. (12) will be more marked because we will now have $R_2 \sim q$ and $R_3 \sim q^2$. DALITZ finds that the net effect of this momentum dependence is small and not experimentally distinguishable at present from constant a and b, although in principle it offers a method of determining the relative parities of strange particles.

(8) Actually there are two distinguishable $T=1$ reaction channels, one for the $\Sigma\pi$ system with wave number q_1 and one for the $\Lambda\pi$ system with wave number q_2. Thus the matrix (13) should be taken to be a 5×5 matrix. In order to reduce the algebraic complexity we have replaced these two channels by a single $T=1$ reaction channel with wave number q. We believe that to the extent that we ignore the energy dependence of q_1, q_2 and the R matrix elements this approximation has no effect on our final results (18)-(22).

where we let the first two rows and columns of the matrix refer to the $T=0$ states and the last two rows and columns refer to the $T=1$ states. Then

$$(14)\qquad \left\{\begin{aligned} A_0 &= a_0 + ib_0 = R_1 + \frac{iqR_2^2}{1-iqR_3}\,, \\ A_1 &= a_1 + ib_1 = R_4 + \frac{iqR_5^2}{1-iqR_6}\,. \end{aligned}\right.$$

As discussed in the introduction the R matrix represents in a phenomenological way the internal dynamics of the strong short range interactions which give rise to the K^- absorption and scattering. Hence we expect deviations from the form (13) for R as a result of violations of charge independence to be small of the order $\Delta m/m \simeq 1\%$. We shall ignore these small changes and assume that (13) with the identifications (14) is a good approximation even when charge independence violations are taken into account in the kinematics.

The kinematic effects which result from the $\overline{K}{}^0$-K^- mass difference arise because the wave number k in the K^-p channel is different from the wave number k' in the $\overline{K}{}^0n$ channel. To take account of these effects we must first transform R from the isotopic spin representation (13) to a charge representation. The first and third rows and columns of (13) refer to states

$$(15)\qquad \left\{\begin{aligned} \chi_0^0 &= \frac{1}{\sqrt{2}}\,(K^-p - \overline{K}{}^0n)\,, \\ \chi_1^0 &= \frac{1}{\sqrt{2}}\,(K^-p + \overline{K}{}^0n)\,. \end{aligned}\right.$$

We now change to a representation in which the rows and columns of the R matrix refer to the following channels.

Row (Column) 1	K^-p
Row (Column) 2	$\overline{K}{}^0n$
Row (Column) 3	$T=0$ reaction channel
Row (Column) 4	$T=1$ reaction channel.

1662

In this representation we find

$$R = \begin{pmatrix} \frac{1}{2}(R_4+R_1) & \frac{1}{2}(R_4-R_1) & \frac{1}{\sqrt{2}}R_2 & \frac{1}{\sqrt{2}}R_5 \\ \frac{1}{2}(R_4-R_1) & \frac{1}{2}(R_4+R_1) & -\frac{1}{\sqrt{2}}R_2 & \frac{1}{\sqrt{2}}R_5 \\ \frac{1}{\sqrt{2}}R_2 & -\frac{1}{\sqrt{2}}R_2 & R_3 & 0 \\ \frac{1}{\sqrt{2}}R_5 & \frac{1}{\sqrt{2}}R_5 & 0 & R_6 \end{pmatrix}. \tag{16}$$

The kinematic effects of the mass difference are then taken into account by using for the matrix B the form

$$B = \begin{pmatrix} \sqrt{k} & 0 & 0 & 0 \\ 0 & \sqrt{k'} & 0 & 0 \\ 0 & 0 & \sqrt{q} & 0 \\ 0 & 0 & 0 & \sqrt{q} \end{pmatrix}. \tag{17}$$

Using (16) and (17) and the general formulas (4) and (5) it is now possible to calculate the cross-sections for elastic and charge exchange scattering and absorption of K^- on protons. When this calculation is performed it is found that the R matrix elements appear only in the combinations (14) so that the results can be expressed in terms of A_1 and A_0. We find

$$\sigma_{\text{el}} = \pi \left| \frac{A_1(1-ik'A_0) + A_0(1-ik'A_1)}{\Delta} \right|^2, \tag{18}$$

$$\sigma_{\text{ex}} = \pi \frac{k'}{k} \left| \frac{A_1 - A_0}{\Delta} \right|^2, \tag{19}$$

$$\sigma_{\text{abs}} = \frac{1}{2}\sigma_{\text{abs}}^{(1)} + \frac{1}{2}\sigma_{\text{abs}}^{(0)}, \tag{20}$$

$$\frac{1}{2}\sigma_{\text{abs}}^{(1)} = \frac{2\pi}{k} b_1 \left| \frac{1-ik'A_0}{\Delta} \right|^2, \qquad \frac{1}{2}\sigma_{\text{abs}}^{(0)} = \frac{2\pi}{k} b_0 \left| \frac{1-ik'A_1}{\Delta} \right|^2, \tag{21}$$

where

$$\Delta = 1 - \tfrac{1}{2}i(k+k')(A_1+A_0) - kk'A_1A_0 .$$

Well above the charge exchange threshold when $k' \to k$ these formulas reduce as they should to those already given by JRW. Near the charge exchange threshold there will be deviations from the JRW formulas. The most important of these from the practical standpoint is the factor k'/k in σ_{ex}. This can of course be obtained on the basis of simple phase space arguments. However, the other deviations from the JRW formulas are interesting. In par-

1663

ticular, below the threshold for charge exchange the $\overline{K}^0 n$ channel is closed and k' is a pure imaginary number [9,10]. Thus if k_0 is the wave number in the K^-p system at the threshold for charge exchange scattering we have

$$k' = \sqrt{k^2 - k_0^2}\,, \qquad \text{above threshold,} \tag{23}$$

and

$$k' = +\,i\sqrt{k_0^2 - k^2}\,, \qquad \text{below threshold.} \tag{24}$$

With this interpretation of k' the formulas (18), (20), (21), (22) give the scattering and absorption cross sections below the charge exchange threshold. Although the cross sections are continuous at $k = k_0$, the fact that $k' \to 0$ at $k = k_0$ gives rise to discontinuous, in fact infinite, derivatives in σ_{el} and σ_{abs}, and the cross-sections thus exhibit cusps.

3. – Examples and discussion.

We have calculated the elastic, exchange, and absorption cross-sections according to the formulas (18)–(22) using the parameters (3) obtained by DALITZ. The results are given in Figs. 1, 2, and 3. Fig. 1 gives the results for Dalitz solution A and Fig. 2 the results for Dalitz solution B. The dotted curves are calculated according to the old JRW formulas

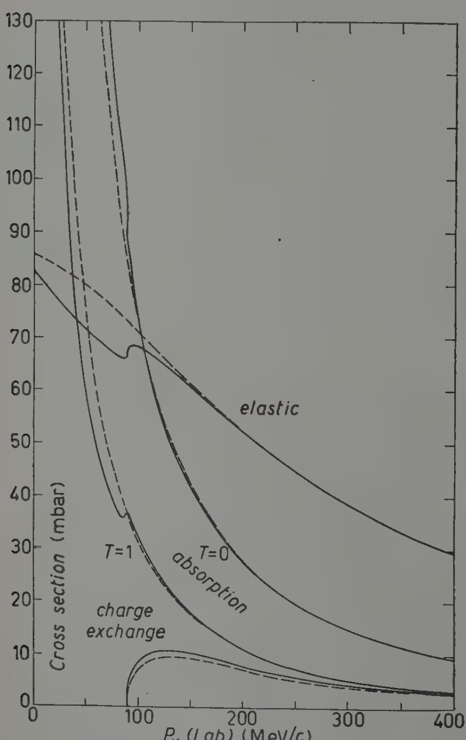

Fig. 1. – Total cross sections as a function of laboratory momentum for the elastic scattering, charge exchange scattering and absorption (into $T=0$ and $T=1$ final states) of K^--mesons on protons. The curves correspond to the Dalitz solution A (Eq. (3)). The solid curves include properly the kinematic effects arising from the K^--$\overline{K}^0$ mass difference, while the dotted curves are calculated neglecting the mass difference (aside from multiplying the charge exchange cross section by the simple phase space factor k'/k). Note the cusps in the elastic scattering and absorption cross sections at the threshold for the charge exchange reaction.

---

(9) E. P. WIGNER: *Phys. Rev.*, **73**, 1002 (1948).
(10) G. BREIT: *Phys. Rev.*, **107**, 1612 (1957).

with $k' = k$ except for the charge exchange cross-sections, where we have multiplied the JRW formula by the phase space factor k'/k.

The elastic and absorption cross-sections according to the formulas (18)–(22) exhibit cusps (*i.e.* the cross-sections have an infinite derivative with respect to wave number) at the threshold of the charge exchange scattering. In the absorption cross-sections the cusps are almost completely masked by the strong $1/v$ dependence of the cross-sections near zero energy. In the elastic scattering cross-sections the cusps are more pronounced.

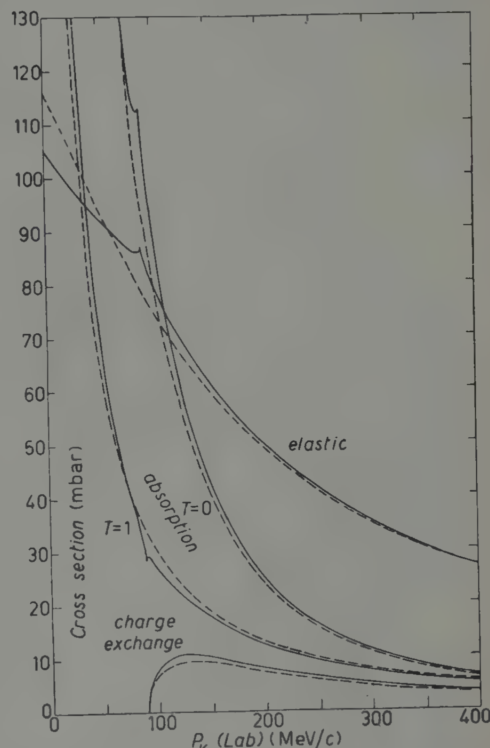

Fig. 2. – Same as Fig. 1, but for Dalitz solution B (Eq. (3)). Note that the cusps are of a different form from those for Dalitz solution A.

There are two points worth mentioning in connection with these cusps. In the first place the cusps in the elastic scattering cross-sections are of different types for the two Dalitz solutions A and B. Hence in principle it is possible to differentiate experimentally between these two solutions. Secondly it can be shown that if the $\overline{K}^0$ has opposite parity to the K^-, a possibility discussed by PAIS (2), there will be no cusps in the S wave cross-sections. The point here is just that if the $\overline{K}^0$n are in a P wave in the final state the additional factor k' in the matrix elements for charge exchange scattering will smooth out the cusps. The elastic scattering cross-section will have a continuous derivative at the threshold for charge exchange scattering and the absorption cross-sections will have discontinuous but finite derivatives at threshold. There will be cusps in the P wave elastic and absorption cross-sections, but these are tiny corrections to the S wave cross-sections at such low energies. Thus in principle it is possible to determine experimentally from the K^- elastic scattering whether the K^- and $\overline{K}^0$ have the same or opposite parities (11).

(11) See in this connection R. K. ADAIR: *Phys. Rev.*, **111**, 632 (1958). who has discussed the possibility of determining whether the Σ and Λ particles have the same or opposite parities by the appearance of cusps in the Λ production cross section at the Σ threshold in πp collisions.

1665

Unfortunately the experimental data available at present are far too crude to differentiate between the various possibilities mentioned above. For a comparison of the elastic and absorption cross-sections as calculated from the old JRW formulas with the experimental data we refer the reader to DALITZ' article [5]. It is evident from Fig. 1 and 2 that the corrections discussed in this paper are small compared to the experimental errors in the cross-section data.

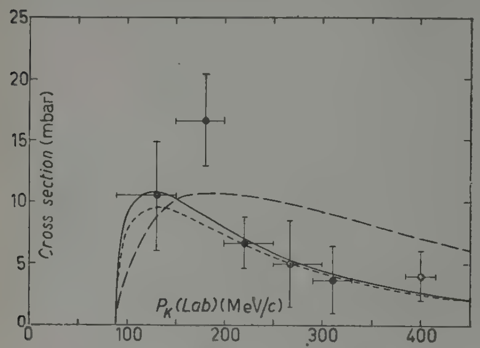

Fig. 3. – Charge exchange scattering cross-section as a function of laboratory momentum for K -mesons on protons. The experimental points are those of ref. [12]. The solid and dotted curves are the same as in Fig. 1. The dashed curve is calculated with Pais' theory for his $\lambda=-1$ and is arbitrarily normalized to have the same peak cross section as the zero effective range theory.

Fig. 3 gives a comparison with the recent experimental data [12] on charge exchange scattering. Again the dotted curve is the JRW formula corrected by the phase space factor k'/k. The solid curve is calculated from Equation (19) using Dalitz solution A (solutions A and B give essentially identical results here). The dashed curve is calculated from Pais's theory [2] in which the K^- and $\overline{K}^0$ have opposite parity [13]. The Pais theory seems to give too high a cross-section at the higher energies. Either the phase space corrected JRW formulas or Equation (19) seems to fit the data reasonably well, although there is an indication that the theoretical curves are somewhat too low. The fit to the charge exchange data can be improved with scattering lengths different from those used by DALITZ, but we did not feel it was worth-while obtaining a new fit with the limited data available at the present time.

* * *

We would like to thank Professors ROSENFEID, SOLMITZ and TRIPP for calling to our attention the problem discussed in this paper.

---

[12] P. EBERHARD, A. ROSENFELD, F. SOLMITZ, R. TRIPP and M. WATSON: *Phys. Rev. Lett.*, **2**, 312 (1959).

[13] The curve in Fig. 3 is for Pais's parameter $\lambda=-1$, and includes dynamic as well as kinematic effects of the $\overline{K}^0$-K^- mass difference.

Added Note

Prof. R. H. DALITZ informs us that he has in preparation a paper in which the R matrix formalism is used to study various aspects of the K^--N interaction. His results for the effects of the $\overline{K}^0$-K^- mass difference are similar to ours.

RIASSUNTO (*)

Si utilizza il formalismo della matrice R di Wigner e Eisenbud per modificare l'analisi in onde S di range zero dello scattering ed assorbimento dei mesoni K^- su protoni proposta da JACKSON, RAVENHALL e WYLD, in modo da tener conto degli effetti cinematici della differenza di massa $\overline{K}^0$-K^-. Si trova che anche con una differenza di massa le sezioni d'urto elastica, di scambio carica e di assorbimento possono esprimersi in termini di due lunghezze di scattering complesse. La forma delle cuspidi può usarsi per distinguere fra serie di lunghezze di scattering altrimenti indistinguibili. Se il $\overline{K}^0$ e il K^- hanno parità opposte non ci sono cuspidi nella sezione d'urto dello scattering elastico, così che in linea di principio è possibile determinare la parità relativa del $\overline{K}^0$ e del K^- dalla dipendenza dall'energia della sezione d'urto dello scattering del K^-.

(*) *Traduzione a cura della Redazione.*

IL NUOVO CIMENTO Vol. XIII, N. 1 1° Luglio 1959

The Attenuation Length of the High Energy Nucleonic Component of the Cosmic Radiation near Sea Level.

K. G. McCracken

Physics Department, University of Tasmania - Hobart

D. H. Johns

Antarctic Division, Department of External Affairs - Melbourne

(ricevuto il 4 Marzo 1959)

Summary. — From the analysis of neutron data obtained at two widely separated stations, it is shown that during 1957 the attenuation length of the high energy nucleonic component of the cosmic radiation near sea level was $(138.1 \pm 0.8)\ \mathrm{g\,cm^{-2}}$ at high geomagnetic latitudes. Analysis of data from a number of stations shows that the amplitudes of Forbush type decreases increase by about 12% per 1000 m increase in station altitude. This is taken as evidence that the value of the attenuation length is sensitive to changes in the rigidity spectrum of the primary radiation, becoming greater as the primary cosmic ray spectrum hardens. It is shown that at sea level near the equator the attenuation length is considerably greater than at high latitudes, having a value of about $159\ \mathrm{g\,cm^{-2}}$. It is shown that the correction for atmospheric change can be the limiting factor in the study of small time variations in the primary intensity by means of a measurement of the nucleonic component deep in the atmosphere.

1. – Introduction.

The counting rate of a cosmic ray neutron monitor varies out of phase with the atmospheric pressure. In order to use the neutron data to study the changes in the primary cosmic ray intensity, allowance must be made for these variation of atmospheric origin. It has been reported that near sea level the relation between neutron counting rate and atmospheric pressure is roughly

exponential [1], that is

$$R(p_0 + \delta p) = R(p_0) \exp\left(-\frac{\delta p}{L}\right),$$

where p is the atmospheric pressure, $R(p)$ is the neutron counting rate at the point where the pressure is p, and L is the attenuation length of the neutron component. In order to compare neutron data obtained at times of different atmospheric pressure, it is the usual practice to use this equation to estimate from the observed counting rate and pressure the counting rate which would have been observed if the pressure had been some other, fixed value, p_0.

It has been reported that the attenuation length in the lower atmosphere is approximately 145 g cm^{-2}, and that this value applies equally well at high latitude and equatorial stations [1,2]. This invariance with respect to primary rigidity suggests that the attenuation length should be invariant with respect to primary spectral change. Evidence is presented here which suggests that the attenuation length at high latitudes is less than 145 g cm^{-2}, and that it does vary during marked changes in the primary spectrum.

2. – Instrumental details.

The University of Tasmania commenced recording the cosmic ray nucleonic component at Hobart during June 1956, and in mid July 1956 a monitor was installed on the slopes of Mt. Wellington, the mountain at whose foot Hobart is situated. In March 1957, a monitor was installed at Mawson, the Australian Antarctic base in Mac-Robertson Land. This latter instrument is operated by the Australian National Antarctic Research Expeditions, for the conduct of whose cosmic ray programme the University of Tasmania is responsible.

The geometries of the monitors are similar to those recommended for use during the International Geophysical Year [3]. In particular, each monitor consists of two completely independent sets of counters and electronic circuits (a so called « duplex neutron monitor »). All atmospheric data have been standardized by frequent checking of the recorders against mercury column barometers.

---

(1) J. A. Simpson and W. C. Fagot: *Phys. Rev.*, **90**, 1068 (1953).
(2) J. A. Simpson, W. Fonger and S. B. Treiman: *Phys. Rev.*, **90**, 934 (1953).
(3) J. A. Simpson: *Annals of the International Geophysical Year*, (New York, 1956), vol. **4**, p. 351.

3. – Determination of the attenuation length.

In theory, a simple regression analysis between neutron counting rate and atmospheric pressure should permit the attenuation length to be determined. In practice, the large fluctuations in neutron counting rate produced by changes in the primary cosmic ray intensity render such a method rather inaccurate ([2]). To obtain accurate values, methods must be employed which make allowance for the primary changes. Three such methods are detailed.

Method A ([2]). – It has been shown elsewhere that the percentage variations in the corrected neutron counting rates at Mawson and Mt. Wellington are very nearly the same ([4]). Thus if a threefold correlation analysis is performed between the corrected Mt. Wellington counting rate and pressure, and the corrected Mawson counting rate, the partial regression coefficient of the Mt. Wellington counting rate upon pressure reveals any residual counting rate against pressure relation freed of the effects of primary intensity variations.

Employing Mawson and Mt. Wellington data corrected using an attenuation length of 145 g cm^{-2}, this type of analysis was performed for seven periods during 1957 of about 30 days each. Similar analyses were performed between the corrected Mawson counting rate and atmospheric pressure, the corrected Mt. Wellington counting rate being used to allow for the primary intensity changes. Daily mean counting rates and pressures were used throughout. Every one of the fourteen analyses showed that the corrected data were still negatively correlated with pressure. From the results of each analysis, an estimate of the attenuation length was obtained. The weighted means of the values found were (138.2 ± 1.1) g cm^{-2} for Mawson, and (139.6 ± 1.2) g cm^{-2} for Mt. Wellington.

Method B. – The monthly mean pressures and counting rates after correction using an attenuation length of 145 g cm^{-2} were calculated for Mt. Wellington and Mawson for the period April 1957 to January 1958. We write them as P_W, P_M, I_W, and I_M, where I_W and I_M are expressed as percentages of the mean value for the whole period. It has been shown that the percentage variations at both stations due to primary intensity changes are very nearly the same ([4]). Let them be represented by $Q(t)$. Let the attenuation length used to correct the data be L, and $L + \delta L$ be the correct value. We assume that the attenuation length is the same at both observatories. Indicating mean values by a bar, the following are good approximations to the truth for the variations in

([4]) K. G. McCRACKEN: *Phys. Rev.*, **113**, 343 (1959).

monthly mean pressure encountered in practice

$$\left.\begin{aligned} I_{\mathrm{W}} &= Q(t) + \alpha(P_{\mathrm{W}} - \bar{P}_{\mathrm{W}}) + 100 \\ I_{\mathrm{M}} &= Q(t) + \alpha(P_{\mathrm{M}} - \bar{P}_{\mathrm{M}}) + 100 \end{aligned}\right\} \text{ where } \alpha = \frac{100\,\delta L}{L^2},$$

and therefore

$$I_{\mathrm{M}} - I_{\mathrm{W}} = \alpha(\delta P_{\mathrm{M}} - \delta P_{\mathrm{W}}), \qquad \text{where } \delta P = P - \bar{P}.$$

In Fig. 1, $I_{\mathrm{M}} - I_{\mathrm{W}}$ and $\delta P_{\mathrm{M}} - \delta P_{\mathrm{W}}$ are plotted against time, and a marked similarity is evident. A correlation analysis showed that the quantities were strongly correlated ($r_{12} = 0.89$). From the value of α found in the correlation analysis, δL was determined, yielding a value of (133.5 ± 2.1) g cm^{-2} for the attenuation length.

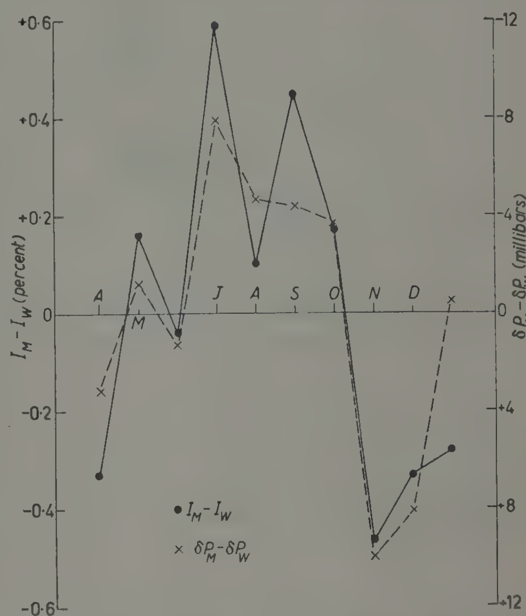

Fig. 1. – Illustrating the dependence of corrected neutron intensity upon atmospheric pressure. $I_{\mathrm{M}} - I_{\mathrm{W}}$ and $\delta P_{\mathrm{M}} - \delta P_{\mathrm{W}}$ are plotted as functions of time.

Method C. – The duplex neutron monitor installed at Mt. Wellington during July 1956 (monitor A) was operated at Hobart for over a month prior to the move. At the time, there was another monitor (monitor B) operating at Hobart. Write the counting rates of monitor A at Mt. Wellington and Hobart as R_{AW}, R_{AH} respectively, and that of monitor B as R_{B}. The ratio of the counting rate of each section of monitor A to the total counting rate of monitor B was calculated for each hour of the month prior to, and the month subsequent to the transfer of monitor A to Mt. Wellington.

The percentage variations in the counting rates of monitor A and B when they were both at Hobart were the same, and so the ratio $R_{\mathrm{AH}}/R_{\mathrm{B}}$ was invariant with respect to primary intensity changes. In the next section it is shown that the percentage variations at Mt. Wellington are greater than those at Hobart by a factor of about 1.09, and consequently, $R_{\mathrm{AW}}/R_{\mathrm{B}}$ was dependent upon primary intensity. However, the counting rate variations at the time

due to primary intensity changes were small ($<4\%$), and so the range of variation of R_{AW}/R_B due to this cause was about 0.4%, which is small enough to be neglected in the present discussion.

The mean values of R_{AW}/R_B and R_{AH}/R_B were calculated, and dividing the second into the first, an estimate was obtained of the ratio of the counting rate of monitor A when at Mt. Wellington to that when at Hobart. From this estimate, and the mean difference in the atmospheric pressure at the two observatories, the attenuation length was calculated. One section of the monitor yielded a value of (134 ± 2) g cm^{-2}, the other a value of (139 ± 2) g cm^{-2}.

While considerable care was taken in the reassembly of monitor A at Mt. Wellington, there were undoubtedly differences in the geometries before and after the move, and these will have introduced errors into the values of the attenuation length. The reproducibility of counting rate reported for monitors of similar construction (2) indicates that the mean of the above values, 136.5 g cm^{-2}, should be within about ± 4 g cm^{-2} of the correct value. A standard error cannot be assigned.

Methods A, B and C all yielded values for the attenuation length which are less than 145 g cm^{-2}. The weighted mean of the results of methods A and B is (138.1 ± 0.8) g cm^{-2}. The result found using method C is consistent with this value. It will be shown that the attenuation length probably increased between 1956 and 1957 as a consequence of the marked hardening of the primary spectrum (4). It is believed that method C was not sufficiently accurate to reveal this change.

4. – Changes in the value of the attenuation length produced by primary spectrum changes.

At time t_0, let the counting rate against atmospheric depth relationship be given by the function $R_0(x)$, where

$$\frac{\mathrm{d}R_0(x)}{\mathrm{d}x} = -\frac{1}{L_0(x)}\, R_0(x)\,,$$

$L_0(x)$ being, by definition, the attenuation length at depth x at time t_0. Between time t_0 and t_1 let a change in primary intensity produce a fractional decrease in counting rate of $g(x)$. Then the counting rate against depth relationship at time t_1 is given by $R_1(x) = R_0(x)\{1 - g(x)\}$. Consequently

$$\frac{\mathrm{d}R_1(x)}{\mathrm{d}x} = \{1 - g(x)\}\, \frac{\mathrm{d}R_0(x)}{\mathrm{d}x} - \frac{\mathrm{d}g(x)}{\mathrm{d}x} \cdot R_0(x)\,,$$

1672

which leads to

$$\frac{\mathrm{d}R_1(x)}{\mathrm{d}x} = -\left\{\frac{1}{L_0(x)} + \frac{1}{1-g(x)}\cdot\frac{\mathrm{d}g(x)}{\mathrm{d}x}\right\} R_1(x)\,.$$

That is, at time t_1, the attenuation length of the radiation in the atmosphere has a new value $L_1(x)$, given by

$$\frac{1}{L_1(x)} = \frac{1}{L_0(x)} + \frac{1}{1-g(x)}\cdot\frac{\mathrm{d}g(x)}{\mathrm{d}x}\,. \tag{1}$$

It would be difficult to determine whether the attenuation length at a given station were variable from a counting rate against pressure regression analysis. However, from the above, it can be seen that comparison of the event amplitudes observed at different atmospheric depths *i.e.*, a determination of $g(x)$, will reveal any variability of attenuation length. Such a comparison is now made.

Let the counting rates observed by recorders 1 and 2 during simultaneous recording periods be R_1 and R_2. It is necessary to find the functional relationship between R_1 and R_2 giving the best fit to N observed (R_1, R_2) pairs. In what follows, any coefficient relating the percentage variation in R_1 to that in R_2 will be called a measure of the R_1, R_2 relative amplitude of the variation. A number of different definitions of the function of best fit can be given, and consequently, there are, corresponding to any set of N pairs (R_1, R_2), a number of values of the R_1, R_2 relative amplitude.

A study of these various measures of relative amplitude has been made (5). The conclusion reached is that for cases where the correlation coefficient between the R_1 and R_2 data is greater than 0.8, the measure of relative amplitude defined as $(\sigma_1/\overline{R}_1)/(\sigma_2/\overline{R}_2)$ where

$$\sigma_i = \sqrt{\frac{1}{N-1}\cdot\sum (R_i - \overline{R}_i)^2} \qquad \text{and} \qquad \overline{R}_i = \frac{1}{N}\sum R_i\,,$$

is the most suitable for the comparison of cosmic ray variations.

Using this definition, and comparing daily mean data, the amplitudes of the neutron variations at a number of observatories relative to those at the sea level observatory of Herstmonceux have been determined, and are listed in Table I. During each period considered, a large Forbush type intensity decrease occurred.

---

(5) K. G. McCracken: *Ph. D. Thesis* (University of Tasmania).

1673

As the amplitude of a cosmic ray variation is a function of geomagnetic latitude, the analysis was restricted to data from observatories which are all at approximately the same geomagnetic latitude. All observatories are above

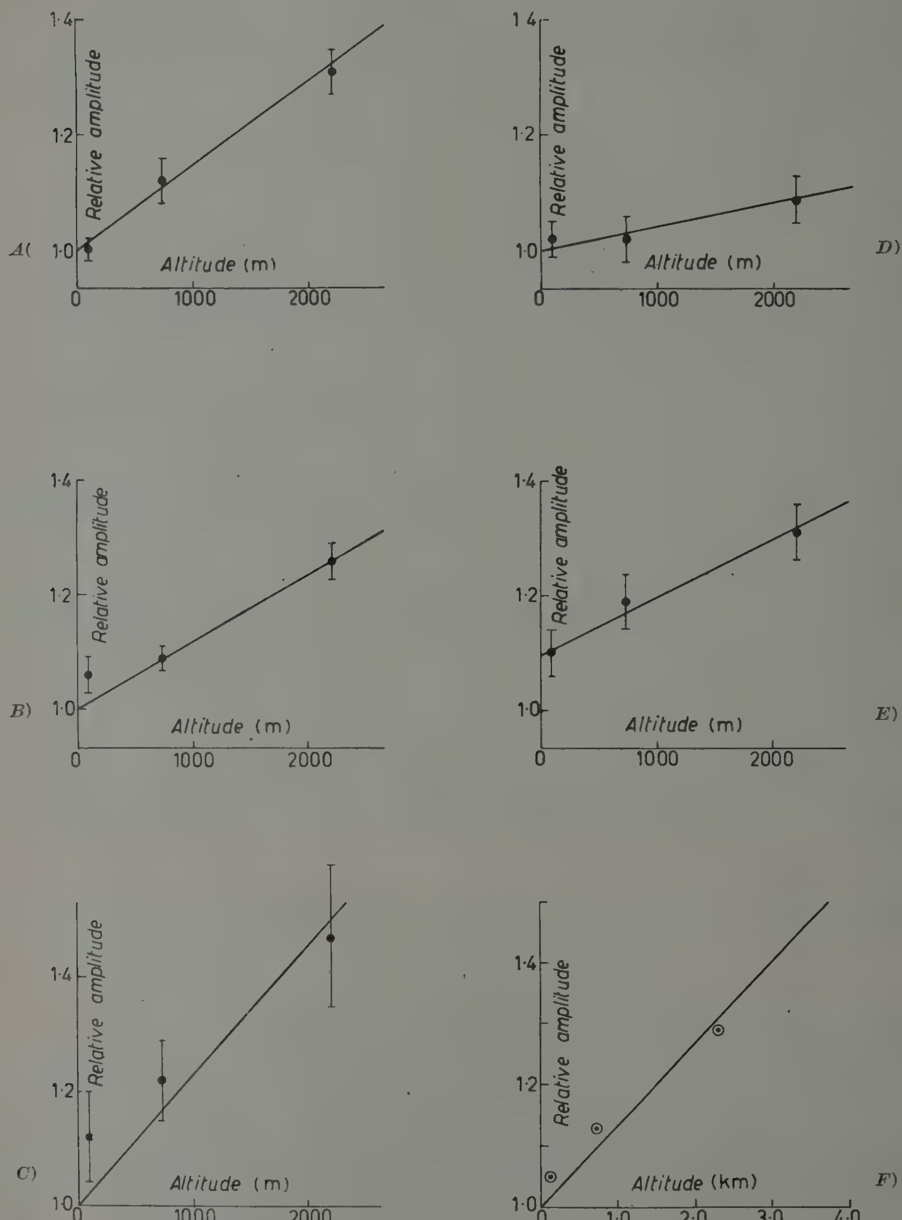

Fig. 2. – Relative amplitude plotted as a function of altitude. The amplitudes are all relative to those observed at the sea level observatory of Herstmonceux. All data were obtained during 1957. Standard errors are shown.

1074

the « knee » in the counting rate against latitude curve (found to be at 52° geomagnetic during 1957 [6]). The values given in Table I are plotted as functions of altitude in Fig. 2. From these graphs, it is clear that the percentage

TABLE I. – *The dependence of event amplitude upon altitude for the neutron component.*

All stations are at approximately the same geomagnetic latitude. Year 1957. The relative amplitudes (R.A.) and correlation coefficients (r_{12}) between various sets of data are given. Standard errors are listed. The geographic co-ordinates and altitudes of the stations are: Herstmonceux, 51° N, 0° E, 20 m; Uppsala, 60° N, 18° E, <100 m; Mt. Wellington, 43° S, 147° E, 725 m; Sulphur Mountain, 51° N, 244° E, 2280 m.

Relative Amplitude \ Period		29 June-28 July	24 Aug.-20 Sept.	21 Sept.-19 Oct.	20 Oct.-13 Nov.	14 Nov.-10 Dec.
Uppsala	R.A.	1.00 ± 0.02	1.06 ± 0.03	1.12 ± 0.08	1.02 ± 0.03	1.10 ± 0.04
Herstmonceux	r_{12}	1.00	0.99	0.93	0.99	0.99
Mt. Wellington	R.A.	1.12 ± 0.04	1.09 ± 0.02	1.22 ± 0.07	1.02 ± 0.04	1.19 ± 0.05
Herstmonceux	r_{12}	0.99	0.99	0.96	0.99	0.98
Sulphur Mt.	R.A.	1.31 ± 0.04	1.26 ± 0.03	1.47 ± 0.13	1.09 ± 0.04	1.31 ± 0.05
Herstmonceux	r_{12}	0.99	0.99	0.92	0.99	0.98

variation in neutron counting rate increases with decreasing atmospheric depth. That is $\mathrm{d}g(x)/\mathrm{d}x < 0$, and by reference to equation (1), it is seen that the attenuation length therefore increases during a Forbush type decrease. From the graph derived from the average of the five observed events, relative amplitude varies by about 12% per 1000 metres increase in altitude, and consequently, it can be shown that during a marked intensity depression (10%), the attenuation length increases by about 2%.

As it is reasonable to expect that the attenuation length will be greatest for the more energetic neutrons produced by primary cosmic rays of high rigidity, and therefore, as it has been shown that during a Forbush type decrease the percentage change in intensity is greater at low than at high rigidities [4], it can be seen that this result is not entirely unexpected. It should be noted in passing that the altitude dependence for the event occurring between 20 October and 13 November, 1957 (Fig. 2-*D*) seems to be

(6) J. R. STOREY, A. G. FENTON and K. G. McCRACKEN: *Nature*, **181**, 1155 (1958).

considerably less marked than those during the other events. This supports the evidence presented elsewhere ([4]) that the rigidity dependence of spectral change during short term events is variable from event to event. Both Fig. 2-*D*, and the data presented in Table II of reference ([4]), indicate that the changes in intensity during the 20 October–13 November event were less dependent upon rigidity than are those during the majority of short term events.

The fact that the attenuation length varies indicates that errors will be present in neutron data corrected using a constant value for the attenuation length. During a period of one or two days, the neutron counting rate can change by 30% due to changes in the atmospheric pressure, and if the attenuation length is 2% in error during this time, a 0.6% variation of atmospheric origin will remain in the corrected data. Correction for this effect would be rather complicated, and it is probably more realistic to accept the fact that errors of this magnitude can exist.

The dependence of the percentage variations in counting rate upon altitude means that some care must be taken when investigating the rigidity dependence of variations by comparison of data obtained at different latitudes. Clearly, indiscriminate comparison of high altitude (3 000 metres) and sea level data will introduce considerable errors.

5. – The attenuation length at low latitudes.

As the attenuation length at sea level is not invariant with respect to spectral change, it is to be expected that it will be greater at low than at high latitudes. The following discussion based upon observations of the variation in neutron counting rate with latitude supports this view.

For a neutron monitor at sea level (atmospheric depth $=1030\ \text{g cm}^{-2}$), the counting rate at geomagnetic latitudes (λ) greater than 55° is 1.77 times that at $\lambda=0$ ([7]). Let the counting rate at an atmospheric depth of $680\ \text{g cm}^{-2}$ at $\lambda=0$ be K times that at sea level. At an atmospheric depth of $680\ \text{g cm}^{-2}$, the counting rate at $\lambda>55°$ is 2.55 times that at $\lambda=0$ ([1]) that is, it is $2.55\,K$ times the sea level counting rate at $\lambda=0$. Hence, on going from sea level to a depth of $680\ \text{g cm}^{-2}$ at $\lambda>55°$, the counting rate changes by a factor of $2.55\,K/1.77=1.44\,K$.

Assume that the attenuation length within that portion of the atmosphere lying between sea level and the $680\ \text{g cm}^{-2}$ level is independent of atmospheric depth. Write the attenuation lengths at $\lambda=0$ and $\lambda>55°$ as $L_0\ \text{g cm}^{-2}$ and

---

([7]) D. C. Rose, K. B. Fenton, J. Katzman and J. A. Simpson: *Can. Journ. Phys.*, **34**, 968 (1956).

L_{55} g cm^{-2} respectively. Between sea level and the 680 g cm^{-2} level there are 350 g cm^{-2} of air, so

$$K = \exp\left[\frac{350}{L_0}\right],$$

$$1.44K = \exp\left[\frac{350}{L_{55}}\right],$$

and eliminating K,

$$L_0 = \frac{L_{55}}{1-(L_{55}/350)\ln 1.44}\,. \tag{2}$$

The latitude surveys considered above were made during the period 1953-1955, that is, the period during which the cosmic ray intensity was at a maximum. There was a marked hardening of the primary spectrum during 1956 ([4,8]), and consequently the value of 138 g cm^{-2} derived for the attenuation length during 1957 will be higher than that pertaining during 1953-1955. Insertion of a value of 136 g cm^{-2} for L_{55} ([9]) in equations (2) yields $L_0 = 158.5$ g cm^{-2}. The non-simultaneity of the determinations of the latitude effect undoubtedly introduces an error into this figure, however, this is unlikely to exceed ± 5 g cm^{-2}, as the primary fluctuations during 1953-1955 were small ([10]). A standard error cannot be assigned.

The fact that the attenuation length at $\lambda \approx 0$ is about 10% greater than the usually accepted value of 145 g cm^{-2} is not as serious as it would seem at first sight, as the atmospheric pressure fluctuations near the equator are small. For example, at the University of Tasmania's observatory at Lae, New Guinea, the day to day variations of neutron counting rate due to atmospheric changes seldom exceed 3%, and therefore, as the attenuation length employed in the correction of the data (145 g cm^{-2}) is about 10% in error, a 0.3% variation of atmospheric origin remains in the corrected data.

6. – Concluding remarks.

When using neutron data to study the time variations in the primary cosmic ray intensity, it is desirable that adequate correction be made for changes in the atmospheric pressure. To this end, it has been demonstrated

---

(8) P. Meyer and J. A. Simpson: *Phys. Rev.*, **106**, 568 (1957).
(9) D. C. Rose and J. Katzman: *Can. Journ. Phys.*, **34**, 1 (1956).
(10) P. Meyer and J. A. Simpson: *Phys. Rev.*, **96**, 1085 (1954).

1677

that during 1957 the average attenuation length at sea level at high latitudes was less than the usually accepted figure of 145 g cm^{-2}. Furthermore, it has been shown that the value of the attenuation length is affected by changes in the spectrum of the primary cosmic radiation.

Obviously, an incorrect value for the attenuation length will result in there being variations of atmospheric origin in the corrected neutron data. Further, as the variation in primary intensity during the solar cycle is strongly rigidity dependent ([4,8]), the attenuation lenght will vary in phase with solar activity. If, as is most convenient, an average value of the attenuation length is used, the magnitude and phase of the variations of atmospheric origin will vary throughout the solar cycle.

For example, during a year when the value of the attenuation length is different from that adopted in the correction of the data, the annual variation of atmospheric pressure will introduce an annual variation into the corrected neutron data. Thus the use of the value of 145 g cm^{-2} during 1957 when the actual value was approximately 138 g cm^{-2} introduced a 0.6% peak to peak annual variation into the Mawson data. During the solar cycle, the amplitude of this annual wave would change. The large day to day pressure fluctuations introduced even greater errors, these sometimes exceeding $\pm 1\%$.

For a large sea level neutron monitor having an average counting rate of 35 000 hr^{-1}, the standard deviation of the daily mean counting rate due to statistical fluctuations is 0.11%. An analysis of the daily mean ratios of the counting rates of the two sections of the Mawson duplex monitor has shown that the standard deviation of the total daily mean counting rate due to equipment variation is less than 0.13% ([5]). On the other hand, the errors introduced by poor choice of attenuation length can exceed $\pm 1\%$, and those due to the variation of attenuation length $\pm 0.5\%$. In addition, there are errors due to the limited accuracy of the pressure recording instruments ([11]). It is therefore clear that the barometric correction can be an important source of error, and that it can be the limiting factor in the study of small amplitude time variations in the primary cosmic ray intensity.

* * *

We are indebted to Dr. D. C. Rose and Dr. B. G. Wilson for supplying the data from Sulphur Mountain, Dr. A. E. Sandström for supplying those from Uppsala, and the Astronomer Royal and Mr. D. R. Palmer for those from Herstmonceux. The other members of the Hobart cosmic ray research group assisted in the maintenance of the Hobart recorder. We would like to

([11]) J. A. Lockwood and A. R. Calawa: *Journ. Atmos. Terr. Phys.*, **11**, 23 (1957).

thank Dr. A. G. FENTON, under whose guidance the work was performed. One of us (K.G. McC.) has participated in the cosmic ray research programme during tenure of an Australian Atomic Energy Commission studentship, and later, a General Motors Holden Research Fellowship.

RIASSUNTO (*)

Dall'analisi dei dati sui neutroni ottenuti in due stazioni molto distanti fra di loro, si dimostra che durante il 1957 la lunghezza d'attenuazione della componente nucleonica di alta energia della radiazione cosmica vicino al livello del mare ad alte latitudini geomagnetiche è stata di (138.1 ± 0.8) g cm^{-2}. L'analisi dei dati di alcune stazioni mostra che le ampiezze dei decrementi di tipo Forbush aumentano di circa il 12% per 1 000 m di aumento dell'altitudine delle stazioni stesse. Ciò dimostra che il valore della lunghezza di attenuazione è sensibile alle variazioni dello spettro di rigidità della radiazione primaria, aumentando coll'indurirsi dello spettro dei raggi cosmici primari. Si mostra che al livello del mare in vicinanza dell'equatore la lunghezza di attenuazione è considerevolmente maggiore che alle alte latitudini, presentando un valore di circa 159 g cm^{-2}. Si dimostra che la correzione per le variazioni atmosferiche può essere il fattore che pone limiti allo studio delle deboli variazioni nel tempo dell'intensità primaria per mezzo della misura della componente nucleonica a grandi profondità atmosferiche.

(*) *Traduzione a cura della Redazione.*

IL NUOVO CIMENTO Vol. XIII, N. 1 1° Luglio 1959

Polarization Effects in Σ^- Hyperons Capture by Deuterons.

O. D. Cheishvili and S. G. Matinyan

Physical Institute of the Georgian Academy of Sciences - Tbilissi

(ricevuto il 9 Marzo 1959)

Summary. — A phenomenological treatment of polarized Σ^--hyperons capture by deuterons with the production of Λ^0-particles is given. The quantitative investigation shows that the study of polarization correlations of these particles allows to obtain certain information about the polarization state of a Σ^--particle.

---

1. – Pais and Treiman (1) have recently considered phenomenologically the effect of a Σ^- hyperon capture by a proton. The study of this effect is very interesting from the point of view of determination of relative parity of Λ and Σ particles and for determination of the degree of polarization of a Σ hyperon not considering its decay as its polarization analyzer. (It is well known that the experiments on the measurement of the up-down asymmetry coefficient in the process of the associated production give quite different results for Λ and Σ particles; this fact makes the problem of determination of the polarization degree for Σ particles very important.)

The effect of polarized Σ^- hyperons capture by deuterons

$$\Sigma^- + d \rightarrow \Lambda^0 + 2n \tag{1}$$

is considered in this article.

The quantitative consideration of this process shows that the deuteron case is rather interesting as a source of some additional information on the problem of determination of the polarization degree of a Σ^- particle.

---

(1) A. Pais and S. B. Treiman: *Phys. Rev.*, **109**, 1759 (1958).

2. – The consideration of the process of a Σ^- hyperon capture by a deuteron is made in the impulse approximation (see for example ([2,3])). In this approximation the amplitude of the capture process of a particle by a deuteron has the following form:

$$T_d = J_{12}T(1, 2) + J_{13}T(1, 3) , \tag{2}$$

where the symbol 1 is used for strange particles and the symbols 2 and 3 for the nucleons constituting the deuteron.

Here

$$J_{1j} = \int \Psi_f^*(\boldsymbol{r}_1, \boldsymbol{r}_2, \boldsymbol{r}_3)\Psi_i(\boldsymbol{r}_1, \boldsymbol{r}_2, \boldsymbol{r}_3)\delta(\boldsymbol{r}_1 - \boldsymbol{r}_j)\, d\boldsymbol{r}_1\, d\boldsymbol{r}_2\, d\boldsymbol{r}_3 , \tag{2$'$}$$

where T is the amplitude of the Σ^- hyperon capture by a proton, given in ([1]) (of course the Σ^- hyperon is captured by one of the deuteron nucleons (proton) to which symbol 2 corresponds.) Ψ_i and Ψ_f are the initial and the final wave functions of the three particle system.

If to make the usual transition from the co-ordinates $\boldsymbol{r}_1$, $\boldsymbol{r}_2$, $\boldsymbol{r}_3$ in expression (2′) to the co-ordinates $\boldsymbol{\rho} = \boldsymbol{r}_2 - \boldsymbol{r}_3$ and $\boldsymbol{R} = (\boldsymbol{r}_2 + \boldsymbol{r}_3)/2$ and to single out explicitly the initial χ_i and the final χ_f spin functions of the three particle system we get:

$$T_d = \int \Phi_g^*(\boldsymbol{\rho})\Phi_d(\varrho) \exp[i\boldsymbol{\varkappa}\boldsymbol{\rho}]\, d\boldsymbol{\rho} \cdot (\chi_f(1, 2, 3), T(1, 2)\chi_i(1, 2, 3)) , \tag{3}$$

where $\Phi_g(\boldsymbol{\rho})$ is the wave function of two neutrons in the final state with the asymptotic momentum $\boldsymbol{g}$; $\Phi_d(\varrho)$ is the wave function of the deuteron, $2\boldsymbol{\varkappa}$ is the momentum transferred to the nucleons as the result of the reaction. In derivation (3) we neglected the interaction of a Σ^- hyperon with the neutrons in the final state.

Below it will be more convenient to introduce symmetric and antisymmetric space wave functions of the system of two neutrons Φ_g^+ and Φ_g^- corresponding to the singlet and triplet spin states selected with the help of the projection operators

$$\Pi_s = \tfrac{1}{4}(1 - \boldsymbol{\sigma}_2\boldsymbol{\sigma}_3) \qquad \text{and} \qquad \Pi_t = \tfrac{1}{4}(3 + \boldsymbol{\sigma}_2\boldsymbol{\sigma}_3) .$$

Performing the calculations we get the following expression for the polari-

---

([2]) G. Chew: *Phys. Rev.*, **80**, 196 (1950).
([3]) I. Ya. Pomerančuk: *Journ. Exp. Theor. Phys.*, **21**, 1113 (1951).

1681

zation vector $\boldsymbol{P}_\Lambda$ of a Λ^0 particle with the spin S produced in the result of the capture of the Σ^- particle, characterized by the spin density matrix ϱ_Σ (and by the polarization vector $\boldsymbol{P}_\Sigma$), by a deuteron:

$$(4)\qquad R_d\boldsymbol{P}_\Lambda = \tfrac{1}{3}\{|F^-|^2\,\mathrm{Tr}[\Pi_t(2,3)T(1,2)\varrho_\Sigma\Pi_t(2,3)T^+(1,2)\boldsymbol{S}] + \\ + |F^+|^2\,\mathrm{Tr}[\Pi_s(2,3)T(1,2)\varrho_\Sigma\Pi_t(2,3)T^+(1,2)\boldsymbol{S}]\},$$

where the trace is taken over the spin variables of all particles,

$$(5)\qquad R_d = \tfrac{1}{3}\{|F^-|^2\,\mathrm{Tr}[\Pi_t(2,3)T(1,2)\varrho_\Sigma\Pi_t(2,3)T^+(1,2)] + \\ + |F^+|^2\,\mathrm{Tr}[\Pi_s(2,3)T(1,2)\varrho_\Sigma\Pi_t(2,3)T^+(1,2)]\},$$

$$F^\pm = \int \Phi_g^{\pm *}\Phi_d \exp[i\boldsymbol{\varkappa\rho}]\,\mathrm{d}\boldsymbol{\rho}\,.$$

Below we consider only the realistic values of the spins of Λ^0 and Σ particles $(\varrho_\Sigma = \frac{1}{2}(1+\boldsymbol{P}_\Sigma\cdot\boldsymbol{\sigma}))$.

It is not difficult to see that in this case there is the following general relation between $\boldsymbol{P}_\Lambda$ and $\boldsymbol{P}_\Sigma$:

$$(6)\qquad R_d\boldsymbol{P}_\Lambda = \alpha\boldsymbol{P}_\Sigma + \beta(\boldsymbol{P}_\Sigma\boldsymbol{N})\boldsymbol{N}\,,$$

where $\boldsymbol{N}$ is the unit vector in the direction of motion of the Λ^0 particle. The values of R_d and α, β are determined by the type of the transition from the initial state to the final state and are connected with the dynamics of the Σ^--particle-proton interaction, resulting in capture.

3. – Let us consider these transitions separately. We shall use the expressions for the transition amplitudes on a free proton given in (1). One must bear in mind that the amplitudes used by Pais and Treiman characterize the transitions between the states of a strange particle-nucleon system. This is the reason why in the consideration of separate types of transitions on a deuteron we especially emphasize this fact. On the other hand when one considers the deuteron case it is necessary to speak about the transitions between the states of a strange particle-two nucleon system. It is easy to see, however, that when the both final nucleons are in the S-state of relative motion (it will be shown below that just in this case some simple definite conclusions about the polarization state of the Σ^- hyperon are obtained) then both these determinations coincide. Therefore from the point of view of the experiments with the deuteron just the particular cases with $\varkappa \approx 0$ given below are of interest.

3·1. *$S \to S$ transitions.* – In this case the amplitude of the capture process of a Σ^- particle by a proton is the following:

$$T = a_1 \Pi_t(1, 2) + a_2 \Pi_s(1, 2)\,,$$

where a_1 and a_2 are the amplitudes of the transitions ${}^3S_1 \to {}^3S_1$ and ${}^1S_0 \to {}^1S_0$ of a strange particle-nucleon system, respectively. (In what follows we use the usual spectroscopic notation.)

As the result of the calculations we get following expressions for R_d, α and β:

$$R_d = \tfrac{1}{16}\{(11|a_1|^2 + 3|a_2|^2 + 2\,\mathrm{Re}\,a_1 a_2^*)\,|F^-|^2 + (|a_1|^2 + |a_2|^2 - 2\,\mathrm{Re}\,a_1 a_2^*)\,|F^+|^2\}\,,$$

$$\alpha = \tfrac{1}{48}\{(25|a_1|^2 + |a_2|^2 + 22\,\mathrm{Re}\,a_1 a_2^*)\,|F^-|^2 - (|a_1|^2 + |a_2|^2 - 2\,\mathrm{Re}\,a_1 a_2^*)\,|F^+|^2\}\,,$$

$$\beta = 0\,.$$

In the case when the impulse transfer to nucleons is small ($\varkappa \approx 0$), $F^- \approx 0$ and

$$\boldsymbol{P}_\Lambda \approx -\tfrac{1}{3}\boldsymbol{P}_\Sigma \tag{7}$$

independently from the assumption made in (1) about coherence or incoherence of the states with a_1 or a_2.

Thus in this case one may obtain some definite information about the polarization of a Σ^- particle by studying the asymmetry in Λ^0 decay both for the case of the Σ^- capture from the continuum and from the bound S-states.

In the case of a free proton capture a simple inequality for $\boldsymbol{P}_\Lambda$

$$\boldsymbol{P}_\Lambda \leqslant \tfrac{2}{3}\boldsymbol{P}_\Sigma$$

is obtained only for the transitions from the S bound states when, as it was shown in (1), the states with a_1 and a_2 are incoherent.

3·2. *$S \to P$ transitions.* – The transition amplitude has the following form:

$$T = (3/2)^{\frac{1}{2}} b_1 \boldsymbol{N}\boldsymbol{S} + 3^{\frac{1}{2}} b_2 \boldsymbol{N}\boldsymbol{S}'\Pi_t + b_3 \boldsymbol{N}\boldsymbol{S}'\Pi_s\,,$$

where $\boldsymbol{S} = \frac{1}{2}(\boldsymbol{\sigma}_1 + \boldsymbol{\sigma}_2)$, $\boldsymbol{S}' = \frac{1}{2}(\boldsymbol{\sigma}_1 - \boldsymbol{\sigma}_2)$; b_1, b_2 and b_3 are the amplitudes of the transitions ${}^3S_1 \to {}^3P_1$, ${}^3S_1 \to {}^1P_1$ and ${}^1S_0 \to {}^3P_0$ of the above mentioned system respectively. The calculations give the following values for R_d, α and β:

$$R_d = \frac{1}{8}\Big\{\Big(5|b_1|^2 + \frac{9}{2}|b_2|^2 + \frac{3}{2}|b_3|^2 + \sqrt{2}\,\mathrm{Re}\,b_1 b_2^* + \sqrt{\frac{2}{3}}\,\mathrm{Re}\,b_1 b_3^* + \frac{1}{\sqrt{3}}\,\mathrm{Re}\,b_2 b_3^*\Big)|F^-|^2 +$$
$$+ \Big(|b_1|^2 + \frac{3}{2}|b_2|^2 + \frac{1}{2}|b_3|^2 - \sqrt{2}\,\mathrm{Re}\,b_1 b_2^* - \sqrt{\frac{2}{3}}\,\mathrm{Re}\,b_1 b_3^* - \frac{1}{\sqrt{3}}\,\mathrm{Re}\,b_2 b_3^*\Big)|F^+|^2\Big\}\,,$$

$$\alpha=\frac{1}{8}\left\{-\left(|b_1|^2+\frac{1}{2}|b_2|^2+\frac{1}{6}|b_3|^2+5\sqrt{2}\,\mathrm{Re}\,b_1b_2^*+5\sqrt{\frac{2}{3}}\,\mathrm{Re}\,b_1b_3^*+\sqrt{\frac{1}{3}}\,\mathrm{Re}\,b_2b_3^*\right)|F^-|^2+\right.$$
$$\left.+\left(|b_1|^2+\frac{1}{2}|b_2|^2+\frac{1}{6}|b_3|^2-\sqrt{2}\,\mathrm{Re}\,b_1b_2^*-\sqrt{\frac{2}{3}}\,\mathrm{Re}\,b_1b_3^*+\sqrt{\frac{1}{3}}\,\mathrm{Re}\,b_2b_3^*\right)|F^+|^2\right\},$$

$$\beta=\frac{1}{4}\left\{\left(3|b_1|^2+\frac{1}{2}|b_2|^2+\frac{1}{6}|b_3|^2+3\sqrt{2}\,\mathrm{Re}\,b_1b_2^*+\sqrt{6}\,\mathrm{Re}\,b_1b_3^*+\frac{5}{\sqrt{3}}\,\mathrm{Re}\,b_2b_3^*\right)|F^-|^2+\right.$$
$$\left.+\left(-\frac{1}{2}|b_2|^2-\frac{1}{6}|b_3|^2+\frac{1}{\sqrt{3}}\,\mathrm{Re}\,b_2b_3^*\right)|F^+|^2\right\}.$$

Let us consider again the case when $\varkappa\approx 0$ (in the experiments that corresponds to the observation of Λ^0 particles with energy higher than a certain energy E_0).

If the capture occurs from a discrete state then according to PAIS and TREIMAN the interference terms with $b_1b_3^*$ and $b_2b_3^*$ are zero. Then if the amplitude b_1 of the transition ${}^3S_1\to{}^3P_1$ predominates over the others we get the simple expression

$$\boldsymbol{P}_\Lambda\approx\boldsymbol{P}_\Sigma\,; \tag{8}$$

in the other extreme case when the main contribution is due to the amplitude b_2 or b_3 (or to them both) we obtain

$$\boldsymbol{P}_\Lambda=\tfrac{1}{3}\boldsymbol{P}_\Sigma-\tfrac{2}{3}(\boldsymbol{P}_\Sigma\boldsymbol{N})\boldsymbol{N}\,. \tag{9}$$

3'3. *$P\to S$ transitions.* – In this case the amplitude T has the form analogous to the form of the amplitude $S\to P$ transition only the unit vector $\boldsymbol{N}$ is now replaced by a unit vector $\boldsymbol{n}$ in the direction of the relative Σ^--P system momentum.

The final expressions for R_d, α and β were averaged over $\boldsymbol{n}$:

$$R_d=\frac{1}{8}\left\{\left(5|c_1|^2+\frac{9}{2}|c_2|^2+\frac{3}{2}|c_3|^2+\sqrt{2}\,\mathrm{Re}\,c_1c_2^*+\sqrt{\frac{2}{3}}\,\mathrm{Re}\,c_1c_3^*+\sqrt{\frac{1}{3}}\,\mathrm{Re}\,c_2c_3^*\right)|F\;|^2+\right.$$
$$\left.+\left(|c_1|^2+\frac{3}{2}|c_2|^2+\frac{1}{3}|c_3|^2-\sqrt{2}\,\mathrm{Re}\,c_1c_2^*-\sqrt{\frac{2}{3}}\,\mathrm{Re}\,c_1c_3^*-\sqrt{\frac{1}{3}}\,\mathrm{Re}\,c_1c_3^*\right)|F^+|^2\right\},$$

$$\alpha=\frac{1}{8}\left\{\left(|c_1|^2-\frac{1}{6}|c_2|^2-\frac{1}{18}|c_3|^2-3\sqrt{2}\,\mathrm{Re}\,c_1c_2^*-\sqrt{6}\,\mathrm{Re}\,c_1c_3^*+\frac{7}{9}\sqrt{3}\,\mathrm{Re}\,c_2c_3^*\right)|F\;|^2+\right.$$
$$\left.+\left(|c_1|^2+\frac{1}{6}|c_2|^2+\frac{1}{18}|c_3|^2-\sqrt{2}\,\mathrm{Re}\,c_1c_2^*-\sqrt{\frac{2}{3}}\,\mathrm{Re}\,c_1c_3^*+\frac{5}{9}\sqrt{3}\,\mathrm{Re}\,c_2c_3^*\right)|F^+|^2\right\},$$

$$\beta=0\,.$$

Here c_1, c_2 and c_3 are the amplitudes of the transitions ${}^3P_1 \to {}^3S_1$, ${}^1P_1 \to {}^3P_1$, ${}^3P_0 \to {}^1S_0$ of the Σ^--p respectively.

In the case when $\varkappa \approx 0$, taking into account that at the capture from a P-state all three amplitudes are incoherent, we obtain the following inequality:

$$\tfrac{1}{9}\boldsymbol{P}_\Sigma \leqslant \boldsymbol{P}_\Lambda \leqslant \boldsymbol{P}_\Sigma\,. \tag{10}$$

The extreme case of this inequality $\boldsymbol{P}_\Lambda \approx \boldsymbol{P}_\Sigma$ occurs when the amplitude c_1 predominates over the others; the other extreme case $\boldsymbol{P}_\Lambda \approx \frac{1}{9}\boldsymbol{P}_\Sigma$ occurs when one of the amplitudes c_2, c_3 predominates over the others. As one had to expect those inequalities could be obtained by a direct averaging of the expressions given in Section 3·2.

3·4. $P \to P$ *Transitions.*

$$T = (3/4)^{\frac{1}{2}}\{\tfrac{1}{3}d_1[4(\boldsymbol{N}\cdot\boldsymbol{n})\Pi_t - 3i\boldsymbol{S}[\boldsymbol{N}\boldsymbol{n}] - (\boldsymbol{n}\cdot\boldsymbol{S})(\boldsymbol{N}\cdot\boldsymbol{S})] +$$
$$+ d_2[i\boldsymbol{S}[\boldsymbol{N}\boldsymbol{n}] + (\boldsymbol{n}\cdot\boldsymbol{S})(\boldsymbol{N}\cdot\boldsymbol{S})] + i\sqrt{2}\boldsymbol{S}'[\boldsymbol{N}\boldsymbol{n}](d_3\Pi_t + d_4\Pi_s) +$$
$$+ 2d_5(\boldsymbol{N}\cdot\boldsymbol{n})\Pi_s + \tfrac{2}{3}d_6[(\boldsymbol{N}\cdot\boldsymbol{n})\Pi_t - (\boldsymbol{n}\cdot\boldsymbol{S})(\boldsymbol{N}\cdot\boldsymbol{S}]\}.$$

The amplitudes d_1, d_2, d_3, d_4, d_5 and d_6 concern the transitions ${}^3P_2 \to {}^3P_2$, ${}^3P_1 \to {}^3P_1$, ${}^3P_1 \to {}^1P_1$, ${}^1P_1 \to {}^3P_1$, ${}^1P_1 \to {}^1P_1$ and ${}^3P_0 \to {}^3P_0$ of the (Σ^--p)-system respectively.

When the conditions for incoherence are fulfilled we obtain (after the averaging over $\boldsymbol{n}$):

$$R_d = \frac{1}{16}\left\{\left(\frac{35}{6}|d_1|^2 + \frac{19}{6}|d_2|^2 + 3(|d_3|^2 + |d_4|^2 + |d_5|^2) + |d_6|^2 + \frac{\sqrt{2}}{3}\operatorname{Re} d_2 d_3^*\right)|F^-|^2 +\right.$$
$$\left. + \left(\frac{5}{6}|d_1|^2 + \frac{5}{6}|d_2|^2 + |d_3|^2 + |d_4|^2 + |d_5|^2 + \frac{1}{3}|d_6|^2 - \frac{\sqrt{2}}{3}\operatorname{Re} d_2 d_3^*\right)|F^+|^2\right\},$$

$$\alpha = \frac{1}{48}\left\{\left(\frac{97}{9}|d_1|^2 + |d_2|^2 + |d_5|^2 + \frac{1}{9}|d_6|^2 - 4\sqrt{2}\operatorname{Re} d_2 d_3^*\right)|F^-|^2 +\right.$$
$$\left. + \left(\frac{11}{9}|d_1|^2 - |d_2|^2 - |d_5|^2 - \frac{1}{9}|d_6|^2 - 2\sqrt{2}\operatorname{Re} d_2 d_3^*\right)|F^+|^2\right\},$$

$$\beta = \frac{1}{24}\left\{\left(-\frac{97}{36}|d_1|^2 + \frac{7}{4}|d_2|^2 - \frac{1}{2}|d_3|^2 - \frac{1}{2}|d_6|^2 - \frac{1}{9}|d_5|^2 + \frac{3}{\sqrt{2}}\operatorname{Re} d_2 d_3^*\right)|F^-|^2 +\right.$$
$$\left. + \left(-\frac{11}{36}|d_1|^2 + \frac{5}{4}|d_2|^2 + \frac{1}{2}|d_3|^2 + \frac{1}{2}|d_4|^2 + \frac{1}{9}|d_5|^2 + \frac{3}{\sqrt{2}}\operatorname{Re} d_2 d_3^*\right)|F^+|^2\right\}.$$

In this case it is difficult to draw any quantitative conclusions about the relation between $\boldsymbol{P}_\Lambda$ and $\boldsymbol{P}_\Sigma$; the same thing has taken place in [1].

As to the problem of determination of an initial predominate state it is solved in the same way as by PAIS and TREIMAN.

* * *

Finally the authors thank Professor G. R. KHUTSISHVILI for valuable discussions and advice.

RIASSUNTO (*)

Si da un trattamento fenomenologico della cattura di iperoni Σ^- polarizzati da parte di deutoni con la produzione di particlelle Λ^0. L'esame quantitativo mostra che lo studio delle correlazioni della polarizzazione di tali particelle permette di ricavare dati sullo studio di polarizzazione di una particella Σ^-.

(*) *Traduzione a cura della Redazione.*

IL NUOVO CIMENTO Vol. XIII, N. 1 1° Luglio 1959

On the Description of Unstable Particles in Quantum Field Theory (*).

M. Lévy

Ecole Normale Supérieure - Université de Paris - Paris

(ricevuto il 9 Marzo 1959)

Summary. — The mass and life-time of an unstable particle may be defined by the real and imaginary parts of a complex pole appearing on the Riemann surface in which its propagator can be continued analytically. This method, which was originally proposed by Peierls, is studied in detail, first on the basis of a special model, then in a more general field theory. The possibility of analytical continuation of the propagator is discussed, using the conditions of causality and unitarity of the S-matrix. The appearance of « unphysical » poles in the various sheets of the Riemann surface is also discussed. It is inferred that a physical principle must be used in each case, in order to select the particular pole which can be correctly interpreted as describing the properties of an unstable particle.

1. – Introduction.

The quantum theoretical treatment of unstable particles has recently become the object of much interest [1-4]. In spite of the fact that most of the so-called elementary particles are unstable, the theoretical situation is still

(*) Supported in part by the United States Air Force through the European Office, Air Research and Development Command.

(1) V. Glaser and G. Källén: *Nucl. Phys.*, **2**, 706 (1956).

(2) P. T. Matthews and A. Salam: *Phys. Rev.*, **112**, 283 (1958). See also the discussion in *Proc. of the Ann. Int. Conf. on High Energy Phys. at CERN* (1958), p. 141.

(3) H. Araki, Y. Munakata, M. Kawaguchi and T. Gotô: *Progr. Theor. Phys.*, **17**, 419 (1957).

(4) G. Höhler: *Zeits. f. Phys.*, **152**, 546 (1958) where the reader will also find more complete references to the literature on the subject.

unsatisfactory, in the sense that no systematical method exists in relativistic quantum mechanics or in field theory to describe unstable systems. For the treatment of atomic decaying states, there is the approximate method of WEISSKOPF and WIGNER [5], which has been extended systematically by HEITLER and his collaborators [6] in the form of a « damping theory ». However, the approximate definition of life-times which comes out of these treatments, although correct in the weak coupling sense, is not consistently obtained as has been pointed out already. In any case, there does not exist at present, even in atomic physics, a rigorous theory to which these various methods can be considered as approximations.

For the description of unstable particles in field theory, there is the additional difficulty that it does not seem possible to define a field φ of an unstable particle which satisfies the usual asymptotic condition, in the sense that φ_{in} and φ_{out} which are the limits of φ when $t \pm \to \infty$ do not exist. Consequently it is not possible to construct a basis of asymptotic stationnary states. Nevertheless, unstable particles cannot all be considered as « bound » systems of stable particles, because of the selection rules of strangeness, isotopic spin, etc. In order to include these selection rules in a complete description of fundamental particles, some elementary fields must be postulated which will correspond to unstable particles. This can be justified in practice by the fact that the interactions responsible for the decay of most unstable particles are very weak; if they are neglected in first approximation, most of the known elementary particles become stable and can be described by the usual method of field theory. The decay interactions can then be treated as a perturbation, along the lines of the atomic treatment. But from a fundamental point of view, this situation is certainly not satisfactory.

One should of course keep in mind that the uncertainty principle fixes severe limits to the « definition » of the mass and life-time of an unstable particle. If m is the mass and $\tau = 1/\Gamma$ the life-time, there will be an uncertainty in the definition of the mass of the order

$$\Delta m \simeq \Gamma . \tag{1.1}$$

Furthermore, since Γ can be considered as a kind of mean square deviation from the average of a mass distribution, there is also an uncertainty on Γ itself of the order

$$\Delta \Gamma \simeq \frac{\Gamma^2}{m} . \tag{1.2}$$

---

[5] V. WEISSKOPF and E. WIGNER: *Zeits. f. Phys.*, **63**, 54 (1930); **65**, 18 (1930).

[6] For a summary, see W. HEITLER: *Quantum Theory of Radiation*, 2nd ed. (Oxford, 1954).

It is therefore clear that m and Γ can be defined uniquely only if Γ is small (*i.e.* if the life time is long). In particular, if the decay occurs through an interaction, the strength of which is characterized by a coupling constant g:

— the mass will be defined with an arbitrariness of the order of g^2;

— the life-time can be defined uniquely to the order g^2, but there will be an arbitrariness of order g^4.

(This arbitrariness can be ascribed, if one wishes, to the production process.) In other words, there will be a large variety of manners to define m and Γ, all consistent with uncertainties (1.1) and (1.2), and any of them can be chosen for a given specific problem. One could then stop to worry about unstable particles, and be contented with the usual perturbation calculation of life-times, since any attempt to go further will only be a matter of personal choice. We think, however, that, from a fundamental point of view, a problem still exists for several reasons.

1) It is desirable to calculate the life-time to the lowest order in a completely consistent way. This is not true in the usual methods of atomic physics. In addition, the extension of these methods to the case of unstable « elementary » particles would imply for these particles not only the existence of a field φ, but also the definition of « free » outgoing and ingoing *states* which is certainly not possible, except in a very approximate and unphysical way.

2) Renormalization of mass and charge is usually based on the existence of « physical states » of the particles under consideration. Special methods must therefore be used for the renormalization of the mass of unstable particles and of the coupling constants of decay interactions.

3) It would be convenient to give a « natural » definition of the parameters m and Γ, for any value of the coupling constant, *which would be independent of the production process.* This definition would apply to metastable states of the type of the $(\frac{3}{2}, \frac{3}{2})$ resonance in π-p scattering as well as to « true » elementary unstable particles [7].

4) Finally, there is a practical problem which is probably the most important and difficult one: although an unstable particle cannot be an exact eigenstate of the total Hamiltonian, we are still able to observe it, if its life-time is not too short, and to make measurements of its properties. We should therefore be able to calculate, for example, the probability to observe the

---

[7] We refer to the work of K. Nishijima: *Phys. Rev.*, **111**, 995 (1958) and W. Zimmermann: *Nuovo Cimento*, **10**, 297 (1958), who have shown that fields representing bound states can be constructed, which obey the usual axioms of local field theory.

particle at time t as a function of t, and this, apart from some normalizing factor, should not depend strongly on the production mechanism. In other words, we should have a satisfactory prescription to describe an unstable particle as a wave packet of exact states of the Hamiltonian and thereby to construct its *time graph* without using unphysical initial conditions, such as the assumption of a « free » state at $t \to -\infty$, etc.

In principle, a fairly unambiguous (if not straightforward) way to define the properties of unstable particles is to investigate cross-sections of the decay products, as well as various reactions involving these products initially or finally. The unstable particle appears then as one of the possible intermediate states in the process, and this should manifest itself as a resonance. However, the definition of mass and life-time obtained from the resonance will vary from one process to the other. Besides, the method may not be very useful in practical cases (think of the difficulty of defining a Λ^0 by means of a resonance around 37 MeV in π^--p scattering!...).

Another method has been suggested by PEIERLS [8] and seems to us the most natural way to define unstable particles, although it may not be feasible in all cases. It consists in investigating the possible existence of poles in the multiple sheets of the Riemann surface into which the Fourier transform of the propagator can be continued analytically. Such poles have already been found in various special cases [9]. It is the main purpose of the present paper to study this method with some detail. Before one can think of using it, however, the main problem is to prove, first of all, that the propagator can actually be continued—at least into a limited region of the second sheet of the Riemann surface in which one may hope to find the complex pole corresponding to the mass and life-time of the particle.

A great advantage of the propagator's method, apart from the fact that it is « natural », and independent from the various production mechanisms, is that it involves only the assumption of a « field » φ, but no asymptotic « free » states into which the particle goes when $t \to \pm\infty$. We shall not discuss, in this paper, the possible methods to construct such a field (which sould vanish when $t \to \pm\infty$). We shall simply assume its existence [10].

Unfortunately, the propagator's method has also a disadvantage: the Riemann surface in a realistic theory will have an infinite number of sheets, a

---

(8) R. E. PEIERLS: *Proc. of the 1954 Glasgow Conf.* (London, 1955), p. 296.

(9) See some of the references given in Höhler's paper (4).

(10) The propagator's method seems also more practical than the method proposed by MATTHEWS and SALAM (2) who define the mass and life-time of an unstable particle by the first and second moments of a certain mass distribution $\varrho(K^2)$. In many instances, these moments, and especially the second, do not exist, if $\varrho(K^2)$ does not decrease very rapidly for large K^2. An example is given in Sect. **3** (see footnote (17)).

new one starting at each value of the energy corresponding to the threshold of a new real process. Each of these sheets will contain poles, and an additional physical principle is necessary to decide which one has the correct physical meaning in order to represent the complex mass of an unstable particle.

Since most of the problems connected with unstable particles are conceptual, it seems convenient to use a field theoretical model in which everything can be calculated exactly. The Lee model (11) is best suited for this purpose and was used already by GLASER and KÄLLÉN (1) and several other authors (3,4). Unfortunately, it turns out that the arbitrariness of the cut-off function, which is nevertheless essential in order to avoid the difficulty of ghosts states (12), introduces a crucial ambiguity in the continuation process. In Section **3**, however, this process is justified by a method where the cut-off function does not appear explicitly; the simple form of the S-matrix unitarity in the Lee model plays then an essential role (13). The analytical continuation of the propagator in a more general theory is studied in Section **4**. It is shown that, from a purely physical argument, *the propagator should only be continued from a limited section of the cut* into the second sheet of the Riemann surface. If one remains in this limited region, the possibility of analytical continuation depends on the analyticity of the S-scattering amplitude in the lower half-plane (14). This analyticity does not seem to follow from causality alone, but probably from a combination of dispersion relations with the unitarity of the S-matrix. An example is given, based on the double representation of scattering amplitudes proposed by MANDELSTAM (15). Finally, the « unphysical » poles of the propagator, which can be found in the other sheets of the Riemann surface accessible from the remaining parts of the cut, are discussed on the basis of a generalization of the Lee model which takes into account the « strong » interaction of the unstable particle in addition to its « weak » decay interaction. The problem of the description of an unstable particle as a wave packet of real states of the Hamiltonian (and therefore the construction of its decay curve as a function of time) is not discussed in the present paper. A qualitative discussion of this problem will be given in a forthcoming note.

---

(11) T. D. LEE: *Phys. Rev.*, **95**, 1329 (1954).

(12) G. KÄLLÉN and W. PAULI: *Dan. Mat. Fys. Medd.*, **30**, no. 7 (1955).

(13) When most of this work was done (especially Sects. **2** and **3**), the author had not yet seen the papers quoted in footnotes (3) and (4), who consider, among other things, the complex pole in the propagator of the Lee model. We feel that there is not much duplication with the present paper, where we are more interested in conditions for the analytical continuation to the pole, rather than in its precise location. Höhler's paper is more concerned with the construction of the time-graph of an unstable particle, and will be discussed in our forthcoming note on this problem.

(14) We are indebted to Prof. LEHMANN for an illuminating discussion on this point.

(15) S. MANDELSTAM: *Phys. Rev.*, **112**, 1344 (1958).

2. – Properties of scattering amplitudes in the Lee model.

This Section does not contain any new result. Its purpose is simply to rewrite the well-known properties of the Lee model in a slightly different form which will be convenient for the discussion of the following Sections.

2·1. *The renormalized Hamiltonian.* – When a stable state of the V-particle exists, the renormalization of mass and charge of the Lee model is, to a large extent, unambiguous. When the V-particle is unstable, the renormalization process becomes quite different and cannot be separated from the determination of the life-time. In this Section the renormalization constants will be exhibited formally, no distinction being made between the two possible cases.

We write the Hamiltonian:

$$H = H_0 + \delta H + H_{\text{int.}}\,, \tag{2.1}$$

where, with the same notations as Källén and Pauli [12], we have set

$$H_0 + \delta H = (m_V - \delta m)N^2 \sum_{\boldsymbol{p}} \psi_V^*(\boldsymbol{p})\psi_V(\boldsymbol{p}) + m_N \sum_{\boldsymbol{p}} \psi_N^*(\boldsymbol{p})\psi_N(\boldsymbol{p}) + \sum_{\boldsymbol{k}} \omega_k a_{\boldsymbol{k}}^* a_{\boldsymbol{k}}\,, \tag{2.2}$$

$$H_{\text{int}} = -\frac{g}{\sqrt{\Omega}} \sum_{\boldsymbol{p}=\boldsymbol{p}'+\boldsymbol{k}} \frac{f(\omega_k)}{\sqrt{2\omega_k}} [\psi_V^*(\boldsymbol{p})\psi(\boldsymbol{p}')a_{\boldsymbol{k}} + \text{c.c.}]\,. \tag{2.3}$$

Here, ψ_V, ψ_N and $a_{\boldsymbol{k}}$ are the usual annihilation operators of the V, N and θ particles respectively, and the corresponding starred quantities the creation operators of the same particles. V and N are treated non-relativistically with no recoil; $\omega_k = (k^2 + \mu^2)^{\frac{1}{2}}$ is the energy of a θ-particle of momentum $\boldsymbol{k}$; g and m_V are the « renormalized » charge and mass of the V-particle. What the latter quantity actually means will have to be defined precisely in each physical case. The unrenormalized mass and charge are given in terms of the two constants δm and N by the relations:

$$\begin{cases} g_0 = \dfrac{g}{N}\,. \\ m_V^0 = m_V - \delta m\,. \end{cases} \tag{2.4}$$

The only conditions which will be required in all cases are:

a) δm *is real*;

b) N^2 *is real and positive.*

1692

N is also related, as is well known, to the V-field renormalization: $\psi_{\text{V}} = \psi_{\text{V}}^0/N$, the corresponding anticommutation relations being written:

$$\{\psi_{\text{V}}^*(\boldsymbol{p}), \psi_{\text{V}}(\boldsymbol{p}')\} = \frac{1}{N^2}\delta_{\boldsymbol{pp}'} \; . \tag{2.5}$$

The relations for the N and θ fields are the usual ones. The total Hamiltonian of the Lee model has two constants of the motion:

$$\begin{cases} Q_1 = \eta_{\text{V}} + \eta_{\text{N}} \, , \\ Q_2 = \eta_{\text{N}} - \eta_{\theta} \, , \end{cases} \tag{2.6}$$

where η_α is the operator representing the number of particles of type (α). Eigenstates of H can therefore be constructed as linear combinations of eigenstates of H_0 corresponding to fixed values of q_1 and q_2, the eigenvalues of Q_1 and Q_2. As usual, we shall write the eigenstates of H_0 corresponding to given numbers of each particle in the form: $|n_{\text{V}}, n'_{\text{N}}, n''_{\theta}\rangle$.

In the following, we shall only be interested in the eigenstates of H corresponding to $q_1 = 1$, $q_2 = 0$. They are related either to the « physical » state of the V-particle (when it exists), or to the (N, θ) scattering states. We consequently consider the eigenvalue problem:

$$H|\Psi(1, 0)\rangle = (m_{\text{N}} + \omega)|\Psi(1, 0)\rangle \, , \tag{2.7}$$

where ω can take any value between $-\infty$ and $+\infty$ (it should not be confused with ω_k). $|\Psi(1, 0)\rangle$ is written in the form:

$$|\Psi(1, 0)\rangle = \beta(\omega)|1_{\text{V}}, 0, 0\rangle + \frac{1}{\sqrt{\Omega}}\sum_{k'}\psi(\omega; \omega_{k'})|0, 1_{\text{N}}, 1_{k'}\rangle \, , \tag{2.8}$$

where Ω is the normalizing volume. Putting this expression into equation (11.7), and setting:

$$\omega_0 = m_{\text{V}} - m_{\text{N}} \, , \tag{11.9}$$

we have the two conditions for β and ψ:

$$\begin{cases} (\omega_0 - \omega - \delta m)\beta(\omega) = \dfrac{g}{N\Omega}\displaystyle\sum_{k'}\frac{f(\omega_{k'})}{\sqrt{2\omega_{k'}}}\psi(\omega; \omega_{k'}) \, , \\[2ex] (\omega_{k'} - \omega)\psi(\omega; \omega_{k'}) = \dfrac{g}{N}\beta(\omega)\dfrac{f(\omega_{k'})}{\sqrt{2\omega_{k'}}} \, . \end{cases} \tag{2.10}$$

2·2. *The physical* V-*particle* ($\omega_0 < \mu$). – The compatibility condition of the two equations (2.10) is written:

$$h(\omega) = 0\,, \tag{2.11}$$

where we have defined:

$$h(\omega) = N^2 \left[\omega + \frac{g^2}{\Omega} \sum_{k'} \frac{f^2(\omega_{k'})}{\sqrt{2\omega_{k'}}} \frac{1}{\omega_{k'} - \omega} + \delta m - \omega_0\right]. \tag{2.12}$$

This function can be defined in the complex ω-plane with a cut on the real axis from $+\mu$ to $+\infty$. Going to continuous values of $\omega_{k'}$, and defining $\Gamma(z)$ as:

$$\Gamma(z) = \frac{g^2}{4\pi} f^2(z)\sqrt{z^2 - \mu^2}\,, \tag{2.13}$$

we have, in the cut plane:

$$h(z) = N^2 \left[z + \frac{1}{\pi N^2} \int_\mu^\infty \frac{\Gamma(\omega')\,\mathrm{d}\omega'}{\omega' - z} + \delta m - \omega_0\right]. \tag{2.14}$$

Asserting that a stable V-particle exists is equivalent to requiring that $h(z)$ has a real root at the value ω_0. In this case, we have:

$$\delta m = -\frac{1}{\pi N^2} \int_\mu^\infty \frac{\Gamma(\omega)\,\mathrm{d}\omega}{\omega - \omega_0}\,. \tag{2.15}$$

Writing the corresponding state as $|V\rangle$, we can also determine N^2 by the two equivalent conditions

$$\langle 0 | \psi_V | V\rangle = 1\,, \tag{2.16a}$$

or

$$\langle N | j | V\rangle = \langle 0, 1_N, 0 | j_0 | 1_V, 0, 0\rangle\,, \tag{2.16b}$$

where j is the renormalized current of the θ-field:

$$j = g(\psi_N^* \psi_V + \text{c. c.}) \tag{2.17}$$

and j_0 the corresponding unrenormalized current. The physical state $|N\rangle$ of the N-particle is identical with the free state $|0, 1_N, 0\rangle$. Note also that both $|V\rangle$ and $|N\rangle$ have to be normalized to unity.

It then follows that:

$$N^2 = 1 - \frac{1}{\pi}\int_{\mu}^{\infty} \frac{\Gamma(\omega)\,\mathrm{d}\omega}{(\omega-\omega_0)^2}\,. \tag{2.18}$$

If $N^2 > 0$, it can be proved [12] that the system does not contain any other root of $h(\omega) = 0$ for $\omega < \mu$. If $N^2 < 0$, there appears the well known ghost state of the V-particle. We exclude this possibility in the following.

2·3. *The scattering states* ($\omega > \mu$). – One finds, for this case:

$$\psi(\omega; \omega') = \sqrt{\Omega}\,\delta_{kk'} + \frac{g\beta(\omega)}{N}\frac{f(\omega')}{\sqrt{2\omega'}}\frac{1}{\omega' - \omega - i\varepsilon}\,, \tag{2.19}$$

with

$$\beta(\omega) = -\frac{gN}{\sqrt{\Omega}}\frac{f(\omega)}{\sqrt{2\omega}}\frac{1}{h(\omega + i\varepsilon)}\,. \tag{2.20}$$

The corresponding S-matrix has been given by Källén and Pauli [12]. We shall more specifically consider the forward scattering amplitude:

$$f_+(\omega) = -\frac{\Gamma(\omega)}{h(\omega + i\varepsilon)}\,. \tag{2.21}$$

(In the following we shall often write:

$$h_\pm \equiv h(\omega \pm i\varepsilon) = \overline{h(\omega)} \pm i\Gamma(\omega)\,, \tag{2.22}$$

where $\overline{h(\omega)}$ is the same function as $h(\omega)$ given by eq. (2.12) but with the integral replaced by its principal part.)

We also consider the function:

$$g_+(\omega) = \frac{f_+(\omega)}{\Gamma(\omega)} = -\frac{1}{h(\omega + i\varepsilon)}\,. \tag{2.23}$$

This function satisfies quite generally a dispersion relation of the type

$$g_+(\omega) = \frac{1}{\pi}\int_{\mu}^{\infty}\frac{\operatorname{Im} g_+(\omega')}{\omega' - \omega - i\varepsilon}\,\mathrm{d}\omega' + \frac{\theta(\mu - \omega_0)}{\omega - \omega_0}\,, \tag{2.24}$$

where the inhomogeneous term on the right hand side appears only when $\omega_0 < \mu$ (the function $\theta(x)$ is defined as $\theta(x) = 0$ for $x < 0$ and $\theta(x) = 1$ for $x > 0$).

Eq. (2.24) can be proved easily by writing:

$$\text{Im}\, g_+(\omega) = \frac{\Gamma(\omega)}{|h(\omega + i\varepsilon)|^2}, \tag{2.25}$$

and by evaluating the integral of the right hand side with the help of the contour C of Fig. 1. We have:

$$\frac{1}{\pi}\int_\mu^\infty \frac{\text{Im}\, g_+(\omega')}{\omega' - \omega - i\varepsilon}\,\mathrm{d}\omega' = -\frac{1}{2\pi i}\int_C \frac{\mathrm{d}z'}{h(z')}\,\frac{1}{z' - \omega - i\varepsilon}. \tag{2.26}$$

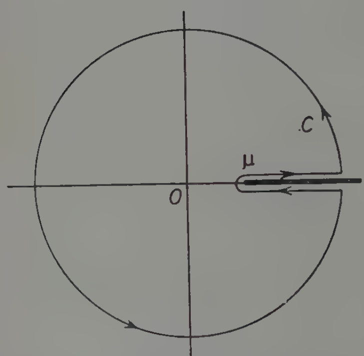

Fig. 1. – Contour of integration necessary to demonstrate the dispersion relation (2.24).

It should also be noted that:

$$h'(\omega_0) = 1, \tag{2.27}$$

because of the definition of N^2 in the case where $\omega_0 < \mu$ (Eq. (2.18)).

The forward scattering amplitude itself does not obey in general a dispersion relation. This is not surprising, since we are dealing with a fixed source theory, for which causality requirements are not automatically fulfilled. If we want f_+ to obey a dispersion relation, *we have to require that $\Gamma(z)$ be an analytical function in the cut plane except for possible poles.* We would then have a relation of the type:

$$f_+(\omega) = \frac{1}{\pi}\int \frac{\text{Im}\, f_+(\omega')}{\omega' - \omega - i\varepsilon}\,\mathrm{d}\omega' + \frac{\Gamma(\omega_0)\theta(\mu - \omega_0)}{\omega - \omega_0} + \sum_i \frac{a_i}{\omega - \omega_i}, \tag{2.28}$$

where the ω_i are the poles of Γ *which are not situated on the cut of* $h(z)$.

The condition of analyticity of $\Gamma(z)$ does not follow « naturally » from the Lee model. However, if we want to consider this model as a kind of simplified image of a more accurate and complicated theory, we may be led to require this condition. This question will be discussed more in detail in Section **3**.

2·4. *Properties of $h(z)$.* – It is convenient to transform slightly the expression (2.14) of $h(z)$ by writing:

$$\left\{\begin{aligned} N^2(\delta m - \omega_0) &= -\frac{1}{\pi}\int_\mu^\infty \frac{\Gamma(\omega')\,\mathrm{d}\omega'}{\omega'} + \alpha, \\ N^2 &= 1 - \frac{1}{\pi}\int_\mu^\infty \frac{\Gamma(\omega')\,\mathrm{d}\omega'}{\omega'^2} + \beta. \end{aligned}\right. \tag{2.29}$$

We then have:

$$h(z) = z\left[1 + \frac{z}{\pi}\int\limits_{\mu}^{\infty} \frac{\Gamma(\omega')\,\mathrm{d}\omega'}{\omega'^2(\omega' - z)}\right] + \alpha + \beta z\,, \tag{2.30}$$

where α and β are two *real* but otherwise arbitrary constants. The function $h - \alpha - \beta z$ is the function which has been considered by PAULI and KÄLLÉN ([12]) (in the case $\omega_0 = 0$). The advantage of the transformation (2.30) is that $h(z)$ remains finite even for infinite cut-off.

We then state two properties of $h(z)$:

1) *If $N^2 > 0$, $h(z)$ cannot have any complex zeros (regardless of the value of ω_0 real).*

This can be seen directly from the expression (2.14) by calculating:

$$\operatorname{Im} h(z) = (\operatorname{Im} z)\left[1 + \frac{1}{\pi N^2}\int\limits_{\mu}^{\infty} \frac{\Gamma(\omega')\,\mathrm{d}\omega'}{|\omega' - z|^2}\right], \tag{2.31}$$

which cannot vanish if $N^2 > 0$.

If $N^2 < 0$, which corresponds to the possibility of ghost states, it is well known that the two real zeros ω_0 and λ (see Ref. ([12])) can be replaced by two complex conjugate roots which are obtained by equating to zero the right hand side of (2.31) (δm being determined by the condition $\operatorname{Re} h(z) = 0$).

2) *If the cut-off function $f(\omega)$ does not have zeros for $\omega > \mu$, then $h_\pm \equiv h(\omega \pm i\varepsilon)$ cannot vanish for $\omega > \mu$.*

This property seems, at first sight, to be a special case of the preceding one. However, this is not quite true when $\operatorname{Im} z \to 0$. We have in this case:

$$\operatorname{Im} h_\pm = \pm\,\frac{\Gamma(\omega)}{N^2}\,. \tag{2.32}$$

The usual method of perturbation theory for treating an unstable particle consists in assuming that there exists an approximate complex zero of $h(z)$ of the type $z \simeq \omega_0 - i\gamma$ where γ is supposed to be a positive quantity infinitely small compared to ω_0. This method is easily seen to be inconsistent, since we have, in this case:

$$\operatorname{Im} h(\omega_0 - i\gamma) \simeq -\left(\frac{\Gamma(\omega_0)}{N^2} + \gamma\right), \tag{2.33}$$

which cannot be made to vanish with a *positive* γ (assuming always $N^2 > 0$).

1697

3. – Definition of the unstable V-particle by means of the propagator.

3·1. *General properties of the propagator.* – As was explained in the introduction, we are looking for a « natural » definition of the mass and life-time of the unstable particle which would be, as much as possible, independent of the production process. For this purpose we consider the propagator, as defined by LEHMANN ([16]):

$$\frac{1}{2}S'_{\mathrm{V}}(t)=\frac{1}{2\pi}\int_{-\infty}^{+\infty}S'_{\mathrm{V}}(\omega)\exp[-i(m_{\mathrm{N}}+\omega)t]\,\mathrm{d}\omega\,, \tag{3.1}$$

with

$$S'_{\mathrm{V}}(\omega)=-i\int_{-\infty}^{+\infty}\frac{\varrho(\omega')\,\mathrm{d}\omega'}{\omega'-\omega-i\varepsilon}\,. \tag{3.2}$$

In this case

$$\varrho(\omega)=\sum_i|\langle 0|\psi_{\mathrm{V}}|i,\,\omega\rangle|^2\,, \tag{3.3}$$

where the summation is extended over all the possible states of H of energy $\omega+m_{\mathrm{N}}=E$. It is easily seen that the only states for which the expectation value of the right hand side does not vanish are the states corresponding to $q_1=1$, $q_2=0$ considered in the last section. We have therefore:

$$\varrho(\omega)=\frac{\Gamma(\omega)}{\pi|h_+(\omega)|^2}\,\theta(\omega-\mu)+\theta(\mu-\omega_0)\,\delta(\omega-\omega_0)\,, \tag{3.4}$$

where the second term on the right hand side appears only when a stable V-particle exists ($\omega_0<\mu$). If $\omega_0>\mu$, GLASER and KÄLLÉN ([1]) have proved that the scattering states form a complete set of states ([17]). Putting the expression (3.4) into (3.2), we find, by making use of the dispersion relation for g_+ (Eq. (2.24)), that we have in all cases:

$$S'_{\mathrm{V}}(\omega)=\frac{i}{h_+(\omega)}\,, \tag{3.5}$$

([16]) H. LEHMANN: *Nuovo Cimento*, **11**, 342 (1954).

([17]) Eq. (3.4) provides an example of a mass density, the first and second moments of which may not exist (see footnote ([10])). In order to prevent the existence of ghost states, it is sufficient that $\Gamma(\omega)$ tends to a constant for $\omega\to\infty$ (this corresponds to $f(\omega)\sim\omega^{-\frac{1}{2}}$ for large ω). On the other hand, for the mass and life-time to be defined by the prescription of Matthews and Salam, $\Gamma(\omega)$ must behave like ω^{-2} for large ω; this corresponds to $f(\omega)\simeq\omega^{-\frac{3}{2}}$ and is, of course, much more restrictive. In a relativistic theory, this would imply that the vertex *operator* $\Gamma(p_1,p_2)$ behaves like W^{-3}, where $W^2=-(p_1+p_2)^2$.

so that, in all cases, we can write:

$$(3.6)\qquad \frac{1}{2}S'_{\mathrm{V}}(t) = -\frac{\exp[-im_{\mathrm{N}}t]}{2\pi i}\int\limits_{\infty+i\varepsilon}^{+\infty+i\varepsilon}\frac{\exp[-izt]}{h(z)}\,\mathrm{d}z\,.$$

An alternate expression can be obtained by dividing the path of integration into two parts, as indicated in Fig. 2. The integral over the path C_1 can be transformed into an integral over real values of ω between μ and $+\infty$, whereas the integral over C_0 gives only a contribution if $\omega_0<\mu$. We then have:

$$(3.7)\qquad \frac{1}{2}S'_{\mathrm{V}}(t)=\exp[-i(\omega_0+m_{\mathrm{N}})t]\theta(\mu-\omega_0)+ \\ +\frac{\exp[-im_{\mathrm{N}}t]}{\pi}\int\limits_{\mu}^{\infty}\frac{\Gamma(\omega')\exp[-i\omega' t]\,\mathrm{d}\omega'}{|h_+(\omega')|^2}\,.$$

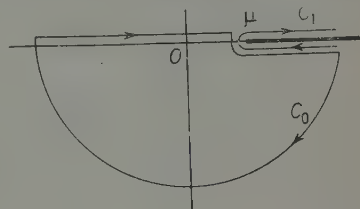

Fig. 2. – The path of integration of Eq. (3.6) is transformed into the sum of C_0 and C_1.

Now, it follows from a well-known theorem in Fourier or Laplace transforms [18] that the second term on the right hand side decreases for large t not as an exponential, but as a certain power of $1/t$. By investigating the asymptotic behaviour of the integral, we find indeed that:

$$(3.8)\qquad \frac{1}{2}S'_{\mathrm{V}}(t)\simeq\exp[-i(m_{\mathrm{N}}+\omega_0)t]\,\theta(\mu-\omega_0)- \\ -\frac{\exp[i\pi/4]}{\sqrt{2\pi}}\frac{g^2}{4\pi}|f(\mu)|^2\exp[-i(m_{\mathrm{N}}+\mu)t]\frac{\sqrt{\mu}}{h^2(\mu)t^{\frac{3}{2}}}+O(t^{-\frac{5}{2}})\,.$$

Let us discuss a little the case $\omega_0>\mu$, for which the first term on the right hand side does not appear. Let us suppose also that $g^2/4\pi$ is small compared to unity as it is always the case for what one usually calls « unstable particles ». All the terms in $t^{-(n+\frac{1}{2})}$ appearing on the right hand side will be proportional to $g^2/4\pi$ and therefore very small. On the other hand, we know that $\frac{1}{2}S'_{\mathrm{V}}(0)=1$ and also that:

$$(3.9)\qquad \frac{1}{4}\int\limits_{-\infty}^{+\infty}S'_{\mathrm{V}}(t)\exp[i(m_{\mathrm{N}}+\omega_1)t]\,\mathrm{d}t=\frac{1}{\Gamma(\omega_1)}\,,$$

---

(18) See, for example, S. Bochner and K. Chandrasekharan: *Fourier Transforms* (Princeton, 1949); G. Doetsch: *Theorie und Anwendung der Laplacetransformation* (Berlin, 1937).

where ω_1 has been chosen in such a way that:

$$\bar{h}(\omega_1) \equiv \operatorname{Re} h_{\pm}(\omega_1) = 0 \tag{3.10}$$

(ω_1 can be made to coincide with ω_0 if δm is appropriately chosen). The integral on the right hand side is proportional to $(g^2/4\pi)^{-1}$, so that it is clear that, in the case $\omega_0 > \mu$, we are missing an important term which does not appear in the asymptotic form but must give a predominant contribution for not too large values of t. We can anticipate that this term will decrease exponentially with t and that, if $\omega_0 > \mu$ and $g^2/4\pi \ll 1$, it will be the main value of $\frac{1}{2}S'_V(t)$ in a very large domain of t. It is therefore natural to look for this term as a definition of the mass and life-time of the unstable V-particle (19). In order to find it, we have to deform the contour of integration of Eq. (3.6) into the second sheet of the Riemann surface constructed from the cut plane on which $h(z)$ is defined. The contour which has to be used is shown in Fig. 3, where all dashed lines belong to the second sheet. However, before something of this kind can be done, we have to ask ourselves whether and under which conditions we can continue analytically the integrand $h^{-1}(z)$ into the second sheet of the Riemann surface.

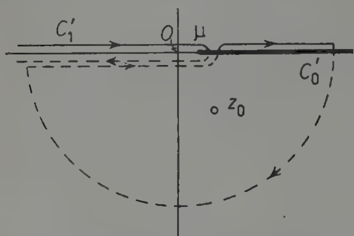

Fig. 3. – The path of integration fo Eq. (3.6) is transformed into the sum of C'_0 and C'_1. Dashed lines represent the parts of the contours which are on the second sheet of the Riemann surface.

3·2. *Analytical continuation of the propagator.* – The function $h(\omega)$ has a jump of $2i\Gamma(\omega)$ when we cross the cut on the real axis. The analytical con-

---

(19) In the Lee model, there is a simple connection between the propagator and the amplitude:

$$b(t) = \langle 1_V, 0, 0\rangle \exp[-iHt] \langle 1_V, 0, 0\rangle ,$$

the square of which is the probability to « observe » the state $|1_V, 0, 0|$ at time t, if $|1_V, 0, 0|$ were the only state present at $t = 0$. This connection is:

$$\frac{1}{2} S'_V(t) = \frac{b(t)}{N^2}.$$

In the framework of the usual treatment of decaying states, $|b(t)|^2$ would be considered as the time-graph of the V-particle, although we know very well that free states like $|l_V, 0, 0\rangle$ do not have much meaning in this case. Consequently, the discussion on the asymptotic behaviour of $S'_V(t)$ can be applied also immediately to $|b(t)|^2$ (see, for example, ref. (4)).

tinuation of $h(z)$ in the second sheet should be therefore

$$H(z) = h(z) + 2i\Gamma(z)\,. \tag{3.11}$$

However, such a continuation would be permissible only if $\Gamma(z)$ is an analytic function, *at least in a certain region in the neighbourhood of a finite segment of the cut.* We have already mentioned in the last section that an analyticity condition may be imposed on $\Gamma(z)$ if we want to have a dispersion relation for the forward scattering amplitude, in spite of the fact that we are dealing with a fixed source theory. On the other hand, it is clear also that special forms of the cut-off function can be chosen which will insure this analytical property. For example, since we cannot take an infinite cut-off, because of the ghost difficulty, we could decide that $f(z)=1$ inside a circle of large radius R and $f(z)=0$ outside. We would then have the possibility to continue $h(z)$ inside the circle of radius R and that would be sufficient, provided that R is large enough.

However, we are not interested here in such special choices of the cut-off function, since our purpose in using the Lee model is not to solve a mathematical exercise, but to illustrate in a simplified manner the conceptual features of a more general and realistic theory. We shall therefore perform the analytical continuation in a different manner, where the cut-off function never appears, *making use in a rather crucial way of the unitarity of the S-matrix.* The Lee model is then only convenient in the sense that the unitarity of the S-matrix can be expressed very simply by the relation:

$$\operatorname{Im} f_+(\omega) = |f_+(\omega)|^2\,, \tag{3.12}$$

because only one intermediate state contributes to the N-θ scattering process.

Going back to the definition (3.1) and (3.2) of the propagator, we write:

$$\left\{\begin{array}{l} \text{in the first sheet:}\quad S_V'^{(1)}(z) = -i\displaystyle\int_\mu^\infty \frac{\varrho(\omega')\,\mathrm{d}\omega'}{\omega'-z}\,, \\ \text{and,} \\ \text{in the second sheet:}\quad S_V'^{(2)}(z) = S_V'^{(1)}(z) + 2\pi\varrho(z)\,. \end{array}\right. \tag{3.13}$$

$\varrho(z)$, defined by (3.3), is the absolute square of a vertex function and, even if we can prove a dispersion relation for the vertex function itself, we have no guarantee that its absolute square will be analytical. We can write however, making use of (3.4) (in the case $\omega_0>\mu$) and (2.21):

$$\varrho(\omega) = -\frac{1}{\pi}\frac{|f_+(\omega)|^2}{f_-(\omega)\,h_-(\omega)}\,, \tag{3.14}$$

1701

where f_- is obtained from f_+ by changing h_+ into h_-. Now, $f_-(\omega)$ and $h_-(\omega)$, which are already defined in the lower half-plane, can be continued immediately; on the other hand $|f_+(\omega)|^2$ can be written:

$$|f_+|^2 = f_-(\omega)[f_-(\omega) + 2i \operatorname{Im} f_+(\omega)] \tag{3.15}$$

and, in general, we will have no information on the analytical properties of $\operatorname{Im} f_+$, from causality alone. However, the simple unitarity relation (3.12) allows us to write:

$$|f_+(\omega)|^2 = \frac{f_-(\omega)}{1 - 2if_-(\omega)}, \tag{3.16}$$

and consequently $\varrho(\omega)$ can be written:

$$\varrho(\omega) = -\frac{1}{\pi} \frac{f_-(\omega)}{h_-(\omega)\,[1 - 2if_-(\omega)]}. \tag{3.17}$$

$\varrho(\omega)$ can then, in this form, be continued in the lower half plane. We find, in this way:

$$S'_V(\omega_-) = \frac{i}{h_- + 2i\Gamma}, \tag{3.18}$$

which is, of course, the same analytical continuation as (3.11). It is clear that this method of analytical continuation will be valid in a more general theory where the S-matrix contains only one term. This will not be the case in general, *except for certain energy regions of the cut*, where some intermediate processes are forbidden by energetic considerations. However, another difficulty will arise in a more general theory, from the fact that a consistent definition of the S-matrix will never make use of the unstable V-particle itself, but only of its stable decay products. This difficulty will be discussed in Section **4**.

3·3. *Existence of a pole and renormalization of mass and coupling constant.* – Assuming then that the propagator can be continued, we evaluate $\frac{1}{2}S'_V(t)$ on the contour of Fig. 3. This gives (for $\omega_0 > \mu$):

$$\frac{1}{2}S'_V(t) = \frac{1}{H'(z_0)} \exp[-i(m_N + z_0)t] - \frac{\exp[-im_N t]}{\pi} \int_{-\infty}^{\mu} \frac{\Gamma(\omega)\exp[-i\omega t]\,d\omega}{h(\omega)H(\omega)}, \tag{3.19}$$

where the function H is defined by (3.11); z_0 is the root of the equation:

$$H(z_0) = 0 \, . \tag{3.20}$$

That such a root exists can be seen directly in the weak coupling limit where it can be calculated without specializing the form of $\Gamma(\omega)$.

Writing

$$z_0 = x_0 - iy_0 \, , \tag{3.21}$$

assuming that $y_0 \simeq O(g^2/4\pi) \ll x_0$ and that $\Gamma(z)$ is continuous around z_0, we can write:

$$h(z_0) \simeq N^2(x_0 - iy_0) + N^2(\delta m - \omega_0) + \frac{1}{\pi} P\int_{\mu}^{\infty} \frac{\Gamma(\omega)\,\mathrm{d}\omega}{\omega - x_0} - i\Gamma(\varkappa x_0) \, . \tag{3.22}$$

Eq. [3.20) can then be split into two parts:

$$\begin{cases} \bar{h}(x_0) = 0 \, , \\ \\ N^2 y_0 - \Gamma(x_0) = 0 \, . \end{cases} \tag{3.23}$$

(See Eq. (2.22) for the definition of $\bar{h}$.) The second equation gives: $y_0 = \Gamma(x_0)/N^2$; the first can always be solved by an appropriate choice of δm, which we only require to be real. The value of y_0 (the inverse half-life) which is so obtained is in agreement with the value deduced from perturbation theory by a special limiting process (1).

There remains to determine the value of the renormalization constants δm and N^2. There is no difficulty for δm, since it is natural to ask that the real part x_0 of the pole coincides with ω_0 (the splitting of the unrenormalized mass into $m_V - \delta m$ was prepared just for that):

$$\textit{1st condition} \qquad x_0 = \omega_0 \, . \tag{3.24}$$

In particular, in the weak coupling limit, this gives

$$\delta m = -\frac{1}{\pi} P\int_{\mu}^{\infty} \frac{\Gamma(\omega)\,\mathrm{d}\omega}{\omega - \omega_0} \, , \tag{3.25}$$

which is the value assumed implicitly by GLASER and KÄLLÉN (1). The determination of N^2 is more ambiguous, and various prescriptions can be given

which are all consistent and differ only by terms of the order of g^4. By analogy with equation (2.27) for the stable case, one could think of requiring the condition:

$$H'(z_0) = 1 ,$$

but this would imply a choice of a complex N^2 which leads clearly to difficulties with the hermitic properties of the field ψ_V, since N^2 is also a field renormalizing factor (ψ_V and ψ_V^* would not be hermitically conjugate). The

$$\text{(3.26)} \qquad \textit{2nd condition:} \qquad |H'(z_0)| = 1$$

has its advantages, because the coefficient of the exponential on (3.19) reduces then to an arbitrary phase factor ([20]). Besides, condition (3.26) can also be justified by an analytical continuation of the state vectors themselves into the second sheet. The continued scattering states do not longer form a complete set; they have to be complemented by two « ghost » states of energies z_0 and z_0^* and zero norm. The ghost state of energy z_0, for example, coincides with the « state » of the V-particle which has been proposed by NAKANISHI ([21]) as a formal solution of the Schrödinger equation, using the theory of complex distribution, except for a « normalizing » factor $N(H'(z_0))^{-\frac{1}{2}}$ which is imposed by the completeness relation written *on the second sheet.* Condition (3.26) follows then from a generalization of (2.16*a*):

$$\text{(3.27)} \qquad |\langle 0|\psi_V|V\rangle|^2 = 1 ,$$

which is a condition on g^2 and not on g.

Another way to define the coupling constant renormalizing factor N^2 would be to require that the N-θ scattering cross-section reduces to its Born approximation when $E = m_N + \omega \to m_V$. When $\omega_0 > \mu$ (stable case), this prescription is identical with conditions (2.16*a*) or (2.16*b*), since these are equivalent to $h'(\omega_0) = 1$. When $\omega_0 > \mu$ the prescription based on the scattering cross-section would correspond to:

$$\text{(3.28)} \qquad |h'(\omega_0)| = 1 .$$

With the choice (3.24) of x_0, it can be seen that conditions (3.26) and (3.28) agree with each other to the order g^4 as could be expected on the basis of incertainty relation (1.2). However, we feel, in the spirit of our general discus-

---

([20]) The coefficient of the exponential in $|b(t)|^2$ becomes also equal to unity (see footnote ([19])).

([21]) K. NAKANISHI: *Progr. Theor. Phys.*, **19**, 607 (1958).

sion of Section **1**, that prescriptions derived from scattering cross-sections should be avoided. In any case, it should be pointed out that this discussion of the coupling constant renormalization is rather academic. Indeed, if the life-time is long (as in the decays due to weak interactions), then the corrections to the renormalization constant due to the decay interaction can easily be neglected (this corresponds, in the present model, to taking $N^2=1$); and if it is short (as in the π^0-decay, for example) the coupling constant renormalization is already known from other phenomena.

4. – Analytical continuation of the propagator in a more general field theory.

We now discuss the analytical properties of the propagator of an unstable particle in a more general field theory. For simplicity, we shall assume that it is a scalar « V » particle represented by a « field » $\Phi(x)$. We do not discuss here the manner in which this field can be defined or constructed. This V particle decays into two stable scalar particles N and θ of masses M and μ. We suppose also that V is not coupled to particles of lower masses, but we do not restrict the number of θ-particles which can be emitted.

4·1. *Relation between the propagator and the scattering amplitude of the decay products.* – According to LEHMANN [16], the propagator $\Delta'_V(x)$:

$$\Delta'_V(x) = \frac{1}{(2\pi)^4}\int \Delta'_V(k^2)\exp[ikx]\,\mathrm{d}_4k\,, \tag{4.1}$$

can be constructed by means of a mass distribution $\varrho(K^2)$. $\Delta'_V(k^2)$ is analytic in the complex $(-k^2)$ plane with a cut starting at $K_0^2=(M+\mu)^2$. It will also have other cuts, starting at $(M+n\mu)^2$, $(n=2, 3$, etc.). Our problem is to decide whether we can continue it in the second (« unphysical ») sheet of the Riemann surface, through the cut starting at K_0^2. For this, we shall have to define a continuation of the analytical function in the first sheet:

$$\frac{1}{2}\Delta_V'^{(1)}(z) = -i\int_{K_0^2}^{\infty}\frac{\varrho(K^2)\,\mathrm{d}K^2}{K^2-z-i\varepsilon}\,, \tag{4.2}$$

into the second sheet by the formula:

$$\tfrac{1}{2}\Delta_V'^{(2)}(z) = \tfrac{1}{2}\Delta_V'^{(1)}(z) + 2\pi\varrho(z)\,, \tag{4.3}$$

and therefore, we have to know if $\varrho(z)$ is analytic in a region of the lower half plane sufficiently large to enable us to reach a pole if there is one.

Now, $\varrho(K^2)$ can be defined by means of a sum over a complete set of states:

$$\varrho(K^2) = 2\pi \sum_n |\langle 0|\Phi(0)|n\rangle|^2\, \delta(k_n^2 + K^2)\,, \tag{4.4}$$

where k_n^2 is the square of the energy-momentum of state $|n\rangle$. The summation must be extended over all the variables which characterize the state $|n\rangle$. In practice, we shall limit ourselves to the states into which the V-particle can decay, namely the physical states $|N, \theta\rangle$ of momenta p and k. They represent one of the terms of the propagator, and if we find a pole in the second sheet, it will correspond to an exponentially decreasing term in $\frac{1}{2}\Delta'_V(x)$ *with a coefficient of the order of unity regardless of the strength of the interaction.* It will represent therefore the dominant term of the propagator (all other poles, if they exist, will contribute more rapidly decreasing exponentials). We can also say that our physical intuition leads us to understand better the meaning of poles in such a term of the propagator rather than in all the others (this question is discussed in Section **4**·3).

With this approximation, $\varrho(K^2)$ will then be expressed in terms of the absolute square of the vertex function:

$$F_+((p+k)^2) = \langle 0|\Phi(0)|p, k\rangle \tag{4.5}$$

through the formula:

$$\varrho(K^2) = |F_+(-K^2)|^2\,. \tag{4.6}$$

With our previous assumptions about the spectrum of states to which the V-particle is related, it is presumably not difficult to prove a dispersion relation [22] for $F_+(-k^2) \equiv F_+(K^2)$:

$$F_+(K^2) = \frac{1}{\pi}\int_{K_0^2}^{\infty} \frac{\operatorname{Im} F_+(K'^2)\, \mathrm{d}K'^2}{K'^2 - K^2 - i\varepsilon}\,, \tag{4.7}$$

where the lower bound of the integral will again be $K_0^2 = (M+\mu)^2$ (this is, in any case, easy to verify in perturbation theory). This means that $F_+(z)$ is analytic in the complex cut-plane, and, in particular, in the lower half of the K^2 plane. However, we are not especially interested in the continuation of F_+ but rather of its absolute square:

$$|F_+|^2 = F_+[F_+ - 2i \operatorname{Im} F_+]\,. \tag{4.8}$$

([22]) References to the work on the vertex function are given in the report of M. L. Goldberger: *Proc. of the Ann. Int. Conf. on High Energy Physics at CERN* (1958), p. 207; see also W. Gilbert: to be published.

We therefore have to study the analytical properties of $\operatorname{Im} F_+$, on which causality does not give us any special information. However, we can restrict ourselves to values of K^2 which are limited by:

(4.9) $$K_0^2 \leqslant K^2 \leqslant K_1^2 = (M+2\mu)^2 .$$

In most of the practical cases, the «mass» of the V-particle will be contained in this range, and even if this is not so, we can always use a slightly different path of integration (see Fig. 4) in order to isolate the pole without crossing the cut outside of the domain (4.9). If the energy of the final state is limited in this way, we can then calculate $\operatorname{Im} F_+$ by the standard techniques which have been used already in connection with other problems [23]. We first write:

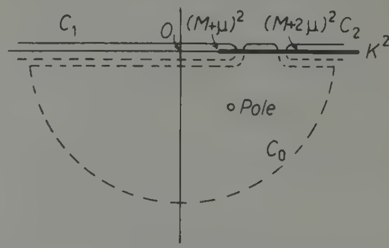

Fig. 4. – Decomposition of the contour of integration in the complex K^2 plane, in order to isolate the «physical» pole. The total path is the sum of C_0, C_1 and C_2. Dotted lines represent the parts of the contours situated on the second sheet.

(4.10) $$F_+ = \frac{i}{\sqrt{2\omega_k}}\int \exp[ikx]\,\mathrm{d}x\,\langle 0|(\varphi(0)),\, j(x))_+|p\rangle ,$$

where $j(x)$ is the current of the θ-particles. Then, in the usual way, we replace (4.10) by:

(4.11) $$F_+ = \frac{i}{\sqrt{2\omega_k}}\int \exp[ikx]\,\mathrm{d}x\,\langle 0|[\varphi(0), j(x)]|p\rangle\,\theta(-x) ,$$

and then take the imaginary part of F_+ by inserting a set of intermediate states:

(4.12) $$\operatorname{Im} F_+ = \frac{\pi}{\sqrt{2\omega_k}}\sum_s \langle 0|\varphi(0)|s\rangle\langle s|j(0)|p\rangle\,\delta(s-p-k) ,$$

where the spatial part of the δ-function must be understood as a Kronecker symbol. If we remain in the domain (4.9), the only states which will contribute to the sum (4.12) will again be the $|p, k\rangle$ states. We therefore have:

(4.13) $$\operatorname{Im} F_+((p+k)^2) = \\ = \frac{\pi}{\sqrt{2\omega_k}}\sum_{p',k'} \langle 0|\varphi(0)|p', k'\rangle\langle p', k'|j(0)|p\rangle\,\delta(p+k-p'-k') .$$

([23]) For example: M. L. Goldberger and S. B. Treiman: *Phys. Rev.*, **111**, 354 (1958); P. Federbush, M. L. Goldberger and S. B. Treiman: *Phys. Rev.*, **112**, 642 (1958); M. L. Goldberger and S. B. Treiman: *Neutral Pion Decay* (preprint).

1707

Now, on the right hand side we recognize, as the first factor, the vertex function $F_+((p'+k')^2)$. The second factor is directly related to the N-θ scattering amplitude $T(p, k; p', k')$

(4.14) $$\langle p', k' | j(0) | p\rangle = (8\omega_k\, p_0 p_0')^{-\frac{1}{2}} T(p, k; p', k')\,,$$

where T is given by the usual expression:

(4.15) $$T = -2i\sqrt{p_0 p_0'}\int \mathrm{d}_4 x \exp\left[i\left(\frac{k+k'}{2}\right)x\right]\theta(x_0)\langle p'|\left[j\left(\frac{x}{2}\right), j\left(-\frac{x}{2}\right)\right]|p\rangle\,.$$

T can be considered as a function of the square of the total energy W^2 and of the square of the momentum transfer Δ^2. Since F_+ depends only on $(p+k)^2$, one sees immediately that the summation on the right hand side of (4.13) involves an average over Δ^2. For convenience, we can use the center of mass system, and write:

(4.16) $$\operatorname{Im} F_+(-W^2) = \frac{1}{32\pi}\,\frac{F_+(-W^2)}{W\sqrt{\omega_k^2-\mu^2}}\int T(W^2, \Delta^2)\,\mathrm{d}\Delta^2\,,$$

so that $\operatorname{Im} F_+/F_+$ *is then simply proportional to the S-scattering amplitude.*

The condition for the continuation of the propagator in the region (4.9) of the cut is therefore that the S-scattering amplitude should be analytic in that region.

4·2. *Analyticity of the S-scattering amplitude.* – The analyticity of the S-scattering amplitudes has not been demonstrated from dispersion relations corresponding to a finite momentum transfer Δ^2. Such relations are usually valid only up to a certain maximum value $\Delta^2_{\max}$, whereas the integration of the scattering amplitude over Δ^2 involves, especially if the energy is sufficiently large, momentum transfers of all possible values. Therefore, even if the methods used to prove dispersion relations are improved in the future, it seems difficult that the analyticity of the S-scattering amplitude can be dmonstrated from causality alone. However, we believe that it is plausible that a combination of dispersion relations with the unitarity of the S-matrix can achieve the desired result. An especially simple case was already considered in Section **3**. A more general example can be obtained from the double representation of scattering amplitudes proposed recently by MANDELSTAM [15]. For simplicity, we shall only consider here the simple case of the scattering of two scalar particles of equal mass M. We write Mandelstam's representation in a slightly different form (neglecting possible contributions from poles which will,

in general, make no difficulty):

$$
\begin{aligned}
(4.17)\qquad T(W^2, \Delta^2) = \frac{1}{\pi}\iint \mathrm{d}\alpha^2\,\mathrm{d}\beta^2\,\frac{\partial\sigma_1(\alpha^2,\beta^2)}{\partial\beta^2}\,\frac{1}{(\alpha^2 - W^2)(\beta^2 + K^2)} + \\
+\frac{1}{\pi}\iint \mathrm{d}\alpha^2\,\mathrm{d}\gamma^2\,\frac{\partial\sigma_2(\alpha^2,\gamma^2)}{\partial\gamma^2}\,\frac{1}{(\alpha^2 - W^2)(\gamma^2 + \Delta^2)} + \\
+\frac{1}{\pi}\iint \mathrm{d}\beta^2\,\mathrm{d}\gamma^2\,\frac{\partial\sigma_3(\beta^2,\gamma^2)}{\partial\gamma^2}\,\frac{1}{(\beta^2 + K^2)(\gamma^2 + \Delta^2)}\,,
\end{aligned}
$$

where, in the center of mass, we have (if θ is the scattering angle):

$$
(4.18)\qquad \left\{
\begin{aligned}
-W^2 &= (p_1 + p_2)^2\,,\\
\Delta^2 &= (p_1 - p_1')^2 = (W^2 - 4M^2)\sin^2\frac{\theta}{2}\,,\\
K^2 &= (p_1 - p_2')^2 = (W^2 - 4M^2)\cos^2\frac{\theta}{2}\,.
\end{aligned}
\right.
$$

In other words, we suppose, in addition, that the Mandelstam weight functions are integrable, and that the corresponding integrals:

$$
(4.19)\qquad \sigma_i(\alpha^2, \beta^2) = \int_0^{\beta^2} \frac{\partial\sigma_i}{\partial\beta'^2}(\alpha^2, \beta'^2)\,\mathrm{d}\beta'^2\,,
$$

exist for all values of α^2 and β^2 of the allowed domain. Then, it can be seen in an elementary way that the scattering amplitude averaged over angles:

$$
(4.20)\qquad t_0(W^2) = \frac{1}{4\pi}\int T(W^2, \Delta^2)\,\mathrm{d}\Omega = \frac{1}{(W^2 - 4M^2)}\int_0^{W^2-4M^2} T(W^2, \Delta^2)\,\mathrm{d}\Delta^2\,,
$$

obeys the following relation:

$$
(4.21)\qquad t_0(W^2) = \frac{1}{\pi}\iint \frac{1}{\beta^2}\,\frac{[\sigma_1(\alpha^2,\beta^2) + \sigma_2(\alpha^2,\beta^2) + 2\sigma_3(\alpha^2,\beta^2)]\,\mathrm{d}\alpha^2\,\mathrm{d}\beta^2}{(\alpha^2 - W^2)(\beta^2 - 4M^2 + W^2)}\,.
$$

The functions σ_i vanish for α^2 and $\beta^2 \leqslant 4M^2$. (They may even vanish outside a smaller domain, as was shown by MANDELSTAM.) In general, therefore, the S-scattering amplitude will be an analytical function of the complex variable W^2 in a plane with two cuts, one from $-\infty$ to 0, the other from $4M^2$ to $+\infty$. There will be consequently no difficulty in continuing the S-scattering

amplitude, and therefore the imaginary part of the vertex operator, in the lower half-plane.

Another well-known example of analyticity of the S-scattering amplitude is given by potential scattering. As is well known, a large class of soluble potentials ([24]) gives for the S-scattering amplitude as a function of $E \simeq k^2$:

$$(4.22) \qquad 2it_0 + 1 = \prod_{n=1}^{N} \frac{k + i\gamma_n}{k - i\gamma_n}.$$

The scattering amplitude will be therefore analytic except for poles at $k^2 = -\gamma_n^2$ which are all located on the negative part of the real axis, where the Maldestam representation led us already to believe the existence of singularities. These poles correspond either to real bound states, or to the so-called « redundant poles » of the S-matrix ([25]).

4.3. *Treatment of the « spurious » poles in the propagator.* – We have already mentioned, in the above discussion, the possible existence of additional poles in the analytical continuation of the propagator through the higher cuts starting at $M+2\mu$, $M+3\mu$, etc. We would like now to discuss the meaning of these poles more in detail with the help of a generalization of the Lee model, in which the V-particle is involved in two interactions instead of one:

$$(4.23a) \qquad V \rightleftarrows N + \theta_1, \qquad (g_1),$$

$$(4.23b) \qquad V \rightleftarrows N + \theta_2, \qquad (g_2).$$

We suppose that the second interaction is much stronger than the first

$$(4.24) \qquad g_2^2 \ll g_1^2,$$

but that the mass μ_2 of the θ_2-particle is such that the rapid decay $V \to N + \theta_2$ is energetically forbidden:

$$(4.25) \qquad m_N + \mu_1 < m_V < m_N + \mu_2.$$

This situation is very close to the physical case of the Λ^0 decay, for example, where the reaction $\Lambda^0 \rightleftarrows p + K$ occurs much more strongly than the decay $\Lambda^0 \to p + \pi$, but is energetically forbidden unless the Λ^0 has a high kinetic energy. The main formulas of this « double Lee model » are given in the Ap-

---

([24]) See, *e.g.*: S. T. Ma: *Rev. Mod. Phys.*, **25**, 853 (1953).
([25]) R. Jost: *Helv. Phys. Acta*, **20**, 256 (1947).

pendix. The Lehmann weight function becomes the sum of two terms:

$$\varrho(\omega) = \frac{\Gamma_1(\omega) + \Gamma_2(\omega)}{\pi|h(\omega + i\varepsilon)|^2}, \tag{4.26}$$

where we have put:

$$\Gamma_i(\omega) = \frac{g_i^2}{4\pi}|f_i(\omega)|^2\sqrt{\omega^2 - \mu_i^2}\,\theta(\omega - \mu_i), \tag{4.27}$$

and

$$h(z) = N^2\left[z - \omega_0 + \delta m + \frac{1}{\pi N^2}\int_0^\infty \frac{\Gamma_1(\omega') + \Gamma_2(\omega')}{\omega' - z}\,d\omega'\right]. \tag{4.28}$$

The propagator retains the form (3.6). If we continue $h(z)$ in the energy region between $m_N + \mu_1$ and $m_N + \mu_2$ we have the continuation:

$$h^{(2)}(z) = h(z) + 2i\Gamma_1(z), \tag{4.29}$$

and it can be seen immediately that there is a pole having the correct physical meaning; the effect of the second interaction (4.23*b*) is simply to change δm and N^2 by what is usually called « renormalization due to strong interactions ». In particular, this pole will tend to the real axis and transform V into a stable particle if $g_1 \to 0$. However, we can also continue $h(z)$ in the energy region higher than $m_N + \mu_2$. Then, the continuation becomes:

$$h^{(3)}(z) = h(z) + 2i\Gamma_1(z) + 2i\Gamma_2(z), \tag{4.30}$$

which has, in the complex plane, a zero with a completely different behaviour. If we make the (physically meaningful) approximation:

$$\Gamma_1(\omega_0) \ll \Gamma_2(\omega_0) \ll m_V - m_N, \tag{4.31}$$

and write for this pole $z_1 = \omega_0 - iy_1$, we find:

$$y_1 = \frac{\Gamma_1(\omega_0) + 2\Gamma_2(\omega_0)}{N^2}, \tag{4.32}$$

which does not go to zero when $g_1 \to 0$. It is therefore clear that this pole does not have the correct physical meaning and should not be considered for the definition of the unstable V-particle [26].

---

[26] It is worth while to note that, even in the stable case of the usual Lee model, an « unphysical » pole in the second sheet of the propagator appears. In the weak coupling limit, its location is approximately at $\omega_0 - 2i(\Gamma(\omega_0)/N^2)$.

Finally, we arrive at the conclusion that the method of continuation which we used in the previous paragraph (namely considering the energy region where the only states which are energetically allowed are the decay states) was not only convenient but necessary. In other words, if the mass and life-time of an unstable particle are to be defined by a pole in the propagator, one has to make a definite prescription, *based only on physical arguments*, to choose the sheet of the Riemann surface into which the propagator has to be analytically continued.

In the above discussion we have implicitly assumed that the decay states are the lowest possible mass states of the spectrum. This may not be always the case; for example, the cascade particle Ξ^- decays into (Λ^0, π^-) states which have a threshold higher than the (n, π^-) states which seem to be forbidden, at least partially. Another example is the π-decay, which we may consider more in detail. There are two possible reactions:

$$(4.33) \qquad \begin{cases} \pi \to \mu + \nu & (g_\mu) \\ \pi \to e + \nu & (g_e) \end{cases}$$

and we know that [27] $g_e^2 \ll g_\mu^2 \ll 1$. On the other hand, we have $m_\pi > m_\mu > m_e$. If the propagator is continued into the sheet corresponding to the cut between m_e and m_μ, the corresponding h-function will be approximately equal to:

$$(4.34) \qquad h^{(2)} \simeq N^2(m_\pi - i\gamma) + i\Gamma_e(m_\pi) - i\Gamma_\mu(m_\pi)\,,$$

where we have written the possible pole as $m_\pi - i\gamma$; Γ_e and Γ_μ are some functions proportional to g_e^2 and g_μ^2 respectively. Since $g_\mu^2 \gg g_e^2$, we see that $h^{(2)}$ has no zero in the lower half-plane. On the other hand, if the continuation is made between m_μ and the next threshold (which will be, in this case, $3m_\pi$), a zero appears, the imaginary part of which has the expected behaviour:

$$(4.35) \qquad \gamma = \frac{\Gamma_e(m_\pi) + \Gamma_\mu(m_\pi)}{N^2}\,.$$

Consequently, no ambiguity will arise in such cases.

---

(27) Actually, we know that g_e^2 and g_μ^2 are of the same order, but that the *matrix elements* for the two reactions, namely $\Gamma_e(m_\pi)$ and $\Gamma_\mu(m_\pi)$ are such that $\Gamma_\mu(m_\pi) \gg \Gamma_e(m_\pi)$. This, however, does not change the argument.

A similar problem will occur when we discuss not the propagator of the unstable particle but its decay probability. This probability can be related (²) to the Lehmann weight function $\varrho(K^2)$, but a great care must be exercised in its definition, in order to prevent unphysical situations to occur. For example, if g_1^2 is large, the uncertainty on the mass of the V-particle is such that there will always be a finite probability for the V-particle to decay through interaction (4.23*b*) rather than (4.23*a*). This is physically acceptable provided that the corresponding partial probability goes to zero when $g_1^2 \to 0$, even if g_2^2 remains large. These problems will be discussed with more detail in a forthcoming note along with the prescriptions to be used in constructing the « time-graph » of an unstable particle.

* * *

A part of this work was done in Geneva, during the fall of 1958, when the author was enjoying the hospitality of C.E.R.N. He would like therefore to express his thanks to the members of the Theoretical Division for numerous discussions and suggestions on this and other related subjects, and especially to Dr. V. GLASER. He is also indebted to Professors A. SALAM and H. LEHMANN for several stimulating conversations.

APPENDIX

« Double » Lee model.

We start from the unrenormalized Hamiltonian:

$$H = H_0 + H_1 \,, \tag{A.1}$$

with:

$$H_0 = m_V^0 \sum_p \psi_V^*(\boldsymbol{p})\psi_V(\boldsymbol{p}) + m_N^0 \sum_p \psi_N^*(\boldsymbol{p})\psi_N(\boldsymbol{p}) + \sum_k \omega_1(k) a_k^* a_k + \sum_k \omega_2(k) b_k^* b_k \,, \tag{A.2}$$

where we have set:

$$\omega_i(k) = (k^2 + \mu_i)^{\frac{1}{2}} \,, \tag{A.3}$$

and

$$(A.4)\qquad H_1 = -\frac{g_1^0}{\sqrt{\Omega}}\sum_{p'=p+k}\frac{f_1(\omega_1)}{\sqrt{2\omega_1}}[\psi_V^*(p')\psi_N(p)a_k + \psi_V(p')\psi_N^*(p)a_k^*] - \\ -\frac{g_2^0}{\sqrt{\Omega}}\sum_{p'=p+k}\frac{f_2(\omega_2)}{\sqrt{2\omega_2}}[\psi_V^*(p')\psi_N(p)b_k + \psi_V(p')\psi_N^*(p)b_k^*]\,.$$

The (a_k, a_k^*), (b_k, b_k^*) are the annihilation and creation operators of particles θ_1 and θ_2 respectively; f_1 and f_2 are two cut-off functions. There are still two constants of the motion:

$$(A.5)\qquad \begin{cases} Q_1 = \eta_V + \eta_N\,, \\ Q_2 = \eta_N - \eta_{\theta_1} - \eta_{\theta_2}\,. \end{cases}$$

The states corresponding to $q_1=1$, $q_2=0$ correspond either to the (N, θ_1) or to the (N, θ_2) scattering states (if we make the assumption (4.25) on the mass spectrum). These states are given by:

$$(A.6)\qquad |N, \theta_i; E\rangle = \beta_i(E)|1_V, 0, 0\rangle + \frac{1}{\sqrt{\Omega}}\sum_{k,j}\psi_{ij}(E; k)|0, 1_N, 1_{k_j}\rangle\,,$$

where the subscript k_j means a θ_j particle with momentum k. The functions β_i are given by:

$$(A.7)\qquad \beta_i(E) = -\frac{g_i^0}{\sqrt{\Omega}}\frac{f_i(\omega)}{\sqrt{2\omega}}\frac{1}{h(\omega+i\varepsilon)}\,,$$

where we have set $E = m_N + \omega$ and $h(z)$ is given by Eq. (4.28) of the text. The functions ψ_{ij} are given by:

$$(A.8)\qquad \psi_{ij}(E; k) = \sqrt{\Omega}\,\delta_{kk_i}\delta_{ij} + g_j^0\beta_i(E)\frac{f_j[\omega_j(k)]}{\sqrt{2\omega_j(k)}}\frac{1}{m_N+\omega_j(k)-E-i\varepsilon}\,,$$

where k_i is such that:

$$(A.9)\qquad k_i^2 + \mu_i^2 = \omega^2 = (E-m_N)^2\,.$$

The corresponding scattering amplitudes are given simply by:

$$(A.10)\qquad f_{i+}(\omega) = -\frac{\Gamma_i(\omega)}{h_+(\omega)}\,,$$

where the functions Γ_i are defined by Eq. (4.27), with $g_i^2=(g_i^0)^2N^2$, the constant N^2 renormalizing *both* coupling constants and being related in the usual way to the ψ_V-renormalization. In Eq. (4.28) of the text, the bare mass of the V-particle has also been replaced by $m_V - \delta m$, where δm is the mass renormalization due to both interactions.

This model can easily be generalized to include n bosons θ_p ($p=1, 2, \ldots, n$) coupled to V and N in such a way that $V \rightleftarrows N+\theta_p$ are the only allowed reactions. If the masses μ_p are chosen such that $\mu_p = p\mu$, the model reproduces many of the features of a more realistic theory where the number of bosons would not be limited.

RIASSUNTO (*)

La massa e la vita media di una particella instabile possono definirsi per mezzo delle parti reale e immaginaria di un polo complesso che appare sulla superficie riemanniana sulla quale il suo propagatore può essere continuato analiticamente. Si studia questo modello, originariamente proposto da PEIERLS, prima sulla base di un modello speciale, poi nel quadro di una teoria di campo più generale. Si discute la possibilità della continuazione analitica del propagatore servendosi delle condizioni di causalità e di unitarietà della matrice S. Si discute anche l'apparizione di poli « non fisici » sulle varie falde della superficie riemanniana. Si deduce che per scegliere correttamente il particolare polo che descriva le proprietà di una particella instabile si deve in ogni caso adottare un principio fisico.

(*) *Traduzione a cura della Redazione.*

1715

IL NUOVO CIMENTO Vol. XIII, N. 1 1° Luglio 1959

Geometrical Generalization of γ_5-Invariance.

S. Watanabe

IBM Research Laboratory - Yorktown Heights, N.Y.

(ricevuto il 12 Marzo 1959)

Summary. — It will be shown that all the free Lagrangians and the well-established strong, intermediate and weak interaction Lagrangians are invariant for a special transformation which has a simple geometrical meaning and is a natural generalization of the γ_5-transformation. This invariance with certain further requirements can limit the possible interaction types to a very small number.

In view of the experimental facts revealing non-conservation of parity, the concepts of chirality and chirality transformation have been introduced (1). Sudharshan and Marshak (2) have shown that the requirement that a four-spinor interaction be invariant for the chirality transformation:

$$\psi \to e^{i\alpha}\gamma_5\psi\,, \qquad \overline{\psi} \to -\, e^{-i\alpha}\overline{\psi}\gamma_5 \tag{1}$$

for *each* of the four spinors *separately* leads to the $(V—A)$-type Fermi-interaction. In such an expression, the spinors have to be arranged in a certain order, and a universal phase-change in (1) must be used for each of them. This transformation, however, does not leave the free Lagrangian of a fermion with

(1) S. Watanabe: *Phys. Rev.*, **106**, 1306 (1957); *Nuovo Cimento*, **6**, 187 (1957); Y. Tanikawa and S. Watanabe: *Phys. Rev.*, **110**, 289 (1958); *Phys. Rev.*, in press.

(2) E. C. G. Sudarshan and R. E. Marshak: *Phys. Rev.*, **109**, 1860 (1958); R. P. Feynman and N. Gell-Mann: *Phys. Rev.*, **109**, 193 (1958).

finite mass invariant [1], unless we perform simultaneously another transformation:

$$m \to -m \,. \tag{2}$$

SAKURAI [3], on the other hand, starting from the fact that each free Lagrangian is invariant for (1) and (2), reached the same conclusion as SUDARSHAN and MARSHAK by requiring the same invariance for the four-spinor interaction. The electromagnetic interaction of a fermion $i\bar{\psi}\gamma_\mu\psi A_\mu$ and the pion-nucleon interaction $i\bar{\psi}\boldsymbol{\tau}\gamma_5\psi\boldsymbol{u}$ remain unchanged for (1), if one further assumes

$$A_\mu \to A_\mu\,, \qquad \boldsymbol{u} \to -\boldsymbol{u}\,. \tag{3}$$

This fact led SALAM [4] to his idea of γ_5-symmetrization. Each of these four transformations, (1), (2), (3), was introduced as necessity presented itself, and no theory is known to derive them from a single point of view. The present letter is intended to propose such a unified point of view.

The present author [5] formerly pointed out that all the known free Lagrangians can be written in an extremely compact invariant form in a five-dimensional flat space (hereinafter referred to as the 5-space), of which a four-dimensional sub-space is the usual Minkowski space and the *space-like* fifth co-ordinate x_5 is the canonical conjugate of the particle-mass. This means that in the usual field equations, m should be replaced as

$$m \to -i\,\partial/\partial x_5 \tag{4}$$

implying that the usual field quantity depends on the x_5-co-ordinate only through a factor, $\exp[imx_5]$. The momentum-energy vector of a particle is complemented by a fifth component m to form a 5-vector whose length is zero. The usual 4-component spinor in the Minkowski space can be considered, as it is, as a spinor for all congruent transformations in the 5-space by extending the usual transformation rule to the 5-space, in particular, assuming that the inversion of the x_5-co-ordinate corresponds to multiplication by γ_5, *i.e.*, (1). In the 5-space, $i\bar{\psi}\gamma_5\psi$ is a pseudo-scalar (of the third kind); $i\bar{\psi}\gamma_\mu\psi$ and $\bar{\psi}\psi$ together form a vector (speudo-vector of the second kind); $\bar{\psi}\gamma_\mu\gamma_\nu\gamma_5\psi$ and

---

(3) J. J. SAKURAI: *Nuovo Cimento*, **7**, 649 (1958); T. OUCHI, K. SENBA and M. YONEZAWA: *Progr. Theor. Phys.* (*Japan*), **14**, 172 (1955); S. WATANABE: *Progr. Theor. Phys.* (*Japan*), **15**, 81 (1956); T. OUCHI: *Progr. Theor. Phys.* (*Japan*), **17**, 743 (1957).

(4) A. SALAM: *Phys. Rev. Lett.*, **2**, 127 (1959).

(5) S. WATANABE: *Sci. Pap. Inst. Phys. Chem. Res.* (*Tokyo*), **39**, 157 (1941); **42**, 1 (1944); *Phys. Rev.*, **76**, 296 (1949). See also Appendix (A) in S. WATANABE: *Phys. Rev.*, **84**, 1008 (1951).

$i\overline{\psi}\gamma_\mu\gamma_5\psi$ together form a pseudo-tensor (of the third kind). A pseudo-scalar field u in the Minkowski space is to be interpreted as a pseudo-scalar in the 5-space. A vector field A_μ of the Minkowski space has to be complemented by a fifth component A_5 which appears to be a scalar in the Minkowski space.

Obviously, if we tilt the x_5-direction, the mass m will change, which is unphysical. However, the form of the free field equations thus obtained is completely invariant for any rotation or inversion in the 5-space, including of course the inversion of the fifth direction. Since this formalism was esthetically appealing, it was suggested (6) to examine whether the requirement of full five-dimensional invariance will not be a useful guide in selecting the right interaction types. The Yukawa-type interactions (without derivatives) of the zeroth order (scalar) and of the first order (vector) according to this criterion are then limited to $\mathcal{L}_S=\overline{\psi}\gamma_5\psi u$ and $\mathcal{L}_V=i\overline{\psi}\gamma_\mu\psi A_\mu+\overline{\psi}\psi A_5$. As far as we remain within the frame-work of 4-component spinors described above, a five-dimensional scalar and a five-dimensional pseudo-vector do not appear. It is interesting that the pion-nucleon interaction emerges as the simplest interaction allowed by the present rule. The electromagnetic interaction of a spinor can be identified as $\mathcal{L}_V$ if for a reason or another A_5 can be equated to zero (6).

It is, in any event, clear that all the four transformations, (1), (2), (3), can now be considered as direct consequences of the inversion of the x_5-axis (which is a space-like co-ordinate). Indeed, the mass, m, being the fifth component of a vector (pseudo-vector of the second kind) changes its sign by the x_5 inversion. The electromagnetic potential, A_μ, being the Minkowski part of a vector (pseudo-vector of the second kind), does not change its sign. The pion field, u, being a pseud-scalar (of the third kind), changes its sign. Thus, we conclude that *all free and interaction Lagrangians are invariant for the simultaneous x_5-inversion of all the fields involved.* Thereby it is assumed that the phase-changes of the spinors in the x_5-inversion are to be suitably chosen.

If we characterize the strong, intermediate and weak interactions in the following fashion, then there will not be too many «allowed» interactions other than the well-established ones. The strong interaction is invariant for all congruent transformations in the 5-space. It is thus invariant for the x_5-inversion of all fields involved simultaneously, but not separately. The electromagnetic interaction is invariant for all congruent transformations in the Minkowski space and invariant for the x_5-inversion of all participating fields separately as well as jointly, but not invariant for the other congruent transformations in the 5-space. The weak interaction is invariant for rotations in the Minkowski-space, time-reversal and the x_5-inversion of all fields, sepa-

(6) S. Watanabe: *Phys. Rev.*, **74**, 1864 (1948).

rately as well as jointly, but not invariant for the other congruent transformations in the 5-space.

Finally, many people (7) have already noticed a formal analogy between the two projection operators, $(1+\tau_3)/2$ and $(1+\gamma_5)/2$, but in the present formalism, this analogy acquires a deeper geometrical meaning, τ_3 and γ_5 corresponding to the « parity » with respect to an additional direction perpendicular to the subspace in which the rotations have a universal meaning (8). The strong interaction distinguishes itself as an invariant for all congruent transformations in the 5-space as well as in the isospin space.

---

(7) Among others, Y. TANIKAWA and A. SALAM: private conversation.
(8) See for instance Sect. **10** in S. WATANABE: *Rev. Mod. Phys.*, **27**, 40 (1955).

RIASSUNTO (*)

Si dimostra che tutto i lagrangiani liberi e i lagrangiani d'interazione forte, intermedia e debole oramai accettati sono invarianti rispetto a una speciale trasformazione che ha un significato geometrico semplice ed è una naturale generalizzazione della trasformazione γ_5. Tale invarianza, in unione a determinate condizioni ulteriori, può limitare a un numero assai ristretto i possibili tipi d'interazione.

(*) *Traduzione a cura della Redazione.*

1719

IL NUOVO CIMENTO Vol. XIII, N. 1 1° Luglio 1959

The Diffusion Coefficient in Dilute H_2-D_2 and ^{3}He-^{4}He Liquid Mixtures.

G. Careri (*), J. Reuss and J. M. Beenakker

Laboratori Nazionali dell'I.N.F.N. - Frascati
Kamerling Onnes Laboratorium - Leiden

(ricevuto il 13 Marzo 1959)

Summary. — An apparatus has been built to measure the diffusion coefficient in liquids at very low temperatures. This technique has been applied to the hydrogen-deuterium dilute mixtures, and the results can be expressed by an Arrhenius type equation as function of the absolute temperature $D = 64 \exp [48/T] \cdot 10^{-5}$ cm²/s. The same technique was more difficult to use for the helium isotope mixtures. The results are affected by large errors and roughly $D = (4 \pm 2) \cdot 10^{-5}$ cm²/s in the temperature range above the λ point.

1. – Introduction.

So far, only the viscosity and heat conductivity have been measured at very low temperature, but no direct measurements of the diffusion coefficient have been reported.

For the above reasons an apparatus has been designed, which seems well adapted to this kind of experiments. It is the purpose of this paper to describe the technique and the results obtained for the hydrogen-deuterium mixtures and some attempts concerning the ^{3}He-^{4}He mixtures (**).

(*) Now at the Istituto di Fisica dell'Università di Padova.

(**) This technique has been very briefly outlined by us a few years ago [1], and in the meantime following our procedure, this apparatus has been used at liquid air temperature by other workers [2].

[1] G. Careri, J. M. Beenakker and K. W. Taconis: *Communication on Congrès de la Physique des Basses Températures* (Paris, 1955), p. 393.

[2] G. Cini-Castagnoli, G. Pizzella and F. P. Ricci: *Nuovo Cimento*, **10**, 309 (1958).

2. – Experimental technique.

The method used in these experiments is substantially the « capillary method » already used in high temperature work (³). In principle, one must allow diffusion to take place between a capillary of length L and an infinite large reservoir. If c_0 is the initial uniform concentration and $\bar{c}$ the average final one in the capillary after a time τ, one has

$$(1)\qquad \frac{\bar{c}}{c_0} = \frac{8}{\pi^2}\sum\left\{(1/(2\pi+1)^2)\cdot \exp\left[-(2n+1)^2\pi^2 D\tau/4L^2\right]\right\},$$

which gives the diffusion coefficient in terms of known quantities, if the capillary concentrations are measured as it is the case.

With reference to Fig. 1, the above conditions have been fulfilled in practice by a brass capillary of 0.5 mm diameter and 40 mm length, closed at both ends by the valves V_1 and V_2. Opening the V_1 valve, the capillary can be brought in contact with the reservoir below the capillary, and opening the upper valve V_2, the capillary can be filled and evacuated. The reservoir volume is about 10^3 times the capillary volume, and can be filled and evacuated independently. With the exception of the capillary and the reservoir which are made of brass and copper respectively, all other elements are of neusilber.

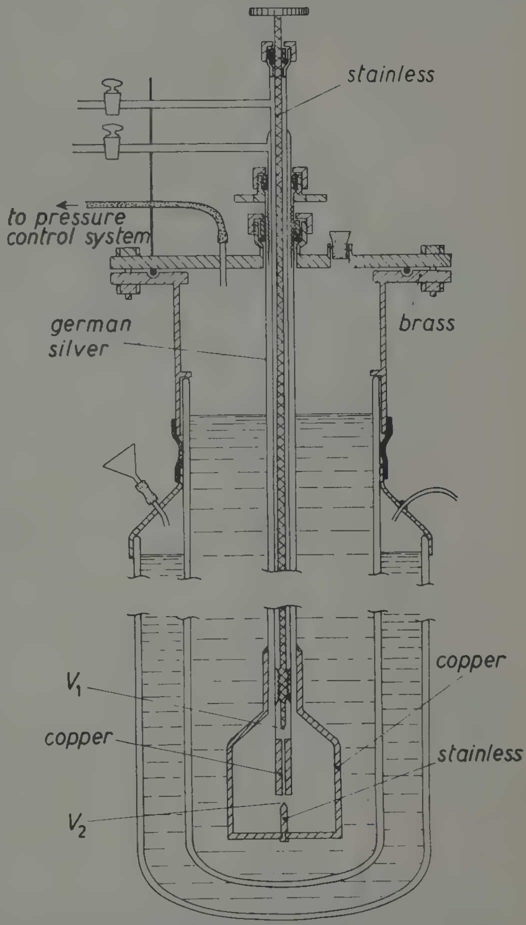

Fig. 1. – The diffusion apparatus. V_1 and V_2 are stainless steel needle valves.

The apparatus is placed in a cryostat, and the valve system is operated from the outside by means of « O rings » sealing. The capillary is connected to a Toeppler pump to take away the mixture from it after the diffusion took place

(³) J. S. ANDERSON and K. SADDINGTON: *Journ. Chem. Soc.*, 8, 381 (1949).

for the time τ, and is accomplished by simply closing the valve V_1 and opening V_2 towards the Toeppler bulb. The Toeppler system is also useful to condense the mixture in the capillary at a pressure somewhat larger than the saturation pressure at the corresponding temperature, this overpressure being needed to avoid bubble formation and incomplete filling of the capillary.

The analysis of the isotopic mixtures has been performed by a Nier type mass spectrometer at the University of Rome. No details of this standard technique will be given here.

3. – Results.

3·1. *The hydrogen-deuterium mixtures.* – A first group of runs has been carried out by placing a 2% deuterium mixture in the capillary and pure hydrogen in the reservoir. In this way the amount of deuterium lost in every run was negligible and the analysis, at the mass spectrometer, very easy; but the results were erratic, since the mixture in the capillary was heavier at the top than at the bottom and convection took place in an uncontrolled way.

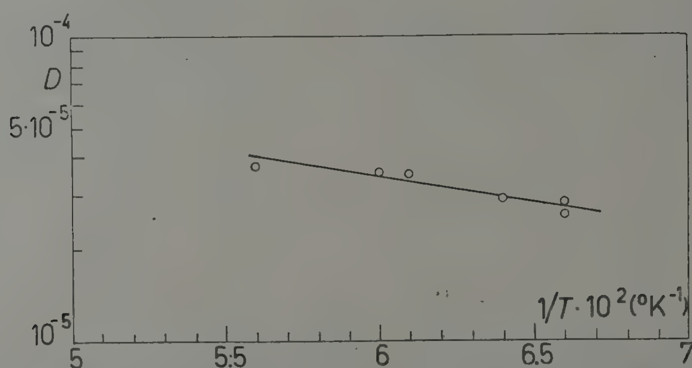

Fig. 2. – The diffusion coefficient of deuterium in liquid hydrogen plotted versus absolute temperature.

In the following runs the heavier mixture was then placed in the reservoir, and pure hydrogen was condensed in the capillary. This being the case, if $c^0_{H_2}$ and $\bar{c}_{H_2}$ are respectively the hydrogen concentration in the reservoir and in the capillary at the end of the run, the deuterium concentration ratio $\bar{c}/c_0$ of eq. (1) will now be given by

$$(\bar{c}_{H_2} - c^2_{H_2})/(1 - c^0_{H_2}) .$$

The concentration in the reservoir $c^0_{H_2}$ was found to change slightly during the runs, for incomplete mixing in the reservoir and especially for a low rate

distillation above the reservoir which tried to increase the hydrogen content in the capillary. The inaccuracy in $c^0_{H_2}$ is believed to be the major source of error in the experimental results.

Of the many runs which have been carried out, the ones carried out when the bath temperature of the cryostat was not sufficiently steady have not been found reproducible. This is easy to understand, since convection currents may easily take place as an effect of the thermal gradients and a long time is needed to remove these gradients. These runs have been discarded, since they were not reproducible and all gave higher values of D, as an obvious result of the convection currents.

In Table I are given the runs which are considered satisfactory and also plotted in Fig. 1 versus $1/T$. These results can be fitted by an Arrhenius type equation

$$D = 64 \exp[48/T] \cdot 10^{-5}\ \text{cm}^2/\text{s}\ .$$

3·2. *The* ^3He-^4He *mixtures.* – Essentially, the same procedure was adopted for the helium mixtures, but now one had the additional operational difficulty of the light mixture being so precious to need to be completely recovered at the end of every run. For the same reason a very small dead space had to be used above the capillary; this caused a larger flow resistance and a long time was then necessary to evacuate the capillary. To avoid that the large difference

TABLE I. – *Diffusion coefficients in hydrogen-deuterium dilute mixtures.*

Time (h)	T (°K)	$c^0_{H_2}$	$\bar{c}_{H_2}$	$\bar{c}/c_0$	$D\cdot 10^5$ cm²/s
1,42′	17.91	0.9776 ± 0.0014	0.9976	0.893 ± 0.006	$3.8\ \pm0.5$
2	15.8	0.9976 ± 0.0014	0.9977	0.897 ± 0.006	2.97 ± 0.37
1,15′	16.66	0.9976 ± 0.0014	0.9980	0.910 ± 0.006	3.55 ± 0.45
1,30′	16.89	0.9976 ± 0.0014	0.9978	0.901 ± 0.006	3.59 ± 0.48
2	15.2	0.9872 ± 0.0010	0.9987	0.898 ± 0.008	2.88 ± 0.45
2,30′	15.2	0.9872 ± 0.0010	0.9986	0.890 ± 0.009	2.67 ± 0.45

in the vapour pressure of the two isotopes should produce some unwanted fractioning during the condensation, it was found necessary to condense in the capillary the mixtures by a quick turbulent flow, and to use the same level in the Helium dewar, when condensing both the standard and the diffusion sample.

Owing to the difficulties of this conventional method and to the very recent attempts of GARWIN and REICH [4] who detected diffusion in these mixtures

[4] R. L. GARWIN and H. A. REICH: *Kamerling Onnes Conference on Low Temperature Physics, Physica* (Sept. 1958), p. 133.

by spin-echoes, we give up our search for a better experimental accuracy. Table II gives the experimental data which show D in these mixture to be roughly temperature independent and to be

$$D = (4 \pm 2)\cdot 10^{-5}\ \text{cm/s}\ .$$

Incidentally, we note that this figure agrees with the extrapolated value reported by other authors (5) above the λ temperature.

TABLE II. – *Diffusion coefficients of dilute* ^{3}He-^{4}He *mixtures.*

Time (h)	T (°K)	c_0 (%)	$\bar{c}$ (%)	$D\cdot 10^5$ cm^2/s
2	2.88	1.01	0.83	3.2 ± 0.8
2	2.88	0.553	0.46	2.8 ± 1.2
2	2.615	0.55	0.457	2.8 ± 1.6
2	3.225	0.561	0.428	5.5 ± 2.2
2^{09}	2.674	0.591	0.449	5.1 ± 0.6
3	3.225	0.610	0.422	5.9 ± 1.4
045	3.2	0.750	0.610	4.08 ± 1.0
(1^{05})	3.2	0.745	0.610	2.8 ± 1.0

4. – Some theoretical remarks.

At present there is not a theory available, which describes irreversible processes in quantum liquids. The work by KIRKWOOD and co-workers has given some justification of the good fit of the Stokes-Einstein equation, but is only limited to classical liquids.

It is perhaps worth noting that the familiar Stokes-Einstein equation

$$D = kT/6\pi\eta r\ ,$$

r being the radius of the sphere and η the viscosity of the medium, also describes our H_2-D_2 results inside the experimental error, if one uses

$$r = 1.95\ \text{Å}\ .$$

This figure has to be compared with the radius calculated from the nearest

(5) J. M. BEENAKKER and K. W. TACONIS: *Progress in Low Temperature Physics*, vol. 1 (Amsterdam, 1955), p. 131.

neighbours distance, which is 1.980 and 1.925 Å for f.c.c. and b.c.c. structures, as calculated by familiar expressions from the liquid hydrogen density.

Similar considerations cannot be made for the ^3He-^4He mixtures due to much larger experimental error. In spite of this large error, this data have proved useful in a comparison (6) with the diffusion coefficient of ions in liquid helium, giving evidence of a clustering around the ions which makes them to diffuse more slowly than ^3He atoms.

* * *

We are indebted to Prof. K. W. TACONIS of the Leiden University, for many useful technical suggestions in the early stage of this work.

(6) G. CARERI, J. REUSS, F. SCARAMUZZI and J. O. THOMSON: *Proc. Int. Conference Low Temperature Physics and Chemistry* (Madison, 1957), p. 155.

RIASSUNTO

È stato costruito un apparecchio per misurare il coefficiente di diffusione in liquidi a bassissime temperature. Questa tecnica è stata applicata a miscele diluite idrogeno-deuterio ed i risultati possono essere espressi da una equazione del tipo Arrhenius in funzioni della temperatura $D = 64 \exp[48/T] \cdot 10^{-5}$ cm²/s. Si sono incontrate maggiori difficoltà nell'usare la stessa tecnica con miscele di isotopi d'elio. I risultati sono affetti da grossi errori e approssimativamente $D = (4 \pm 2) \cdot 10^{-5}$ cm²/s per temperature superiori al punto λ.

IL NUOVO CIMENTO Vol. XIII, N. 1 1° Luglio 1959

Limitations on the Nucleon Form Factors due to Causality Requirements.

B. Bosco and V. De Alfaro

Istituto di Fisica dell'Università - Torino
Istituto Nazionale di Fisica Nucleare - Sezione di Torino

(ricevuto il 14 Marzo 1959)

Summary. — Starting from the spectral representation of the form factors, we investigate what kind of functions one has to use in order to represent the nucleon charge and magnetic moment distributions.

In the present note we wish to point out some simple properties of the nucleon charge and magnetic moment densities in the configuration space. These properties follow quite simply from facts which seem to us summarize the present field theoretical situation of the problem.

It is well known that the Fourier transform $F(q^2)$ of such functions admits a spectral representation of the form (1):

$$F(q^2) = \frac{1}{\pi}\int_{\gamma^2}^{\infty} \frac{g(\sigma^2)}{\sigma^2 + q^2}\, d\sigma^2 , \tag{1}$$

where $\gamma = 2\mu$ for the isotopic vector part $F^v(q^2)$, and $\gamma = 3\mu$ for the iso-scalar part.

In fact, such dispersion relations have been proved (2) under some restric-

---

(1) G. F. Chew, R. Karplus, S. Gasiorowicz and F. Zachariasen: *Phys. Rev.*, **110**, 265 (1958), hereafter referred to as CKGZ; P. Federbush, M. L. Goldberger and S. B. Treiman: *Phys. Rev.*, **112**, 643 (1958), hereafter referred to as FGT.

(2) H. J. Bremermann, R. Oehme and J. G. Taylor: *Phys. Rev.*, **109**, 2178 (1958).

tive conditions from the general properties of the field theory. Unfortunately the condition under which (1) is proved for the nucleon form factors is that the relation $\mu > (\sqrt{2}-1)m$ holds between the pion and nucleon masses.

However it is generally believed that the representation (1) is still valid without such unphysical restriction and, indeed, it has been proved by NAMBU (³) in every order of perturbation theory.

In references (1) evaluations of the spectral functions g have been attempted but for the moment no completely satisfactory form for the g is yet available.

In this paper we want to derive some properties of the form factors which follow from the representation (1), and from some very general assumptions on the spectral functions.

Let us consider the co-ordinate space form factors $f(r)$ (⁴) given by

$$f(\boldsymbol{r}) = \frac{1}{(2\pi)^3}\int \mathrm{d}^3 q \exp[-i\boldsymbol{q}\boldsymbol{r}]F(q^2)\,.$$

One immediately gets

$$f(r) = \frac{1}{2\pi^2}\int\limits_{\gamma^2}^{\infty} g(\sigma^2)\,\frac{\exp[-\sigma r]}{r}\,\mathrm{d}\sigma^2\,. \tag{2}$$

If we perform the substitution $\sigma = \gamma + t$ we obtain

$$f(r) = \frac{1}{\pi^2}\,\frac{\exp[-\gamma r]}{r}\int\limits_{0}^{\infty}(\gamma+t)g\left((\gamma+t)^2\right)\exp[-tr]\,\mathrm{d}t\,. \tag{3}$$

Equation (2) shows us a quite simple relation between the spectral function $g(\sigma^2)$ and $f(r)$. Indeed one can say that $\pi^2 r f(r) e^{\gamma r}$ is the Laplace transform of the function

$$G(t) = (\gamma+t)\,g((\gamma+t)^2)\,. \tag{4}$$

This elementary observation enables us to apply some quite general theorems (⁵) (Abelian or Tauberian theorems) which connect the asymptotical behaviour of the function near the origin with the asymptotical behaviour of its Laplace transform at infinity.

(³) Y. NAMBU: *Nuovo Cimento*, **6**, 1064 (1957).

(⁴) We use here $f(r)$ to indicate any of the Fourier transforms of $F_{1,2}^{v,s}(q^2)$; to be more specific $f(r)$ indicates any of the four functions $\varrho^{s,v}(r)$, $\mu^{s,v}(r)$.

(⁵) G. DOETSCH: *Theorie und Anwendung der Laplace-Transformation* (Berlin, 1937); *Teoria degli sviluppi asintotici dal punto di vista delle trasformazioni funzionali* (Roma 1954).

We are thus led to analyze the behaviour of the spectral functions near threshold.

Strictly speaking we have until now no general theorems about the behaviour of these spectral functions near threshold; however all the calculations made up to date (6) show that the spectral functions vanish at the lower limit of integration, and, what is more interesting, their behaviour is of the form

$$g((\gamma+t)^2) \sim at^\lambda\,, \qquad \text{where } \lambda > 0.$$

These results can be supported in the case of the iso-vector part of the nucleon form factors by a quantitative calculation in the sense that if we consider the pion as a structureless particle we can get a model independent result about the threshold behaviour of the spectral functions.

Indeed FGT and CKGZ have shown that in this case the spectral functions are connected with the pion nucleons scattering amplitudes in the non physical region.

The explicit formulae they give read (FGT (3,10), (3,11)):

$$g_1^v(\sigma^2) = \frac{e}{16\pi}\frac{1}{\sigma}\,\mathrm{Re}\left\{M^*(-\sigma^2)\int\limits_{-PQ/m}^{PQ/m}\mathrm{d}\nu\left[2\frac{m^3}{P^3}\nu A_2(\nu,-\sigma^2)-\right.\right.$$
$$\left.\left.-m\frac{Q^2}{P}\left\{\frac{m^2}{P^2}\left(\frac{3m^2\nu^2}{P^2Q^2}-1\right)-\left(1-\frac{m^2\nu^2}{P^2Q^2}\right)\right\}B_2\,(\nu,-\sigma^2)\right]\right\}\theta(\sigma^2-4\mu^2)\,,$$

$$g_2^v(\sigma^2) = \frac{e}{32\pi}\frac{1}{\sigma}\,\mathrm{Re}\left\{M^*(-\sigma^2)\int\limits_{-PQ/m}^{PQ/m}\mathrm{d}\nu\left[\frac{m^2Q^2}{P^3}\left(\frac{3m^2\nu^2}{P^2Q^2}-1\right)B_2(\nu,-\sigma^2)-\right.\right.$$
$$\left.\left.-\frac{m\nu}{P^2}A_2(\nu,-\sigma^2)\right]\right\}\theta(\sigma^2-4\mu^2)\,,$$

$$P=\left(\frac{\sigma^2}{4}-m^2\right)^{\frac{1}{2}};\qquad Q=\left(\frac{\sigma^2}{4}-\mu^2\right)^{\frac{1}{2}},$$

where $M(-\sigma^2)$ is the pion form factor. The $A_2(\nu,-\sigma^2)$ and $B_2(\nu,-\sigma^2)$ are the isotopic spin flip amplitudes as defined in CHEW, LOW, GOLDBERGER, and NAMBU (7).

---

(6) CKGZ; FGT; J. D. WALECKA: to be published on *Nuovo Cimento*; B. BOSCO and V. DE ALFARO: to be published on the *Phys. Rev.*

(7) G. F. CHEW, M. GOLDBERGER, F. E. LOW and Y. NAMBU: *Phys. Rev.*, **106**, 1337 (1957).

The structure of these formulae allows quite easy derivation of the threshold limit, and the result is:

$$g_1^v((2\mu+t)^2) \underset{t\to 0}{\sim} \frac{e}{24\pi}\mu^{\frac{1}{2}} t^{\frac{3}{2}}\,\mathrm{Re}\,\{B_2(0,-4\mu^2)+A_2'(0,-4\mu^2)\}\,, \tag{5}$$

$$g_2^v((2\mu+t)^2) \underset{t\to 0}{\sim} \frac{-e}{96\pi}\frac{\mu^{\frac{1}{2}}}{m} t^{\frac{3}{2}}\,\mathrm{Re}\,\{P_0 A_2'(0,-4\mu^2)\}\,, \tag{6}$$

with

$$M(-4\mu^2)=1\,,\qquad P=(\mu^2-m^2)^{\frac{1}{2}}\,,$$

where use has been made of the hypothesis that $A_2'(\nu,-\sigma^2)=(\partial/\partial\nu)A_2(\nu,-\sigma^2)$, and $B_2(\nu,-\sigma^2)$ exist and are regular for $\nu\to 0$, $\sigma^2\to 4\mu^2$ (if someone of them vanishes the power will be increased). This hypothesis is probably verified in the case of no pion-pion interaction [8].

It is apparent that a disagreement exists for threshold behaviour between our formulae and the first order perturbation theory results obtained by CKGZ. Indeed we obtain $g_1^v\sim t^{\frac{3}{2}}$; $g_2^v\sim t^{\frac{3}{2}}$ while in perturbation theory one obtains $g_1^v\sim t^{\frac{3}{2}}$; $g_2^v\sim t^{\frac{5}{2}}$. This is due to the fact that in the Born approximation $A_2=0$.

At this point let us see what are the consequences of the properties just stated for the g's on the behaviour of $f(r)$ for large r.
In this case one of the Abelian theorems recalled above states that if the function $G(t)$ can be represented for $t\to 0$ by

$$G(t)\underset{t\to 0}{\sim} ct^{\Lambda}$$

then its Laplace transform $\pi^2 r f(r)e^{\gamma r}$ for $r\to\infty$ can be asymptotically represented by

$$\pi^2 r f(r)\exp[\gamma r]\sim c\,\frac{\Gamma(1+\Lambda)}{r^{1+\Lambda}}\,.$$

Γ is the Euler function.

Taking into account (4), (5) and (6), we get, in the case of the iso-vector part of charge and magnetic moment densities, which we denote respectively by $\varrho^v(r)$ and $\mu^v(r)$:

$$\varrho^v(r)\underset{r\to\infty}{\sim} C_1^v\,\frac{\Gamma(\frac{5}{2})}{r^{\frac{7}{2}}}\exp[-2\mu r]\,, \tag{7}$$

$$\mu^v(r)\underset{r\to\infty}{\sim} C_2^v\,\frac{\Gamma(\frac{5}{2})}{r^{\frac{7}{2}}}\exp[-2\mu r]\,, \tag{8}$$

---

[8] This could be seen, for example, by Mandelstam's representation (S. MANDELSTAM: preprint) in which all the lower integration limits are $4m^2$. At the present time it is difficult to predict how the pion-pion interaction would affect the spectral functions at $\sigma^2\to 4\mu^2$.

where C_1^v and C_2^a are given by:

$$C_1^v = \frac{e}{12\pi^3}\,\mu^{\frac{3}{2}}\,\mathrm{Re}\,\{B_2(0, -4\mu^2) + A_2'(0, -4\mu^2)\}\,, \tag{9}$$

$$C_2^v = \frac{-e}{48\pi^3}\,\mu^{\frac{3}{2}}\,\mathrm{Re}\,\{P_0 A_2'(0, -4\mu^2)\}\,. \tag{10}$$

In a similar way, if $g_1^s((3\mu+t)^2)$ and $g_2^s((3\mu+t)^2)$ behave for $t \to 0$ like respectively $C_1^s t^{\alpha_1}$ and $C_2^s t^{\alpha_2}$ (9), we obtain

$$\varrho^s(r) \underset{r\to\infty}{\sim} C_1^s\,\frac{3\mu}{\pi^2}\,\frac{\Gamma(1+\alpha_1)}{r^{2+\alpha_1}}\exp[-3\mu r]\,, \tag{11}$$

$$\mu^s(r) \underset{r\to\infty}{\sim} C_2^s\,\frac{3\mu}{\pi^2}\,\frac{\Gamma(1+\alpha_2)}{r^{2+\alpha_2}}\exp[-3\mu r]\,. \tag{12}$$

Concluding we wish to summarize our results in the following two points:

1) Our discussion allows to deduce a necessary condition to which asymptotically the charge and magnetic moment densities in the configuration space must satisfy.

2) From formulae (7), (8), (11), (12), one sees that the experimental determination of $C_{1.2}^{v.s}$ gives, by means of the relation (4), direct information about the threshold behaviour of the spectral functions, and, in the case of the vector part, this is directly connected to quantities which represent the pion nucleon scattering amplitude in the non physical region.

* * *

We are deeply indebted to Prof. S. FUBINI for encouragement and illuminating criticism.

We have also beneficiated of discussions with many people which we wish to thank here, particularly Prof. M. VERDE, Prof. R. HOFSTADTER and many physicists of the CERN theoretical Division in Geneva.

---

(9) From formulae (3.55), (3.56) of FGT, one sees that if the quantities α, β, H satisfy reasonable properties such a behaviour could be deduced.

RIASSUNTO (*)

Partendo dalla rappresentazione spettrale dei fattori di forma, si esamina quale tipo di funzioni si debba usare per rappresentare le distribuzioni della carica del nucleone e del suo momento magnetico.

(*) *Traduzione a cura della Redazione.*

IL NUOVO CIMENTO Vol. XIII, N. 1 1° Luglio 1959

On Parity Conservation in Strong Interactions.

N. Dallaporta

Istituto di Fisica dell'Università - Padova
Istituto Nazionale di Fisica Nucleare - Sezione di Padova

(ricevuto il 16 Marzo 1959)

Summary. — The analogy in respect to γ_5 invariance between the two component Dirac equation for the neutrino and the Schremp-Gürsey type equation describing bayrons is used in order to express the lagrangian for strong interactions as the sum of two types of parity non-conserving terms formally similar to those adopted for weak interactions. These terms however, when suitably grouped, may be shown to compensate each other in order that parity is always conserved and the conventional lagrangian is obtained; the compensation is a consequence of the fact that the number and disposition of the baryon states in the elementary particle scheme is such as to allow this grouping of compensating pairs; the original asymmetry remains only detectable in the mass differences between baryons which may naturally be thus interpreted as a consequence of it.

1. – One of the main problems at the present moment facing the study of the interactions of elementary particles consists in the right choice of the fundamental spinors which have to represent the different kinds of fermions interacting. Should we consider either strong or weak interactions, the main element is always a fermion pair which appears directly twice in a weak four fermion interaction, or once in a strong interaction coupled with a boson which may, in turn, be considered in the sense of the Fermi and Yang (1), Sakata (2), and Okun (3) compound models as composed also of fermion pairs.

(1) E. Fermi and C. N. Yang: *Phys. Rev.*, **76**, 1739 (1949).
(2) S. Sakata: *Progr. Theor. Phys.*, **16**, 686 (1956).
(3) L. B. Okun: *Proc. of the Annual Intern. Conf. on High Energy Physics at CERN* (1958), p. 223.

A definite answer to this problem of the choice of spinors representing fermions has been given in the case of the neutrino by the so-called two-component theory. The wave equation for the neutrino

$$\gamma^\mu \frac{\partial}{\partial x_\mu} \chi_\nu = 0\,, \tag{1}$$

may be separated in the γ_5 representation into 2-component spinor equations of type

$$(-\sigma\cdot p + E)\chi'' = 0\,,$$

$$(+\sigma\cdot p + E)\chi' = 0\,.$$

The four independent free particle solutions correspond to given eigenvalues of γ_5, energy E, and helicity H.

As a consequence of this fact, eq. (1) is invariant for the γ_5 transformation (4)

$$\chi_\nu' \to \exp[i\gamma_5\theta]\chi_\nu$$

and the Pauli transformation (5)

$$\chi_\nu \to a\chi_\nu + b\gamma_5\chi_\nu^c \qquad |a|^2+|b|^2=1$$

and if χ_ν is a 4 spinor solution, then both $\varkappa_\nu' = \alpha\chi_\nu$ and $\varkappa_\nu'' = \beta\chi_\nu$ are also 2 spinor solutions of eq. (1), (with $\alpha = (1+\gamma_5)/2$, $\beta = (1-\gamma_5)/2$).

Of the quantities γ_5, E, H, the only physically observable one is the helicity which, therefore, allows the distinction of only two different physical states corresponding to different signs of energy. Now, the main point of the two-component theory consists in considering always one of the two types only, let us say $\varkappa_\nu' = \alpha\chi_\nu$ as representing the neutrino. This is equivalent to the following assumption: as the two solutions $\varkappa_\nu'$, $\varkappa_\nu''$ differ from each other only for the sign of γ_5, no physical meaning may be attributed to the value of γ_5: so only one choice of γ_5 is preserved and the other is discarded as physically inexistent, and only this selected solution $\varkappa'$ is then used in all interactions involving neutrinos.

In the case of charged leptons (or baryons acting in weak interactions), the basic reasons operating for the choice of the adequate spinors are less clear cut and they are in fact differently formulated in the different attempts of SUDARSHAN and MARSHAK (6), FEYNMAN and GELL-MANN (7) and SAKURAI (8)

---

(4) B. TOUSCHEK: *Nuovo Cimento*, **5**, 1281 (1957).

(5) W. PAULI: *Nuovo Cimento*, **6**, 204 (1957).

(6) E. C. SUDARSHAN and R. MARSHAK: *Proc. Intern. Conf. on Mesons and recently discovered Particles* (Padua-Venice, Sept. 1957), V, 14 (1957); *Phys. Rev.*, **109**, 1860 (1957).

(7) R. P. FEYNMAN and M. GELL-MANN: *Phys. Rev.*, **109**, 193 (1958).

(8) J. J. SAKURAI: *Nuovo Cimento*, **7**, 649 (1958).

aiming to express them in order to interpret correctly the experimental facts. In this case, the spinor obeys the complete Dirac equation

$$\left(\gamma^\mu \frac{\partial}{\partial x_\mu} + m\right)\chi_l = 0 , \tag{2}$$

which is not separable; and as now a given fermion state is not only physically distinguishable by the value of helicity but also by the sign of the charge, if one defines the sign of energy according to the sign of electric charge as is customary, then, for each charge sign one has two different values of helicity and therefore one should need the four component solutions to describe the complete situation.

However, in this case a supplementary principle is introduced, which in all cases amounts to selecting only one of the two possible spinor combinations

$$\varkappa' = (p + p'\gamma_5)\chi_l , \qquad \varkappa'' = (p - p'\gamma_5)\chi_l \tag{3}$$

(with $p = p'$ for leptons and $p \neq p'$ for baryons), let us say $\varkappa' = (p + p'\gamma_5)\chi_l$ and discard the other $\varkappa'' = (p - p'\gamma_5)\chi_l$, the result of which selection in the case $p = p'$, leads to the $V-A$ coupling type theory, to parity non-conservation in weak interactions and more generally to what is commonly called chirality invariance. Thus, even in this more complicated case, the further limitation in the choice of the spinors due to the chirality principle operates in order to select a solution corresponding to a single sign of γ_5.

2. – Up to now, no corresponding attempts have been made for the strong interactions and it could therefore be tempting to see whether an approach aiming to translate in an appropriate manner for them what has been done for the weak ones could in effect succeed in explaining and justifying in a coherent way some of their known properties.

As we shall now see, and contrarily to what could be expected owing to the more complicated structure of the baryons operating in strong interactions in respect to the leptons operating in the weak ones, it appears that a selecting rule for the spinors representing baryons in this case may be formulated in a very similar way as for the neutrino; and in the present note we should like to present a preliminary attempt which could be termed a « neutrino-like » approach for treating the baryons in strong interactions. Such a name indicates that the main line of thought followed throughout will stress the analogy which may be found between the invariance properties of the neutrino Dirac equation on one side and the invariance properties of the Schremp-Gürsey (S-G)

type equations ([9]) on the other side, which, according to previous work ([10]), may be assumed to describe in a wider sense the behaviour of baryons.

In fact, for free baryons the S-G equation may be written ([10]):

$$\left[\Gamma^\mu \frac{\partial}{\partial x^\mu} + m\Gamma_5\right] X = 0\,, \tag{4}$$

where Γ^μ and Γ_5 are 8×8 matrices

$$\Gamma^\mu = \begin{vmatrix} 0 & \gamma^\mu \\ \gamma^\mu & 0 \end{vmatrix}, \qquad \Gamma_5 = \begin{vmatrix} -\gamma_5 & 0 \\ 0 & \gamma_5 \end{vmatrix},$$

and $X = \begin{vmatrix} \chi \\ \tilde{\chi} \end{vmatrix}$ represents an 8 spinor.

The physical necessity of describing a baryon with at least 8-components may be easily understood when we recall that now, apart from helicity and electric charge, baryon states are labelled also by the baryonic number. If, as is customary, we associate the definition of the energy sign of a state with a given value of the baryonic number, then we have in each case two possible assignments of electric charge and two assignments for helicity which obviously double the number of the components needed to describe the situation with respect to the lepton case.

No other degree of freedom is required due to hypercharge since, as it has often been observed in the discussion of the baryon schemes ([11,12]), hypercharge and electric charge are not independent in the labelling of the baryon states, as the sign of charge is always linked to the sign of hypercharge in the meson fields. This allows to interchange the roles of electric charge and hypercharge and to treat baryon pairs with opposite signs of electric charge and/or hypercharge on the same footing; the actual 8 component representation of baryon states ([10]) refers to anyone of these pairs.

Now, like the neutrino and unlike the charged lepton case, the S-G equation is reducible and separable into two 4 component Dirac equations, each of which mixes two components of χ with two components of $\tilde{\chi}$. Further, the components mixed in a given equation have opposite eigenvalue of γ_5.

As a consequence of this situation, eq. (4) is invariant for the γ_5, the

([9]) E. J. Schremp: *Phys. Rev.*, **99**, 1603 (1955) F. Gürsey: *Nuovo Cimento*, **7**, 411 (1958).

([10]) N. Dallaporta and T. Toyoda: *Nuovo Cimento*, **12**, 593 (1959).

([11]) N. Dallaporta: *Proc. Int. Conf. on Mesons and recently discovered Particles* (Padua-Venice, Sept. 1957), V, 3 (1957); *Nuovo Cimento*, **7**, 200 (1958).

([12]) P. Budini, N. Dallaporta and L. Fonda: *Nuovo Cimento*, **9**, 316 (1958).

Toyoda [13] and the Pauli transformations, if:

$$\left.\begin{aligned} \chi &\to \exp[i\gamma_5\theta]\chi \\ \tilde{\chi} &\to \exp[-i\gamma_5\theta]\tilde{\chi} \end{aligned}\right\} \gamma_5 \text{ transformation .}$$

$$\left.\begin{aligned} \chi &\to \exp i[\varepsilon + (1-\varepsilon)\gamma_5]\theta\chi \\ \tilde{\chi} &\to \exp i[\varepsilon - (1-\varepsilon)\gamma_5]\theta\tilde{\chi} \end{aligned}\right\} \text{Toyoda transformation .}$$

$$\left.\begin{aligned} \chi &\to a\chi + b\gamma_5\chi^c \\ \tilde{\chi} &\to a\tilde{\chi} - b\gamma_5\tilde{\chi}^c \end{aligned}\right\} \text{Pauli transformation .}$$

And if χ and $\tilde{\chi}$ are a 4 spinor pair solution of the S-G equation, also the pairs (A) $\alpha'\chi$, $\beta'\tilde{\chi}$ or (B) $\beta'\chi$, $\alpha'\tilde{\chi}$ (where $\alpha' = p + p'\gamma_5$, $\beta' = p - p'\gamma_5$) constitute two other types of solutions of it.

We consider that we should assume $p \neq p'$ for the general solution in the present case, as already in weak interactions such a condition holds for the baryonic parity non-conserving factors. Moreover, only the case $p \neq p'$ guarantees the existence of eight baryonic states, as is required by the physical situation just discussed.

Here also the difference between solutions (A) and (B) is just an interchange of sign of γ_5 which does not lead to any physical distinction. At this point therefore, we could try to generalize the procedure adopted for the neutrino case and formulate the following assumption: when in a degenerate problem, the degenerate solutions can be grouped into two types differing only from each other according to the eigenvalue of γ_5 which cannot be observed, only one of these two possible types of solutions is used to describe the fermions, while the other is discarded; and only the selected solution is used in all interaction expressions.

As for the neutrino, we therefore select only one of the two pairs (A) and (B), let us say

$$X_1 = \begin{vmatrix} \beta' & \chi \\ \alpha' & \tilde{\chi} \end{vmatrix}, \tag{6}$$

to represent the fermions in the baryon interactions.

As a consequence of this assumption, it follows that the fundamental fermion pairs in all strong interactions should appear coupled in a form of the

---

([13]) T. TOYODA: *Nucl. Phys.*, 8, 661 (1958).

types either

$$\bar{\chi}_a \Gamma(q + q'\gamma_5)\chi_b \quad \text{or} \quad \bar{\chi}_a \Gamma(q - q'\gamma_5)\chi_b \tag{6a}$$

similar to those adopted for weak interactions in all the papers previously quoted.

Let us now precise our assumptions concerning the general behaviour of the interactions involving the spinors selected to represent a baryon pair. According to our previous work [10], if we should require, as is physically observed, that the definite charge states ψ, $\tilde{\psi}$, which will be introduced in the following, should be separated in the final equations, then the interaction terms contained in the Lagrangian from which the S-G equation can be derived, should be only of the following types (*)

$$\bar{X}_1\Gamma^\mu X_1 \quad \bar{X}_1\Gamma_5^\mu X_1 \quad \bar{X}_1\Gamma'^\mu X_1 \quad \bar{X}_1\Gamma_5'^\mu X_1 \quad \bar{X}_1\Gamma_5 X_1 \quad \bar{X}_1\Gamma_5' X_1\,, \tag{7}$$

where the Γ not yet defined, are the following 8×8 matrices [8]

$$\Gamma_5^\mu = \begin{vmatrix} 0 & \gamma^\mu\gamma_5 \\ -\gamma^\mu\gamma_5 & 0 \end{vmatrix}, \qquad \Gamma'^\mu = \begin{vmatrix} 0 & -\gamma^\mu \\ \gamma^\mu & 0 \end{vmatrix},$$

$$\Gamma_5'^\mu = \begin{vmatrix} 0 & \gamma^\mu\gamma_5 \\ \gamma^\mu\gamma_5 & 0 \end{vmatrix}, \qquad \Gamma_5' = \begin{vmatrix} \gamma_5 & 0 \\ 0 & \gamma_5 \end{vmatrix},$$

and $\bar{X}_1 = |\bar{\tilde{\chi}}\beta'\,\bar{\chi}\alpha'|$ is the adjoint of $X_1(6)$. Let us define

$$(p + p'\gamma_5)^2 = q + q'\gamma_5\,, \qquad (p - p'\gamma_5)^2 = q - q'\gamma_5\,.$$

Therefore, the only possible interaction forms are:

$$\left.\begin{array}{ll} (8) & \bar{\chi}\gamma^\mu(q - q'\gamma_5)\chi \pm \bar{\tilde{\chi}}\gamma^\mu(q + q\gamma_5)\tilde{\chi}\,. \\ (8a) & \bar{\chi}\gamma^\mu\gamma_5(q - q'\gamma_5)\chi \pm \bar{\tilde{\chi}}\gamma^\mu\gamma_5(q + q'\gamma_5)\tilde{\chi} \end{array}\right\} \quad \text{in case of } VA \text{ types}$$

$$\left.\begin{array}{ll} (9) & \bar{\chi}(q + q'\gamma_5)\tilde{\chi} \pm \bar{\tilde{\chi}}(q - q'\gamma_5)\chi \\ (9a) & \bar{\chi}\gamma_5(q + q'\gamma_5)\tilde{\chi} \pm \bar{\tilde{\chi}}\gamma_5(q - q'\gamma_5)\chi \end{array}\right\} \quad \text{in case of } STP \text{ types}$$

(sign + gives S and V, sign — gives A and P).

(*) I am indebted to Prof. T. Toyoda for clarifying this point.

1736

(8) and (8*a*) are equivalent forms, and so are (9) and (9*a*). Therefore, it will be sufficient in what follows to consider only the first one in each case.

3. – We shall now consider the physical meaning of the spinors χ and $\tilde{\chi}$. This may be exemplified by introducing into the S-G equation the electromagnetic and baryonic interactions, as was done in the other paper [10]. The wave equations may then be written into two different ways:

$$\left[\Gamma^\mu\left(\frac{\partial}{\partial x_\mu}-ig\varphi_\mu-ie\Gamma_5A_\mu\right)+m\,\Gamma_5\right]X=0\,, \tag{10a}$$

$$\left[\Gamma^\mu\left(\frac{\partial}{\partial x^\mu}-ig\Gamma_5\varphi_\mu-ieA_\mu\right)+m\Gamma_5\right]X=0\,, \tag{10b}$$

A_μ electromagnetic field, φ_μ baryonic field.

If we assume form (10*a*) for the S-G equation, then, χ, $\tilde{\chi}$ represent a solution corresponding to a definite sign of the baryonic number, but to a mixture of different electric or hypercharge states. If, instead, we consider equation (10*b*) then the χ, $\tilde{\chi}$ correspond to a definite sign of the electric charge or of the hypercharge but to a mixture of different baryonic number states. If we want, as will be required by the final results, to use a representation in which both baryonic number and electric charge and hypercharge are simultaneously observable, we must separate the S-G equation according to the substitutions

$$X=\begin{vmatrix}\chi\\ \tilde{\chi}\end{vmatrix}=\begin{vmatrix}\beta & \alpha\\ \alpha & -\beta\end{vmatrix}\begin{vmatrix}\psi\\ \tilde{\psi}\end{vmatrix}, \tag{11a}$$

in the first case

$$X=\begin{vmatrix}\chi\\ \tilde{\chi}\end{vmatrix}=\begin{vmatrix}\beta & \alpha\\ \alpha & -\beta\end{vmatrix}\begin{vmatrix}\psi^c\\ \tilde{\psi}^c\end{vmatrix}, \tag{11b}$$

in the second case. Now, the ψ, $\tilde{\psi}$ are 4-spinors which are solutions of the normal Dirac equation. Each pair of ψ, $\tilde{\psi}$ may be interpreted as representing either $\Sigma^+\Sigma^-$ or p-Ξ^+; or n-Ξ^0 by substituting a hypercharge interaction to the electromagnetic one; or even Y^0Z^0, if we would consider a similar kind of solutions also for the completely neutral states into our consideration. A similar but somewhat more complicated interpretation will be proposed in the following.

Let us now apply our transformations (11*a*) or (11*b*) to the baryon terms (8) or (9); they are respectively changed into the following expressions, which we

may term the conventional forms of the baryon factors in strong interactions:

$$(12)\qquad \begin{cases} [-\overline{\psi}(q+q')\gamma^{\mu}\gamma_5\psi+\overline{\tilde{\psi}}(q-q')\gamma^{\mu}\gamma_5\tilde{\psi}] & \text{for sign } - \text{ in (8)},\\ [\overline{\psi}(q+q')\gamma^{\mu}\psi+\overline{\tilde{\psi}}(q-q')\gamma^{\mu}\tilde{\psi}] & \text{for sign } + \text{ in (8)}, \end{cases}$$

$$(13)\qquad \begin{cases} [\overline{\psi}(q+q')\gamma_5\psi+\overline{\tilde{\psi}}(q-q')\gamma_5\tilde{\psi}] & \text{for sign } - \text{ in (9)},\\ [\overline{\psi}(q+q')\psi-\overline{\tilde{\psi}}(q-q')\tilde{\psi}] & \text{for sign } + \text{ in (9)}. \end{cases}$$

We may incidentally note that the two transformations ($11a$) and ($11b$) although defining states χ, $\tilde{\chi}$ of a different physical meaning lead, when the initial form (8), (9) for the interaction is postulated, to the same final forms (12), (13). Therefore, as the treatment of the two substitutions ($11a$) and ($11b$) is analogous and the results are equivalent, we shall consider only the first of them.

With a substitution of type ($11b$) the transformation leading from (8) to (12) has been first proposed by D'ESPAGNAT [14] but was given another physical meaning.

We may now assume, according to what we know up to now on the nature of meson fields, that pion interactions, being pseudoscalar, are of type (9), while we may postulate (but this is unessential for what follows), that K-interactions are of type (8); we then obtain as main interaction terms:

$$(14)\qquad i\,[(-)\overline{\psi}(f+f')\gamma^{\mu}(\gamma_5)\psi+\overline{\tilde{\psi}}(f-f')\gamma^{\mu}(\gamma_5)\tilde{\psi}]\,\frac{\partial K}{\partial x_{\mu}}\,,\qquad \left\{\begin{array}{l}\text{for } K\text{'s; (factor in ( ) to}\\ \text{be considered, if } \partial K/\partial x^{\mu}\\ \text{is of } A \text{ type).}\end{array}\right.$$

$$(15)\qquad i[\overline{\psi}(g+g')\gamma_5\psi+\overline{\tilde{\psi}}(g-g')\gamma_5\tilde{\psi}]\,\pi \qquad \text{for } \pi\text{'s}$$

Now, if we compare in (8) or (9) and in (12) or (13) the forms of the baryonic factors, it is immediately apparent that, while (8) or (9) contain each two different parity non-conserving terms, parity is evidently conserved in expressions (12) or (13). It must be stressed, however, that the change between the two groups of formulae is only a formal one, and that of course parity has always been conserved in both cases and is inherent in forms (8) or (9) as it is in (12) or (13); this being implicit in the choice of the interactions (7) which have been selected to represent the strong interactions. The aim of the present derivation is then simply to show that parity conservation in this case, as apparent in (12) or (13), may be thought of as due to an internal compensation between two parity non-conserving terms as those present in (8) or (9) and that, if we admit all original interactions as being of type ($6a$), this compensation occurs because the scheme of the baryon elementary states

---

(14) B. D'ESPAGNAT: *Nuovo Cimento*, **9**, 920 (1958).

is such as to allow to combine always two different χ and $\tilde{\chi}$ states into equation pairs such as (4); while it might not occur if only one of these χ states in each pair should exist.

In this way, one may say that, under such an approach, the properties of strong interactions and especially conservation of parity, instead of being considered as something intrinsic due to the high symmetries which some time ago were postulated to hold for them, may be rather thought of as being fundamentally similar to those of weak interactions, the parity conservation being only a compensation effect happening to be effective for strong interactions (and not for the weak ones), due to the right number and disposition of the baryon states in the fundamental scheme. Such a point-of-view, quite different from those based on highly symmetrical Lagrangians adopted up to now in most of the theoretical works ([15]) on strong interactions, may perhaps appear more up to date after some recent attempts ([16]) on the application of the postulated high symmetries to the strong reactions observed, have shown much disagreement between the data and the theoretical expectations.

The original asymmetry which, owing to this compensation, disappears for what concerns parity, may however still be found in the mass difference between baryons, which are a consequence of it. In fact, it may be seen, by comparing (8), (9) with (12), (13) that, just by starting from parity non-conserving terms which possess all the same interaction constants, we arrive at parity conserving terms for which the interaction constants $q \mp q'$ are different.

This feature may be used to explain in a simple way the mass differences of the baryons and to derive them from a fundamental aspect of the interactions.

Let us further note that our tentative assumption of a V or A type interaction for K-mesons could differentiate them naturally from the pion interactions.

4. – We shall now write the whole Lagrangian of strong interactions expressed in terms of type (8) or (9) and transform it according to (11*a*) or (11*b*) into the familiar form of definite charge and baryonic number states.

As isospin baryon scheme, we shall use first the doublet approximation in the form proposed by Tiomno ([17]) and the author ([11]). According to it,

---

([15]) B. d'Espagnat and J. Prentki: *Nucl. Phys.*, **1**, 33 (1956); A. Salam: *Nucl. Phys.*, **2**, 173 (1956); B. d'Espagnat, J. Prentki and A. Salam: *Nucl. Phys.*, **3**, 446 (1957); M. Gell-Mann: *Phys. Rev.*, **106**, 1296 (1957); J. Schwinger: *Phys. Rev.*, **104**, 1164 (1956); *Ann. Phys.*, **2**, 407 (1957).

([16]) A. Pais: *Phys. Rev.*, **110**, 574 (1958); **112**, 624 (1958).

([17]) J. Tiomno: *Nuovo Cimento*, **6**, 69 (1957).

we write the original Lagrangian as [18]:

$$
\begin{aligned}
(16)\qquad \mathcal{L} = i\Big[&\{\bar{\chi}_J\Gamma^\mu_n(f_n - f'_n\gamma_5)\omega_i\chi_J \mp \bar{\tilde{\chi}}_J\Gamma^\mu_n(f_n + f'_n\gamma_5)\omega_i\tilde{\chi}_J + \\
&+ \bar{y}_J\Gamma^\mu_n(f_n - f'_n\gamma_5)\omega_i y_J \mp \bar{\tilde{y}}_J\Gamma^\mu_n(f_n + f'_n\gamma_5)\omega_i\tilde{y}_J\}\frac{\partial K_{ni}}{\partial x_\mu} + \\
&+ \{\bar{\chi}_L\Gamma^\mu_c(f_c - f'_c\gamma_5)\zeta_i\chi_L \mp \bar{\tilde{\chi}}_L\Gamma^\mu_c(f_c + f'_c\gamma_5)\zeta_i\tilde{\chi}_L + \\
&+ \bar{y}_L\Gamma^\mu_c(f_c - f'_c\gamma_5)\zeta_i y_L \mp \bar{\tilde{y}}_L\Gamma^\mu_c(f_c + f'_c\gamma_5)\zeta_i\tilde{y}_L\}\frac{\partial K_{ci}}{\partial x_\mu} + \\
&+ \{\bar{\chi}_N(g + g'\gamma_5)\tau_i\tilde{\chi}_N - \bar{\tilde{\chi}}_N(g - g'\gamma_5)\tau_i\chi_N + \\
&+ \bar{y}_N(g + g'\gamma_5)\tau_i\tilde{y}_N - \bar{\tilde{y}}_N(g - g'\gamma_5)\tau_i y_N\}\pi_i\Big].
\end{aligned}
$$

In this expression, π_i indicates the usual isospin vector pion field, K_n the neutral K field and K_c the charged K field, defined as:

$$
K_n = \begin{vmatrix} K_{n1} \\ K_{n2} \end{vmatrix} \qquad
\begin{aligned}
K_{n1} &= \frac{1}{\sqrt{2}}(K^*_x + K_n) \\
K_{n2} &= \frac{1}{\sqrt{2}i}(K^*_n - K_n)
\end{aligned}
$$

$$
\pi = \begin{vmatrix} \pi_1 \\ \pi_2 \\ \pi_3 \end{vmatrix} \qquad
\begin{aligned}
\pi_1 &= \frac{1}{\sqrt{2}}(\pi + \pi^*) \\
\pi_2 &= \frac{1}{\sqrt{2}i}(\pi - \pi^*)
\end{aligned}
$$

$$
K_c = \begin{vmatrix} K_{c1} \\ K_{c2} \end{vmatrix} \qquad
\begin{aligned}
K_{c1} &= \frac{1}{\sqrt{2}}(K^*_c + K_c) \\
K_{c2} &= \frac{1}{\sqrt{2}i}(K^*_c - K_c)
\end{aligned}
$$

τ, ω and ζ are three isospin vectors ruling respectively the emission and absorption of pions, neutral K's and charged K's as defined in [13,18]. τ has of course three components, while ω and ζ owing to the fact that the third component of neutral hypercharge of the K_n and the K_c triplet has never been observed, are defined only by their first two components and represent only rotations in the ω and ζ spin space perpendicular to their third axis.

([18]) N. DALLAPORTA: *Nuovo Cimento*, **11**, 142 (1959).

All the baryons are represented by 8-component spinors of the $\chi, \tilde{\chi}$ type, which we now define, according to (11a), by the $\psi, \tilde{\psi}$ type states:

$$(17)\quad \begin{cases} \begin{vmatrix} \chi_N \\ \tilde{\chi}_N \end{vmatrix} = \begin{vmatrix} \beta & \alpha \\ \alpha & -\beta \end{vmatrix} \begin{vmatrix} N_1 \\ N_4 \end{vmatrix}, & \begin{vmatrix} \chi_J \\ \tilde{\chi}_J \end{vmatrix} = \begin{vmatrix} \beta & \alpha \\ \alpha & -\beta \end{vmatrix} \begin{vmatrix} J_1 \\ J_4 \end{vmatrix}, \quad \begin{vmatrix} \chi_L \\ \tilde{\chi}_L \end{vmatrix} = \begin{vmatrix} \beta & \alpha \\ \alpha & -\beta \end{vmatrix} \begin{vmatrix} L_1 \\ L_4 \end{vmatrix}, \\ \begin{vmatrix} y_N \\ \tilde{y}_N \end{vmatrix} = \begin{vmatrix} \beta & \alpha \\ \alpha & -\beta \end{vmatrix} \begin{vmatrix} N_2 \\ N_3 \end{vmatrix}, & \begin{vmatrix} y_J \\ \tilde{y}_J \end{vmatrix} = \begin{vmatrix} \beta & \alpha \\ \alpha & -\beta \end{vmatrix} \begin{vmatrix} J_2 \\ J_3 \end{vmatrix}, \quad \begin{vmatrix} y_L \\ \tilde{y}_L \end{vmatrix} = \begin{vmatrix} \beta & \alpha \\ \alpha & -\beta \end{vmatrix} \begin{vmatrix} L_2 \\ L_3 \end{vmatrix}, \end{cases}$$

where

$$(18)\quad \begin{cases} N_1 = \begin{vmatrix} p \\ n \end{vmatrix}, & N_2 = \begin{vmatrix} \Sigma^+ \\ Y^0 \end{vmatrix}, & N_3 = \begin{vmatrix} Z^0 \\ \Sigma^- \end{vmatrix}, & N_4 = \begin{vmatrix} \Xi^0 \\ \Xi^- \end{vmatrix}, \\ J_1 = \begin{vmatrix} p \\ \Sigma^+ \end{vmatrix}, & J_2 = \begin{vmatrix} n \\ Y^0 \end{vmatrix}, & J_3 = \begin{vmatrix} Z^0 \\ \Xi^0 \end{vmatrix}, & J_4 = \begin{vmatrix} \Sigma^- \\ \Xi^- \end{vmatrix}, \\ L_1 = \begin{vmatrix} n \\ \Sigma^- \end{vmatrix}, & L_2 = \begin{vmatrix} p \\ Z^0 \end{vmatrix}, & L_3 = \begin{vmatrix} Y^0 \\ \Xi^- \end{vmatrix}, & L_4 = \begin{vmatrix} \Sigma^+ \\ \Xi^0 \end{vmatrix}, \end{cases}$$

applying the formulae (17) into (16) we get easily:

$$(19)\quad \mathcal{L} = i\Big[\{(-)\bar{J}_1(f_n + f'_n)\Gamma^\mu_n(\gamma_5)\omega_i J_1 + \bar{J}_4(f_n - f'_n)\Gamma^\mu_n(\gamma_5)\omega_i J_4 +$$
$$+ (-)\bar{J}_2(f_n + f'_n)\Gamma^\mu_n(\gamma_5)\omega_i J_2 + \bar{J}_3(f_n - f'_n)\Gamma^\mu_n(\gamma_5)\omega_i J_3\}\frac{\partial K_{ni}}{\partial x_\mu} +$$
$$+ \{(-)\bar{L}_1(f_c + f'_c)\Gamma^\mu_c(\gamma_5)\zeta_i L_1 + \bar{L}_4(f_c - f'_c)\Gamma^\mu_c(\gamma_5)\zeta_i L_4 +$$
$$+ (-)\bar{L}_2(f_c + f'_c)\Gamma^\mu_c(\gamma_5)\zeta_i L_2 + \bar{L}_3(f_c - f'_c)\Gamma^\mu_c(\gamma_5)\zeta_i L_3\}\frac{\partial K_{ci}}{\partial x_\mu} +$$
$$+ \{\bar{N}_1(g + g')\gamma_5\tau_i N_1 + N_4(g - g')\gamma_5\tau_i N_4 +$$
$$+ \bar{N}_2(g + g')\gamma_5\tau_i N_2 + \bar{N}_3(g - g')\gamma_5\tau_i N_3\}\pi_i\Big].$$

The factors in brackets occur if K couplings are of A type. This is the well known parity conserving Lagrangian of the doublet approximation.

However, the most interesting feature now, which has been naturally introduced in it, consists in the different interaction constants of the different terms, which allow to obtain different self masses. Let us discuss briefly which more likely assumptions are to be made in order to obtain the experimental data.

Let us first suppose that in the K interactions, the two constants f and f' have a rather similar value. The distribution of the different coupling constants

$f+f'$ or $f-f'$ in relation to interactions may then be better visualized in the scheme (Fig. 1), representing the K terms of (19). Each baryon state is linked by two interactions, a neutral and a charged one to its neighbours and in each case these two interactions are both the same for nucleons $(f+f')$ and for Ξ's $(f-f')$. One may then choose the f and f' signs and values in order to fit the experimental masses of the nucleons and the Ξ's. Intermediate Y hyperons are coupled with a $f+f'$ term and a $f-f'$ term. It is then rather likely that the self masses of these states should turn out to be intermediate between nucleons and Ξ's as is in fact required. Moreover the masses of all four hyperon states should turn out to be equal (we do not consider here the $\Lambda\Sigma$ splitting) to each other in this approximation, if the coupling types of K_n and K_c interactions are equal. This could even be true for opposite parity of the K_n and K_c interaction ([16]) provided that self energy integrals for the V and A couplings should turn out to give about the same contribution and the interaction should be practically linear in the interaction constants.

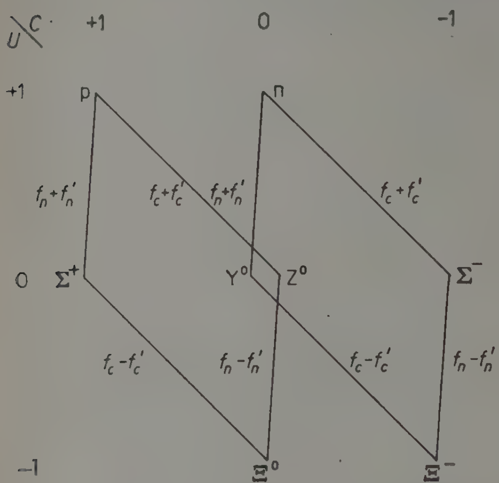

C = electric charge U = hypercharge.

Fig. 1.

If we now introduce also the pion interactions, it is easily seen that the best agreement is obtained if we suppose that in this case the g and g' constants turn out to be widely different (*i.e.* $g' \ll g$). Then, the self masses due to pion interaction are practically equal for all baryons and this allows a kind of global symmetry to be effective. The assumption $f \sim f'$, $g' \ll g$ leads moreover to the Pais condition for the validity of charge independence in the doublet approximation.

Should we try the opposite choice, *i.e.* $f' \ll f$, $g \simeq g'$, then all K self masses should obviously be about equal, while the $g+g'$ value for pion-nucleon

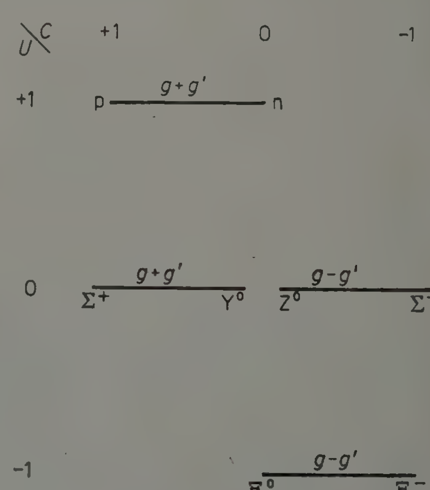

C = electric charge U = hypercharge

Fig. 2.

interactions, and the $g-g'$ value for pion-Ξ interactions would yield also different self masses for nucleons and Ξ's. In this case, however (Fig. 2) in the doublet approximation, the two hyperon pion doublets Σ^+Y^0, $Z^0\Sigma^-$ would be coupled by widely different constants and therefore it would turn out to be difficult to explain the similar mass values of all Y hyperons. Moreover Pais' condition should no more be valid and charge independence should break down for $\Sigma\Lambda\pi$ interactions. Therefore, the first choice seems best in agreement with experimental evidence.

We may remark that the present approach to interpret strong interactions has been formulated in order to obtain the doublet approximation which is the more comprehensive scheme that can be postulated. Should the real scheme turn out to be different, one should probably be obliged to revise or change at least part of the assumptions we have made. And if this were the case, it could perhaps happen that the compensation of the different parity non conserving terms could in the real scheme be not so complete, in order that in some occasions strong interactions not conserving parity could be realized, as some experimental indications concerning neutral hyperon interactions might indicate [19]. And this situation could of course be connected with the further experimental evidence of violation of the doublet approximation [16,20].

However, we would like to stress that, even if further refinements will probably be necessary in order to meet these facts, the present approach, just by aiming to start from expressions for the strong interactions with similar form and invariance properties as those for the weak ones, obtains in this way, with the assumptions $f \simeq f'$, $g' \ll g$, in a quite natural manner the different values of the baryon masses; and this perhaps may open different possibilities of interpreting these mass differences in respect to previous attempts.

* * *

I am indebted to Prof. P. Budini and prof. T. Toyoda for discussing many questions of interest related to the present subject, and to prof. J. Prentki for a critical revision of some important points.

---

(19) A. N. Salmeron and A. Zichichi: *Nuovo Cimento*, **11**, 461 (1959).
(20) A. Pais: *Phys. Rev. Lett.*, **1**, 418 (1958).

RIASSUNTO

L'analogia nei riguardi della invarianza in γ_5 tra l'equazione di Dirac a due componenti del neutrino e le equazioni del tipo di Schremp-Gürsey che descrivono i barioni viene usata per esprimere il lagrangiano delle interazioni forti come somma di due tipi di termini non conservanti la parità, formalmente simili a quelli in uso per le interazioni deboli. Questi termini però possono venire raggruppati in modo da far vedere che si compensano vicendevolmente, che sono equivalenti ai termini del lagrangiano convenzionale e che la parità viene sempre conservata. Questo compenso appare quale conseguenza del fatto che il numero e la disposizione degli stati barionici nello schema delle particelle elementari è tale da consentire questo raggruppamento; l'asimmetria originaria si manifesta solo nelle differenze di massa tra i barioni che possono così spiegarsi in modo naturale come conseguenza di essa.

IL NUOVO CIMENTO Vol. XIII, N. 1 1° Luglio 1959

Verallgemeinerung der Grundformel der relativistischen Mechanik für einige praktisch wichtige Nichtinertialsysteme.

N. St. Kalitzin

Physikalisches Institut bei der Bulgarischen Akademie der Wissenschaften - Sofia

(ricevuto il 16 Marzo 1959)

Zusammenfassung. — Die Grundformel der Relativitätsmechanik eines Massenpunktes $\boldsymbol{F}=(\mathrm{d}/\mathrm{d}t)(m\boldsymbol{v}/\sqrt{1-(v/c)^2})$ wird für die sogenannten « nichtrelativistische » Systeme verallgemeinert. Bei den nichtrelativistischen Systemen kann man die Begriffe der universellen Zeit und des starren Körpers einführen, also gilt für diese Systeme der Satz von Coriolis der klassischen Kinematik. Die neue Gleichung lautet $\boldsymbol{F}+\boldsymbol{S}_f+\boldsymbol{S}_c+\boldsymbol{S}_k=$ $=(\mathrm{d}_p\mathrm{d}t)(m\mathrm{d}/\sqrt{1-(v/c)^2})$, hierbei bedeutet $\boldsymbol{S}_f$ die Fuhrungskraft, $\boldsymbol{S}_c$ die Corioliskraft. $\boldsymbol{S}_k$ ist eine neue Trägheitskraft, welche nur bei relativistischen Geschwindigkeiten $\boldsymbol{v}$ des Massenpunktes auftritt. Die neue Gleichung wird auch im Gebiet der allgemeinen Relativitätstheorie abgeleitet und es wird eine Anwendung der Theorie für die Raketen mit relativistischen Antriebsteilchen gegeben.

1. – Die Grundformel der Relativitätsmechanik

$$\boldsymbol{F}=\frac{\mathrm{d}}{\mathrm{d}t}\left(\frac{m\boldsymbol{v}}{\sqrt{1-(v^2/c^2)}}\right), \tag{1}$$

ist bekanntlich nur für Inertialsysteme gültig. Hierbei bedeutet m die Ruhmasse eines Massenpunktes, $\boldsymbol{v}$ seine Geschwindigkeit, $\boldsymbol{F}$ die auf den Punkt wirkende Kraft.

Es ist durchaus wahrscheinlich, daß in der nahen Zukunft der Antrieb der Raketen durch Wegschleudern relativistischer Teilchen erfolgen wird. Die Raketen sind aber keine Inertialsysteme und für solche ist die unmittelbare Anwendung von Gl. (1) nicht möglich. Die Erde selbst ist auch kein Inertialsystem. Also verlangt die Praxis selbst eine Verallgemeinerung der Grund-

formel (1) der Relativitätsmechanik für nichtinertiale Systeme. Diese Verallgemeinerung läßt sich in der Tat vollführen auf Grund der allgemeinen Relativitätstheorie. Diese Verallgemeinerung ist aber bei der praktischen Berechnung recht kompliziert und im allgemeinen Fall ist die engültige Lösung nicht zu erreichen.

In dieser Arbeit wollen wir eine einfachere Verallgemeinerung von Gl. (1) ableiten, wobei ihr Gültigkeitsbereich für einige Nichtinertialsysteme erweitert wird. Für diesen Zweck betrachten wir Systeme, welche gegenseitig nichtrelativistische Geschwindigkeiten besitzen und so kleine Beschleunigungen und Gravitationsfelder haben, daß für alle diese Systeme eine gemeinsame universelle Zeit t und einen invarianten Abstand zwischen je zwei beliebigen Punkten jedes Systems definiert werden kann. Solche Systeme werden wir als « nichtrelativistiche Systeme » bezeichnen. Wenn also K und K' zwei nichtrelativistische Systeme sind, $\mathrm{d}t$ und $\mathrm{d}t'$ die Zeitintervalle zwischen zwei Ereignissen gemessen von K und von K' und $\mathrm{d}l$ und $\mathrm{d}l'$ die Entfernungen zwischen zwei Punkten gemessen von K und K', dann gilt nach unserer Definition

$$\mathrm{d}t = \mathrm{d}t' , \qquad \mathrm{d}l = \mathrm{d}l' . \tag{2}$$

Für die nichtrelativistischen Systeme ist die Gleichzeitigkeit ein absoluter Begriff, man kann bei diesen Systemen den Begriff des starren Körpers benutzen. Offenbar haben die nichtrelativistichen Systeme eine sehr große praktische Bedeutung. Insbesondere sind z.Z. sämtliche uns bekannte makrophysikalische Systeme auf der Erde, die Erde selbst eingeschlossen, nichtrelativistiche Systeme.

Wir betrachten nun zwei nichtrelativistiche Systeme K und K', von welchen das eine System, z.B., K', ein Intertialsystem sei. Wir betrachten aus diesen beiden Systemen die Bewegung eines Massenpunktes P, welcher sich mit relativistichen Geschwindigkeiten in Bezug auf K und K' bewegt. Wir bezeichnen die Geschwindigkeit und die Beschleunigung des Punktes P in Bezug aud K mit $\boldsymbol{v}$ und $\boldsymbol{b}$, und entsprechend in Bezug auf K' mit $\boldsymbol{v}'$ und $\boldsymbol{b}'$. Da beide Systeme K und K' die Bedingungen der klassischen Kinematik befriedigen, so lassen sich sofort die Grundsätze der relativen Bewegung der klassischen Kinematik für diesen Fall (relativistische Geschwindingkeit des Punktes P) verallgemeinern. Wir haben

$$\boldsymbol{v}' = \boldsymbol{v}_f + \boldsymbol{v} \approx \boldsymbol{v} , \tag{3}$$

$$\boldsymbol{b}' = \boldsymbol{b} + \boldsymbol{b}_f + \boldsymbol{b}_c \tag{4}$$

(der Satz von Coriolis). Hierbei bedeuten $\boldsymbol{v}_f$ und $\boldsymbol{b}_f$ die Führungsgeschwindigkeit und die Führungsbeschleunigung des Punktes P vom System K, in wel-

chem sich der Massenpunkt P im betrachteten Zeitpunkt befindet. $\boldsymbol{b}_c$ ist die Coriolisbeschleunigung des Punktes P. (In der vorliegenden Theorie wird das Verhältnis v_f/c wie auch v_f/v überall vernächlässigt.)

Wenn $\boldsymbol{\omega}$ der Vektor der Winkelgeschwindigkeit des Systems K in Bezug auf K' bedeutet und wenn $\boldsymbol{\epsilon}$ den Vektor der Winkelbeschleunigung von K bezeichnet, dann haben wir nach dem Satz von Coriolis

$$\boldsymbol{b}_f = \boldsymbol{b}_0 + \boldsymbol{\epsilon}\times\boldsymbol{r} + \boldsymbol{\omega}\times(\boldsymbol{\omega}\times\boldsymbol{r})\,, \tag{5}$$

$$\boldsymbol{b}_c = 2\boldsymbol{\omega}\times\boldsymbol{v}\,. \tag{6}$$

$\boldsymbol{b}_0$ ist die Beschleunigung des Ursprungs O des Systems K, $\boldsymbol{r}$ ist der Radiusvektor von O nach P. $\boldsymbol{b}_0$ ist die Translationsbeschleunigung, $\boldsymbol{\epsilon}\times\boldsymbol{r}$ ist die Tangentialbeschleunigung und $\boldsymbol{\omega}\times(\boldsymbol{\omega}\times\boldsymbol{r})$ ist die Zentripetalbeschleunigung.

Wie wir vorausgesetzt haben, ist das System K' ein Inertialsystem. Also gilt in diesem System die Gleichung

$$\boldsymbol{F} = \frac{\mathrm{d}'}{\mathrm{d}t}\left(\frac{m\boldsymbol{v}'}{\sqrt{1-(v'/c)^2}}\right), \tag{7}$$

oder

$$\boldsymbol{F} = \frac{m\boldsymbol{b}'}{\sqrt{1-(v'/c)^2}} + m\,\frac{\boldsymbol{v}'(\boldsymbol{v}'\boldsymbol{b}')}{c^2\sqrt{1-(v'/c)^2}^{\,3}}\,. \tag{8}$$

Wenn wir (3) und (4) in (8) einsetzen und beachten, daß $\boldsymbol{v}_f$ nichtrelativistisch ist, so erhalten wir

$$\boldsymbol{F} = \frac{m}{\sqrt{1-(v/c)^2}}\,(\boldsymbol{b}+\boldsymbol{b}_f+\boldsymbol{b}_c) + m\,\frac{\boldsymbol{v}}{c^2\sqrt{1-(v/c)^2}^{\,3}}\,(\boldsymbol{v}\boldsymbol{b}+\boldsymbol{v}\boldsymbol{b}_f)\,, \tag{9}$$

wobei die Beziehung

$$\boldsymbol{v}\boldsymbol{b}_c = 2\boldsymbol{v}(\boldsymbol{\omega}\times\boldsymbol{v}) = 0 \tag{10}$$

benutzt wurde. Außerdem haben wir die Definition der nichtrelativistischen Systeme ausgenutzt, also die fiktiven Gravitationsfelder so schwach vorausgesetzt, daß wir die Kraft $\boldsymbol{F}$ für alle nichtrelativistische Systeme als invariant betrachten können.

Wenn $\boldsymbol{v}$ nichtrelativistisch ist, dann geht Gl. (9) in die bekannte Formel der Newtonschen Mechanik für nichtinertiale Systeme über.

Aus (9) folgt

$$\boldsymbol{F}\boldsymbol{v} = \frac{m}{\sqrt{1-(v/c)^2}^{\,3}}\,(\boldsymbol{v}\boldsymbol{b}+\boldsymbol{v}\boldsymbol{b}_f)\,. \tag{11}$$

Mit Hilfe von (11) kann man die Gleichung (9) in die Form

$$\boldsymbol{F} = \frac{m}{\sqrt{1-(v/c)^2}}\,(\boldsymbol{b}+\boldsymbol{b}_f+\boldsymbol{b}_c) + \frac{(\boldsymbol{F}\boldsymbol{v})}{c^2}\,\boldsymbol{v}\,, \tag{12}$$

bringen. Umgekehrt, wenn wir (12) mit $\boldsymbol{v}$ skalar multiplizieren, dann erhalten wir (11) und daraus und aus (12) ergibt sich die Gl. (9). Also sind die Gleichungen (9) und (12) gleichwertig.

Formel (9) kann auch in der Form geschrieben werden

$$\boldsymbol{F} + \boldsymbol{S}_f + \boldsymbol{S}_c + \boldsymbol{S}_k = \frac{d}{dt}\left(\frac{m\boldsymbol{v}}{\sqrt{1-(v/c)^2}}\right), \tag{13}$$

wobei

$$\boldsymbol{S}_f = -\frac{m}{\sqrt{1-(v/c)^2}}\boldsymbol{b}_f = -\frac{m}{\sqrt{1-(v/c)^2}}\left(\boldsymbol{b}_0 + \boldsymbol{\epsilon}\times\boldsymbol{r} + \boldsymbol{\omega}\times(\boldsymbol{\omega}\times\boldsymbol{r})\right), \tag{14}$$

die Führungskraft bedeutet und

$$\boldsymbol{S}_c = -\frac{m}{\sqrt{1-(v/c)^2}}\boldsymbol{b}_c = -\frac{2m}{\sqrt{1-(v/c)^2}}\boldsymbol{\omega}\times\boldsymbol{v}, \tag{15}$$

ist die Corioliskraft. $\boldsymbol{S}_k$ ist eine neue Trägheitskraft, welche nur bei relativistischen Geschwindigkeiten $\boldsymbol{v}$ auftritt,

$$\begin{aligned}\boldsymbol{S}_k = &-\frac{m\boldsymbol{v}}{c^2\sqrt{1-(v/c)^2}^{\,3}}(\boldsymbol{v}\boldsymbol{b}_f) = \\ &= -\frac{m\boldsymbol{v}}{c^2\sqrt{1-(v/c)^2}^{\,3}}\left(\boldsymbol{v}\boldsymbol{b}_0 + \boldsymbol{v}\cdot\boldsymbol{\epsilon}\times\boldsymbol{r} + \boldsymbol{v}\cdot\boldsymbol{\omega}\times(\boldsymbol{\omega}\times\boldsymbol{r})\right).\end{aligned} \tag{16}$$

Die Differentiation nach der Zeit auf der rechten Seite von (13) ist in Bezug auf dem System K auszuführen.

Gleichung (9) oder (13) stellt die Grundgleichung der Relativitätsmechanik eines Massenpunktes dar, welcher sich mit relativistischer Geschwindigkeit $\boldsymbol{v}$ in einem nichtinertialen und nichtrelativistischen System K bewegt. Gleichung (13) hat die gleiche Form wie die Grundgleichung (1) der Relativitätsmechanik für ein Inertialsystem, nur muß man zu der Kraft $\boldsymbol{F}$ noch die Führungskraft $\boldsymbol{S}_f$, die Corioliskraft $\boldsymbol{S}_c$ und die neue Kraft $\boldsymbol{S}_k$ hinzufügen.

Wenn das System K eine ebene Bewegung in Bezug auf das System K' ausführt, dann steht der Vektor $\boldsymbol{\omega}$ senkrecht zu $\boldsymbol{r}$ und wir haben

$$\boldsymbol{S}_f = -\frac{m}{\sqrt{1-(v/c)^2}}(\boldsymbol{b}_0 + \boldsymbol{\epsilon}\times\boldsymbol{r} - \omega^2\boldsymbol{r}), \tag{17}$$

$$\boldsymbol{S}_c = -\frac{2m}{\sqrt{1-(v/c)^2}}\boldsymbol{\omega}\times\boldsymbol{v}, \tag{18}$$

$$\boldsymbol{S}_k = -\frac{m\boldsymbol{v}}{c^2\sqrt{1-(v/c)^2}^{\,3}}(\boldsymbol{v}\boldsymbol{b}_0 + \boldsymbol{v}\cdot\boldsymbol{\epsilon}\times\boldsymbol{r} - \boldsymbol{v}\boldsymbol{r}\omega^2). \tag{19}$$

Wenn hierbei $\epsilon = 0$ (das System rotiert gleichmäßig) und $\boldsymbol{b}_0 = 0$, dann ergibt sich aus (17) und (19)

$$\boldsymbol{S}_f = \frac{m\omega^2}{\sqrt{1-(v/c)^2}}\,\boldsymbol{r}\,, \tag{20}$$

$$\boldsymbol{S}_k = \frac{m\omega^2(\boldsymbol{vr})}{c^2\sqrt{1-(v/c)^2}^3}\,\boldsymbol{v}\,. \tag{21}$$

Zur Kontrolle der erhaltenen Resultate betrachten wir die zu Gl. (7) gehörige Energiegleichung im Inertialsystem K' (die vierte Komponente der Kraft im Raum von Minkowski)

$$\boldsymbol{Fv}' = \frac{\mathrm{d}'}{\mathrm{d}t}\left(\frac{mc^2}{\sqrt{1-(v'/c)^2}}\right). \tag{22}$$

Wir setzen in (22) die Formeln (3) und (9) ein und erhalten

$$\frac{m}{\sqrt{1-(v/c)^2}^3}(\boldsymbol{bv}+\boldsymbol{b}_f\boldsymbol{v}) = \frac{\mathrm{d}'}{\mathrm{d}t}\left(\frac{mc^2}{\sqrt{1-(v'/c)^2}}\right) = \tag{23}$$
$$= \frac{m\boldsymbol{v}'\boldsymbol{b}'}{\sqrt{1-(v'/c)^2}^3} = \frac{m\boldsymbol{v}(\boldsymbol{b}+\boldsymbol{b}_f+\boldsymbol{b}_c)}{\sqrt{1-(v/c)^2}^3} = \boldsymbol{Fv}\,.$$

Gleichung (23) stellt wegen (10) in der betrachteten Näherung eine Identität dar.

2. – Da unsere Gleichung (9) oder (13) mit den Mitteln der speziellen Relativitätstheorie und der klassischen Kinematik abgeleitet ist und für nichtinertiale Systeme gültig sein soll, bei welchen Systemen die allgemeine Relativitätstheorie gültig ist, so ist es angebracht, diese Gleichung im Gebiet der allgemeinen Relativitätstheorie zu prüfen. Zum diesen Zweck betrachten wir ein gleichmäßig rotierendes System K. Das Intervall zwischen zwei benachbarten Punkten in K lautet (wir benutzen Zylinderkoordinaten r, φ, z, t)

$$\mathrm{d}s^2 = (c^2-\omega^2r^2)\,\mathrm{d}t^2 - 2\omega r^2\,\mathrm{d}\varphi\,\mathrm{d}t - \mathrm{d}z^2 - r^2\,\mathrm{d}\varphi^2 - \mathrm{d}r^2\,. \tag{24}$$

Unsere Koordinaten sind

$$x_1 = r\,;\quad x_2 = z\,;\quad x_3 = \varphi\,;\quad x_4 = t\,.$$

Der Fundamentaltensor von

$$-\,\mathrm{d}s^2 = g_{ik}\,\mathrm{d}x^i\,\mathrm{d}x^k\,,\qquad i, k = 1, 2, 3, 4 \tag{25}$$

lautet

$$g_{11} = 1\,; \qquad g_{22} = 1\,; \qquad g_{33} = r^2\,;$$
$$g_{44} = \omega^2 r^2 - c^2\,; \qquad g_{34} = \omega r^2 = g_{43}\,.$$

Die Determinante ist

$$g = -\,c^2 r^2$$

also

$$g^{11} = 1; \qquad g^{22} = 1; \qquad g^{33} = \frac{1}{r^2} - \frac{\omega^2}{c^2}\,; \qquad g^{34} = g^{43} = \frac{\omega}{c^2}; \qquad g^{44} = -\frac{1}{c^2}.$$

Die nichtverschwindenden Christoffelschen Symbole lauten

$$\Gamma^1_{33} = -\,r; \qquad \Gamma^1_{34} = -\,\omega r; \qquad \Gamma^1_{44} = -\,\omega^2 r; \qquad \Gamma^3_{13} = \frac{1}{r}; \qquad \Gamma^3_{14} = \frac{\omega}{r}. \tag{26}$$

Die Gleichung der geodätischen Linie lautet

$$\frac{\mathrm{d}^2 x^i}{\mathrm{d}s^2} + \Gamma^i_{kl}\,\frac{\mathrm{d}x^k}{\mathrm{d}s}\,\frac{\mathrm{d}x^l}{\mathrm{d}s} = 0\,, \tag{27}$$

oder

$$\frac{\mathrm{d}^2 r}{\mathrm{d}s^2} - r\left(\frac{\mathrm{d}\varphi}{\mathrm{d}s}\right)^2 - 2\omega r\,\frac{\mathrm{d}\varphi}{\mathrm{d}s}\,\frac{\mathrm{d}t}{\mathrm{d}s} - \omega^2 r\left(\frac{\mathrm{d}t}{\mathrm{d}s}\right)^2 = 0\,;$$

$$\frac{\mathrm{d}^2 z}{\mathrm{d}s^2} = 0\,; \qquad \frac{\mathrm{d}^2\varphi}{\mathrm{d}s^2} + \frac{2}{r}\,\frac{\mathrm{d}r}{\mathrm{d}s}\,\frac{\mathrm{d}\varphi}{\mathrm{d}s} + 2\,\frac{\omega}{r}\,\frac{\mathrm{d}r}{\mathrm{d}s}\,\frac{\mathrm{d}t}{\mathrm{d}s} = 0\,; \qquad \frac{\mathrm{d}^2 t}{\mathrm{d}s^2} = 0\,. \tag{28}$$

Das gleiche Gleichungssystem (28) erhält man indem man nach Hilbert die zum Variationsproblem

$$\delta\int\left[(c^2 - \omega^2 r^2)\left(\frac{\mathrm{d}t}{\mathrm{d}s}\right)^2 - 2\omega r^2\,\frac{\mathrm{d}\varphi}{\mathrm{d}s}\,\frac{\mathrm{d}t}{\mathrm{d}s} - \left(\frac{\mathrm{d}z}{\mathrm{d}s}\right)^2 - r^2\left(\frac{\mathrm{d}\varphi}{\mathrm{d}s}\right)^2 - \left(\frac{\mathrm{d}r}{\mathrm{d}s}\right)^2\right]\mathrm{d}s = 0\,, \tag{29}$$

gehörigen Differentialgleichungen aufstellt. Sie haben die Gestalt

$$\frac{\mathrm{d}}{\mathrm{d}s}\left(\frac{\partial V}{\partial\,\mathrm{d}x^k/\mathrm{d}s}\right) - \frac{\mathrm{d}V}{\partial x^k} = 0\,, \tag{30}$$

wenn V den Integranden bedeutet.

Die vierte Gleichung (28) ergibt uns sofort das Integral

$$\left(\frac{\mathrm{d}s}{\mathrm{d}t}\right)^2 = c^2 - \omega^2 r^2 - 2\omega r^2\,\frac{\mathrm{d}\varphi}{\mathrm{d}t} - \left(\frac{\mathrm{d}z}{\mathrm{d}t}\right)^2 - r^2\left(\frac{\mathrm{d}\varphi}{\mathrm{d}t}\right)^2 - \left(\frac{\mathrm{d}r}{\mathrm{d}t}\right)^2 = \text{konst}\,. \tag{31}$$

Die dritte und die vierte Gleichungen von (28) ergeben das Integral

$$\omega r^2 \frac{dt}{ds} + r^2 \frac{d\varphi}{ds} = \text{konst} . \tag{32}$$

Aus (31) und (32) ergibt sich

$$\omega r^2 + r^2 \frac{d\varphi}{dt} = A = \text{konst} , \tag{33}$$

oder

$$\frac{d\varphi}{dt} = \frac{A}{r^2} - \omega . \tag{34}$$

Der Ausdruck (34) in die erste Gleichung von (28) eingesetzt ergibt

$$\frac{d^2 r}{dt^2} = \frac{A^2}{r^3} . \tag{35}$$

Die allgemeine Lösung der Gleichung (35) lautet

$$r^2 = -\frac{A^2 + (C_1 t - C_2)^2}{C_1} , \tag{36}$$

C_1, C_2, beliebige Konstanten. (Es gibt noch eine Sonderlösung von (35), nämlich

$$r^2 = 2t\sqrt{-A^2} + C_3 , \qquad C_3 = \text{Konstante},$$

welche aber komplexe Werte für r liefert). In (36) muß offenbar

$$C_1 < 0 \tag{37}$$

angesetzt werden. Aus (36) ergibt sich

$$\frac{dr}{dt} = -\frac{C_1 t - C_2}{r} . \tag{38}$$

Aus (31), (34), (38) und (36) erhalten wir

$$\left(\frac{ds}{dt}\right)^2 = c^2 + C_1 = \text{konst} . \tag{39}$$

1751

Die erste und die dritte Gleichung von (28) lauten dann

$$\frac{d^2r}{dt^2} - r\left(\frac{d\varphi}{dt}\right)^2 - 2\omega r\frac{d\varphi}{dt} - \omega^2 r = 0\,, \qquad \frac{d^2\varphi}{dt^2} + \frac{2}{r}\frac{dr}{dt}\frac{d\varphi}{dt} + 2\frac{\omega}{r}\frac{dr}{dt} = 0\,. \tag{40}$$

Auf Grund der zweiten Gleichung von (28) können wir einfach ansetzen

$$z = 0\,. \tag{41}$$

Die Gleichungen (40) bestimmen die geodätischen Linien im gleichmäßig rotierenden System K. Um zum ruhenden Inertialsystem K' überzugehen, müßen wir die Transformation

$$r = r'\,; \qquad z = z'\,; \qquad \varphi = \varphi' - \omega t \tag{42}$$

ausführen. Dann geht das Linienelement (24) in

$$ds^2 = c^2\,dt^2 - dz'^2 - r'^2\,d\varphi'^2 - dr'^2 \tag{43}$$

über, also in das Linienelement des Minkowskiraumes in Zylinderkoordinaten. Durch die Transformation (42) gehen die Gleichungen der geodätischen Linie (40) in die Gleichungen

$$\frac{d^2r'}{dt^2} - r'\left(\frac{d\varphi'}{dt}\right)^2 = b'_r = 0\,, \qquad r'\frac{d^2\varphi'}{dt^2} + 2\frac{dr'}{dt}\frac{d\varphi'}{dt} = b'_\varphi = 0 \tag{44}$$

über. b'_r und b'_φ sind die Komponenten der Beschleunigung im System K' in Zylinderkoordinaten. Also ist die Beschleunigung $\boldsymbol{b}'$ in K' gleich Null. Gleichungen (44) bestimmen die geodätischen Linien im Raum von Minkowski. Aus Gleichung (8) folgt dann

$$\boldsymbol{F} = 0\,. \tag{45}$$

Bei kleinen Winkelgeschwindigkeiten ω können wir bei Vernachlässigung der Glieder mit ω/c^2 den Begriff des starren Körpers und der universellen Zeit t einführen, (vergl. z.B. (1), S. 293), und infolgedessen auch die Beschleunigungen

$$\boldsymbol{b}_f = \boldsymbol{\omega}\times(\boldsymbol{\omega}\times\boldsymbol{r}) = -\,\omega^2\boldsymbol{r} \tag{46}$$

---

(1) L. Landau und E. Lifschitz: *Theorie des Feldes* (Moskau, 1948).

und

$$\boldsymbol{b}_c = 2\boldsymbol{\omega}\times\boldsymbol{v}\,. \tag{47}$$

In Zylinderkoordinaten haben wir die folgenden Vektoren

$$\boldsymbol{r} = (r,\ 0,\ 0)\,,$$

$$\boldsymbol{\omega} = (0,\ 0,\ \omega)\,,$$

$$\boldsymbol{v} = \left(\frac{\mathrm{d}r}{\mathrm{d}t},\ r\frac{\mathrm{d}\varphi}{\mathrm{d}t},\ 0\right),$$

$$\boldsymbol{b} = \left(\frac{\mathrm{d}^2 r}{\mathrm{d}t^2} - r\left(\frac{\mathrm{d}\varphi}{\mathrm{d}t}\right)^2,\quad r\frac{\mathrm{d}^2\varphi}{\mathrm{d}t^2} + 2\frac{\mathrm{d}r}{\mathrm{d}t}\frac{\mathrm{d}\varphi}{\mathrm{d}t},\ 0\right),\quad \boldsymbol{\omega}\times\boldsymbol{v} = \left(-\omega r\frac{\mathrm{d}\varphi}{\mathrm{d}t},\ \omega\frac{\mathrm{d}r}{\mathrm{d}t},\ 0\right). \tag{48}$$

Die Gleichungen (40) und (44) lassen sich in der Form schreiben

$$\boldsymbol{b}' = \boldsymbol{b} + \boldsymbol{b}_f + \boldsymbol{b}_c\,. \tag{49}$$

Das ist aber gerade die Verallgemeinerung des Satzes von Coriolis, Gl. (4).

Jetzt wollen wir nachweisen, daß auch die Grundformel (9) oder (13) in diesem Spezialfall der allgemeinen Relativitätstheorie gültig ist. Aus (49), (44) und (45) folgt, daß wir hierfür nur die Beziehung

$$\boldsymbol{v}\boldsymbol{b} + \boldsymbol{v}\boldsymbol{b}_f = 0 \tag{50}$$

nachzuweisen haben.

Wenn wir die Lösung (36) in die Komponenten (48) von $\boldsymbol{v}$ und $\boldsymbol{b}$ einsetzen, dann ergibt sich

$$\left\{\begin{aligned} \boldsymbol{v} &= \left(\frac{-C_1 t - C_2}{r},\ \frac{A}{r} - \omega r,\ 0\right), \\ \boldsymbol{b} &= \left(2\frac{A}{r}\omega - r\omega^2,\ 2\omega\frac{C_1 t - C_2}{r},0\right), \\ \boldsymbol{v}\boldsymbol{b}_f &= \boldsymbol{v}\boldsymbol{\omega}\times(\boldsymbol{\omega}\times\boldsymbol{r}) = -\boldsymbol{r}\boldsymbol{v}\omega^2\,, \end{aligned}\right. \tag{51}$$

$$\boldsymbol{v}\boldsymbol{b} + \boldsymbol{v}\boldsymbol{b}_f = -(C_1 t - C_2)\omega^2 + (C_1 t - C_2)\omega^2 = 0\,. \tag{52}$$

Wir betrachten noch den Fall, wenn auf den Massenpunkt die Lorentzsche Kraft des elektromagnetischen Feldes wirkt. Die Bewegungsgleichungen lauten in diesem Falle nach (1), S. 286,

$$mc\left(\frac{\mathrm{d}^2 x^i}{\mathrm{d}s^2} + \Gamma^i_{kl}\frac{\mathrm{d}x^k}{\mathrm{d}s}\frac{\mathrm{d}x^l}{\mathrm{d}s}\right) = \frac{e}{c}F^i_k u^k\,, \tag{53}$$

F_{ik} Tensor des elektromagnetischen Feldes, $u^k = \mathrm{d}x^k/\mathrm{d}s$. Gleichungen (53) lassen sich in unserem gleichmäßig rotierenden System so schreiben

$$(54)\qquad \left\{\begin{aligned} & mc\left[\frac{\mathrm{d}^2 r}{\mathrm{d}s^2} - r\left(\frac{\mathrm{d}\varphi}{\mathrm{d}s}\right)^2 - 2\omega r\frac{\mathrm{d}\varphi}{\mathrm{d}s}\frac{\mathrm{d}t}{\mathrm{d}s} - \omega^2 r\left(\frac{\mathrm{d}t}{\mathrm{d}s}\right)^2\right] = \frac{e}{c}F^1_k u^k\,,\\ & mc\frac{\mathrm{d}^2 z}{\mathrm{d}s^2} = \frac{e}{c}F^2_k u^k\,,\\ & mc\left(\frac{\mathrm{d}^2\varphi}{\mathrm{d}s^2} + \frac{2}{r}\frac{\mathrm{d}r}{\mathrm{d}s}\frac{\mathrm{d}\varphi}{\mathrm{d}s} + 2\frac{\omega}{r}\frac{\mathrm{d}r}{\mathrm{d}s}\frac{\mathrm{d}t}{\mathrm{d}s}\right) = \frac{e}{c}F^3_k u^k\,,\\ & mc\frac{\mathrm{d}^2 t}{\mathrm{d}s^2} = \frac{e}{c}F^4_k u^k\,. \end{aligned}\right.$$

Dabei ist F^i_k der Tensor des elektromagnetischen Feldes in Zylinderkoordinaten.

Wenn wir die Glieder mit ω^2/c^2 und ω/c^2 vernachlässigen, dann erhalten wir aus (54) unmittelbar die Gleichung (12), d.h. die Gl. (9). Aus Gl. (12) ergibt sich die Gleichung (11) oder

$$(55)\qquad \boldsymbol{Fv} = \frac{m}{\sqrt{1-(v/c)^2}^3}(\boldsymbol{vb} + \boldsymbol{vb}_f + \boldsymbol{vb}_c)\,.$$

Aus der vierten Gleichung von (54) ergibt sich

$$\frac{\mathrm{d}}{\mathrm{d}t}\left(\frac{mc^2}{\mathrm{d}s/c\,\mathrm{d}t}\right) = \boldsymbol{Fv}\,,$$

oder

$$(56)\qquad \frac{\mathrm{d}'}{\mathrm{d}t}\frac{mc^2}{\sqrt{1-(v'/c)^2}} = \boldsymbol{Fv}\,.$$

Hierbei bedeutet v' die Geschwindigkeit im absoluten Koordinatensystem, was aus (43) sofort zu sehen ist.

Der Vergleich von (55) mit (56) ergibt bei $r^2\omega^2 \ll c^2$

$$(57)\qquad \boldsymbol{vb}' = \boldsymbol{vb} + \boldsymbol{vb}_f + \boldsymbol{vb}_c\,,$$

d.h. den Satz von Coriolis.

3. – Zur Illustration der Theorie wollen wir die Bewegung einer Rakete betrachten, welche Teilchen mit relativistischen Geschwindigkeiten wegschleudert. Die Bewegung der Rakete selbst soll nichtrelativistisch sein. Die dabei

auftretenden Beschleunigungen sollen auch so klein sein, daß die Rakete als ein nichtrelativistisches System aufgefaßt werden kann. (Solche Raketen werden wir noch lange Zeit zu bauen haben). In jedem Augenblick werden wir zu der Rakete nur diese Teilchen hinzuzählen, welche in diesem Augenblick sich innerhalb einer Kontrollfläche befinden, welche durch die Oberfläche der Rakete und durch den Ausgangsquerschnitt der Düsen gebildet ist.

Nach GANTMACHER und LEVIN (²) betrachten wir in einem gegebenen Zeitpunkt einen starren Körper S, welcher aus der Rakete entstehen würde, wenn die Rakete im Moment t erstarren würde und keine Teilchen wegscheudern würde. Der Körper S ist unbeweglich mit dem Korpus der Rakete verbunden und vom Augenblick t an bewegt er sich zusammen mit der Rakete. Die Bewegungsgröße des körpers S bezeichnen wir mit $\boldsymbol{Q}$.

Gleichzeitig betrachten wir das System Σ, welches aus sämtlichen Teilchen besteht, welche zum Zeitpunkt t der Rakete angehören. Im Zeitpunkt t fällt das System Σ mit der Rakete zusammen, in den darauffolgenden Zeitpunkten werden sich einige von den Teilchen des Systems Σ außerhalb der Rakete befinden. Das System Σ und der Körper S haben unveränderliche Masse, gleich der Masse der Rakete im Augenblick t. Die Bewegungsgröße des Systems Σ in Bezug auf ein Inertialsystem, welches als unbeweglich betrachtet wird, bezeichnen wir mit $\boldsymbol{K}$. Es sei $\boldsymbol{F} = \mathrm{d}\boldsymbol{K}/\mathrm{d}t$ der Vektor der Außenkräfte, welche im Augenblick t auf die Rakete (also auch auf das System Σ) wirken.

Die Bewegung einiger Teilchen des Systems Σ ist relativistich. Wir betrachten die Bewegung jedes Teilchens des Systems Σ als zusammengesetzt: das Teilchen bewegt sich in bezug auf den Körper S, und der Körper S führt die Führungsbewegung aus. Die absolute, die relative und die Führungsgeschwindigkeit eines Teilchens bezeichnen wir entsprechend mit $\boldsymbol{v}_a$, $\boldsymbol{v}_r$, $\boldsymbol{v}_f$. Entsprechend bezeichnen wir die Beschleunigungen mit $\boldsymbol{b}_a$, $\boldsymbol{b}_r$ und $\boldsymbol{b}_f$. Außerdem führen wir noch die Coriolisbeschleunigung $\boldsymbol{b}_c$ ein. $\boldsymbol{v}_r$ und $\boldsymbol{b}_r$ sind gleich Null für sämtliche Teilchen des Raketenkorpus. Wir haben

$$
(58)\quad \boldsymbol{F} = \frac{\mathrm{d}\boldsymbol{k}}{\mathrm{d}t} = \sum \frac{\mathrm{d}}{\mathrm{d}t}\left(\frac{m\boldsymbol{v}_r}{\sqrt{1-(v_r/c)^2}}\right) + \sum \frac{m}{\sqrt{1-(v_r/c)^2}}\boldsymbol{b}_f + \\
+ \sum \frac{m(\boldsymbol{v}_r\boldsymbol{b}_f)}{c^2\sqrt{1-(v_r/c)^2}^{\,3}}\boldsymbol{v}_r + \sum \frac{m}{\sqrt{1-(v_r/c)^2}}\boldsymbol{b}_c\,.
$$

(Der Einfachheit halber haben wir bei den Summen die Indices i der Teilchen weggelassen, also anstatt v_{ri}, m_i einfach $\boldsymbol{v}_r$, m geschrieben.)

Bei sämtlichen Teilchen, für welche v_r, wie v_a nichtrelativistisch ist (v_f ist immer nichtrelativistisch), kann man $(v_r/c)^2$ in der Formel (58) vernachlässigen.

(²) F. R. GANTMACHER und L. M. LEVIN: *Prikladnaja mathematika i mechanika*, **11**, 301 (1947).

1755

Wir bezeichnen mit $\boldsymbol{v}_{1r}$ die relative Geschwindigkeit des Teilchens im Augenblick $t_1 = t + \mathrm{d}t$. Dann erhalten wir für den elementaren Geschwindigkeitszuwachs in bezug auf den Raketenkorpus $\delta \boldsymbol{v}_r = \boldsymbol{v}_{1r} - \boldsymbol{v}_r = \boldsymbol{b}_r \mathrm{d}t$ und deswegen

$$\sum \frac{\mathrm{d}}{\mathrm{d}t}\left(\frac{m\boldsymbol{v}_r}{\sqrt{1-(v_r/c)^2}}\right) = \sum\left(\frac{m}{\sqrt{1-(v_r/c)^2}}\frac{\delta \boldsymbol{v}_r}{\mathrm{d}t} + \frac{m(\boldsymbol{v}_r \delta \boldsymbol{v}_r/\mathrm{d}t)\boldsymbol{v}_r}{c^2\sqrt{1-(v_r/c)^2}^3}\right), \tag{59}$$

(δ bedeutet das Differential eines Vektors in bezug auf den Raketenkorpus. Das Differential in Bezug auf dem Ausgangskoordinatensystem bezeichnen wir mit d).

Es bezeichne $\boldsymbol{K}_r$ die Bewegungsgröße in bezug auf den Raketenkorpus dieser Teilchen, welche sich im Augenblick t innerhalb der Rakete befinden, und $\boldsymbol{K}_{r1}$ die Bewegungsgröße der Teilchen, welche sich im Zeitpunkt $t + \mathrm{d}t$ in der Rakete befinden. Also

$$\left\{\begin{aligned} &\delta \boldsymbol{K}_r = \boldsymbol{K}_{r1} - \boldsymbol{K}_r; \qquad \sum \frac{m}{\sqrt{1-(v_r/c)^2}}\boldsymbol{v}_r = \boldsymbol{K}_r; \\ &\sum \frac{m}{\sqrt{1-(v_{1r}/c)^2}}\boldsymbol{v}_{1r} = \boldsymbol{K}_{r1} + \boldsymbol{R}_r \mathrm{d}t. \end{aligned}\right. \tag{60}$$

Dabei ist $\boldsymbol{R}_r \mathrm{d}t$ die Bewegungsgröße (bei der relativen Bewegung) dieser Teilchen, welche im Zeitintervall $\mathrm{d}t$ durch die Ausgangsquerschnitte der Düsen ausgetreten sind. $\boldsymbol{R}_r$ ist die Begewungsgröße in Bezug auf dem Raketenkorpus der Sekundenmasse der Teilchen, welche durch die Düsen hinaustreten, $\delta \boldsymbol{K}_r$ ist der elementare Zuwachs der relativen Bewegungsgröße der Teilchen, welche sich innerhalb der Kontrollfläche befinden.

Der Vektor $\boldsymbol{R}_r$ hat die Dimension einer Kraft. Die Kraft $\boldsymbol{R}_r$ bezeichnet man als die Resultante der reaktiven Kräfte, oder einfach die reaktive Kraft.

Aus (59) und (60) folgt

$$\sum \frac{\mathrm{d}}{\mathrm{d}t}\left(\frac{m\boldsymbol{v}_r}{\sqrt{1-(v_r/c)^2}}\right) = \boldsymbol{R}_r + \frac{\delta \boldsymbol{K}_r}{\mathrm{d}t}. \tag{61}$$

Dann erhalten wir aus (58)

$$\begin{aligned} \boldsymbol{F} = \boldsymbol{R}_r + \frac{\delta \boldsymbol{K}_r}{\mathrm{d}t} + \sum \frac{m}{\sqrt{1-(v_r/c)^2}}\boldsymbol{b}_f + {} \\ + \sum \frac{m\boldsymbol{v}_r}{c^2\sqrt{1-(v_r/c)^2}^3}(\boldsymbol{v}_r \boldsymbol{b}_f) + \sum \frac{m}{\sqrt{1-(v_r/c)^2}}\boldsymbol{b}_e. \end{aligned} \tag{62}$$

Wenn wir die Bewegungsgröße $\boldsymbol{Q}$ des starren Körpers S in Bezug auf dem absoluten System durch die Gleichung

$$\frac{\mathrm{d}\boldsymbol{Q}}{\mathrm{d}t} = \sum m\boldsymbol{b}_f\,, \tag{63}$$

einführen, dann nimmt die Gleichung (62) die Gestalt

$$\frac{\mathrm{d}\boldsymbol{Q}}{\mathrm{d}t} = \boldsymbol{F} - \boldsymbol{R}_r - \frac{\delta \boldsymbol{K}_r}{\mathrm{d}t} - \sum m\left(\frac{1}{\sqrt{1-(v_r/c)^2}} - 1\right)\boldsymbol{b}_f - \\ - \sum \frac{m(\boldsymbol{v}_r\boldsymbol{b}_f)}{c^2\sqrt{1-(v_r/c)^2}^3}\,\boldsymbol{v}_r - \sum \frac{m}{\sqrt{1-(v_r/c)^2}}\,\boldsymbol{b}_c\,. \tag{64}$$

an. Gleichung (64) drückt den Satz der Bewegungsgröße für die erstarrte Rakete, d.h. für den starren Körper S, aus.

RIASSUNTO (*)

Si generalizza la formula fondamentale della Meccanica relativistica $\boldsymbol{F} = (\mathrm{d}/\mathrm{d}t)\cdot(m\boldsymbol{v}/\sqrt{1-(v/c)^2})$ per i sistemi cosiddetti « non relativistici ». Per questi si possono introdurre i concetti di tempo universale e di corpo rigido, e pertanto vale la legge di Coriolis della Cinematica classica. La nuova equazione è $\boldsymbol{F}+\boldsymbol{S}_f+\boldsymbol{S}_c+\boldsymbol{S}_k = (\mathrm{d}/\mathrm{d}t)(m\boldsymbol{v}/\sqrt{1-(v/c)^2})$, dove $\boldsymbol{S}_c$ è la forza conduttrice, $\boldsymbol{S}_f$ la forza di Coriolis, $\boldsymbol{S}_k$ è una nuova forza d'inerzia che sorge soltanto a velocità relativistiche $\boldsymbol{v}$ del punto materiale. Si deriva la nuova equazione anche nell'ambito della teoria della relatività generale e se ne mostra una applicazione alla teoria dei razzi con particelle propulsive relativistiche.

(*) *Traduzione a cura della Redazione.*

IL NUOVO CIMENTO Vol. XIII, N. 1 1° Luglio 1959

Heat Flush and Mobility of Electric Charges in Liquid Helium

I. – Non Turbulent Flow.

G. Careri, F. Scaramuzzi (*) and J. O. Thomson (**)

Istituto di Fisica dell'Università - Padova
Istituto Nazionale di Fisica Nucleare - Sezione di Padova

(ricevuto il 20 Marzo 1959)

Summary. — With the aim of a quantitative check of the Landau-Pomerančuk picture of the movement of foreign atoms in liquid helium II, an experiment has been performed in which some elementary charged particles could be dragged perpendicular to their motion in an electric field by a stream of excitations in non-turbulent flow. Using known values for the mobility of charged particles in He II, the drift velocity of the charges parallel to the stream of excitations has been found to be equal to the normal fluid velocity in the temperature range above 1.18 °K. Working under similar conditions, the apparatus has then been used to obtain mobilities at temperatures near 1 °K. The mobility is found to go exponentially with decreasing temperature, and this behaviour is discussed in terms of elastic scattering of the charges by the rotons.

1. – Introduction.

In liquid helium a foreign particle must collide only with the excitations and not with the superfluid liquid, insofar as the particle moves with a velocity lower than the one needed to itself create the excitations. This statement has been put forward by Landau and Pomerančuk [1] to explain the dynamical

(*) On leave of absence from the University of Bari.

(**) Present address: Department of Physics, University of Tennessee, Knoxville, Tenn., U.S.A.

[1] L. D. Landau and I. Pomerančuk: *Dokl. Akad. Nauk USSR*, **59**, 669 (1948).

properties of dilute solutions of ^{3}He in ^{4}He, and in particular the non participation of ^{3}He in superfluid motion, discovered by DAUNT [2] and LANE [3] and their co-workers. This point of view is now widely accepted (especially by the Russian workers) and has been used as a reasonable assumption to derive results that are consistent with experiment [4]. However it is our impression that a direct and quantitative check of the fact that impurities do not interact with the superfluid has yet to be made [*].

The Landau-Pomerančuk statement is quite general, and one is tempted to apply it to the case of electric charges dissolved in liquid helium, where now the movement of these charged foreign particles can be more easily produced and controlled than in the case of the ^{3}He atoms. Furthermore the detectable number of impurities can be so small as not to affect at all the normal fluid density of the liquid. With this aim, a heat flush experiment has been performed and is described in the following, in which some elementary charged particles could be dragged by a stream of excitations perpendicular to their motion in an electric field. The drift velocity of the charges in the direction of the excitation flow, v_i, has been found to be equal to the normal fluid velocity, v_n.

As it will appear from the following, to make this quantitative check possible, the mobilities must be independently known as they are now thanks to the recent work of MEYER and REIF [5].

Once this relation, $v_i = v_n$ is verified for one temperature, it seems plausible to extend it to all temperatures if certain experimental conditions, to be mentioned below, are still fulfilled. Thus this experiment can yeld the ionic mobilities at other temperatures.

The experimental conditions fulfilled in this paper are such as to avoid turbulent flow, in order to make a quantitative check of the Landau picture. New and very interesting phenomena occur for heat flows larger than the turbulent threshold, but they will be presented at a later time.

For reasons that will become evident in the following, the terms « positive and negative charges » will be used as well as « positive and negative ions »;

---

(2) J. G. DAUNT, R. E. PROBST, H. L. JOHNSTON, L. T. ALDRICH and A. O. NIER: *Phys. Rev.*, **72**, 502 (1947).

(3) C. T. LANE, H. A. FAIRBANK, L. T. ALDRICH and A. O. NIER: *Phys. Rev.*, **73**, 256 (1948).

(4) J. J. M. BEENAKKER and K. W. TACONIS: *Progress in Low Temperature Physics* (Amsterdam, 1955), chap. VI.

(*) The best evidence concerning this check seems to be in the analysis of second sound in dilute solutions of ^{3}He; however the ideality of these mixtures had to be assumed and the effective mass of ^{3}He obtained in this way is a temperature dependent quantity: see, for instance, K. R. ATKINS: *Liquid Helium* (Cambridge, 1959), p. 284.

(5) L. MEYER and F. REIF: *Phys. Rev.*, **110**, 279 (1958).

(6) W. F. VINEN: *Proc. Roy. Soc.*, **243**, 400 (1957).

this is due to the still unknown complex type of clustering that the elementary particles are likely to form in liquid helium.

Preliminary presentations of these results have been given at the Madison (7) and Leiden (8) International Conferences on low temperatures Physics.

2. – The apparatus.

The apparatus is essentially a ionization chamber with several detecting electrodes, where the ionic currents are measured as a function of the heating produced by an electric resistance.

The apparatus is shown schematically in Fig. 1. The radioactivity, composed of an electrochemically deposited layer of ^{210}Po, emits α-particles of range of the order of 0.2 mm in liquid helium. These α-particles ionize intensely the helium within this small distance from the active electrode. An electric field is applied across the chamber which draws a small fraction of the ions of one sign from the ionized region toward the four collecting electrodes. Provision is made for measuring the current on each of these collecting electrodes while the other three are grounded. A constantan wire heater located at the bottom of the chamber supplied the heat current densities used.

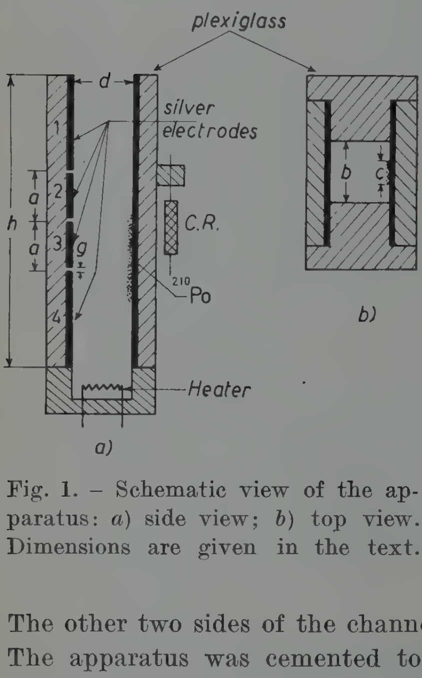

Fig. 1. – Schematic view of the apparatus: *a*) side view; *b*) top view. Dimensions are given in the text.

The heat flow channel was formed on two sides by plexiglass walls, which, due to the fact that their dielectric constant is much greater than that of helium, also served to improve the uniformity of the field in the channel. The other two sides of the channel were formed by the electrodes themselves. The apparatus was cemented together using a plexiglass cement, with the wires passing through small holes also tight with plexiglass cement. Care was taken to ensure that only a negligeable amount of heat escaped through the walls of the apparatus or along the wires or electrodes. However, no special precautions were taken to ensure that the channel was actually superfluid tight,

(7) G. CARERI, J. REUSS, F. SCARAMUZZI and J. O. THOMSON: *Proc. Fifth Int. Conference on Low Temperature Physics and Chemistry* (Madison, U.S.A., 1957), p. 79.

(8) G. CARERI, F. SCARAMUZZI and J. O. THOMSON: *Proc. Kamerlingh Onnes Conference on Low Temperature Physics*, in *Physica* (Sept. 1958), p. 139.

since such a small leak would not have affected the results of the experiment significantly.

The temperature was monitored by means of an ALLEN and BRADLEY [9] carbon resistor and held constant within 10^{-3} °K by means of a throttling valve. The resistor was also used to measure the temperature below 1.2 °K, after being calibrated against the vapour pressure of helium between 1.2 and 2.2 °K. The error in this extrapolation is of the order of 0.02 °K, which was negligible in this experiment. The lowest temperatures were reached by pumping with an oil booster pump of throughput about $2\cdot10^{4}$ μm/l/s (Edwards 9B3). The Dewar system was provided with a nitrogen pocket around the pumping tube which served to cool the lip of the Dewar and to reduce the pumping impedance. This pocket roughly halved the heat leak in the helium bath.

The small ionization currents were measured with a vacuum tube electrometer capable of detecting currents down to $3\cdot10^{-15}$ A flowing across a $10^{11}\,\Omega$ resistor. In practice the changes in current measured were of the order of 10^{-13} A. The output of the electrometer was amplified and displayed on a stripchart recorder. For some of the later measurements, a vibrating reed electrometer was employed.

The nominal dimensions of the chamber used in these experiments and the area of the channel section (at room temperature) were as follows (see Fig. 1 for the designation of the dimensions):

a	b	c	d	g	h	A
10	10	6	8	0.1	60 mm	80 mm²

In the previous experiments, briefly reported at the Madison Conference [7], a cylindrical geometry was used. This had the disadvantage that the field was not uniform along the radius, and therefore quantitative data were difficult to obtain. The results of this cylindrical apparatus were actually used to design the plane geometry apparatus, and were consistent with the latter more exact results. Therefore the results of the cylindrical geometry will not be reported here.

3. – Analysis of data.

Upon heating, it was observed from the change in current on plates No. 2 and No. 4 (Fig. 1) that the ions have a drift velocity upward in the direction of the heat current that is proportional to the heat current density, as is shown in Fig. 2. This proportionality is a quantitative evidence of a heat flush phe-

---

[9] J. R. CLEMENT and E. H. QUINNEL: *Rev. Sci. Instr.*, **23**, 213 (1952).

nomenon similar to the one already observed by LANE and co-workers ([3]) for the ^{3}He-^{4}He mixtures, and stressed by LANDAU and POMERANČUK ([1]) to be a peculiar behaviour of the impurities in liquid helium II regardless of the nature of the impurities themselves. In this picture we expect that the average velocity with which the ions are carried upwards is the normal fluid velocity, v_n, if the following four conditions are satisfied:

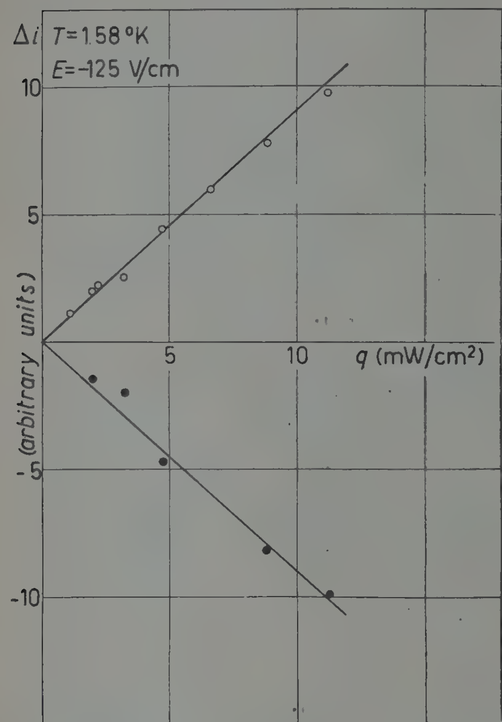

Fig. 2. – A typical plot of the change in current in plate 2 (white points) and plate 4 (black points) due to the heat flush effect, versus heat input. From the slope of the best fitted straight line a value of v_i^0 is calculated.

a) the mean free path of the ion is small compared with the dimensions of the apparatus, such that the vertical component of the ionic velocity quickly reaches equilibrium with the drift velocity of the normal fluid;

b) the energy gained from the electric field between collisions by a ion is less than its energy of thermal agitation: it is not certain that this condition is necessary; however it was fulfilled in these experiments;

c) the maximum velocity reached by the ions is small compared with the velocity of sound in liquid (*i.e.* small compared with the velocity required to create excitations); this condition is satisfied if *b*) is satisfied;

d) the density of vortices in the superfluid is small.

Since all of these conditions were met in this experiment, we may check the relation (for motion in the direction of the heat flow)

$$v_i = v_n \tag{1}$$

from the measured currents as a function of the heat current density on the various electrodes.

A simplified calculation that neglects the finite range of the α-particles

1762

and assumes that v_i is constant over the whole channel section (instead of the Poiseuille distribution (*)) proceeds as follows. The angle α, that the trajectory of the ion makes with the field will be given by:

$$\operatorname{tg}\alpha = \frac{v_i(\dot{q})}{\mu E} = \frac{z(\dot{q})}{d}, \tag{2}$$

z being the displacement along the heat flow and μ the mobility. This displacement will be proportional to the change in current observed on plates No. 2 and No. 4

$$z(\dot{q}) = c\,\Delta i(\dot{q}). \tag{3}$$

The constant c can be determined measuring the current on plate No. 3 without heat input

$$a = c i_3 \tag{4}$$

and, from (2), (3) and (4) we have

$$v_i(\dot{q}) = \mu E \frac{a}{i_3} \frac{\Delta i(\dot{q})}{d}.$$

Since this experiment shows that there is a linear dependence between Δi and $\dot{q}$, we introduce the drift velocity per unity heat input

$$v_i^0 = \frac{v_i(\dot{q})}{\dot{q}} \tag{5}$$

and write

$$v_i^0 = \frac{\mu E a}{i_3 d} \frac{\Delta i}{\dot{q}}, \tag{6}$$

(*) The Poiseuille distribution is easily introduced multiplying v_i by a geometrical factor. Experimental evidence on flow in small channels (EDWARDS: *Thesis* [10], etc.) indicates that such a flow pattern is in accord with experiment. The fact that phonons and rotons, each having different viscosities, will show different flow patterns near the walls has no effect on our wide channel experiment, since at short distance from the walls both excitations will have the same velocity due to their mutual interactions. The correction to the excitation velocity profile, for our rectangular channel, is to increase the effective normal fluid velocity, by a factor 1.28. However, there is some incertitude when applying this correction to our experimental data, due to a possible lack of hydrodynamical equilibrium in the channel during the runs. It must be emphasized that a somewhat different numerical factor would have left in practice the position of the experimental data of Fig. 3, and the relative conclusions unchanged.

[10] D. O. EDWARDS: *Thesis* (Oxford, University 1957).

where $\Delta i/\dot{q}$ is the slope of the experimental curves (Fig. 2). This procedure can be applied to the plate No. 2, as well as to the plate No. 4. This value of v_i^0 deduced from (6) must now be compared with the value of v_n^0 (the normal fluid velocity per unity of heat input), deduced from the familiar hydrodynamical equation for the entropy conservation in liquid helium II, which now simply requires

$$\dot{q} = \varrho S v_n T, \tag{7}$$

S being the entropy per gram and ϱ the density, and T the absolute temperature. This comparison can be made for temperatures larger than 1.18 °K by help of the mobilities measured by MEYER and REIF ([5]) and is found to be satisfactory (see Table I). For matter of presentation we reverse the argument and give in Fig. 3 the mobilities derived from our experimental data assuming equation (1) to hold, and compare them with the ones already measured ([5]) and indicated by the solid lines.

This procedure can be now extended to temperatures lower than 1.18 °K provided that the above experimental conditions are still fulfilled; the values of the mobilities derived in this manner are also shown in Fig. 3.

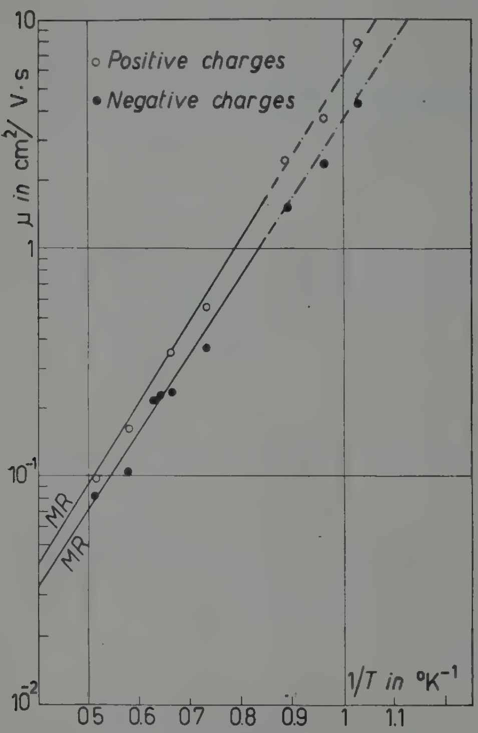

Fig. 3. – Plot of the log of the mobilities versus $1/T$. Solid lines are the data by MEYER and REIF ([5]).

However it must be said that the threshold for turbulence in a large channel is not a well defined value ([6]), and therefore an appreciable amount of turbulence could also exist in some of our runs, if, in the middle of the run, the critical heat current was exceeded. This was noticeable sometimes as a systematic difference in the behaviour of the No. 2 and No. 4 plates, and a general tendency of the Δi versus $\dot{q}$ plot to deviate from the straight line. In this somewhat uncertain situation the averages of the results of the two plates have been given in Table I and Fig. 3. But when turbulence memory effects are certainly excluded (because the threshold has never been reached in that run), the two plates had quite the same behaviour, as indicated in the quoted example (Fig. 2). However, a fuller discussion of these effects will be presented later, but we want here only to say that the true « subturbulent » mobility in

this kind of apparatus must be intended as the limiting value of the mobility derived when the heat input goes to zero.

TABLE I.

	T	μ (*)	v_i^0	v_n^0
a) positive charges	1.947	0.102	4.6	4.36
	1.734	0.173	10.5	9.05
	1.508	0.354	22.4	22.3
	1.372	0.618	51.4	42.6
b) negative charges	1.947	0.078	4.15	4.36
	1.733	0.127	11.3	9.05
	1.585	0.197	14.2	16.0
	1.560	0.211	18.1	17.7
	1.508	0.253	23.8	22.3
	1.372	0.430	59.1	42.6

(*) Data from MAYER and REIF (5).

4. – Discussion of the mobilities.

The mechanism for the mobility when only the He II excitations are effective to the ion drift, must be analogous to the diffusion of ^{3}He in a dilute solution of ^{3}He in ^{4}He, with the addition of a slow drift due to the electric field. Of course there are differences due to the larger sizes and masses of the ionic complexes, but the treatment must follow closely the one employed by GIAROV and HALATNIKOV (11) for the case of dilute solutions ^{3}He-^{4}He. These authors find by inspection of the collision integrals that the process involving collisions with phonons may be discarded in comparison with the ^{3}He-roton and the ^{3}He-^{4}He ones, as one expects classically due to the low phonon momentum.

For extremely dilute solutions and low temperatures the treatment by GIAROV and HALATNIKOV reduces to the simple gas-kinetic one

$$D = \tfrac{1}{3}\lambda\bar{v}\,,$$

$\bar{v}$ being the average thermal velocity (without the zero point kinetic energy), λ the mean free path which is now only determined by the roton-^{3}He col-

(11) V. N. GIAROV and I. M. HALATNIKOV: *Dokl. Akad. Nauk USSR*, **43**, 1007 (1953).

lisions, namely

$$\lambda = \frac{1}{\sigma_{^3\mathrm{He}-\varrho} N_\varrho}\,,$$

N_ϱ being the roton density and $\sigma_{^3\mathrm{He}-\varrho}$ the cross-section of the process. If this simplified treatment is applied to the experiments of GARWIN and REICH [12], who measured the diffusion coefficient of ^{3}He in ^{4}He, one gets a temperature independent cross-section $\sigma_{^3\mathrm{He}-\varrho} \simeq 10^{-13}\ \mathrm{cm}^2$, similar to the one obtained by GIAROV and HALATNIKOV from the data of BEENAKKER *et al.* (they actually give $1/\tau = \bar{v}\sigma_{^3\mathrm{He}-\varrho} N_\varrho$). The Δ/k value for these experiments lies around 9 °K. The value of this cross-section is rather large, and corresponds to an interaction radius of about 18 Å. We note however that this is the mean distance between rotons at 1.5 °K, right when the roton gas starts to show a non ideal behaviour due to its high density.

A completely similar treatment might then be used for the mobility in our very dilute ionic system. Here the interaction between the ions themselves is not important, as can be seen from the experimental results, which are independent of the intensity of the ionic sources. Therefore we write the gas kinetic expression

$$\mu = \frac{e\lambda}{m\bar{v}}\,,$$

m being an effective mass for the movement in the liquid medium. Assuming again the roton scattering to be the dominant process, we then use the Landau-Halatnikov expression for the roton density and get

$$\mu = \frac{\pi^2}{2}\,\frac{e\hbar^3}{\sigma_{i\varrho} m_\varrho^{\frac{1}{2}} m^{\frac{1}{2}} p_0^2}\,\frac{1}{kT}\exp[\Delta/kT]\,, \tag{8}$$

$\sigma_{i\varrho}$ being the ion-roton cross-section, m and p_0 the roton effective mass and momentum.

Our experimental data, as well as those of MEYER and REIF [5], fit a straight line when $\log\mu$ is plotted versus $1/T$. The equation (8) on the same plot (if $\sigma_{i\varrho}$ and m are independent of temperature), has a slope

$$S = T + \frac{\Delta}{k}\,. \tag{9}$$

Therefore the experimental slope indicates Δ/k somewhat lower than that found

---

[12] R. L. GARWIN and H. A. REICH: *Proc. Kamerlingh Onnes Conference on Low Temperature Physics*, in *Physica* (Sept. 1958), p. 133.

by other workers, that is

$$\text{for positive charges} \qquad \Delta/k \simeq 7.3\ ^\circ\mathrm{K}\,,$$

$$\text{for negative charges} \qquad \Delta/k \simeq 6.9\ ^\circ\mathrm{K}\,.$$

Postulating some extreme values of the effective mass of the ion, one can calculate the value of the mean free path and cross-section of the ions in the excitation gas. These values, based on the Landau-Halatnikov analysis of the roton constants from thermodynamic data, are shown in Table II. It must

TABLE II. – *The mean free paths λ and the cross-sections $\sigma_{i\varrho}$ for postulated values of the effective mass.*

effective mass in $m_{^4\mathrm{He}}$ units		1	10	100
positive charges	λ (Å)	17.5	55.3	175
	$\sigma_{i\varrho}$ (cm²)	$5.7\cdot10^{-13}$	$1.8\cdot10^{-13}$	$0.57\cdot10^{-13}$
negative charges	λ (Å)	10.8	34.2	108
	$\sigma_{i\varrho}$ (cm²)	$9.3\cdot10^{-13}$	$2.9\cdot10^{-13}$	$0.93\cdot10^{-13}$

be said that a large amount of clustering must exist around the charges in order to make possible such large values of m. Actually, with a convenient value of m lying around 15 helium masses, the cross-section can be made the same as the ^{3}He-roton one.

However, a large value of the ion-roton cross-section can be expected because, if we think a roton as a local compression of the medium, the ion will interact with it at large distances owing to the polarization forces (*). Also an explanation of our value of Δ may lie in the intense polarization forces of electric charges, that will cause a local compression of the medium, and make a roton easier to be formed in the neighbourhood of the charges than elsewhere. But here again we must call attention that all the above figures have been obtained under the assumption of the independency of the cross-section from temperature.

The different behaviour between positive and negative charges is more

---

(*) This possibility has been kindly pointed out to us by professor R. P. FEYNMAN during a very useful discussion. Thanks are also due to professor L. MEYER for many useful discussions on these points.

difficult to explain. It might be due to zero point energy motion which will cause the negative charge to behave as a bubble if the negative ion is supposed to be a free electron. Therefore one should have a cross-section larger for the negative than for the positive charges, and a more intense compression of the medium around the charge.

The fact that the plot of $\log \mu$ against $1/T$ remains linear down below 1 °K, where the phonon density exceeds the roton density indicates that phonon-ion collisions are unimportant. It will be interesting to extend the measurements down below 0.6 °K, where rotons are extremely scarce and phonon collisions will therefore be important. In this region, we should find that

$$\mu \sim T^{-4} ,$$

(assuming that the phonon-ion cross-section is independant of temperature).

Finally vortices may also interact with the charges and this possibility must not be discarded even in subturbulent conditions. This point will be further discussed in a subsequent publication.

* * *

One of the authors (J. O. THOMSON) wishes to express appreciation to the « Commissione Americana per gli Scambi Culturali con l'Italia » for a Student Fulbright Grant to Italy during which time this work was carried out.

RIASSUNTO

È stato realizzato un esperimento in cui alcune particelle cariche vengono trascinate in direzione perpendicolare al loro moto in un campo elettrico da un flusso non turbolento di eccitazioni, allo scopo di controllare il modello di Landau e Pomerančhuck sul moto di particelle estranee in He II. Usando valori noti della mobilità, (fino a 1.18 °K) si è calcolata la velocità delle cariche nella direzione del flusso di eccitazioni e la si è trovata uguale alla velocità del fluido normale. Lavorando in condizioni analoghe è stato possibile calcolare la mobilità a temperature inferiori a 1.18 °K fino a circa 1 °K. S'è trovato che la mobilità varia esponenzialmente con $1/T$ e s'è discusso questo comportamento in termini di scattering elastico delle cariche coi rotoni.

Solvent Effect on the Intensity of CN Stretching Vibration for some Nitriles.

A. FOFFANI, C. PECILE and F. PIETRA

Istituto di Chimica-Fisica dell'Università - Padova

(ricevuto il 12 Marzo 1959)

The present situation as to the effect of the medium on electronic and vibrational spectra is typical of a field which is attracting a rapidly increasing body of interest. In the case of electronic spectra a very promising approach appears to be that by KOSOWER [1], who proposed the use of the transition energies corresponding to some appropiate charge-transfer bands as an empirical measure of solvent polarity; these transition energies (designated as Z-values) are linear functions of the Winstein-Grünwald Y-value,which is a kinetic measure of the ionizing power of the medium.

In the case of vibrational spectra, concerned with our present measurements, the theoretical treatments up to present proposed [2] are essentially focused on the evaluation of the extent of electrostatic solute-solvent interactions; the first equation to be deduced, that by Kirkwood-Bauer-Magat (KBM), correlates in a simple way the frequency shifts with the dielectric constant of the medium; in a similar way equations were proposed connecting the intensity shifts with the dielectric properties of the solvent. Subsequent more refined treatments, which consider the interaction energy as an additional perturbation to the harmonic oscillator Hamiltonian and which again make use of the «reaction field» approach (where the reaction field is the mean electric field acting on the vibrating molecule owing to the charge distribution induced in the neighbouring molecules), suffer from the limitation to require, for their testing, the knowledge of molecular parameters and other data hardly available. In the rather limited number of cases where testing was possible, there were found only a very few instances of agreement with theory; this is pointing out to the important fact that purely electrostatic interactions are playing only a minor part on the total interaction energy, which should be presumably strongly influenced by local solute-solvent association effects.

On this regard, very promising is the semiempirical approach by BELLAMY and

(1) E. M. KOSOWER: *Journ. Am. Chem. Soc.*, **80**, 3253, 3261, 3267 (1958).

(2) See A. D. BUCKINGHAM: *Proc. Roy. Soc.*, A **248**, 169 (1958); A. D. E. PULLIN: *Spectrochim. Acta*, **13**, 125 (1958); D. G. REA: *Journ. Opt. Soc. Am.*, **49**, 90 (1959); and references therein.

PULLIN [3], who have observed that, if one orders a series of solvents according to their increasing effect on the frequency and the intensity of a particular bond vibration (starting from the corresponding vapour value), the order is approximately the same for many different solutes, but generally it changes drastically if one changes the bond vibration in study; in particular, BELLAMY studied X—H and C=O vibrations, and he found in both cases an order for the solvents entirely different from that predicted by the KBM equation and similar electrostatic approachs. There is no break between the behaviour of polar and non-polar solvents, suggesting that in the latter solvents the type of solute-solvent interaction is not qualitatively different from that active in the former; it seems that an important factor determining the solvent effect, particularly in the case of X-H vibrations, is the proton-donating power of the solute and the proton-accepting power of the solvent.

We have now extended the study to C≡N vibrations, both isolated and conjugated to other vibrating groups, finding in the latter case a singular behaviour and generally confirming the previous observations.

1. – Experimental.

The infrared spectrometer was a Perkin-Elmer mod. 12C single beam one, modified to double pass, with CaF_2 optics; frequency calibration in the triple bond region was performed with the aid of the CO band at 4.67μ; the spectral slit width was $(4\div5)$ cm^{-1}, which is about a half of the mean half intensity band width for our C≡N bands (see later); the mechanical slit width was of the order of 0.07 mm, the cell thickness generally 1 mm and only in a few cases 0.1 mm. We estimate an accuracy of our frequency values of about ± 2 cm^{-1}.

The A values reported are integrated absorption intensities, obtained by the Wilson-Wells method as extended by RAMSAY (see Ramsay's II method [4]); every A figure was determined by 5 to 6 measurements at different concentrations (in the range 0.1 to 0.3 moles/l), and extrapolating to zero concentration; the wing correction was always performed, its amount being of the order of 5 to 10% of the total value; the bands were integrated over a range of 50 cm^{-1} on both sides; in the case of acetonitrile a graphic correction was performed before integration, to eliminate a partial overlapping on its short wavelength wing; the A unit is moles^{-1} liter cm^{-2}. In all other cases the C≡N bands examined appeared well developed and free from partial overlappings or deformations depending from solvent. The intensity values for benzonitrile from [5] and [6] reported in Table I were not corrected for the wings; those by THOMPSON appeared systematically lower than those by BROWN, and for the purpose of comparison they were raised by about 15%. Our figures for the cyanpyridines in chloroform are in good agreement with the corresponding values by SENSI and GALLO [7].

The frequency values for C=O and C=C bands of acrylonitrile and ketonitriles were obtained on a Perkin-Elmer mod. 21 instrument with NaCl optics.

The solvents used were purity grade further treated by standard methods; aceto- and acrylo-nitriles and the cyanpyridines were pure commercial products purified before use; benzoyl- and acetylcyanides were prepared from the corresponding halogenides with cuprous cyanide [9].

---

(3) L. J. BELLAMY, R. L. WILLIAMS and H. E. HALLAM: *Trans. Far. Soc.*, **54**, 1120 (1958); **55**, 14 (1959); L. B. ARCHIBALD and A. D. E. PULLIN: *Spectrochim. Acta*, **12**, 34 (1958).

(4) D. A. RAMSAY: *Journ. Am. Chem. Soc.*, **74**, 72 (1952).

(5) T. L. BROWN: *Journ. Am. Chem. Soc.*, **80**, 794 (1958).

(6) H. W. THOMPSON, G. STEEL and M. R. MANDER: *Trans. Far. Soc.*, **52**, 1451 (1956); **53**, 1402 (1957).

(7) P. SENSI and G. GALLO: *Gazz. Chim. Ital.*, **85**, 235 (1955).

(8) H. W. THOMPSON and A. V. GOLTON, in R. W. HENDRICKS: *Thesis* (Brown University, 1956).

(9) W. TSCHELINZEFF and W. SCHMIDT: *Ber.*, **62**, 2211 (1929); *Organic Syntheses*, coll. vol. **3**, 112.

2. – Results and discussion.

Table I reports the frequency (cm^{-1} units) and intensity values and the half intensity band widths so far obtained for the C≡N bands.

The present solvent order, which in a good approximation (see Fig. 1 and Table I) is the same for all the six compounds examined, is very similar to the one found for C=O bonds (see [3]), and differs markedly from the situation observed for X-H bonds; this is particularly

TABLE I.

	CH_3CN			$CH_2{=}CHCN$			CH_3COCN			C_6H_5COCN		
Solvent	$\nu(CN)$	$A\cdot10^{-3}$	$\Delta\nu_{\frac{1}{2}}$	$\nu(CN)$	$A\cdot10^{-3}$	$\Delta\nu_{\frac{1}{2}}$	$\nu(CN)$	$A\cdot10^{-3}$	$\Delta\nu_{\frac{1}{2}}$	$\nu(CN)$	$A\cdot10^{-3}$	$\Delta\nu_{\frac{1}{2}}$
vapour	2267	0.18 [c]		2241	0.06 [c]			—			—	
n-hexane		—			—			—		2223	3.70	16
CCl_4	2257	0.61	11	2232	0.65	10	2221	2.85	10	2221	3.40	16
C_6H_6	2255	0.96	11	2229	0.94	9	2221	2.70	10	2222	3.30	15
C_2Cl_4	2257	0.54	11	2232	0.55	9	2221	2.72	10	2221	3.70	16
$CHCl_3$	2258	1.02	10	2232	1.40	11	2223	2.50	11	2224	3.00	16
CH_2Cl_2		—			—		2223	2.45	10	2224	2.80	15
CH_3NO_2	2254	1.20	11	2230	1.55	11	2225	1.90	11	2225	2.70	16

	C_6H_5CN			3-Cyanpyridine			4-Cyanpyridine		
n-hexane	2234	1.50 [a]							
CCl_4	2232	2.15	10	2235	1.50	12	2240	0.48	10
C_6H_6		—		2235	2.20	12	2239	0.90	10
C_2Cl_4	2231 [b]	1.90 [a]		2236	1.55	13	2240	0.47	10
$CHCl_3$	2230 [b]	3.50 [a]		2237	2.75	13	2241	1.05	11
CH_2Cl_2		—		2235	3.70	14		—	
CH_3NO_2	2230 [b]	2.50 [b]		2236	3.05	12	2241	1.20	10

([a]) values from [5], not corrected for the band wings; ([b]) values from [6]; ([c]) values from [8].

If one looks at the intensity values, it is apparent that, for all the compounds studied, the dielectric Polo-Wilson relation (2) is not followed, as in the cases examined in [3]; in fact, also in the present case the order of increasing solvent effect (starting from the clearly non-polar solvents) is quite different from that predicted by the above mentioned relation; this is again pointing out to the small contribution of dielectric factors to the medium effects on bond vibrations involving polar bonds.

evident if one compares the position of chloroform in the two cases studied by BELLAMY. The limited number of solvents for which we have presently intensity values does not permit of extending too much the parallelism between C=O and C≡N bonds as to the type of solute-solvent interaction which is effective in each case. We think however that, if one limits the study (as in the present case) to solvents for which the general form of the band, as mainly reflected in its $\Delta\nu_{\frac{1}{2}}$ value, does not change drastically,

the situation should not essentially change.

The singular behaviour of ketonitriles, as emphasized by the corresponding plot of Fig. 1, seems to us of particular interest, in that the direction of the solvent effect is inverted, *i.e.* in polar solvents the intensity is lower than in non-polar ones; the relative solvent order is however maintained, and the plot of *A* values for

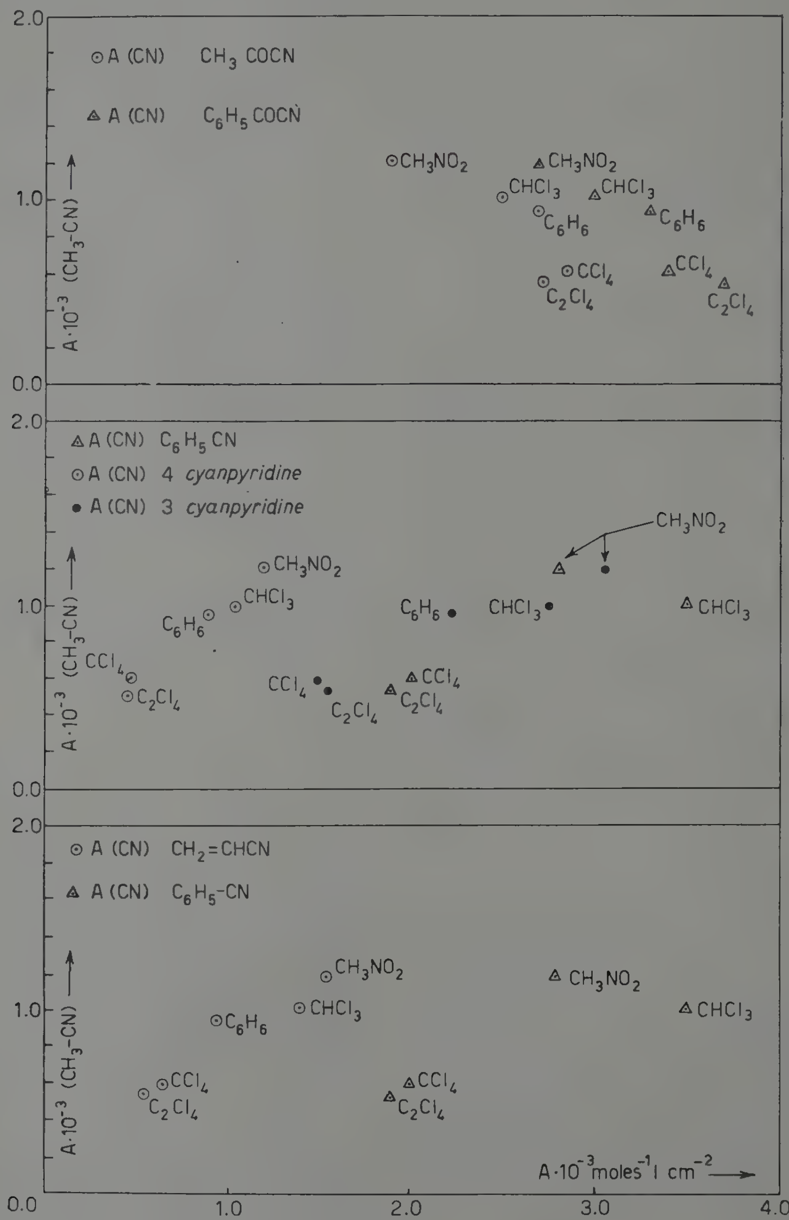

Fig. 1.

1788

acetylcyanide against those for benzoylcyanide shows a regular trend. Such a behaviour is presumably connected with the presence in these two molecules of molecules of the form R—CO—CH_2—CN, with separated dipoles, in the hope to get a better knowledge on these very interesting competitive solvent effects.

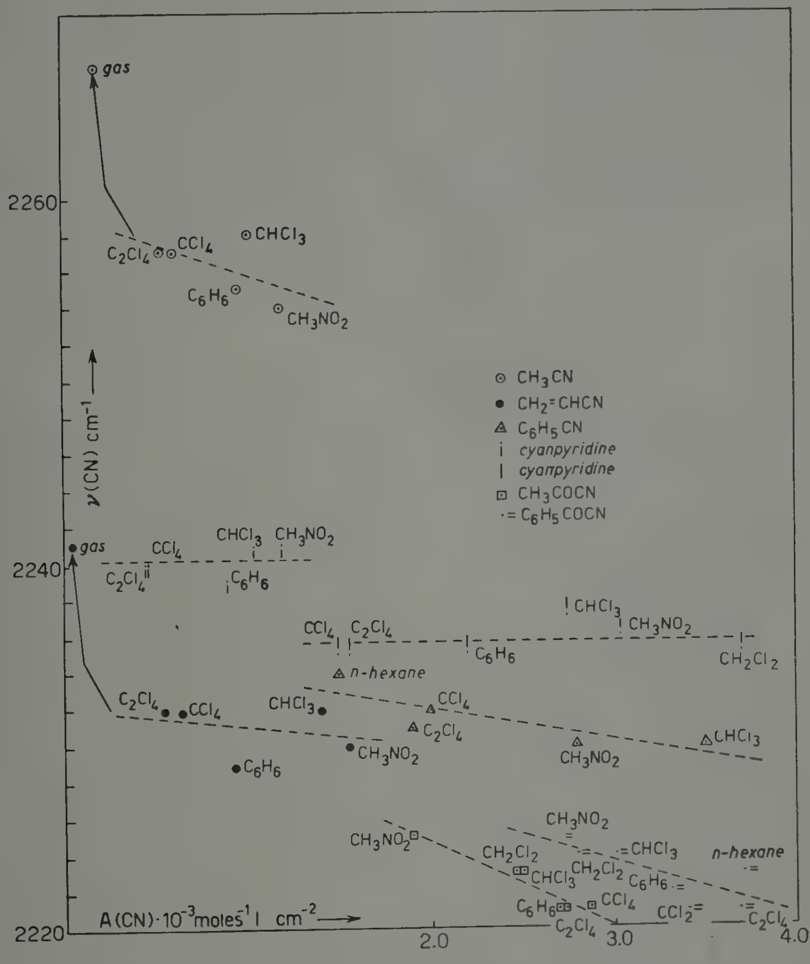

Fig. 1.

two competing free dipoles, whose interaction with the solvent is eventually of similar nature, possibly through dipole-dipole association effects. We are planning to go further into the study of molecules of this kind, extending it to

It is to be noted that the figures of Table I for benzene and n-hexane were obtained on 0.1 mm cell, so as to reduce, in the single-beam operation, the influence of solvent absorption. The higher concentration (of about (1÷2) moles/l) so

1789

necessary might cause some influence on the values due to concentration effects (see also [10]).

The discussion has hitherto focused on the intensities of the bands, because the corresponding frequency values, being very little influenced by the solvent and having being recorded with CaF_2 optics are not sufficiently accurate to permit of an equally good comparison; in defect of LiF values we have limited ourselves to a rough comparison of the general trend of frequency-intensity dependence, as from Fig. 2. In this figure the ordinate scale has been markedly enlarged in order to show the trend of the diagrams, which is similar to that observed [3] for carbonyl compounds, again with the exception of the two ketonitriles.

Introductory measurements on C=O and C=C bands of the ketonitriles and of acrylonitrile, showed some difficulty in the evaluation of the intensities, owing to partial overlapping from neighbouring bands. As to the frequencies, the C=O band appears to be much less solvent dependent than in the cases referred to in [3]; the same is valid for the two C=C bands of acrylonitrile at 6.1μ. We reserve to a later study under higher resolution a re-examination of the question.

[10] E. L. Zhukova: *Optika i Spek.*, **4**, 750 (1958).

IL NUOVO CIMENTO VOL. XIII, N. 1 1° Luglio 1959

Possible Example of an Interaction in Emulsion Produced by a Deuteron of $\sim 10^{13}$ eV.

P. K. ADITYA (*) (**)

Physics Honours School, Panjab University - Chandigarh

(ricevuto il 4 Aprile 1959)

In high energy disintegrations initiated by singly charged particles of the cosmic radiation secondary interactions produced by neutral particles have been usually observed (1-8). It is conventional to assume the neutral particles to be neutral mesons of long lifetime or neutral baryons created as nucleon-antinucleon or hyperon-antihyperon pairs. This is possible as long as the energy of the secondary interaction is reasonably well of the same order as that expected for the secondary particles created in the disintegration.

In a recent communication (9), we considered the possibility that some of the neutral interactions (events produced by neutral particles) observed as secondary events in high energy showers could be initiated also by the neutrons of the original projectile. It was pointed out that, apart from a neutron being produced by charge exchange of the primary proton, in case the singly charged particle be the nucleus of a heavy isotope of hydrogen, those neutrons of the projectile which get stripped off in the first interaction might contribute to secondary neutral interactions. As an example of the process we shall first describe the characteristics of two interactions (5) which we have interpreted as being due to the proton and neutron of a deuteron of $\sim 10^{13}$ eV. This is followed be an approximate estimate of the proportion of deuteron interactions at very high altitudes in the atmosphere.

(*) Formerly known as Prem Kumar.

(**) At present at the Institute for Theoretical Physics, University of Copenhagen.

(1) J. H. MULVEY: *Proc. Roy. Soc.*, A **221**, 367 (1954).

(2) E. LOHRMANN: *Zeits. f. Naturfor.*, **2** a, 561 (1956).

(3) F. D. HÄNNI, C. LANG, M. TEUCHER, H. WINZELER and E. LOHRMANN: *Nuovo Cimento*, **6**, 1473 (1956).

(4) F. A. BRISBOUT, C. DAHANAYAKE, A. ENGLER, Y. FUJIMOTO and D. H. PERKINS: *Phil. Mag.*, **1**, 605 (1956).

(5) P. KUMAR: *Proc. 45th. Ind. Sci. Cong.*, III-3, Abs. n. 9 (Jan, 1958).

(6) B. EDWARDS, J. LOSTY, D. H. PERKINS, K. PINKAU and J. REYNOLDS: *Phil. Mag.*, **3**, 237 (1958).

(7) E. LOHRMANN and M. W. TEUCHER: *Phys. Rev.*, **112**, 587 (1958).

(8) M. SCHEIN and D. M. HASKIN: *Suppl. Nuovo Cimento*, **8**, 710 (1958).

(9) P. K. ADITYA: *Nuovo Cimento*, **11**, 872 (1959).

The primary interaction of the type $(30+26)_s$ was produced by a singly charged particles of the cosmic radiation, observed in a stack of stripped emulsions exposed in the stratosphere above India, at 19° geomagnetic latitude [10]. The event was detected while following back the ensuing cascades of high energy, needed for another investigation [11]. The primary particle made an angle of 11° to the zenith, the core traversing 2.5 cm per emulsion and left the stack after 10 cm axial length. The collimation of ten tracks within a cone of $1.5\cdot10^{-2}$ rad, indicated the primary energy to be very high. At 1420 μm from the primary event (called hereafter as A) another interaction (called as B) of the type $(5+14)_n$ took place near the air surface of the emulsion, so that the angular distribution of its shower particles could be obtained only in the next emulsion. From target diagrams of the core made at 3600 μm, 4600 μm, and 8400 μm from the origin of A and the angular distribution of the tracks from A, it was possible to find the integral angular distribution of the particles emitted from B. Proper account was taken of the electron pairs materializing in the core since these tracks could be identified by their characteristic closeness in the begining and subsequent development of electron pairs on or around them. Unfortunately none of the two interactions could be safely considered as a nucleon-nucleon collision, especially A, because the collision occured with a heavy nucleus of the emulsion. Assuming the interactions to be elementary nucleon-nucleon collisions, the velocity β_c of the c.m. system was deduced from the angular distributions, giving $\gamma_c(A)=31\pm6$ and $\gamma_c(B)=56\pm15$, where $\gamma_c=[1-\beta_c^2]^{-\frac{1}{2}}$. As may be seen, the estimated energy difference is appreciable especially since it is in contradiction to the expectations, event B having apparently an energy greater than that of A. This pointed out the fallaciousness of the assumption about the collisions being elementary. For event A all the usual checks of symmetrical distribution of tracks in the c.m. system were made by using the conventional trasformation relations. The angular distribution in the c.m. system was in accordance with a $\cos^2\theta$ type distribution and the symmetry allowed the removal of about six mesons on the basis of having been created by secondary processes occurring during the collision. The energy of high energy electron-positron pairs from A was obtained from shower development and other means [11]. This evidence was also against the energy being $\sim$2000 GeV as obtained from the angular distribution of the shower tracks. The removal of 6 mesons as mentioned before, allowed the energy of A to be raised to about $(4\pm1)\cdot10^{12}$ eV, and we consider this to be a reliable estimate. The proximity of event B did not allow many measurements to be made on it. Apart from the angular distribution of its narrowly collimated shower tracks, two high energy pairs clearly pointing to B confirmed the very high energy involved in the event. It was not possible from the experimental data, to increase the energy of A beyond that of B, or to decrease the energy of B below that of A, the two being at most and probably of the same order. This excluded the possibility of the event B being due to a particle emitted from A and made it difficult to assume the neutral particle to be even a neutron created by the charge exchange process. It appeared that if the singly charged primary particle were a deuteron or a triton instead of the normally assumed proton, there would be no difficulty in interpreting the event. To support this idea, we consi-

(10) R. R. DANIEL, G. FRIEDMANN, D. LAL, YASH PAL and B. PETERS: *Proc. Ind. Acad. Sci.*, **40** A, 151 (1954).

(11) P. K. ADITYA: *Nuovo Cimento*, **11**, 546 (1959).

dered it desiderable to obtain an approximate estimate of the ratio of deuteron to proton interactions expected in a stack exposed in the stratosphere.

It is not possible to distinguish by direct means between deuterons or protons and neither between the interactions produced by them. The enormous flux of protons coming in the primary cosmic ray beam, obscures the presence of heavy singly charged particles. In stacks exposed at a particular altitude in the stratosphere, there is however one observable quantity that may be used to estimate the magnitude of secondary processes. This is the ratio of interactions produced by neutrons and singly charged particles, all within same energy limits and preferably at such high energies that any possible contribution of those disintegrations that may be produced by neutrons and deuterons ejected from the target nuclei may be safely neglected. For $n_s \geqslant 5$ *i.e.*, energy $\geqslant 15$ GeV, it is possible to identify unambigously the neutral stars. Since both neutrons and deuterons are assumed to arise almost entirely from identical secondary processes, *i.e.* fragmentations occuring near the top of the atmosphere, it is logical to employ the observations on neutral stars to predict the proportion of deuteron interactions. The assumptions and results of such an approximate estimate are the following:

a) For all primary particles of $Z \geqslant 1$ having the same energy per nucleon, the relative numbers of protons (P), α-particles (α), medium nuclei (M, $6 \leqslant Z \leqslant 9$) and heavy nuclei ($H$, $Z \geqslant 10$) are 6000, 400, 30 and 6 respectively. The flux of light nuclei ($3 \leqslant Z \leqslant 5$) is assumed small and has been neglected.

b) There are no neutrons, deuterons or tritons incident with the primary cosmic ray beam [12].

c) The interaction mean free path values for P, α, M and H in g cm^{-2} of atmosphere are 60, 35, 25 and 18 respectively.

d) The proportion of secondary particles is negligible as compared to the primary flux i.e., no account is taken of the particles $Z \geqslant 2$ arising from fragmentation of heavy primary nuclei.

e) Among those protons which produce inelastic collisions in the atmosphere, the inelasticity is small and half the number maintain identity after emerging out while the other half undergo charge exchange.

f) Denoting by $F_{i \to s}$, the fragmentation probability for the production of singly charged particles s, from a heavy primary nucleus i, and assuming that protons and deuterons are equally abundant among the fragmentation products [13], we adopt for the atmosphere the following values for the fragmentation probability:

$$F_{\alpha \to s} = 0.77\ (^{14}) \quad \text{or} \quad F_{\alpha \to (P \text{ or } N \text{ or } D)} = 0.38\,,$$
$$F_{M \to s} = 1.7\ \ (^{16}) \quad \text{or} \quad F_{M \to (P \text{ or } N \text{ or } D)} = 0.85\,,$$
$$F_{H \to s} = 4.0\ \ (^{16}) \quad \text{or} \quad F_{H \to (P \text{ or } N \text{ or } D)} = 2.0\,.$$

---

(12) Neutrons and tritons because of being unstable cannot be expected in the high energy primary radiation. There might however be some deuterons, but their flux is unpredictable and might be very small as compared to the proton flux. Some calculations on this value have been made by SINGER [S. F. SINGER: *Suppl. Nuovo Cimento*, **8**, 549 (1958)].

(13) To be published separately.

(14) This value is based upon 136 singly charged particles that emerged without participation from 176 collisions produced by α-particles in emulsion (15). The fragmentation probability in air might be a little less than this value, but it has not been possible for us to take any account of this.

(15) M. V. K. APPA RAO, R. R. DANIEL and K. A. NEELAKANTAN: *Proc. Ind. Acad. Sci.*, **43**, 181 (1956).

(16) These values are based upon the fragmentation probabilities observed for collision of heavy primary nuclei with light nuclei of the emulsion and those derived for air (17).

(17) J. H. NOON and M. F. KAPLON: *Phys. Rev.*, **97**, 769 (1955).

g) In emulsion the interaction mean free path of neutrons and protons is 35 cm ([15]) and that of deuterons is 15 cm ([13]).

The calculated percentage of interactions that would be produced by neutrons and deuterons in ratio to those by protons, (all observed in a stack exposed at a particular altitude), has been plotted in Fig. 1. For comparison some of the experimental points ([18]) have also been included. (see Table I). These are based upon interactions of $n_s \geqslant 5$ (energy $\geqslant$ 15 GeV) produced by singly charged and neutral particles. One might expect that some of the singly charged particle interactions are due to mesons created in high energy disintegrations, so that the N/P ratio is essentially $N/(P+M)$, M for mesons. This effect will however gain importance at depths $\geqslant$ interaction mean free path, *i.e.* 60 g cm^{-2}. It may be mentioned that on account of the simplified assumptions, the absolute values of N/P or D/P might not be correct, but the ratio N/D would not be very sensitive to the approximations, because both N and D

TABLE I. – *Experimentally observed ratios of the interactions produced by neutral particles to those produced by singly charged particles, observed at various depths in the atmosphere.* The number of interactions marked with (*) are derived from the results, assuming the quoted errors to be statistical. A combation of (*b*), (*c*) and (*d*) yields a value of 14.6 ± 3.1 at 15 g cm^{-2}, while (*f*) and (*g*) give a value of 26 ± 5 at 40 g cm^{-2}.

Sub-reference in ([18])	Selection criteria	Depth in the atmosphere (**) (g cm^{-2})	Secondary interactions		Ratio neutral to charged
			neutral	charged	
(*a*)	$E > 10^{12}$ eV	$8 \div 10$	2	27	7.4 ± 5.3
(*b*)	$E \geqslant 10^{11}$ eV	14	12	79	15 ± 4.3
(*c*)	$n_s \geqslant 5$	16	6 (*)	60 (*)	10 ± 4
(*d*)	$n_s \geqslant 5$	16	4 (*)	12 (*)	32 ± 15
(*e*)	E, $(10^{10} \div 10^{13})$ eV	20	9	31	29 ± 9
(*f*)	$n_s \geqslant 5$	40	23	96	24 ± 5
(*g*)	$n_s \geqslant 5$	40	7	20	35 ± 13
(*h*)	$n_s \geqslant 5$	50	89	294	30 ± 3
(*i*)	$n_h < 5$, $n_s \geqslant 6$	8	8	52	15 ± 5.5

(**) In these values, no account has been taken of the amount of packing material of the stack.

([18]) (*a*) E. LOHRMANN: private communication (Feb. 1959).
(*b*) H. WINZELER: private communication (March 1959). The data were collected by E. LOHRMANN, M. TEUCHER and H. WINZELER.
(*c*) A. ENGLER, U. HABER-SCHAIM and W. WINKLER: *Nuovo Cimento*, **12**, 930 (1954).
(*d*) H. YAGODA: *Canad. Journ. Phys.*, **34**, 122 (1956).
(*e*) I. GUREVIĆ, A. P. MIŠAKOVA, B. A. NIKOLSKIJ and L. V. SURKOVA: *Suppl. Nuovo Cimento*, **8**, 786 (1958).
(*f*) M. W. TEUCHER: *Zeits. f. Naturfor.*, **8 a**, 127 (1953).
(*g*) G. BERTOLINO and D. PESCETTI: *Nuovo Cimento*, **12**, 630 (1954).
(*h*) U. CAMERINI, J. H. DAVIES, P. H. FOWLER, C. FRANZINETTI, H. MUIRHEAD, W. O. LOCK, D. H. PERKINS and G. YEKUTELI: *Phil. Mag.*, **42**, 1241 (1951).
(*i*) J. GIERULA and M. MIĘSOWICZ: private communication (March 1959). Data collected in a collaboration experiment at Krakow, Praha and Warsaw, and published by CIOK *et al.*: *Nuovo Cimento*, **10**, 741 (1958).

are secondary particles. We find that for a stack exposed under about 15 g cm^{-2} out of 100 interactions of the same energy those produced by protons, neutrons and deuterons would be 84, 12 and 4 respectively.

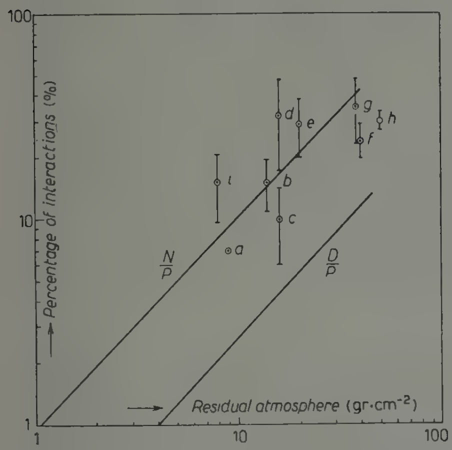

Fig. 1. – Variation of the percentage of interactions produced in an emulsion stack by neutrons and deuterons as compared to those produced by protons, plotted against the amount of residual atmosphere in g cm^{-2}. The line shows the result of an approximate calculation (see text). The experimental points are those mentioned in Table I and reference (18).

The percentage of deuteron interactions being so small, their presence is not directely detectable. There would be no appreciable influence of their presence on the composition of shower particles, as thought earlier (9). Their presence may however be felt through other characteristics of deuteron interactions. For instance, in a case an example of which has been described above, one might observe two interactions one being apparently a secondary from the other and the characteristics of the two events being similar within experimental errors. The latter event can be neutral or charged depending upon whether the first interaction is produced by the proton or neutron of the deuterons, respectively. SCHEIN and HASKIN (8) have observed a neutral interaction of $2\cdot10^{12}$ eV in the core of an interaction produced by a singly charged particle of $5\cdot10^{12}$ eV. Though in this case the measured energies allow the possibility of the neutral particle being a neutron produced by charge exchange of the proton, if one expects some energy uncertainity, two collisions might have had similar characteristics.

While in those cases in which both the nucleons of the deuteron (or three in the case of a triton) participate in the collision, the meson multiplicity would be much different from that expected for the collision of a single nucleon of energy equal to that obtained from the angular distribution of the shower. Such an interaction is expected to look much different from another in which the increased meson multiplicity results from multiple collisions within the target nucleus (*).

* * *

This investigation is part of a programme of work on high energy phenomena, started earlier. Thanks are due Professor B. M. ANAND for encouragement. I am thankful to Professor B. PETERS for laboratory facilities at the Tata Institute of Fundamental Research, Bombay and for the loan of the plates. I thank Drs. LOHRMANN, MIĘSOWICZ and WINZELER for private communications.

(*) *Note added in proofs.* - Since the communication of this paper, there has appeared an article by BRISBOUT *et al.* (*Nuovo Cimento*, **11**, 484 (1959)) in which a large cosmic ray jet (shower P.8 of BRISBOUT *et al.*: *Phil. Mag.*, **4**, 605 (1956)) has been described. They have found that for a straightforward explanation, the characteristics of the event require the primary to be a deuteron. This is in accordance with our suggestion.

Further, while giving arguments as explanation of the observation of two « groups » of jets involving about the same energy but different multiplicity, DILWORTH *et al.* (*Nuovo Cimento*, **10**, 1261 (1953)) did not consider the probability of some of their interactions having been produced by deuterons, which possibility can explain the phenomena observed by them. It would be useful to confirm this with increased statistics and at higher energies.

1795

IL NUOVO CIMENTO Vol. XIII, N. 1 1° Luglio 1959

The Parity of K-Mesons and Dispersion Relations.

M. M. Islam

Department of Mathematics, Imperial College of Science and Technology - London

(ricevuto il 15 Aprile 1959)

The dispersion relations for K-nucleon scattering offer a powerful means for determining the parities and strengths of K-meson interactions and a number of authors have considered this problem ([1-3]). Since experimental data both in the low energy region ([4 5]) and in the high energy region ([6]) have now greatly increased, it is of interest to see the present situation by using these data.

The dispersion relation of Matthews and Salam (eq. 10 of ref. ([1])) and of Igi (eq. (2.5) of ref. ([2])) have been considered on the assumption that Λ and Σ have the same parities. Since the dispersion relation of Matthews and Salam is not very sensitive to low energy data but is slowly convergent in the high energy region, while that of Igi, though sensitive to low energy K^+-p data, is yet much more convergent in the high energy region, so it is to be seen whether essentially the same conclusions could be reached using these two relations.

In evaluating the integrals in Matthews and Salam's dispersion relation, σ_{sc}^+ has been taken to be constant throughout at a value 15 mb $\sigma^-(=\sigma_{sc}^- + \sigma_{ab}^-)$ has also been taken to be constant at a value 40 mb from 120 K-meson K.E. to 2 GeV K-meson K.E. ([6]). In the region $(0 \div 120)$ K.E. the elastic scattering contribution has been evaluated graphically using the combined emulsion and bubble chamber data. The charge exchange scattering has been taken to one fifth of the elastic scattering. The contribution due to absorption in the $(0 \div 120)$ K.E. energy region as well as in the unphysical region $(\omega_{\Lambda\pi} - m_K)$ has been evaluated assuming a constant value 7 of $|k|\sigma_{ab}^-$.

([1]) P. T. Matthews and A. Salam: *Phys. Rev.*, **110**, 569 (1958). See also C. Goebel: *Phys. Rev.*, **110**, 572 (1958).

([2]) K. Igi: *Progr. Theor. Phys.*, **20**, 403 (1958).

([3]) D. Amati and B. Vitale: *Nuovo Cimento*, **7**, 190 (1958); D. Amati: *Phys. Rev.* (to be published); E. Galzenati and B. Vitale: *Phys. Rev.* (to be published).

([4]) M. F. Kaplon: *Ann. Int. Conf. on High Energy Phys. CERN* (1958), p. 171.

([5]) J. E. Lannutti S. Goldhaber, G. Goldhaber, W. W. Chupp, S. Giambuzzi, C. Marchi, G. Quareni and A. Wataghin: *Phys. Rev.*, **109**, 2121 (1958).

([6]) H. C. Burrowes, D. O. Caldwell, D. H. Frisch, D. A. Hill, D. M. Ritson and R. A. Schulter: *Phys. Rev. Lett.*, **2**, 117 (1959).

The dispersion relation of Matthews-Salam is now written in the following form [7]:

$$(1)\quad (\pm b) + a = \frac{1}{6\pi^2}\left[\int_1^{1+t} k'\sigma_{sc}^-(\omega')\left(\frac{1}{\omega'-1}-\frac{1}{\omega'+1}\right)d\omega' + \int_{\omega_{\Lambda\pi}}^{1+t} |k'|\,\sigma_{ab}^-\left(\frac{1}{\omega'-1}-\frac{1}{\omega'+1}\right)d\omega' + \right.$$

$$\left. + \sigma^-\int_{1+t}^{5} k'\left(\frac{1}{\omega'-1}-\frac{1}{\omega'+1}\right)d\omega' - \sigma^+\int_1^5 k'\left(\frac{1}{\omega'-1}-\frac{1}{\omega'+1}\right)d\omega'\right] + [\text{B.S.}]\,,$$

where $t = 120/M_K$. We take $\sigma_{el}^c(\theta=0) = 4.5$ mb.

Inserting the calculated values term by term, we get

$$(\pm 1.68) + 0.86 = 0.72 - 0.14 + 1.37 - 0.73 + [\text{B.S.}]\,.$$

If we now take the positive sign corresponding to K^--p potential attractive, we get

$$(2a)\qquad [\text{B.S.}] = 1.32\,, \qquad \text{(K-meson pseudoscalar)},$$

and taking the negative sign, corresponding to K-p repulsive potential,

$$(2b)\qquad [\text{B.S.}] = -2.04\,. \qquad \text{(K-meson scalar)}.$$

Igi's dispersion relation (eq. (2.5) of ref. [2]) has been used at threshold and for this purpose ω is put egual to $1+h$ and then the limit when h is negligible compared to 1 is taken. The first term in Igi's formula becomes

$$\frac{1}{4}[D_-(1) - D_+(1)] + \frac{1}{2}\left(\frac{\partial D_+}{\partial W_l}\right)_{W_l=0},$$

where W_l = K-meson K.E. in lab.

If we write $\sigma_{sc}^+(1) = 4\pi a^2$ and $\sigma_{sc}^-(1) = 4\pi b^2$ we get

$$D_+(1) = -\frac{M_p+1}{M_p}\,a\,, \qquad D_-(1) = \frac{M_p+1}{M_p}\,(\pm b)\,,$$

and

$$\left(\frac{\partial D^+}{\partial W_l}\right)_{W_l=0} = \frac{M_p}{M_p+1}\,a^3 - \frac{a}{M_p+1}\,.$$

Assuming that σ_{sc}^+ is a constant. We now write Igi's dispersion relation at threshold in the following form:

$$(3)\quad (\pm b) + a + \left(\frac{\partial D_+}{\partial W_l}\right)_{W_l=0}\cdot\frac{2M_p}{M_p+1} = \frac{M_p}{M_p+1}\cdot\frac{1}{\pi^2}\left[\int_{1+t}^{\infty}\frac{d\omega'\sigma^+}{k'(\omega'-\omega)} + \int_1^{1+t}\frac{\sigma_{sc}^-(\omega')\,d\omega'}{k'(\omega'+\omega)} + \right.$$

$$\left. + \int_{\omega_{\Lambda\pi}}^{1+t}\frac{|k'|\,\sigma_{ab}^-\,d\omega'}{k'^2(\omega'+\omega)} + \int_{1+t}^{\infty}\frac{\sigma^-\,d\omega'}{k'(\omega'+\omega)}\right] + \frac{4M_p}{M_p+1}\cdot 2F\,.$$

---

(7) The unit used is $c = \hbar = m_K = 1$, the unit of length being $1/K = (c\hbar/m_K) = 0.4\cdot 10^{-13}$ cm.

Inserting values term by term, we have

$$(4)\qquad (\pm 1.68) + 0.86 + 0.16 = \frac{0.66}{\pi^2}\,[-9.38 + 10.27 - 2.10 + 16.77] + \frac{4M_p}{M+1}\cdot 2F\,.$$

If we take the positive sign we get,

$$(5a)\qquad 4\,\frac{M_p}{M_p+1}\cdot 2F = 1.67\,,$$

which corresponds to pseudoscalar K-meson.

On the other hand, if we take the negative sign we get

$$(5b)\qquad 4\,\frac{M_p}{M_p+1}\cdot 2F = -1.68\,,$$

which corresponds to scalar K-meson.

If now, instead of taking σ^+ constant, a linear variation of it with energy of the form $\sigma^+(\omega') = m(\omega' - \omega) + \sigma(\omega)$ is considered in the energy range 1 to $1+t$ and then a constant value $\sigma^+(\omega') = \sigma^+(1+t)$ up to infinity, we shall have

$$\left(\frac{\partial D_+}{\partial W_l}\right)_{W_l=0} = \frac{M_p}{M_p+1}\,a^3 - \frac{a}{M_p+1} - \frac{1+M_p}{M_p}\cdot\frac{m}{8\pi a}\,,$$

and

$$\int_1^\infty \frac{\sigma^+(\omega')\,d\omega'}{k'(\omega'-\omega)} = m\log\frac{1+(t/(2+t))^{\frac12}}{1-(t/(2+t))^{\frac12}} + mt^{\frac12}(2+t)^{\frac12} - \sigma_+(1+t)\,.$$

Kaplon has reported a K^+-p cross-section equal to (13.5 ± 2.8) mb in the energy range $(20 \div 100)$ MeV. The maximum value of m permitted within this experimental error is obtained by taking $\sigma^+ = 13.5 - 2.8$ at 20 MeV K.E. and $\sigma^+ = 13.5 + 2.8$ at 100 MeV K.E. This value of m comes out to be 21.61. Using this value, we shall now get, instead of eq. (4), the following equation, term by term:

$$(\pm 1.68) + 0.68 - 2.57 = \frac{0.66}{\pi^2}\,[19.66 + 10.27 - 2.10 + 16.77] + 4\,\frac{M_p}{M_p+1}\cdot 2F\,.$$

If we take the positive sign, corresponding to K^--p potential attractive, then

$$4\,\frac{M_p}{M_p+1}\cdot 2F = -3.17\,.$$

If the negative sign is taken, corresponding to K^--p potential repulsive, then

$$4\,\frac{M_p}{M_p+1}\cdot 2F = -6.52\,.$$

1798

Therefore, we find that the K-meson comes out to be scalar irrespective of the sign of the K-p potential.

Summarizing, we can say that the Matthews-Salam dispersion relation gives a pseudoscalar or scalar K-meson according to K^--p potential attractive or repulsive, though the experimental data of BURROWES *et al.* (6) do not indicate that the contribution due to the energy region beyond $5m_K$ will be negligible. Igi's dispersion relation also gives a pseudoscalar or a scalar K-meson, if σ^+ is taken to be constant in the low energy region and the K^--p potential is considered attractive or repulsive respectively. However, within the limit of the present data on K^+-p scattering, we can have K-meson scalar, irrespective of the sign of the K^--p potential, if we take a linear variation of σ^+ with energy. The values of the coupling constants (8) are

$$\frac{g^2}{4\pi} = \left.\begin{matrix} 7.26 & \text{ps.} \\ 0.78 & \text{s.} \end{matrix}\right\} \text{Matthews-Salam}\,,$$

$$\frac{g^2}{4\pi} = \left.\begin{matrix} 4.60 & \text{ps.} \\ 0.32 & \text{s.} \end{matrix}\right\} \text{Igi (constant } \sigma^+)\,.$$

* * *

I wish to express my thanks to Dr. P. T. MATTHEWS and Prof. A. SALAM for their interest and encouragement. An overseas scholarship of the Royal Commission for the Exhibition of 1851 is gratefully acknowledged.

(8) The bound state term of Matthews-Salam is given by

$$[\text{B.S.}] = -2\,\frac{M_p}{M_p+1}\,p[X(\Lambda) + X(\Sigma)]\,.$$

While the constant $2F$ of Igi is given by

$$2F = -p[X(\Lambda) + X(\Sigma)]\,,$$

[see DALITZ: *Ann. Int. Conf. on High Energy Phys. CERN.* (1958), p. 187].

IL NUOVO CIMENTO Vol. XIII, N. 1 1° Luglio 1959

Determination of the Meson-Nucleon Coupling Constant from Nucleon-Nucleon Scattering.

H. McManus

Chalk River Laboratories - Chalk River, Ontario, Canada

(ricevuto il 5 Maggio 1959)

In the process of calculating the nuclear scattering of high energy nucleons (1), the various spin dependent components of the two nucleon scattering amplitude were tabulated as a function of energy and angle, using the phase shifts derived from the G-T potential (2). Now Chew (3,4) has pointed out that if these amplitudes have certain analytic properties, the π-meson nucleon coupling constant can be determined by extrapolating their real part into the unphysical region. The point of view taken here is that as the G-T potential gives a fair account of nucleon-nucleon scattering in the region $(0 \div 300)$ MeV, it serves as a convenient summary of the experimental data, and the extrapolation can be carried out from the already tabulated quantities.

The two nucleon amplitude may be written

$$M = A + C(\sigma_{1n} + \sigma_{2n}) + B\sigma_{1n}\,\sigma_{2n} + \\ + E\sigma_{1q}\,\sigma_{2q} + F\sigma_{1p}\sigma_{2p}\,,$$

the notation being that of Bethe (5), where the coefficients A, B etc. are angle and isotopic spin dependent. Each of these coefficients, except C, has, according to Chew (3), a simple pole in the unphysical region at $t = \pm t_0$, where t is the cosine of the scattering angle in the CM system, and

$$t_0 = 1 + m^2/2k^2\,.$$

Here m is the π-meson Compton wave number and k the nucleon CM wave number. The residue at these poles is proportional to the meson-nucleon coupling constant, which can be determined (3,6) from the relation

$$K_j(-t_0) = \underset{t\to -t_0}{L}(t+t_0)\,\mathrm{Re}\,M_j(t) = \\ = \varepsilon\delta_T\,\frac{f^2M^2}{k^2\sqrt{M^2+k^2}}\,,$$

where $M_j(t)$ stands for any of the scattering coefficients A, B, etc., M is the nucleon Compton wave number, and

$$\begin{aligned}\varepsilon &= +1\,, \quad M_j = A, F\,,\\ &\, -1\,, \quad M_j = B, E\,,\end{aligned}$$

(1) A. Kerman, H. McManus and R. Thaler: *Phys. Rev. Lett.*, **2**, 172 (1959).

(2) J. Gammel and R. Thaler: *Phys. Rev.*, **107**, 291, 1337 (1957).

(3) G. F. Chew: *Phys. Rev.*, **112**, 1380 (1958)

(4) G. F. Chew: *Proc. CERN High Energy Conference* (1958), p. 93.

(5) H. Bethe: *Ann. Phys.*, **3**, 190 (1958).

(6) M. L. Goldberger, Y. Nambu and R. Oehme: *Ann. Phys.*, **2**, 226 (1957).

$$\delta_T = \tfrac{1}{2} \qquad \text{for p-p scattering,}$$

$$= 1 \qquad \text{for n-p scattering:}$$

The parameter f^2 is the square of the dimensionless meson-nucleon coupling constant as defined, for example, in BETHE (7).

The tabulated coefficients were used to determine the $K_j(-t_0)$ by straight line extrapolation from the values at 140° and 160°. The results are listed in Table I.

Energy (MeV)	f^2
310	0.071 ± 0.029
156	0.072 ± 0.016
90	0.050 ± 0.018

where the error quoted is that due to the scatter in the estimates from individual amplitudes. These values are compatible with those deduced (4) from meson nucleon scattering and photopion production, which lead to $f^2 \sim 0.085 \pm .01$, and with the result obtained by CZIFFRA (8,4), by extrapolation of the 90 MeV n-p scattering cross-section.

TABLE I. – *Table of f^2 corresponding to individual scattering amplitudes.*

	Scattering amplitudes			
Energy	A	B	E	F
p-p 310	0.042	0.099	0.057	−0.036
n-p 310	0.062	0.072	0.029	−0.006
p-p 156	0.056	0.088	0.070	−0.007
n-p 156	0.059	0.054	0.053	0.020
p-p 90	0.032	0.068	0.068	0.018
n-p 90	0.044	0.048	0.018	0.024
p-p 40	−0.025	0.054	0.051	0.005
n-p 40	0.013	0.054	0.016	0.017

The values obtained are reasonably consistent, except at 40 MeV, and for the coefficient F. The present two nucleon scattering and polarization data give more information on the coefficients A, B and C than on the other coefficients, which involve the components of spin in the scattering plane, and which enter only in the combination $|E|^2+|F|^2$. Taking the proton-proton results which should be more reliable, as there is more experimental information, and the amplitudes A and B only, we find

The results presented in this note show that the smoothed experimental data as represented by a phenomenological potential support Chew's conjecture. More complete scattering information would determine the coefficients A, B, etc. directly from experiment (5), and enable a direct check to be made. The poles in the scattering amplitude can be understood as arising from the one meson exchange term (6) and con-

(7) H. BETHE and F. DE HOFFMANN: *Mesons and Fields*, vol. **2** (1955).

(8) P. CZIFFRA and M. J. MORAVCSIK: *Bull. Am. Phys. Soc.*, **8**, E. 8 (1958).

stitute an invariant separation of the effect of the distant part of nuclear forces which determines the higher phase shifts. CZIFFRA *et al.* [9] have calculated the phase shifts for $L > 5$ from the pole contributions as a function of the coupling constant f^2 and have adjusted the phase shifts for $L < 5$ to fit the p-p scattering experiments at 310 MeV. In this way an improved fit was found to the 310 MeV data, the best results being obtained for $f^2 \sim 0.08$.

---

[9] P. CZIFFRA, M. MACGREGOR, M. MORAVCSIK and H. STAPP: UCRL-8510 (unpublished); *Bull. Am. Phys. Soc.*, **1**, T7 (1959).

IL NUOVO CIMENTO Vol. XIII, N. 1 1° Luglio 1959

Wave Operators in Multichannel Scattering (*).

M. N. Hack
Argonne National Laboratory - Lemont, Ill.

(ricevuto l'11 Maggio 1959)

1. – Introduction.

The convergence to the wave operators is one of the characteristic properties of scattering systems. In the multichannel case of scattering, it means the existence of the wave operators as the limits

$$\Omega_{\pm}^{(\alpha)}\varphi = \lim_{t\to\mp\infty} \exp[iHt]\exp[-iH_\alpha t]\varphi \qquad \text{for } \varphi\in D_\alpha\,, \tag{1}$$

in the sense of strong convergence, where D_α is the subspace spanned by the asymptotic states of the channel α (the subspace of Hilbert space on which the strong limits converge), H_α is the channel Hamiltonian (the sum of the kinetic energy operators plus the internal energies of the various free particles and fragments in the channel), H is the total Hamiltonian of the system, and we take $\hbar=1$. The operators $\Omega_{\pm}^{(\alpha)}$ are evidently isometric on D_α, since they are strong limits of unitary operators, and for convenience are set equal to zero on the orthogonal complement of D_α (1).

In single-channel scattering, where H_α is simply the kinetic energy operator and D_α is the entire space, the existence of the strong limits (1) has been proved for potentials which are locally square-integrable and which, roughly speaking, fall off faster than $1/r$ at large distances from the scatterer (2). In the multichannel case the convergence has been postulated as a basic requirement for scattering systems (1), although a verification for specific Hamiltonians has so far been available (3) only for the case in which H_α is the sum of the kinetic energies of all the particles and D_α is the entire Hilbert space, *i.e.*, for the particular channel where all particles are free.

(*) Work performed under the auspices of the U. S. Atomic Energy Commission.

(1) J. M. Jauch: *Helv. Phys. Acta*, **31**, 661 (1958).

(2) J. M. Cook: *Journ. Math. Phys.*, **36**, 82 (1957); M. N. Hack: *Nuovo Cimento*, **9**, 731 (1958); J. M. Jauch and I. I. Zinnes: *Nuovo Cimento*, **11**, 553 (1959); S. T. Kuroda: to be published.

(3) S. T. Kuroda: reference (2).

In this note we derive some important consequences of, and conditions for, the convergence to the wave operators in the case of multichannel scattering, and demonstrate the convergence for the typical multichannel systems with quadratically integrable interactions.

2. – Asymptotic vanishing of the interaction in scattering states.

An outgoing-wave scattering state originating in the channel α of a multichannel scattering system (or an ingoing-wave scattering state terminating in this channel) is defined as a state vector ψ in the range of the wave operator $\Omega_+^{(\alpha)}$ (or $\Omega_-^{(\alpha)}$). Such a state can be characterized as one for which the interaction in the channel α eventually becomes negligible (in the past or future respectively) and the further development of the state is governed by the channel Hamiltonian. In a precise form, this idea may be expressed as follows:

The state ψ is an ingoing-wave scattering state terminating in the channel α if and only if

$$\exp[-iHu]\exp[-iHt]\psi \simeq \exp[-iH_\alpha u]\exp[-iHt]\psi\,, \tag{2}$$

as $t\to\infty$, uniformly in $u\geqslant 0$. (A corresponding assertion holds in the outgoing case with $t\to-\infty$, and $u\leqslant 0$. The sign $\simeq$ denotes that the difference of the two terms tends strongly to zero.)

To show the sufficiency of the condition, suppose that condition (2) is satisfied, *i.e.*, given $\delta>0$ there is a T such that

$$\|\exp[-iHu]\exp[-iHt]\psi-\exp[-iH_\alpha u]\exp[-iHt]\psi\|<\delta\,,$$

for $t\geqslant T$ and all $u\geqslant 0$.

[The norm is defined as usual by $\|f\|=(f,f)^{\frac{1}{2}}$.] On setting $t'=t+u$ and making use of the invariance of the norm to transformation by the unitary operator $\exp[iH_\alpha t']$, we have

$$\|\exp[iH_\alpha t']\exp[-iHt']\psi-\exp[iH_\alpha t]\exp[-iHt]\psi\|<\delta\,,$$

for $t'\geqslant t\geqslant T$.

But since the norm is unchanged by an interchange of the two terms, this inequality holds for all $t\geqslant T$, $t'\geqslant T$. Hence by the completeness property of Hilbert space there exists a φ such that

$$\varphi=\lim_{t\to\infty}\exp[iH_\alpha t]\exp[-iHt]\psi\,,$$

and this is equivalent to $\exp[-iHt]\psi\simeq\exp[-iH_\alpha t]\varphi$ as $t\to\infty$ or

$$\psi=\lim_{t\to\infty}\exp[iHt]\exp[-iH_\alpha t]\varphi\,.$$

The necessity of the condition (2) is proved by reversing the steps of the argument, and the outgoing case can be treated similarly.

3. – Structure of the Hamiltonian of multichannel scattering systems.

As shown by JAUCH [1], the convergence theorem and the properties of the channel Hamiltonians lead to the orthogonality theorem. Let $R_{\pm}^{(\alpha)}$ denote the subspaces spanned by the outgoing- and ingoing-wave scattering states originating and terminating in channel α (the ranges of $\Omega_{\pm}^{(\alpha)}$). The projection operators on these subspaces are

$$F_{\pm}^{(\alpha)} = \Omega_{\pm}^{(\alpha)}\Omega_{\pm}^{(\alpha)*} . \tag{3}$$

The orthogonality theorem asserts the orthogonality of the subspaces $R_{+}^{(\alpha)}$ and $R_{+}^{(\alpha')}$ (and similarly in the ingoing case), or equivalently $F_{\pm}^{(\alpha)}F_{\pm}^{(\alpha')}=0$ for $\alpha'\neq\alpha$. The series of projection operators $F_{\pm}=\sum\limits_{\alpha} F_{\pm}^{(\alpha)}$ therefore converge and are the projections on the subspaces $R_{\pm}=\sum\limits_{\alpha}\oplus R_{\pm}^{(\alpha)}$.

The intertwining relations [JAUCH [1]]

$$\exp[iHt]\Omega_{\pm}^{(\alpha)} = \Omega_{\pm}^{(\alpha)}\exp[iH_{\alpha}t] \tag{4}$$

follow directly from the convergence theorem and the vanishing of $\Omega_{\pm}^{(\alpha)}$ on $D_{\alpha}^{\perp}$: For $\varphi\in D_{\alpha}$,

$$\lim_{\tau\to\pm\infty}\exp[iH\tau]\exp[-iH_{\alpha}\tau]\exp[iH_{\alpha}t]\varphi = \\ = \lim_{\tau\to\pm\infty}\exp[iHt]\exp[iH(\tau-t)]\exp[-iH_{\alpha}(\tau-t)]\varphi . \tag{5}$$

Thus (4) holds on D_{α} and $\exp[iH_{\alpha}t]$ leaves D_{α} invariant for each t. Therefore it also leaves the orthogonal complement $D_{\alpha}^{\perp}$ invariant. But since by definition $\Omega_{\pm}^{(\alpha)}$ are equal to zero on $D_{\alpha}^{\perp}$, (4) holds also on $D_{\alpha}^{\perp}$ and hence on the entire space.

We also make use of a well known theorem on the reduction of an operator by a direct sum of orthogonal reducing subspaces [4]. Let $\{R^{(\alpha)}\}$ be a finite or infinite family of mutually orthogonal subspaces; let $\{F^{(\alpha)}\}$ be the corresponding family of projections; let R denote the subspace $\sum\limits_{\alpha}\oplus R^{(\alpha)}$ and F the projection on R. Let H be a closed linear operator which is reduced by each subspace $R^{(\alpha)}$. Then R reduces H. An element f in R belongs to the domain of H if and only if both $F^{(\alpha)}f\in\mathcal{D}_H$ for each α and $\sum\limits_{\alpha}\|HF^{(\alpha)}f\|^2<\infty$, in which case $Hf=\sum\limits_{\alpha}HF^{(\alpha)}f$.

With these preparations we can prove the following theorem.

The Hamiltonian H of a multichannel scattering system is reduced by the subspace $R_{\pm}$, and the part of H in $R_{\pm}$ is given by

$$H_{\pm}=\sum_{\alpha}\oplus\,\Omega_{\pm}^{(\alpha)}H_{\alpha}\Omega_{\pm}^{(\alpha)*} .$$

(Here $\Omega_{\pm}^{(\alpha)}$ and $\Omega_{\pm}^{(\alpha)*}$ are regarded as restricted to the subspaces D_{α} and $R_{\pm}^{(\alpha)}$ on which they are isometric.)

---

(4) M. H. STONE: *Linear Transformations in Hilbert Space* (New York, 1932), p. 152, Theorem 4.26.

First we note that the subspaces $R_\pm^{(\alpha)}$ reduce H, since by (5) $\exp[iHt]$ leaves $R_\pm^{(\alpha)}$ invariant for all t. Also, H is evidently closed, since for the physical systems it is always a self-adjoint operator (5). Hence all the hypotheses of the theorem noted above are satisfied, and we conclude from it that $R_\pm$ reduce H and

$$Hf = \sum_\alpha HF_\pm^{(\alpha)} f\,, \qquad \text{for } f \in \mathcal{D}_H \cdot R_\pm\,.$$

To complete the proof, it will be shown that

$$HF_\pm^{(\alpha)} = H\Omega_\pm^{(\alpha)}\Omega_\pm^{(\alpha)*} = \Omega_\pm^{(\alpha)} H_\alpha \Omega_\pm^{(\alpha)*}\,. \tag{6}$$

From (4) we have

$$\frac{1}{t}\,\Omega_\pm^{(\alpha)}\,(\exp[iH_\alpha t] - I)\varphi = \frac{1}{t}\,(\exp[iHt] - I)\,\Omega_\pm^{(\alpha)}\varphi\,.$$

For $\Omega_\pm^{(\alpha)}\varphi \in \mathcal{D}_H$, the right-hand side has a limit, $iH\Omega_\pm^{(\alpha)}\varphi$, as $t \to 0$ (by Stone's theorem (6)). Therefore for $\varphi \in D_\alpha$ and $\Omega_\pm^{(\alpha)}\varphi \in \mathcal{D}_H$, also $(1/t)(\exp[iH_\alpha t] - I)\,\varphi$ has a limit, $iH_\alpha\varphi$, as $t \to 0$ since $\exp[iH_\alpha t]$ leaves D_α invariant and $\Omega_\pm^{(\alpha)}$ are isometric on D_α. This shows that

$$H\Omega_\pm^{(\alpha)}\Omega_\pm^{(\alpha)*} \subseteq \Omega_\pm^{(\alpha)} H_\alpha \Omega_\pm^{(\alpha)*}\,, \tag{7}$$

since the ranges of $\Omega_\pm^{(\alpha)*}$ are equal to D_α. On the other hand, from the relations $\Omega_\pm^{(\alpha)} H_\alpha \subseteq H\Omega_\pm^{(\alpha)}$ which likewise follow from (4), we have

$$\Omega_\pm^{(\alpha)} H_\alpha \Omega_\pm^{(\alpha)*} \subseteq H\Omega_\pm^{(\alpha)}\Omega_\pm^{(\alpha)*}\,. \tag{8}$$

From equations (3), (7) and (8), equation (6) follows.

Under the completeness hypothesis (7) that $R_+ = R_- = N$ holds for the Hamiltonians of the physical scattering systems, where N is the orthogonal complement of the subspace spanned by the proper functions (if any) of H, it follows from the above theorem that the « continuum part » of H (the restriction of H to $R_+ = R_- = N$) is given by

$$H_c = \sum_\alpha \oplus\ \Omega_\pm^{(\alpha)} H_\alpha \Omega_\pm^{(\alpha)*}\,.$$

Since D_α reduces H_α (by the invariance of D_α to $\exp[iH_\alpha t]$ for all t), this relation expresses that the continuum part of the total Hamiltonian decomposes in two ways, into its parts in the subspaces $R_+^{(\alpha)}$ or in $R_-^{(\alpha)}$ respectively, where each of these parts is unitarily equivalent to the part of H_α in D_α, the isometric operator furnishing the unitary equivalence being the wave operator $\Omega_+^{(\alpha)}$ or $\Omega_-^{(\alpha)}$.

---

(5) T. Kato: *Trans. Amer. Math. Soc.*, **70**, 195 (1951).

(6) See, *e.g.*, F. Riesz and B. Sz.-Nagy: *Functional Analysis* (New York, 1955), pp. 384-385.

(7) J. M. Jauch: reference (1). The equality of R_+ and R_- (unitarity property of the S-operator) means in the single-channel case that if the conditon (2) holds for either $t \to -\infty$ or $t \to +\infty$, it holds for both. However the equality of $R_+^{(\alpha)}$ and $R_-^{(\alpha)}$ will not in general hold in the multichannel case, since by the orthogonality theorem it would exclude scattering into or out of the channel. An exception (cf. Sect. **4**) is in the channels where all particles are bound.

4. – Convergence to the wave operators in many-body scattering.

We consider the typical multichannel system with the total Hamiltonian given by

$$H=\sum_j (\boldsymbol{p}_j^2/2m_j)+\sum_j V_j(\boldsymbol{r}_j)+\sum_{i<j} V_{ij}(\boldsymbol{r}_i-\boldsymbol{r}_j)\,,$$

and demonstrate the convergence to the wave operators for the case [8] where the V_j and V_{ij} are quadratically integrable functions of their arguments, for $i, j = 1, 2, \ldots, N$.

We first discuss the case of $N=3$ and then the generalization to arbitrary N. As will be clear from the discussion which follows, the V_j can be treated in the same way as the V_{ij} (they augment the number of channels and give additional terms in V_α) and therefore no generality will be lost by carrying out the proof under the assumption that the V_j all vanish identically.

Consider the channel for which particle 1 is scattered by a fragment consisting of particles 2 and 3 bound together. The channel Hamiltonian is

$$H_\alpha=\frac{\boldsymbol{p}_1^2}{2m_1}+\frac{\boldsymbol{P}^2}{2M}+E_\alpha\,;$$

where $\boldsymbol{P}=\boldsymbol{p}_2+\boldsymbol{p}_3$, $M=m_2+m_3$, and $|E_\alpha|$ is the binding energy of the fragment. The interaction in the channel α is

$$V_\alpha=V_{12}+V_{13}\,.$$

We introduce the center-of-mass coordinates, $\boldsymbol{R}=(1/M)(m_2\boldsymbol{r}_2+m_3\boldsymbol{r}_3)$, and the relative coordinates, $\boldsymbol{r}=\boldsymbol{r}_2-\boldsymbol{r}_3$, for the fragment. The class of functions of the form

$$\varphi=g(\boldsymbol{r}_1)G(\boldsymbol{R})u_\alpha(\boldsymbol{r})\,,$$

where $g(\boldsymbol{r}_1)$ and $G(\boldsymbol{R})$ are Fourier transforms of Gaussian packets [2] of the form $\exp[-a^2(\boldsymbol{p}-\boldsymbol{p}')^2]$ with fixed $a^2>0$, are a convenient choice of a dense set of functions in the subspace D_α of functions of the form $f(\boldsymbol{r}_1,\boldsymbol{R})u_\alpha(\boldsymbol{r})$, where $u_\alpha(\boldsymbol{r})$ is the fixed bound-state function for the particles 2 and 3, and $f(\boldsymbol{r}_1,\boldsymbol{R})$ is square-integrable in $\boldsymbol{r}_1,\boldsymbol{R}$. By evaluation of the Fourier transform, one obtains

$$\left|\left(\exp\left[i\,\frac{p_1^2}{2m_1}\,t\right]g\right)(\boldsymbol{r}_1)\right|^2=\left[4\left(a^4+\left(\frac{t}{2m_1}\right)^2\right)\right]^{-\frac{3}{2}}\exp\left[-c(\boldsymbol{r}_1-\boldsymbol{b})^2\right],$$

where

$$\boldsymbol{b}=\frac{t}{m_1}\boldsymbol{p}_1'\,,\qquad c=\frac{1}{2}\,\frac{a^2}{a^4+(t/2m_1)^2}\,,$$

and a similar relation holds for G.

---

[8] This corresponds to the case treated by J. M. COOK: reference [2], in single-channel scattering.

1807

In order to demonstrate the convergence to the wave operators, it suffices (²) to show that

$$\int_{\infty}^{\infty} \| V_\alpha \exp [iH_\alpha t]\varphi \| \mathrm{d}t < \infty \,. \tag{9}$$

By virtue of the triangle inequality, it is enough to verify (9) for each term in V_α separately. For the first term we have

$$\| V_{12} \exp [iH_\alpha t]\varphi \|^2 =$$

$$= \iiint V_{12}^2(\boldsymbol{r}_{12}) \left[4\left(a^4 + \left(\frac{t}{2m_1}\right)^2\right)\right]^{-\frac{3}{2}} \exp [-c(\boldsymbol{r}_1 - \boldsymbol{b})^2] \cdot$$

$$\cdot \left|4\left(a^4 + \left(\frac{t}{2M}\right)^2\right)\right|^{-\frac{3}{2}} \exp \left| - C\left(\frac{m_2\boldsymbol{r}_2 + m_3\boldsymbol{r}_3}{M} - \boldsymbol{B}\right)^2\right| u_\alpha^2(\boldsymbol{r}_{23})\, \mathrm{d}\boldsymbol{r}_1\, \mathrm{d}\boldsymbol{r}_2\, \mathrm{d}\boldsymbol{r}_3 \leqslant$$

$$\leqslant \iiint V_{12}^2(\boldsymbol{r}_{12}) \left|4\left(a^4 + \left(\frac{t}{2m_1}\right)^2\right)\right|^{-\frac{3}{2}} \left|4\left(a^4 + \left(\frac{t}{2M}\right)^2\right)\right|^{-\frac{3}{2}} \cdot$$

$$\cdot \exp [-C(\boldsymbol{R} - \boldsymbol{B})^2]\, u_\alpha^2(\boldsymbol{r})\, \mathrm{d}\boldsymbol{r}_{12}\, \mathrm{d}\boldsymbol{r}\, \mathrm{d}\boldsymbol{R} = K \cdot \left[4\left(a^4 + \left(\frac{t}{2m_1}\right)^2\right)\right]^{-\frac{3}{2}},$$

where K is a constant. One obtains a similar bound for the second term in V_α, and consequently condition (9) is satisfied.

The remaining channels, *i.e.*, the channels obtained by permutations (⁹) of 1, 2, 3, as well as the channels where 1, 2, 3 are all free or all bound (each bound state of a fragment counting as a separate channel) can all be treated similarly; the interactions are of course assumed sufficiently strong to bind the various fragments described, otherwise even fewer channels need to be considered. In the channels where all particles are bound, $V_\alpha = 0$, the wave operators reduce to the identity, and $R_+^{(\alpha)} = R_-^{(\alpha)} = D_\alpha$.

The generalization to an arbitrary channel of the N-particle system will now be clear. In the evaluation of $\| V_{ij} \exp [iH_\alpha t]\varphi \|$ for each interaction term $V_{ij}(\boldsymbol{r}_i - \boldsymbol{r}_j)$ in V_α, each of the variables $\boldsymbol{r}_i, \boldsymbol{r}_j$ occurs in an exponential function, either as a term in a center-of-mass coordinate of a fragment or as a free-particle coordinate. We drop one of these exponentials as we did above, and introduce in place of the omitted center-of-mass or free-particle coordinate the new variable $\boldsymbol{r}_{ij} = \boldsymbol{r}_i - \boldsymbol{r}_j$. The factor $[4(a^4 + (t/2m)^2)]^{-\frac{3}{2}}$ associated with the omitted exponential is then left over as before, and so condition (9) is again satisfied.

(⁹) For indistinguishable particles, the appropriate antisymmetric or symmetric linear combinations can be formed from the scattering states thus obtained.

IL NUOVO CIMENTO Vol. XIII, N. 1 1° Luglio 1959

Conservation Laws in General Relativity.

C. Cattaneo

Istituto Matematico dell'Università - Pisa

(ricevuto il 13 Maggio 1959)

1. – Introductory considerations.

In this short Note we shall show, by means of a suitable method of projection and by adopting the relative standard quantities defined in two previous papers [1], that conservation principles can be formulated for any possible physical system in a gravitational field. This formulation does not yet give conservation laws without sources, like those of Einstein and many other Authors (I shall here simply mention the important result recently obtained by C. Møller [2]). However the present formulation, by its simplicity and generality and its purely tensor character, proves the physical content of the relative standard quantities and shows the advantages of the « projection method ».

Let V_4 be the space-time manifold, x^i [3] physically admissible co-ordinates; $ds^2 = g_{ik}\,dx^i\,dx^k$ the space-time metric $(+++-)$; $\boldsymbol{\gamma}$ the unitary vector oriented like the line x^4 ($\gamma^\alpha=0$, $\gamma^4=1/\sqrt{-g_{44}}$; $\gamma_i=g_{i4}/\sqrt{-g_{44}}$); T_x the tangent vector space at the point x, Θ_x and Σ_x (or sometime simply Θ and Σ) the sub-spaces of T_x respectively parallel and orthogonal to $\boldsymbol{\gamma}$. The ∞^3 ideal particles having the lines x^4 as world lines form the *physical frame of reference* S associated to the co-ordinates x^i.

Every vector $\boldsymbol{V}$ of T_x can be uniquely decomposed in two vectors, $\boldsymbol{V}=\boldsymbol{A}+\boldsymbol{N}$, belonging respectively to Θ_x and Σ_x:

$$A_i = -\gamma_i\gamma_k V^k\,, \qquad N_i = \gamma_{ik}V^k\,, \tag{1}$$

where the tensors $-\gamma_i\gamma_k$ and $\gamma_{ik}=g_{ik}+\gamma_i\gamma_k$ act as *time-projector* and *space-projector* respectively. Similarly, since the symbolic decomposition $T_x=\Sigma_x+\Theta_x$ induces on $T_x\otimes T_x$ the decomposition $T_x\otimes T_x=\Sigma\otimes\Sigma+\Sigma\otimes\Theta+\Theta\otimes\Sigma+\Theta\otimes\Theta$, every double tensor A_{ij} can be uniquely decomposed into the sum of four tensors belonging respectively to the above mentioned sub-spaces of $T_x\otimes T_x$. These tensors will be

(1) C. Cattaneo: *Nuovo Cimento*, **10**, 318 (1958) and **11**, 733 (1959). These papers will be in the following quoted as I and II.

(2) C. Møller: *Ann. Phys.*, **4**, 347 (1958).

(3) Latin indexes vary from 1 to 4; greek indexes from 1 to 3.

called the four *natural projections* of A_{ij} and they will be indicated by $\mathcal{P}_{\Sigma\Sigma}(A_{ij})$, $\mathcal{P}_{\Sigma\Theta}(A_{ij})$, $\mathcal{P}_{\Theta\Sigma}(A_{ij})$, $\mathcal{P}_{\Theta\Theta}(A_{ij})$. They can be obtained from A_{ij} by means of the two *projectors* $-\gamma_i\gamma_k$ and γ_{ik} in the following way:

$$(2)\qquad \begin{cases} \mathcal{P}_{\Sigma\Sigma}(A_{ij}) = \gamma_{ir}\gamma_{js}A^{rs}\,, & \mathcal{P}_{\Sigma\Theta}(A_{ij}) = -\gamma_{ir}\gamma_j\gamma_s A^{rs}\,, \\ \mathcal{P}_{\Theta\Sigma}(A_{ij}) = -\gamma_i\gamma_r\gamma_{js}A^{rs}\,, & \mathcal{P}_{\Theta\Theta}(A_{ij}) = \gamma_i\gamma_j\gamma_r\gamma_s A^{rs}\,. \end{cases}$$

For a simmetrical tensor $A_{ij}=A_{ji}$ the natural decomposition may be written

$$(3)\qquad A_{ij} = \tilde{A}_{ij} + \tilde{A}_i\gamma_j + \gamma_i\tilde{A}_j + A\gamma_i\gamma_j\,,$$

where we have put $\tilde{A}_{ij}=\mathcal{P}_{\Sigma\Sigma}(A_{ij})=\gamma_{ir}\gamma_{js}A^{rs}$, $\tilde{A}_i=-\gamma_{ir}\gamma_s A^{rs}$, $A=\gamma_r\gamma_s A^{rs}$ (the symbol $\sim$ indicates the spatial character of the tensors and vectors). Similar considerations can be applied to tensors of any order.

Some important properties of the physical frame of reference S can be characterized by means of the following tensors: the *space-time vortex tensor*, $\Omega_{ij} = \partial_i\gamma_j - \partial_j\gamma_i$; the *space vortex tensor* $\tilde{\Omega}_{ij}=\mathcal{P}_{\Sigma\Sigma}(\Omega_{ij})=\gamma_4[\tilde{\partial}_i(\gamma_j/\gamma_4) - \tilde{\partial}_j(\gamma_i/\gamma_4)]$, $(\tilde{\Omega}_{i4}= - \tilde{\Omega}_{4i}=0)$; the *curvature vector* of the lines x^4, $\tilde{\Omega}_i=\gamma^4\Omega_{4i}\equiv\gamma^r\Omega_{ri}$, $(\tilde{\Omega}_4=0)$; the *tensor of Killing*, $K_{ij}=\nabla_i\gamma_j+\nabla_j\gamma_i$; the *spatial tensor of deformation* or *Born tensor* $\tilde{K}_{ij}=\mathcal{P}_{\Sigma\Sigma}(K_{ij})= =\gamma^4\partial_4\gamma_{ij}$, $(\tilde{K}_{i4}=\tilde{K}_{4i}=0)$. For instance the vanishing of $\tilde{\Omega}_i$, or of $\tilde{K}_{ij}$, or of $\tilde{\Omega}_{ij}$ characterizes respectively the *geodesic* frames, the *rigid* (or *stationary*) frames in the sense of Born, and the *spatially irrotational* frames (orthogonality of the congruence of the lines x^4).

With the same tensors we can express, as we have shown in I and II, the gravitational force mG_α acting on a freely gravitating test particle:

$$(4)\qquad mG_\alpha = mG'_\alpha + mG''_\alpha = mc^2\Omega_{\alpha r}\gamma^r + mc\tilde{\Omega}_{\alpha\beta}v^\beta\,,$$

($m=m_0(1-v^2/c^2)^{-\frac{1}{2}}$, $v^\alpha=\mathrm{d}x^\alpha/\mathrm{d}T$, $v^2=\gamma_{\alpha\beta}v^\alpha v^\beta$, $\mathrm{d}T=-(1/c)\gamma_i\mathrm{d}x^i$ being the relative standard quantities [1] of the particle (mass, velocity, magnitude of the velocity, time) with respect to the physical frame of reference S. By means of these tensors we can also express the energy absorbed by the particle from the field per unity of relative standard time T:

$$(5)\qquad mc^2\Omega_{\alpha r}\gamma^r v^\alpha - \tfrac{1}{2}\,mc\gamma^4\partial_4\gamma_{\alpha\beta}v^\alpha v^\beta\,.$$

The two terms can be interpreted respectively as the work of the gravitational force per unit time T and as the energy directly absorbed from the frame, if it is not stationary.

2. – Conservation equations (with sources) for any physical system.

In accordance with the general definition of the relative standard interval of time between to infinitely close events ($\mathrm{d}T= -(1/c)\gamma_i\mathrm{d}x^i$), we shall call *local standard time interval*, relative to a given place point (x^α) of the system of reference S, the

quantity $\delta T_0 = -(1/c)\gamma_4 dx^4$ which coincides with the proper time interval of the reference particle (x^α) itself.

The *local* variation of any quantity $q(x^i)$ (that is its variation obtained by leaving unaltered the spatial co-ordinates x^α) with respect to the local time, that we shall call — in a not very proper sense — local time derivative of q, is evidently $\delta q/\delta T_0 = c\gamma^4\partial_4 q$.

Moreover let us consider an infinitesimal tube of lines x^4 and the element ΔS of the physical frame represented by the tube. Let ΔS_0, function of x^4, be the *proper volume* of this element, that is to say the volume of the normal section of the tube.

The variation of ΔS_0 is given by well known formula (4): $\gamma^4\partial_4(\Delta S_0) = \Delta S_0 \nabla_j \gamma^j$, so that its local time derivative may be written: $\delta(\Delta S_0)/\delta T_0 = c\Delta S_0 \nabla_j \gamma^j$.

Let us now consider any physical system whose symmetrical energy-momentum tensor A_{ij} must satisfy, because of the gravitational equations, the conditions

$$\nabla_j A_i{}^j = 0 . \tag{6}$$

By decomposing the tensor A_{ij} according to equation (3), we give now the following definitions: $h = A = \gamma_r\gamma_s A^{rs}$ = *relative standard density of energy*, per unit of proper volume of frame; $\mu = h/c^2$ = *relative standard density of mass*; $\tilde{g}_i = \tilde{A}_i/c$ = = *relative standard density of momentum*, per unit of proper volume of frame ($\tilde{g}_4 = 0$); $\tilde{S}_i = c\tilde{A}_i = c^2\tilde{g}_i$ = *relative standard density of energy current*, per unit of proper volume of frame and per unit of local time ($\tilde{S}_4 = 0$); $\tilde{A}_{ij} = \gamma_{ir}\gamma_{js}A^{rs}$ = *relative standard density of momentum current*, per unit of proper volume of frame and per unit of local time ($\tilde{A}_{i4} = \tilde{A}_{4i} = 0$). If we apply, for instance, the above mentioned definitions to a pure-matter scheme we obtain:

$$h = \mu_0 c^2/[1-(v^2/c^2)], \quad \mu = \mu_0/[1-(v^2/c^2)], \quad \tilde{g}_\alpha = \mu v_\alpha , \quad \tilde{S}_\alpha = c^2\mu v_\alpha , \quad \tilde{A}_{\alpha\beta} = \mu v_\alpha v_\beta , \tag{7}$$

v^α being the relative standard velocity of the particles of the system.

By means of these definitions, the scalar projection of (6) onto Θ_x, multiplied by ΔS_0, the proper volume of an element ΔS of the physical frame, may be written

$$\Delta S_0 \nabla_i \tilde{S}^i + c\Delta S_0 \gamma^4 \partial_4 h + c\Delta S_0 h \nabla_i \gamma^i = c^2 \Omega_{\alpha r}\gamma^r(\tilde{g}^\alpha \Delta S_0) - \frac{c}{2}\gamma^4\partial_4\gamma_{\alpha\beta}(\tilde{A}^{\alpha\beta}\Delta S_0). \tag{8}$$

According to our definitions, in the first term in the left hand side we recognize, with the help of the Green theorem, the amount of energy that goes out of ΔS per unit of the local time. On the other hand the second and the third term give, together, the increase per unit of local time $\big(\delta(h\Delta S_0)/\delta T_0\big)$ of the energy contained in ΔS, so that the whole left hand side is nothing else than the *non balanced* increase of the energy contained in ΔS. On the right hand side the first term, which is the scalar product of the gravitational field G'_α by the momentum $\tilde{g}^\alpha \Delta S_0$ contained in ΔS, may be identified (apart from the substitution of mv^α by $\tilde{g}^\alpha \Delta S_0$) with the first term of (5); the second term, apart from the substitution of $mv^\alpha v^\beta$ by $\tilde{A}^{\alpha\beta}$, may be identified with the second term of (5). The whole right side hand of (8) may then be interpreted as the energy absorbed by the system from the gra-

(4) See, for instance, J. L. SYNGE: *Relativity: The Special Theory* (Amsterdam, 1956), p. 280.

vitational field: thus (8) seems really to express, in a *local* form, the principle of conservation of energy.

In a similar way one can deduce from (6) a principle of conservation of the relative momentum; in fact (6) projected into Σ_x and multiplied by ΔS_0, gives

$$\Delta S_0 \nabla_j \widetilde{A}_\alpha{}^j + c\Delta S_0 \gamma^4 \partial_4 \widetilde{g}_\alpha + c\Delta S_0 \widetilde{g}_\alpha \nabla_j \gamma^j = \mu \Delta S_0 c^2 \Omega_{\alpha r} \gamma^r + c \widetilde{\Omega}_{\alpha\beta} \widetilde{g}^\beta \Delta S_0 \,. \tag{9}$$

The first term can be interpreted as the amount of momentum flowing out of the fixed element of space ΔS, per unit of local time. The second and third term give the increase, in the same time, of the momentum contained inside ΔS; so the whole left hand side gives the non balanced increase of the momentum. On the other hand the right hand side, being the gravitational force (cfr. (4)) acting on the volume ΔS ($\widetilde{g}^\alpha \Delta S_0$ taking the place of mv^α) can be interpreted as a source of momentum.

Details and calculations will be given in a forthcoming paper.

A New Method for the Determination of the Meson-Nucleon Coupling Constant from the 33 Phase Shift.

A. Martin
CERN - Geneva

(ricevuto il 18 Maggio 1959)

The ordinary way to get the meson nucleon coupling constant from the 33 phase shift consists in extrapolating the Chew-Low plot to zero total energy of the meson. The method we propose here is free of assumptions on the energy dependence of the phase shift and just requires that, in the low energy region, the cut off factor could be taken equal to unity. The starting equation may be the Low equation (1) or its relativistic generalization (2):

$$g_3(\omega_q) = \frac{4}{3}\frac{q^3 f^2}{\mu^2\omega_q} + \frac{q^3}{\pi}\int_\mu^\infty \frac{v^2(k)}{k^3}\frac{|g_3(\omega_k)|^2 \mathrm{d}\omega_k}{\omega_k-\omega_q-i\varepsilon} + \frac{q^3}{\pi}\int_\mu^\infty \frac{C(\omega_k)\,\mathrm{d}\omega_k}{\omega_k+\omega_q}, \tag{1}$$

where

$$g_3(\omega_q) = \frac{\exp[i\delta_{33}(q)]\sin\delta_{33}(q)}{v^2(q)},$$

q is the c.m. momentum, and ω_q is the total c.m. energy minus the nucleon mass. $C(\omega_q)$ is a function of the meson nucleon phase shifts and takes into account recoil effects. When the phase shift is supposed to be known one can write for the quantity $f(\omega_q) = g_3(\omega_q)/q^3$ a linear integral equation of the Mushkelishvili-Omnès type (3):

$$f(\omega_q) = \frac{4}{3}\frac{f^2}{\omega_q\mu^2} + \frac{1}{\pi}\int_\mu^\infty \frac{f(\omega_k)\exp[-i\delta(k)]\sin\delta(k)\,\mathrm{d}\omega_k}{\omega_k-\omega_q-i\varepsilon} + \frac{1}{\pi}\int_\mu^\infty \frac{C(\omega_k)\,\mathrm{d}\omega_k}{\omega_k+\omega_q}. \tag{2}$$

This equation has a finite number of solutions for $0<\delta<\pi$. We keep the solution which vanishes when f^2 and C go to zero (so called « physical solution »). We easily

---

(1) F. E. Low: *Phys. Rev.*, **97**, 1392 (1955).
(2) G. Chew, M. Goldberger, F. E. Low and Y. Nambu: *Phys. Rev.*, **106**, 1337 (1957).
(3) R. Omnès: *Nuovo Cimento*, **8**, 316 (1958).

obtain $f(\omega_q)$, and finally, the cut off factor:

$$(3) \qquad v^2(q)f^2 + \frac{3}{4}\,\frac{\omega_q\mu^2}{\pi}\int\limits_{\mu}^{\infty}\frac{C'(\omega_k)\,\mathrm{d}\omega_k}{\omega_k+\omega_q} = \frac{3}{4}\,\frac{\mu^2\omega_q\sin\delta(q)}{q^3}\exp\left[-\frac{\omega_q}{\pi}\,P\int\limits_{\mu}^{\infty}\frac{\delta(k)\,\mathrm{d}\omega_k}{\omega_k(\omega_k-\omega_q)}\right],$$

where

$$C'(\omega_q) = C(\omega_q)\exp\left[\frac{\omega_q}{\pi}\int\limits_{\mu}^{\infty}\frac{\delta(k)\,\mathrm{d}\omega_k}{\omega_k(\omega_k+\omega_q)}\right].$$

Consequently the product of the coupling constant by the cut off factor can be expressed in terms of the 33 phase shift and of an unknown smooth function going to zero for $\omega_q=0$. One can estimate the unknown term by assuming that the main contribution to it comes from the 33 resonance and from $1/M$ terms. One sees that it is small (less than 0.02ω) and smooth in the positive energy region. Therefore we suggest to plot the right hand side of (3) and to extrapolate it to $\omega_q=0$ to get f^2, since, below the resonance, it is reasonable to take $v^2=1$. One might be more ambitious and try to get the cut off factor from equation (3). The lack of information on $C(\omega_k)$ and on the high energy behaviour of the phase shift (above 400 MeV) makes this impossible.

In order to compute the principal value integral, we have assumed the following analytic form for the phase shift:

$$(4) \qquad \delta_{33}(\omega) = 180^\circ\left[\alpha\left(\frac{\omega'}{\omega'+1.2}\right)^{\frac{3}{2}} + (1-\alpha)\,\frac{\omega'^4}{(1.12)^4+\omega'^4}\right] + $$

$$+\,500^\circ\times\beta\times\frac{\omega'^4}{(\omega'^4+5)(\omega'^4+5.5)(\omega'^4+6)},$$

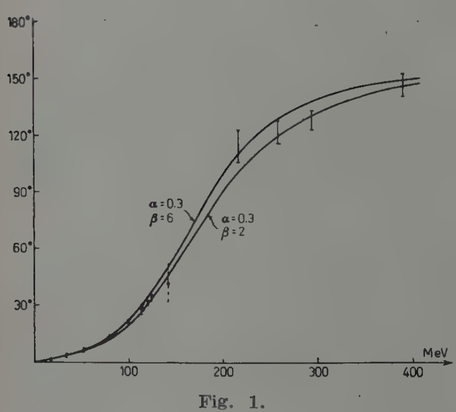

Fig. 1.

where $\omega'=\omega-1$, in units $\mu=1$. Fig. 1 represents the 33 phase shift versus laboratory energy [4,5]. The two curves correspond to $\alpha=0.3$, $\beta=2$ and $\alpha=0.3$, $\beta=6$. The best fit is given by $\alpha=0.31$, $\beta=4.2$. We have computed the right hand side of (3) for these three couples of values. The extrapolated values are very close to each other and we have only represented on Fig. 2 the points corresponding to $\alpha=0.31$, $\beta=4.2$. We get $f^2=0.099\pm0.003$. Since this value is large as compared to those derived from exact dispersion relations [6] we

(4) H. Anderson and W. Davidson: *Nuovo Cimento*, 5, 238 (1957).
(5) S. Barnes, B. Rose and G. Giacomelli: NYO-2170, to be published in the *Phys. Rev.*
(6) G. Salzmann and H. Schnitzer: NYO-2272, to be published in the *Phys. Rev.*

have tried to get f^2 as small as possible. The curve $\alpha=0.28$, $\beta=4.2$ is clearly below the low energy values of δ_{33}. It leads to a value of $f^2=0.093\pm0.002$ (Fig. 2), which is still rather large. This is a general feature of the extrapolations starting from the Low equation (7).

Formula (4) assumes that $\delta_{33}(\infty)=\pi$. In fact, around the cut off energy, the phase shift returns to zero, more or less smoothly according to the sharpness of the cut off. To estimate the importance of this effect we cut the principal value integral at some large energy Ω. This is equivalent to multiplying the exponential factor by $\Omega/(\Omega-\omega_q)$. It turns out that the extrapolated value of f^2 is unaffected by this factor. One might hope to get the cut off energy in this way, by adjusting Ω to get $v^2=1$ in the low energy region. Unfortunately the uncertainty on $C(\omega_q)$ makes such an estimate very unprecise. It seems that a cut off energy lower than the commonly accepted value would be favoured.

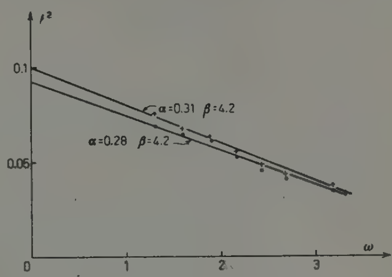

Fig. 2.

* * *

Mr. KLEIN is acknowledged for the numerical computations. The author is indebted to Professors FIERZ, FUBINI, STANGHELLINI, AMATI and VITALE for interesting discussions, and thanks Professor FIERZ and Professor BAKKER for hospitality at the CERN Theoretical Study Division.

(7) M. CINI, S. FUBINI and A. STANGHELLINI: *Nuovo Cimento*, 3, 1380 (1956).

IL NUOVO CIMENTO VOL. XIII, N. 1 1° Luglio 1959

Energy Bands in Silicon Crystals.

F. BASSANI

Istituto di Fisica Teorica dell'Università - Pavia

(ricevuto il 30 Maggio 1959)

The results of energy-band calculations performed at special symmetry points of the reduced zone in silicon crystals have been reported earlier by T. O. WOODRUFF (1) and F. BASSANI (2). The points at which results have been given are the point Γ ($\boldsymbol{k} = 0$) and the point X ($\boldsymbol{k} = 2\pi a^{-1}(1, 0, 0)$). The method of Orthogonalized Plane Waves was used in the form described by T. O. WOODRUFF (1).

In the present letter we present new results for the energy values at two more points of the reduced zone, the point L ($\boldsymbol{k} = 2\pi a^{-1}(\frac{1}{2}, \frac{1}{2}, \frac{1}{2})$) and the point $\Delta(\frac{1}{2})$ ($\boldsymbol{k} = 2\pi a^{-1}(\frac{1}{2}, 0, 0)$).

The general method and the essential parameters which enter the calculations in the case of silicon have been fully described in references (1) and (2). The symmetry analysis required in this framework is the same for all diamond structures and has been described in detail elsewhere (3). The trial wave functions have been constructed from the sets of plane waves $\langle\frac{1}{2}, \frac{1}{2}, \frac{1}{2}\rangle$, $\langle\frac{3}{2}, \frac{1}{2}, \frac{1}{2}\rangle$, $\langle\frac{1}{2}, \frac{3}{2}, \frac{3}{2}\rangle$, $\langle\frac{3}{2}, \frac{3}{2}, \frac{3}{2}\rangle$ and $\langle\frac{5}{2}, \frac{1}{2}, \frac{1}{2}\rangle$ at the point L, and from the sets of plane waves $\langle\frac{1}{2}, 0, 0\rangle$, $\langle\frac{1}{2}, 1, 1\rangle$, $\langle\frac{3}{2}, 0, 0\rangle$, $\langle\frac{3}{2}, 1, 1\rangle$, $\langle\frac{1}{2}, 2, 0\rangle$ and $\langle\frac{5}{2}, 0, 0\rangle$ at the point $\Delta(\frac{1}{2})$. It does not seem necessary to give the values of the orthogonality coefficients required at the two points of interest, because they can easily be evaluated from the explicit expressions for the core wave functions given by WOODRUFF (1). The Fourier coefficients of the potential depend only on the reciprocal lattice vectors and are also given in Woodruff's paper (1).

The results for the energies of the valence states and of the lowest conduction states at the point L and at the point $\Delta(\frac{1}{2})$ are given in Table I and Table II respectively. They have been obtained by solving the secular determinantal equations with the Electronic Computer of the Engineering School of Milan.

From Table I and from the results of reference (1) and (2) it can be seen that the separation between the top valence state $L_{3'}$ and the lowest conduction state L_3 is larger than the corresponding separations at the points Γ and X and that the relative positions of the energy states at the various points yield an energy-band structure

(1) T. O. WOODRUFF: *Phys. Rev.*, **103**, 1159 (1956).

(2) F. BASSANI: *Phys. Rev.*, **108**, 263 (1957).

(3) F. BASSANI and V. CELLI: *Nuovo Cimento*, **11**, 805 (1959).

TABLE I. – *Energies (in Rydbergs) of valence and conduction states in* Si *at the point* L $(\boldsymbol{k} = 2\pi a^{-1}(\frac{1}{2}, \frac{1}{2}, \frac{1}{2}))$.

	$L_1(1)$	$L_{2'}(1)$	$L_{3'}(1)$	$L_3(1)$	$L_1(2)$	$L_{2'}(2)$
E_1	-0.992	-1.196	-0.718	-0270	—	—
E_2	-1.073	-1.237	-0.772	-0.356	-0.296	$+0.037$
E_3	-1.173	-1.260	-0.839	-0.363	-0.310	$+0.036$
E_4	-1.180	-1.278	—	—	-0.351	$+0.036$
E_5	-1.198	-1.291	—	—	-0.364	-0.044

The subscripts attached to E indicate the order of the secular equation solved in obtaining the energies.

consistent with experimental data. The order of the energy levels in Table I is the same as that obtained by PHILLIPS with his interpolation scheme [4], but all energies lie consistently higher with respect to the energies at the point Γ $(\boldsymbol{k} = 0)$. This is probably due to the fact that plane waves of higher energy should be included in our procedure which makes use of calculated theoretical values for the crystal potential and the core states. On the other hand, the fact that the sequence of the energy states and their relative positions at different points in the zone are essentially determined by a small number of plane waves and have been shown to be independent of the details of the crystal potential [5] seems to furnish a justification for the validity of the interpolation scheme of Phillips.

TABLE II. – *Energies (in Rydbergs) of valence and conduction states in* Si *at the point* $\Delta(\frac{1}{2})$ $(\boldsymbol{k} = 2\pi a^{-1}(\frac{1}{2}, 0, 0))$.

	Δ_1	Δ_5	$\Delta_{2'}$	$\Delta_1(2)$	$\Delta_{2'}(2)$	$\Delta_5(2)$
E_1	-1.264	-0.676	-0.567	—	—	—
E_2	-1.337	-0.807	-0.789	-0.409	-0.264	0.139
E_3	-1.386	-0.827	-0.789	-0.477	-0.317	-0.196
E_4	-1.388	-0.884	-0.841	-0.533	-0.318	-0.212
E_5	—	—	-0.845	—	-0.355	—

The subscripts attached to E indicate the order of the secular equation solved in obtaining the energies.

The results of Table II must be compared with Fig. 1 of reference [2] and Fig. 5 of reference [4]. They suggest a much smoother variation of E versus $\boldsymbol{k}$ than was obtained in reference [2], in agreement with the criticism of Phillips to the validity of a tight binding interpolation scheme.

---

[4] J. C. PHILLIPS: *Phys. Rev.*, **112**, 685 (1958).

[5] F. BASSANI: *Journ. Phys. and Chemistry of Solids*, **8**, 375 (1959). See also reference [3].

LIBRI RICEVUTI E RECENSIONI

A. MESSIAH – *Mécanique quantique*, Dunod, Paris 1959, Tome I, pag. XV+430.

Questo volume comprende le prime delle cinque parti che costituiranno l'opera complessiva. È basato su lezioni date da MESSIAH al Centro di Studi Nucleari di Saclay a partire dal 1953.

Dalle due parti incluse nel primo volume la prima è dedicata al formalismo quantistico ed alla sua interpretazione, la seconda allo studio di particolari sistemi semplici. Nella prima parte vengono trattati le origini sperimentali e teoriche della teoria quantistica, la teoria di Schrödinger, i sistemi unidimensionali, l'interpretazione statistica e le relazioni di indeterminazione, il formalismo quantistico, il limite classico, e, negli ultimi due capitoli, il formalismo generale della meccanica quantistica. Nella seconda parte sono trattati i potenziali centrali, i problemi di urto, l'intersezione coulombiana, e l'oscillatore armonico a una e a più dimensioni. Due appendici trattano delle distribuzioni delta e delle funzioni speciali e formule relative.

La scelta degli argomenti, l'ordine delle esposizioni si adeguano ad un corso universitario di meccanica quantistica. Il secondo volume completerà la trattazione con una discussione delle proprietà di simmetria, dei metodi di approssimazione e di elementi di teoria relativistica. Il lavoro di MESSIAH ci sembra tuttavia notevole per le due seguenti ragioni. Primo vi è raggiunto un brillante esempio di equilibrio tra la parte formale e la parte fisica-interpretativa. È noto come in parecchi trattati di meccanica quantistica il peso è spostato ora sull'uno ora sull'altro aspetto della teoria, a scapito, in alcuni casi, dell'approfondimento dei concetti, in altri casi della descrizione dei metodi. Secondo, pur essendo impostato nelle linee tradizionali, il testo contiene in parecchie parti spunti didatticamente moderni ed originali, come ad esempio una trattazione moderna della teoria dello scattering ispirata a lavori di CHEW e LOW, una trattazione semplice ma sufficiente delle funzioni improprie colla teoria delle distribuzioni, la discussione degli ensemble statistici, l'uso frequente della rappresentazione di Heisenberg, di solito poco adoperata in problemi di teoria di particelle.

Infine ci è apparsa molto soddisfacente la drastica riduzione ad alcune paginette di tutta l'antica teoria dei quanti, dall'innegabile valore storico e didattico, ma alla cui descrizione bisogna essere disposti a rinunciare se si vuole far posto a nozioni più moderne. È fatale che con l'evolversi della teoria la discussione di quelli che furono stadi provvisori, anche se importantissimi storicamente, debba necessariamente venire sfrondata e ridotta a pochi cenni. Anche in termini di pura didattica, personalmente riteniamo che le generazioni nuove siano più facili ad impadronirsi direttamente dei punti di vista moderni, che

non a ripercorrere per tappe storiche il cammino che ha portato alla formulazione di questi punti di vista. Vorremmo così augurarci che nei prossimi anni possa avvenire una ulteriore evoluzione nella pratica di insegnamento e nella forma di esposizione della meccanica quantistica, in maniera che non siano più presentate in forme disgiunte e quasi contrapposte le teorie non relativistiche e quelle relativistiche, e soprattutto siano evitate quelle costruzioni contraddittorie e vacillanti per presentare inesistenti teorie relativistiche di una sola particella, cui sempre si ricorre, anche qui forse in parte per lascito storico, nel proposito di non includere concetti di teoria dei campi nel nostro insegnamento universitario.

R. GATTO

Annual Review of Nuclear Science; Vol. 8, Editore EMILIO SEGRÈ, Annual Reviews Inc., Palo Alto, California 1958, pag. VII+417; dollari 7.50.

Questo volume ottavo di *Annual Review of Nuclear Science* comprende tredici articoli su argomenti di scienza nucleare.

Apre la serie un bellissimo articolo di GIAN CARLO WICK sui principi di invarianza in fisica nucleare. L'articolo è limitato, come spiega l'autore, a quelle operazioni di simmetria sulle quali la fisica nucleare ha qualcosa di nuovo da dire: parità, inversione di tempo, coniugazione di carica; ed inoltre sono discussi lo spin isotopico e le leggi di conservazione dei barioni e dei leptoni. La discussione di queste proprietà di simmetria è svolta in maniera rigorosa e completa e nello stesso tempo molto chiara e accessibile.

L'articolo di WICK è seguito da un articolo di FESHBACH sul modello ottico e la sua giustificazione. L'autore mostra dapprima la possibilità di una derivazione rigorosa del potenziale ottico generalizzato e dell'approssimazione dovuta a Brueckner mediante la introduzione della massa effettiva; quindi l'approssimazione mediante scattering multipli per fenomeni di alta energia; e, per fenomeni di bassa energia, lo studio delle sezioni d'urto mediante sulla energia, il formalismo di Kapur e Peierls ed il modello ad accoppiamento intermedio. Il resto dell'articolo descrive l'enorme lavoro accumulato in questi ultimi anni per una caratterizzazione fenomenologica dei potenziali ottici nucleari. È notevole come da questo studio empirico siano emersi in maniera definita importanti dati qualitativi sul potenziale ottico nucleare, quale ad esempio il diverso comportamento della energia della parte reale e della parte immaginaria, e la presenza del termine spin orbita apparentemente confinato alla superficie del nucleo. Manca una discussione approfondita della teoria di Brueckner che richiederebbe uno spazio molto maggiore.

L'articolo di FRY sugli iperframmenti è piuttosto breve e si limita agli aspetti sperimentali del problema più alcuni cenni molto qualitativi della teoria.

Segue l'ottima rassegna di SEGRÉ sugli antinucleoni. L'autore discute dapprima le verifiche sperimentali delle proprietà dell'antiprotone previste dalla teoria di Dirac, e quindi espone in dettaglio i risultati sperimentali sullo scattering e sull'annichilazione ed i vari modelli teorici proposti. Vengono anche riportati i pochi dati relativi agli antineutroni. È compreso sulla rassegna un esame dei limiti superiori assegnabili per la quantità di antimateria presente nella galassia e per la sua intensità di produzione, e la eventuale relazione con l'energia emessa da radiostelle.

La spettroscopia dei raggi gamma per mezzo di diffrazione diretta su cristalli viene discussa da DU MOND nell'articolo seguente. Vengono esposti i principi di

funzionamento degli spettrometri a cristallo incurvato. Il resto dell'articolo descrive lo spettrometro a due cristalli recentemente realizzato con successo a Chalk River.

Di affascinante lettura è l'articolo di JUDD sui recenti progressi concettuali nel campo degli acceleratori di particelle. L'articolo è esplicitamente scritto per non specialisti. Oltre ad esporre i più recenti progressi nel campo della progettazione di acceleratori JUDD espone anche idee recentissime, ancora non di certa realizzazione, che potranno divenire attuali ed importanti nel prossimo futuro, come ad esempio la proposta di far collidere due beam in senso opposto, che viene ora seriamente considerata dai fisici delle Università del Midwest, ed originali proposte russe come quella di usare guide d'onda riempite di plasma negli acceleratori lineari, e quella dovuta a Veksler di generare il campo acceleratore della interazione coerente di un piccolo gruppo di particelle con un plasma o con onde elettromagnetiche.

L'articolo seguente è di NEHER sulla radiazione cosmica primaria. L'autore passa in rassegna i dati sulla composizione chimica dei primari, sulla loro distribuzione in energia, e sulle loro fluttuazioni. Il resto dell'articolo tratta del problema dell'origine dei raggi cosmici.

Seguono gli articoli di SUESS, sulla radioattività della atmosfera e della idrosfera, di ALDRICH e WETHERILL sulla cronologia della terra mediante decadimento radioattivo, di CAMERON sulla astrofisica nucleare, di MOYER sul controllo dei rischi da radiazioni in ricerche di fisica, di WOOD sulla radiobiologia cellulare ed infine un articolo di QUASTLER sulla teoria dell'informazione in radiobiologia, la cui lettura ci ha svelato un campo di ricerche nuovissimo e promettente di sviluppi.

R. GATTO

Direttore responsabile: G. POLVANI

Tipografia Compositori - Bologna

Questo fascicolo è stato licenziato dai torchi il 25-VI-1959

1820